Mendelova univerzita v Brně
Agronomická fakulta
Ústav chemie a biochemie

Progresivní nástroje pro identifikaci bakterie
Staphylococcus aureus

Disertační práce
Studijní obor: 4106V017 Zemědělská chemie

Vedoucí práce:
Doc. RNDr. Pavel Kopel, Ph.D.

Školitel specialista: *Vypracovala:*
Mgr. Markéta Vaculovičová, Ph.D.   Ing. Kristýna Číhalová

Brno 2016

PROHLÁŠENÍ

Prohlašuji, že disertační práce na téma „Progresivní nástroje pro identifikaci bakterie *Staphylococcus aureus*" je samostatným autorským dílem podle Autorského zákona. Nositelem majetkového autorského práva je pracoviště a univerzita.

Výsledky práce shrnuté v této závěrečné práci byly financovány z veřejných prostředků z Evropských fondů a státního rozpočtu České republiky. Vzniklé dílo jako celek je chráněno autorským zákonem. Užití tohoto díla pro další šíření a využívání je vázáno na uzavřenou výhradní licenční smlouvu.

Podle § 12 autorského zákona platí, že autorské dílo lze užít jen se svolením autora. Základní informace o práci jsou přístupné všem žadatelům a jsou plně k dispozici (abstrakt). V případě zájmu o využití díla pro další užití (výuka, prezentace, konference, komerční účely) je zapotřebí se řídit licenčními podmínkami.

Licenční podmínky jsou dány licenční smlouvou, kde na jedné straně je pracoviště vzniku díla a děkana nebo rektora univerzity (nositel majetkového autorského práva) a na druhé straně je žadatel o využití výsledku. Realizátor závěrečné práce podléhá licenčním podmínkám, pokud jeho práci chce použít pro jiné účely než ukončení studia. Užití § 29 zákona užití pro osobní potřebu citace není dotčeno.

Disertační práce a výsledky v ní prezentované jsou dílem vypracovaným na Ústavu chemie a biochemie působícím na půdě Agronomické fakulty Mendelovy univerzity v Brně a mohou být použity k dalšímu prezentování případně ke komerčním účelům jen se souhlasem vedoucího disertační práce a děkana. V opačném případě se jedná o porušení zákona.

dne ……………………………………………

podpis…………………………………………

Poděkování

Na prvním místě bych chtěla poděkovat profesoru Vojtěchu Adamovi a profesoru Renému Kizekovi za příležitost být součástí jejich týmu, za cenné rady, připomínky a čas, který věnovali mně a mojí práci.

Děkuji Markétě Vaculovičové a Pavlu Kopelovi za odborné vedení mé práce.

Dagmar Hegerové, Lukáši Nejdlovi, Aně Marii Jimenez Jimenez, Sylvii Skaličkové, Lukáši Richterovi a Davidu Hynkovi patří velký dík za ochotu a pomoc při konzultacích a interpretaci výsledků práce.

Děkuji všem spoluautorům za pomoc při vědecké práci a přípravě publikací, které jsou experimentální součástí této disertační práce.

Poděkování patří také Úrazové nemocnici v Brně, p.o. za poskytnutí stěrů z infekčních ran hospitalizovaných pacientů, ze kterých jsme mohli izolovat bakterie a provádět experimenty.

Dále bych chtěla poděkovat všem kolegům z Ústavu chemie a biochemie, ve kterých jsem našla nejen kolegy, ale i velké přátele, díky nimž byla pro mne práce radostí a zábavou.

Velký dík patří mé rodině za psychickou podporu během studií, za pevné zázemí a oporu. Poděkování patří i mým přátelům a mému příteli za podporu, pochopení a důvěru.

Abstrakt

Přítomnost bakterie *Staphylococcus aureus* (*S. aureus*) a jeho rezistentní formy meticilin-rezistentní *S. aureus* (MRSA) jsou v infekcích stále častější a léčba se stává čím dál komplikovanější především kvůli vzrůstající rezistenci. Včasná identifikace mikrobiomu infekční rány vede k nasazení správné léčby a tím k ušetření pacienta od vzniku abscesů, amputací končetin či dokonce smrti.

Předkládaná práce s názvem „Progresivní nástroje pro identifikaci bakterie *Staphylococcus aureus*" je zaměřena na studium výskytu těchto bakterií v klinických vzorcích, návrh a zhotovení nových detekčních metod založených na magnetické separaci a vyhodnocení vlivu účinku antibiotik a nanočástic kovů na růst a tvorbu biofilmu, genovou expresi a proteinové složení u *S. aureus* a MRSA.

Nejvíce zastoupený mikroorganismus v infekčním mikrobiomu je *S. aureus* a v našich studiích byl použit jako modelová bakterie pro návrh rychlých, přesných a citlivých detekčních technik, které využívají nepřímé detekce jako je: i) detekce produktu biochemické reakce bakteriálních enzymů s matricí, ii) detekce amplifikovaného genu za použití zlatých nanočástic jako indikátorových sond, iii) stanovení detekčních oligonukleotidů po sendvičovém zachycení bakterie mikro a nanočásticemi a iv) multiplexní detekce kvantových teček využívajících sendvičového zachycení fragmentu specifického genu vybraných bakterií. Na navržené detekční metody navazuje porovnání vlivu účinku samotných β-laktamových antibiotik a jejich komplexů se selenovými nanočásticemi na nerezistentní a rezistentní formu *S. aureus*. V případě MRSA bylo použitím komplexů antibiotik a selenových nanočástic dosaženo výrazné inhibice růstu bakterií a tvorby biofilmu, změny genové exprese a proteinového složení.

Klíčová slova: *Staphylococcus aureus*, infekce, antibiotikum, rezistence, magnetická separace, nanočástice, inhibice

Abstract

The presence of infections caused by *Staphylococcus aureus* (*S. aureus*) and its resistant form - methicillin-resistant *S. aureus* (MRSA) - are more frequent and treatment with increasing resistance becomes increasingly complicated. Early identification of microbiome in the infectious wounds leads to implementation of the correct treatment and thereby saving the patient from the formation of abscesses, amputation of limbs or even death.

Presented thesis entitled "Progressive tools for the identification of Staphylococcus aureus" is focused on the study of the occurrence of these bacteria in clinical samples, design and construction of new detection methods based on magnetic separation and evaluation of the effects of antibiotics and metal nanoparticles on growth and biofilm formation, gene expression and protein composition in *S. aureus* and MRSA.

The most abundant microorganism in microbiome of infections is *S. aureus* and in our studies was used as model bacteria for the design of fast, accurate and sensitive detection techniques utilizing indirect detection such as: i) detection of product of biochemical reaction between bacterial enzymes and matrix, ii) detection of the amplified gene using gold nanoparticles as an indicator probe, iii) determination of the detection oligonucleotides after sandwich capture of bacteria between micro and nanoparticles, and iv) a multiplex detection of quantum dots using sandwich capture of specific gene from selected bacteria. Subsequently, an influence effect of β-lactam antibiotics and their complexes with selenium nanoparticles to non-resistant and resistant form of *S. aureus* was investigated. The significant inhibition of bacterial growth and biofilm formation as well as changes in gene expression and protein composition were achieved in MRSA by using the complexes of antibiotics and selenium nanoparticles.

Key words: *Staphylococcus aureus*, infections, antibiotic, resistance, magnetic separation, nanoparticles, inhibition

OBSAH

1 ÚVOD

Svět v jaké podobě ho vidíme, není až tak úplně jednoznačný, jak se zdá. Mnoho procesů, které byly pro člověka vždy jasnou věcí, ale zároveň záhadou, byly objasněny až postupem času s příchodem objevitelů, vědy a moderních technik.

Bakteriální předci byli ve skutečnosti na Zemi první živé organismy, i když o těchto faktech víme poměrně málo. Mikrobiologická historie několika posledních staletí je pro nás z hlediska příčin, přenosu a léčby nemocí mnohem známější. Jeden z nejdůležitějších objevů byl uskutečněn v 17. století Robertem Hookem, jehož teorie zní: „Všechny živé věci jsou složeny z buněk".

Jedním z klíčových kroků, kdy lidem došlo, že mikroorganismy jsou spjaty s chorobami, bylo zjištění původu kvašení během výroby alkoholických nápojů. Louis Pasteur tak zjistil, že mikroorganismy, zvané kvasinky, dokáží převést cukry na alkohol v nepřítomnosti vzduchu. Tento proces zvaný fermentace se používá k výrobě vína a piva. V přítomnosti vzduchu ovšem dochází ke vzniku kyseliny octové, což je během zkvašování cukrů s cílem vzniku etanolu nežádoucí. Řešení problému takto zkaženého piva či vína Pasteur vyřešil inhibicí většiny bakterií teplem. Tento proces zvaný pasterizace je důležitým krokem při výrobě potravin a zamezuje tak jejich kažení.

Jak je známo, mnoho druhů nemocí souvisí s bakteriemi, ale do poměrně nedávné doby nebyly jejich příčiny úplně jasné. Účinné léčby chorob bývaly dříve objeveny obvykle metodou „pokus-omyl". Zjištění, že kvasinky hrají klíčovou roli během kvasných procesů, upozornilo vědce na možnost vztahu mezi mikroorganismy a rostlinami či zvířaty, zejména možnost způsobení onemocnění právě mikroorganismy (teorie nemoci z bakterií). Teorie nemoci z bakterií byla v té době těžce přijatelný koncept. Pro lidi narozené v Pasteurově době bylo nemyslitelné, aby „neviditelní" mikrobi mohli být transportováni vzduchem, držet se na oblečení či lůžkovinách a že mohou být přenášeny z jedné osoby na druhou.

V roce 1860 anglický chirurg Joseph Lister aplikuje teorii nemoci z bakterií do léčebných procedur, což spočívalo v aplikaci fenolu, který zabíjí bakterie, na pooperační rány. Listerova technika byla jedním z prvních lékařských pokusů o kontrolu a eliminaci infekcí způsobených mikroorganismy. Ve skutečnosti, jeho nálezy prokázaly, že mikroorganismy způsobují infekce operační rány. S prvním důkazem toho, že bakterie skutečně způsobují onemocnění, přišel Robert Koch.

Objevením tyčinkovité bakterie zjistil příčinu onemocnění antrax u dobytka v Evropě. Bakterie izolovaná z krve uhynulého dobytka je dnes známá jako *Bacillus anthracis*. Tyto poznatky byly během posledního století významné a velmi důležité pro rozvoj diagnostiky bakteriálních onemocnění.

Poté, co byl objasněn vztah mezi mikroorganismy a nemocemi, lékařská mikrobiologie začala klást důraz na hledání látek, které by mikroorganismy mohly ničit. Léčba pomocí chemických látek se nazývá chemoterapie. Chemické látky produkované přirozeně bakteriemi a houbami jsou antibiotika a chemoterapeutika vyrobené z chemických látek v laboratoři jsou syntetické léčiva. Úspěch chemoterapie je založen na vyšším stupni jedovatosti látky na bakterie než na hostitele infikovaného mikroby.

Moderní objevy v mikrobiologii se snaží řešit rezistenci vůči léčivům, identifikovat rychle, přesně a citlivě bakterie a viry a vyvíjet nové vakcíny. Základy položené v době Pasteura a Kocha, Zlatý věk mikrobiologie, zajistily předpoklad pro monumentální úspěchy mikrobiologického vývoje v průběhu 20. století. Nové obory mikrobiologie jako je imunologie, virologie, molekulárně-biologické technologie zabývající se rekombinantní DNA mají zásadní a převratnou ve výzkumu praktických aplikací všech oblastí mikrobiologie.

Detekci bakterií vědci posunuli z klasických kultivačních metod na molekulární úroveň, a to díky studiu genomu, proteinového složení a metabolických drah bakterií. Výskytem infekčního onemocnění se zvyšují požadavky na rychlost, přesnost a citlivost detekce bakteriálního kmene, léčbu a eliminaci výskytu bakteriální infekce, což je řešeno chemoterapeutiky a antibiotiky. Avšak roky nadužívání či dokonce zneužívání těchto léčiv vytvořilo u bakterií odolnost přežívat v prostředí ošetřovaném léčivy. Náhodné mutace bakteriálních genů přispívají k bakteriální rezistenci vůči antibiotikům. Bakterie odolné vůči antibiotikům, z nichž nejvýznamnější je právě MRSA, se staly celosvětovou zdravotnickou krizí. Dnešní výzkum se zabývá vývojem nových antibakteriálních léčiv, která nejsou založena na bázi antibiotik, ale směřují spíše k nanotechnologiím, ve kterých moderní výzkum nalézá stále širší uplatnění.

2 CÍLE PRÁCE

- Sumarizovat informace o bakteriích *Staphylococcus aureus (S. aureus),* jejich vlastnostech a rezistenci k meticilinovým antibiotikům

- Vyhodnotit metody stanovení bakterie *S. aureus* a testovat nové, rychlé a citlivé metody stanovení této bakterie a meticilin-rezistentního *S. aureus* (MRSA)

- Vyhodnotit přítomnost bakterie *S. aureus* u vzorků klinických stěrů infekčních ran

- Porovnat efekt antibiotik a komplexů nanočástic selenu a antibiotik na *S. aureus* a MRSA

3 LITERÁRNÍ PŘEHLED

3.1 Stafylokoky

3.1.1   Taxonomické zařazení

Stafylokoky představují vhodný model pro ilustraci jednotlivých aspektů a problematiky bakteriální taxonomie ve všech třech jejích částech: klasifikace (definice skupin a vztahů mezi nimi), názvosloví (pojmenování skupin) a identifikace (přiřazení nových izolátů do nových nebo již vzniklých pojmenovaných skupin). Vědci zabývající se taxonomií se často střetávají v názorech, týkajících se zařazení jednotlivých bakterií do taxonomického systému u bakterií rodu *Staphylococcus* a *Micorococcus (Vandamme a kol., 1996)*.

Dle časné taxonomické historie měla na tuto problematiku velký vliv Society of American Bacteriologist Committee a byl vytvořen Bergey's Manual, první vydaný taxonomický řád, který byl postupně doplňován. Tato raná klasifikace byla ovlivněna převážně morfologickými aspekty mikroorganismů. Postupně nastávaly v Bergeyho manuálu různé změny, které již do klasifikace stafylokoků zahrnuly další postupně objevované aspekty, jako je vztah ke kyslíku, biochemická aktivita bakterií, podrobná studie DNA, vznik rezistencí na antibiotika aj. V současnosti je uplatňováno 8. vydání Bergeyho manuálu *(Kawamura a kol., 1998)*.

Podle Bergeyho manuálu systematické bakteriologie je taxonomické zařazení bakterií rodu *Staphylococcus* popsáno následovně:

Kmen: Firmicutes

Třída: Bacilli

Řád: Bacillales

Čeleď: *Staphylococcaceae*

Čeleď Staphylococcaceae zahrnuje bakteriální rody a to *Staphylococcus, Salinicoccus, Nosocomiicoccus, Jeotgalicoccus* a *Macrococcus*. Jednotlivé rody zahrnují dále své druhy a poddruhy. Nejvíce zástupců bakteriálních druhů tvoří rod *Staphylococcus (Amoozegar a kol., 2014)*.

Taxonomie stafylokoků se díky moderním molekulárně-biologickým metodám rozšiřuje

také na úrovni poddruhové. Na základě fenotypových odlišností a fylogenetické příbuznosti jsou dnes známy např. poddruhy *S. equorum* subspecies *equorum* a *S. equorum* subsp. *linens (Kawamura, Hou, Sultana, Hirose, Miyake, Shua Ezaki, 1998), S. succinus* subsp. *succinus (Lambert a kol., 1998)* a *S. succinus* subsp. *casei (Place a kol., 2002).* Významným stafylokokem v humánních klinických vzorcích je např. *S. hominis* subsp. *novobiosepticus (Kloos a kol., 1998).*

3.1.2 Morfologie a anatomie stafylokoků

Vzhledem k různorodosti a četnosti zastoupení čeledí a rodů bakterií, jsou bakterie prvotně rozpoznávány a děleny podle tvaru na koky, kokobacily, tyčinky a dále vibria, spirily či spirochety. Pomocí tvaru a seskupení lze bakterie prvotně klasifikovat pod mikroskopem a již zařadit podle morfologie. Důležitá je i anatomická stavba bakterií, která je spolu s biochemickými procesy klíčová pro navržení vhodných metod detekce. *Staphylococcus* v řečtině je přeložen "staphyle", což znamená hrozen vína a "kokkos", což znamená kok. Pojmenování vyplývá z tvorby shluků koků pod mikroskopem, který se podobá hroznům. Jedná se o grampozitivní (G^+) koky o průměrné velikosti 0,5 - 1,5 μm. Jakožto většina G^+ bakterií, je i *S. aureus* řazen morfologicky mezi koky *(Forsyth a kol., 2002).* Buňky jsou sférické, uspořádané po jedné, ve dvojicích, čtveřicích, v nepravidelných shlucích, v krátkých řetízcích nejčastěji o třech buňkách, či v typickém uskupení trsu hroznů. Hroznovité seskupení pozorovatelné pod mikroskopem stafylokoky tvoří proto, že se na rozdíl od blízkých příbuzných streptokoků, dělí ve dvou rovinách. Streptokoky se dělí v jedné rovině a tvoří tak řetězce. Stafylokoky jsou nepohyblivé, nesporulující, poměrně odolné vůči podmínkám zevního prostředí *(Adams a kol., 2009).*

3.1.2.1 Pouzdro

Pouzdro, též zvané kapsule bakterie je polysacharidová vrstva, která se nachází vně bakteriální buňky. Jedná se o dobře organizovanou vrstvu, která je špatně omyvatelná z povrchů a může být příčinou různých onemocnění. Na povrchu ploch, či v trubkách

s tekutými potravinami, dokonce i v lidském organismu vzniká přítomností bakterií tvořící pouzdra slizovitá vrstva.

Pouzdro je považováno za faktor virulence, protože zvyšuje schopnost bakterií vyvolávat nemoci. Pouzdro chrání bakterii před pohlcením makrofágy tak, že antigenní struktury jsou díky pouzdru pro protilátky nedostupné, a nemůže nastat fagocytóza. Dochází tedy k bakteriální perzistenci v krevním řečišti infikovaných hostitelů. Další neopomenutelnou vlastností pouzdra je ochrana bakterie proti vysychání a napomáhání buňce přilnout k povrchu, ochrana před napadením bakteriálními viry a před detergenty *(Dunne a kol., 1994; Standish a kol., 2012).*

3.1.2.2 Buněčná stěna

Stafylokoky patří ke G^+ bakteriím, jejichž buněčná stěna vykazuje vysoký obsah peptidoglykanu a zároveň postrádá vnější membránu a vrstvu lipopolysacharidů. Tato skutečnost pak ovlivňuje výsledek diagnostického barvení dle Grama, kdy G^+ bakterie můžeme pozorovat pod mikroskopem modrofialové, zatímco gramnegativní (G^-) červené *(Rao, 1997; Archunan, 2004; Kayser a kol., 2011).* **Peptidoglykan** tvoří antigenní strukturu bakterie, který navozuje v lidském organismu tvorbu interleukinu-1, který představuje jednu z klíčových molekul imunitního systému a tvoří významnou součást tzv. cytokinové sítě, která zajišťuje regulaci a koordinaci různých složek obrany organismu v případě infekce, zánětu, poranění nebo stresu. Peptidoglykan také slouží jako aktivátor sérových a membránových glykoproteinů, endotoxinů bakterií a je na něm navázána kyselina teichoová a protein A *(Marraffini a kol., 2006; Dreisbach a kol., 2011).* **Kyselina teichoová** je hlavní součástí buněčné stěny bakterií a její název je označení pro skupinu polysacharidů navázaných přes fosfodiesterové vazby. Vzhledem k různorodosti navázaných skupin (cukry, aminokyseliny) existuje množství teichoových kyselin a na jejich základě lze určit sérotyp bakterie. To znamená, že proti různým sérotypům téhož druhu mikroorganismu se tvoří různé typy protilátek. Krom toho, že se jednotlivé sérotypy liší v antigenní struktuře, mohou vykazovat rovněž rozdílnou druhovou vnímavost, virulenci, patogenitu či odolnost vůči vnějšímu prostředí. V mikrobiologii je serotyp považován za taxonomickou jednotku. **Protein A** má antifagocytární a antikomplementární účinek a váže se na Fc fragment imunoglobulinu G (IgG), čehož se využívá u diagnostické koagulační reakce *(Verhoef a*

kol., 1979; Hartford a kol., 1999; Cox a kol., 2008). Další součástí antigenní struktury jsou **adheziny** sloužící jako kolonizační faktory, které způsobují adhezi stafylokoků na mezibuněčné nebo buněčné struktury jako je fibrinogen, fibronektin či kolagen *(Nandakumar a kol., 2005; Dreisbach, van Dijla Buist, 2011).* Jak již bylo zmíněno, rozdíly v antigenní struktuře se vyskytují v rámci jednoho druhu bakterie, stejně jako rezistence vůči antibiotikům. Studie zabývající se septickou artritidou prokázala, že meticillin-rezistentní *S. aureus* obsahující na svém povrchu **plasmin-sensitive surface protein** (Pls protein) způsobuje větší zátěž na modelu myších ledvin než kmen bez Pls proteinu. Pls protein můžeme tedy zařadit mezi faktory virulence pro septické artritidy a sepse *(Josefsson a kol., 2005).* Vazebné povrchové proteiny bakterií jsou důležité z hlediska bakteriální kolonizace na hostitelských matricích. Povrchové proteiny bakterie *S. aureus* byly popsány jako virulentní faktory v různých modelech infekce, jejichž přesné mechanismy nebyly dosud zjištěny.

3.1.2.3 Cytoplazmatická membrána

Cytoplazmatická membrána je biologická membrána oddělující vnitřek buňky od vnějšího prostředí. Tato membrána je semipermeabilní. Je propustná pro některé ionty a organické molekuly, což je způsobeno difuzí pronikavých molekul, což závisí hlavně na jejich náboji, polaritě a molární hmotnosti molekuly. Ovládá také pohyb látek ven z buněk. Její základní funkcí je chránit buňku před okolními vlivy. Podílí se na adhezi buňky, výměně iontů, buněčné signalizaci. Dále hraje roli při ukotvení cytoskeletu a udává tvar buňky *(Singer a kol., 1972; Budin a kol., 2012).*

3.1.2.4 Cytoplazma

Cytoplazma je materiál uvnitř živé buňky s výjimkou buněčného jádra. Skládá se z cytosolu (gelovitá látka uzavřená v buněčné membráně) a organel, které tvoří vnitřní strukturu buňky. Obsah prokaryotických buněk, které nemají jádro, je obsažen v cytoplazmě. Buněčné jádro eukaryotických buněk je odděleno od cytoplazmy a nazývá se nukleoplazma.

Cytoplazma je tvořena z 80 % vody a je bezbarvá. V cytoplazmě dochází k většině buněčných metabolických aktivit, jako je glykolýza a procesy buněčného dělení *(Singera Nicolson, 1972).*

3.1.2.5 Genetika a studium genomu

Genom bakterie *S. aureus* obsahuje jeden kružnicový **chromozom** o velikosti 2700 - 2800 kb a soubor variabilních přídatných genetických elementů jako jsou plazmidy, bakteriofágy, inzerční sekvence, transpozony a genomové ostrovy patogenity. Zatímco bakteriální chromozom nese informace nezbytné pro zajištění důležitých fyziologických funkcí organizmu, přídatné genetické elementy udělují buňce např. odolnost vůči antibiotikům a zvyšují její virulenci *(Mlynarczyk a kol., 1998; Kuroda a kol., 2001).*

Plazmidy jsou extrachromozomální genetické elementy s autonomním replikačním systémem, které významně ovlivňují fenotypový projev bakterií. Většina přirozeně se vyskytujících kmenů *S. aureus* obsahuje jeden a více plazmidů, které můžeme podle Novicka rozdělit do čtyř různých tříd podle velikosti.

Plazmidy se stejným replikačním kontrolním systémem nemohou stabilně koexistovat v jedné hostitelské buňce. Tento jev označujeme jako inkompatibilitu. Její příčinou je soutěžení o replikační aktivátory a citlivost k replikačním inhibitorům *(Paulsson, 2002).* Na začátku 70. let 20. století navrhli Datta a Hedges klasifikaci plazmidů založenou na testu inkompatibility, podle kterého se u *S. aureus* rozlišuje 15 inkompatibilních skupin *(Hedges a kol., 1974).*

Pojmem **bakteriofág** označuje virus napadající bakterie. Indukují se prostřednictvím UV záření nebo mitomycinu C a do bakteriálního chromozomu se integrují na specifickém místě typickým Campbellovým mechanizmem *(Duncan a kol., 1978).*

Začlenění DNA fága (fágový genom) do genomu bakterie a vznik profága může být příčinou lyzogenní konverze. Součástí některých profágů mohou být genetické determinanty virulence *(Boyd a kol., 2002).*

Inzerční sekvence (IS elementy) jsou sekvence DNA o délce 700 - 2500 bp. Vyznačují se schopností transpozice, což je proces přemístění sekvence DNA z jednoho místa genomu na jiné. Kromě genů pro svou vlastní transpozici neobsahují žádnou genetickou

informaci. Inzerční sekvence se vyskytují jednotlivě nebo vytváří složený transpozon. Mohou být součástí prokaryotického i eukaryotického genomu *(Mahillon a kol., 1998)*.

Transpozony jsou sekvence DNA, které se stejně jako IS elementy vyznačují schopností transpozice. Přemísťují se pomocí enzymu transponáza, která je využívána na vyštěpení a opětovné zabudování do genomu. Mimo genů pro svou vlastní transpozici obsahují navíc jeden nebo více strukturních genů, které se projevují ve fenotypu buňky. Obvykle jsou to geny kódující rezistenci k antibiotikům *(Stewart a kol., 2001)*.

Genomové ostrovy patogenity (GOP) jsou variabilní genetické elementy, které výrazně zvyšují patogenitu bakterií. Jejich součástí jsou geny kódující faktory virulence, což jsou toxiny, adhesiny, invasiny. Nachází se u patogenních kmenů G$^+$ i G$^-$ bakterií *(Hacker a kol., 1997)*.

3.1.2.6 Ribozomy

Bakteriální ribozom je cytoplazmatický nukleoprotein, jehož hlavní funkcí je sloužit jako místo pro translaci mRNA. Skládá se z malé podjednotky (30S) a velké podjednotky (50S). Při syntéze proteinu se ribozom pohybuje podél molekuly mRNA, přečtením kodonu a přiřazením správné aminokyseliny dochází k syntéze proteinu. Při dosažení stop kodonu je překlad zastaven, mRNA a protein jsou uvolněny *(Czernilo.Ap a kol., 1974)*. Ribozomy se vyskytují v bakteriální buňce v hojném počtu. Bakteriální buňka obsahuje asi 10 000 ribozomů, což činí až 30 % hmotnosti buňky. Ribozomy se skládají z malé ribozomální podjednotky, která čte RNA a velké podjednotky, spojující aminokyseliny za vzniku polypeptidového řetězce. Malá podjednotka bakteriálního ribozomu má funkci asociace s RNA během překladu a dekódování a velká podjednotka slouží jako centrum peptidyl-transferázy, což je místo pro vznik peptidové vazby *(Benne a kol., 1987)*.

3.1.2.7 Bičík

Bičík vyčnívá z buňky některých prokaryotických i eukaryotických buněk. Jeho primární úlohou je pohyb, má ale také funkci smyslové organely, jelikož je citlivý na přítomnost chemických látek v prostředí a teplotu vně buňky *(Wang a kol., 2005)*.

Bičíky jednotlivých druhů bakterií se liší proteinovým složením a mohou tvořit toxiny (*E. coli* O157: H7) *(He a kol., 1996).*

Vzhledem k tomu, že *S. aureus* nenese na svém povrchu bičík ani pili, pak se jedná o bakterii nepohyblivou.

3.1.3 Fyziologie stafylokoků

Původní skupina zahrnující stafylokoky i mikrokoky byla rozdělena na základě vztahu ke kyslíku *(Evans a kol., 1955)*. Obligátně aerobní koky byly zařazeny do rodu *Micrococcus*, zatímco většina fakultativně anaerobních koků vytvořila rod *Staphylococcus*. Vztah stafylokoků ke kyslíku je fakultativně anaerobní.

Stafylokoky syntetizují katalázu, což je enzym, který dokáže přeměnit molekuly peroxidu vodíku na kyslík a vodu. Tento fakt indikuje patogenitu bakterie, která může být infekční a způsobovat onemocnění *(Otero a kol., 2006)*. Téměř každý z kmenů produkuje koagulázu, která přeměňuje fibrinogen na fibrin, který způsobuje srážení krve *(Sinha a kol., 1999)*. Oxidáza produkovaná rody *Micrococcus* a *Kocuria* (tvoří cytochrom a, b, c a d) je další fyziologický parametr, který je při stanovení stafylokoků pozorován jako negativní test. Stafylokoky jsou tedy oxidáza-negativní. U většiny stafylokoků jsou nalézány pouze cytochromy a a b, výjimku představují druhy *Staphylococcus lentus*, *Staphylococcus vitulinus*, *Staphylococcus sciuri* a *Staphylococcus fleurettii*, které mají navíc cytochrom c. Přítomnost cytochromu c u nich podmiňuje produkci oxidázy *(Kwok a kol., 2003)*.

Stafylokoky patří mezi chemoorganotrofy, některé druhy mívají metabolismus převážně respiratorní, jiné převážně fermentativní. Jako zdroj uhlíku a energie využívají cukry nebo aminokyseliny, případně oboje. Rozličné cukry mohou metabolizovat za aerobních podmínek a tvorby kyselin. Hlavními konečnými produkty pak bývají kyselina octová a CO_2. Zdroj dusíku pro stafylokoky představují organické látky, aminokyseliny a vitamín skupiny B. Některé druhy jsou schopny jako jediný zdroj dusíku využívat $(NH_4)_2SO_4$. Anorganické zdroje dusíku mohou využívat např. novobiocin rezistentní druhy *S. sciuri* a *S. xylosus (Emmett a kol., 1975)*. Stafylokoky jsou nepohyblivé bakterie, které netvoří spory a jsou schopny žít bez kyslíku.

3.1.4 Molekulární patogeneze *S. aureus*

I když více než 20 druhů *Staphylococcus* jsou popsány v Bergey's Manual (2001), pouze *Staphylococcus aureus* a *Staphylococcus epidermidis* jsou významné při interakci s lidmi *(Guerrero, 2001)*. *S. aureus* kolonizuje především nosní sliznice, ale vyskytovat se může i v ostatních anatomických lokalitách, včetně kůže, ústní dutiny a

gastrointestinálního traktu *(Wendt a kol., 2007)*. *S epidermidis* se nejčastěji vyskytuje na kůži *(Heilmann a kol., 2003)*.

S. aureus exprimuje mnoho potenciálních faktorů virulence. Jsou to povrchové proteiny, podporující kolonizaci hostitelských tkání; faktory, které inhibují fagocytózu (kapsle, imunoglobulin vázající protein A). Toxiny vyvolávající poškození hostitelské tkáně a onemocnění. Koaguláza-negativní stafylokoky jsou obvykle méně virulentní a exprimují tedy méně virulentní faktory *(Novick a kol., 1993; Piette a kol., 2009)*.

3.1.4.1 *Mechanismus patogenity*

Vylepšováním faktorů virulence ve stresových podmínkách u *S. aureus* je klíčovým faktorem k umožnění přetrvávat v krevním řečišti nebo tvořit sekundární ohniska nákazy hluboko v tkáních, kam se dostanou přes poškozenou kůži či sliznici nosních dírek. Bez ohledu na dostupnost antibiotik je *S. aureus* klinicky velmi významný G^+ kok.

Patogenita u *S. aureus* začíná **adhezí a kolonizací**, kdy dochází k přilnutí bakterie k povrchu kůže, či sliznic a tím umožnění kolonizace krevního řečiště, sliznic, apod. Pro tento účel hraje důležitou roli kyselina teichoová *(Weidenmaier a kol., 2004)*. Dále nastává **invaze**, při které *S. aureus* narušuje kožní bariéru vylučováním exfoliačních toxinů a hemolyzinů a dalších enzymů ničících tkáně *(Lowy, 1998; Amagai a kol., 2000)*. Infekce může být spuštěna při ohrožení imunitního systému nebo při lokalizovanému zánětu *(Harraghy a kol., 2007)*. Vyhnutí se imunitní odpovědi je tzv. **evaze**, při které *S. aureus* vylučuje anti-opsonizační proteiny *(Haas a kol., 2004)*. Na tomto procesu se nejvíce podílí protein A, který má anti-fagocytační vlastnosti a vyskytuje se na povrchu *S. aureus*. Kromě toho, *S. aureus* vylučuje leukotoxiny (Panton-Valentine leukocidin) lyzující leukocyty a dále exprimuje superantigeny (např. enterotoxiny) *(McCormick a kol., 2001)*, které rozvrací imunitní odpověď silnou polyklonální stimulací a expanzí specifických receptorů k T-lymfocytům, kdy následuje potlačení T-buněk do anergického stavu *(Wang a kol., 1998)*.

Exprese genů pro **tvorbu biofilmu** nastává při vyčerpání živin či kyslíku a bakterie vstupuje do stacionární fáze. Ve stacionární fázi, kdy jsou bakterie přilnuty, je *S. aureus* odolný vůči antimikrobiálním látkám. Slizovitá matrice biofilmu poskytuje též ochranu před imunitními buňkami a průnikem antibiotik *(Proctor a kol., 1998; Patel, 2005)*.

Extracelulární proteinové toxiny přispívají k patogenezi široké škály infekcí způsobené bakterií *S. aureus*. Produkce toxinu přispívá především na patogenitě této bakterie *(Stevens a kol., 2007)*. **Panton-Valentine leukocidin** jsou póry-tvořící toxiny spadající do skupiny leukotoxinů *(Grumann a kol., 2014)*, což jsou cytotoxiny podílející se na tvorbě pórů na membránách polymorfonukleárních buněk a způsobují buněčnou smrt, apoptózu nebo nekrózu *(Kobayashi a kol., 2010)*. Panton-Valentine leukocidin je jedním z nejvíce virulentních stafylokokových toxinů nekorzující zápal plic, kůži a infekce měkkých tkání *(Lina a kol., 1999)*, který je přítomen ve většině CA-MRSA *(DeLeo a kol., 2010)*.

Dokonce neúmyslné užívání β-laktamových antibiotik indukuje zvýšenou produkci toxinů u MRSA a dochází tak ke zhoršení průběhu infekce a následně léčby *(Stevens, Ma, Salmi, McIndoo, Wallacea Bryant, 2007)*.

Další skupinou jsou **exfoliativní toxiny** které se dělí na skupiny A, B a D. Funkčně se jedná o isoformy enzymů s vysokou druhovou specifitou *(Becker a kol., 2003)*. Obsahují serin specifický pro glutamát a proteázovou aktivitou a selektivně štěpí peptidovou vazbu v extracelulární oblasti lidského desmogleinu, což způsobí adhezi bakterie na povrch buňky *(Nishifuji a kol., 2008)*. Tímto způsobem usnadňují exfoliativní toxiny bakteriální kožní invazi a uvolněním keratinocytů mohou způsobit stafylokokový syndrom opařené kůže *(Grumann, Nubela Broker, 2014)*.

3.1.4.2 Patogeneze MRSA

Samostatnou pozornost z hlediska patogeneze si zaslouží MRSA pro svoji vysokou morbiditu a mortalitu při vzniku epidemie. MRSA je možné rozdělit do dvou genotypově odlišných skupin HA-MRSA (healthcare-acquired MRSA) a CA-MRSA (community associated MRSA), které jsou různě zaměřené a překrývají se a způsobují různá onemocnění *(Ito a kol., 2003)*.

3.1.4.3 Healthcare-acquired MRSA (HA-MRSA)

MRSA byla poprvé objevena v 60. letech 20. století, ale její problematika vzrostla až v 90. letech téhož století, a to zejména na jednotkách intenzivní péče, kde se stala jednou z hlavních příčin nosokomiálních infekcí. Nemocniční kmen (HA-MRSA) nese

na svém genomu stafylokokovou chromozomální kazetu (SCC*mec* I-III), kde se nachází geny rezistence (SCC*mec* typ I) nebo multirezistence (SCC*mec* typ II-III) k antibiotikům *(Gonzalez a kol., 2006)*. Je zajímavé, že při vyjmutí z prostředí zdravotnických zařízení způsobuje HA-MRSA onemocnění jen zřídka. V důsledku toho bylo stanoveno, že HA-MRSA je kmen, který může přežívat jen v prostředí vystaveném působení antibiotik. Pro správný úhel pohledu tohoto hlediska vykazuje HA-MRSA delší generační dobu pro srovnání s meticilin-citlivým *S. aureus* (MSSA) *(Deurenberg a kol., 2008)*.

3.1.4.4 Community associated MRSA (CA-MRSA)

CA-MRSA je definován jako MRSA přítomen u lidí, kteří nepodstoupili v průběhu roku rizikové faktory jako je hospitalizace nebo chirurgický zákrok, permanentní katetr, dialýza či dlouhodobý pobyt v pečovatelském zařízení. Předešlé výzkumy prokázaly rozdíly v demografii pacienta a byly porovnány s HA-MRSA izolované od pacientů z pečovatelských zařízení *(Fraser a kol., 2008)*. Pacienti s CA-MRSA jsou obvykle mladší než pacienti s HA-MRSA. U CA-MRSA izolátů bylo prokázáno, že jsou citlivější na antibiotika bez β-laktamového původu a fylogenetické testování poukazuje na zřetelné rozdíly v genomu těchto bakterií. Spektrum působení této bakterie je soustředěno na kůži a měkké tkáně jako jsou abscesy. CA-MRSA může také způsobovat lišej, folikulitidu nebo furunkulózu a ve vzácných případech může způsobit invazivní infekce, jako jsou společné infekce, nekrotizující zápal plic a sepse *(DeLeo, Otto, Kreiswirtha Chambers, 2010)*.

3.2 Rezistence u *S. aureus*

Výskyt stále více druhů bakterií odolných vůči antibakteriálním látkám pramení z mnoha faktorů, které zahrnuje rozsáhlé a někdy nevhodné používání antimikrobiálních látek, rozsáhlé užívání těchto látek jako stimulátorů růstu v krmivu pro zvířata a nárůst mezinárodního cestovního ruchu. Problematika rezistence je nejvýznamnější u G^+ stafylokoků, pneumokoků a enterokoků *(Stewarta Costerton, 2001)*. Kmeny bakterií *S. aureus* vzhledem k užívání antibiotik vyvinuly rezistenci vůči penicilinu, cefalosporinu, meticilinu, vancomycinu a linezolidu *(Bingen a kol., 2006; Bourgeois-Nicolaos a kol., 2006)*. Mortalita bakterémie způsobené *S. aureus* je přibližně 10 – 30 % bez ohledu na

dostupnost antibiotik *(van Hal a kol., 2012)*. Vývoj nových antibakteriálních komponent inhibujících růst rezistentních bakterií je novodobým trendem, který se dostává rychle na trh a pokrývá tak velmi žádanou poptávku této skupiny léčiv. Při testování antibakteriálních vlastností látek se velmi osvědčily nanočástice, konkrétně nanočástice kovů. Stříbrnými nanočásticemi jsou ošetřeny plochy a obvazy v lékařství a tyto nanočástice si získaly zaslouženou popularitu a využití *(Ansari a kol., 2015)*. Selenové nanočástice prokázaly efektivní účinek proti meticilin-rezistentní bakterii *S. aureus*, produkt je na trhu osvědčený a zajišťuje tak ošetření infekčních ran u domácích mazlíčků i hospodářských zvířat *(Chudobova a kol., 2014; Cihalova a kol., 2015)*. Stejně jako u antibiotik, tak i u antibakteriálních nanočástic může vzniknout bakteriální rezistence právě proti těmto komponentům.
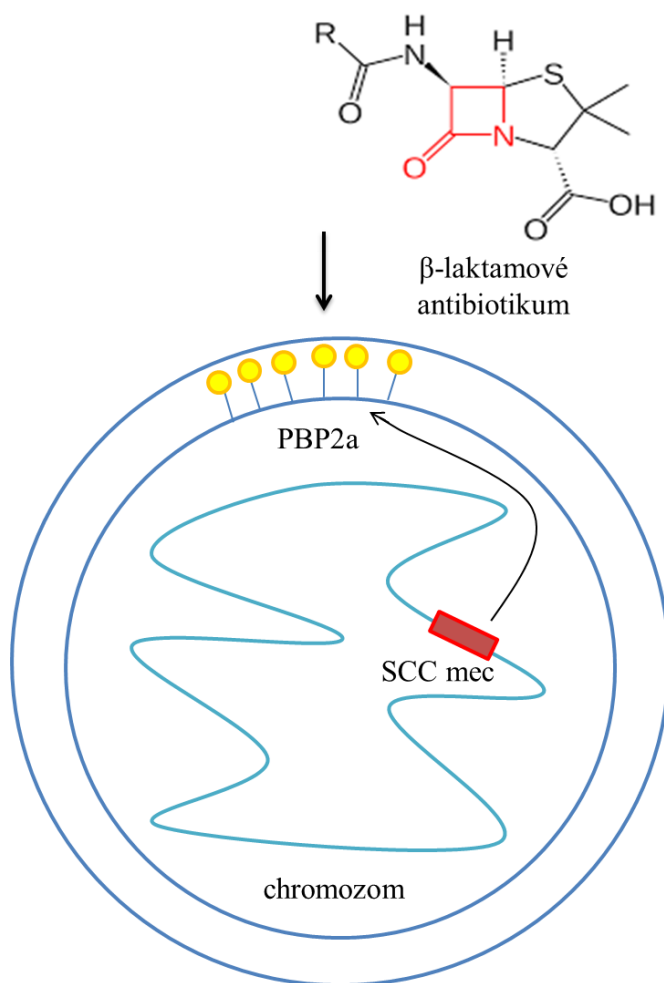
3.2.1 Vznik rezistence *S. aureus* na antibiotika

Ironií trendu vzniku stále více rezistentních bakterií je období výrazně lepšího pochopení molekulárních mechanismů bakteriální rezistence, což vede k inovaci a vývoji nových léčiv a terapeutických činidel. Rezistence na antibiotika může být buď přirozená, což je vrozená necitlivost bakterie k antibiotiku nebo získaná, která vzniká fenotypickou adaptací nebo genetickými změnami. Získaná rezistence bakterií vůči antibiotikům vzniká nejčastěji horizontálním přenosem genetické informace a modifikací genu na chromozomu *(Gill a kol., 2005; Deurenberga Stobberingh, 2008; Chambers a kol., 2009)*.

3.2.2 Mechanismus účinku β-laktamových antibiotik na *S. aureus*

β-laktamová antibiotika jsou širokou třídou antibiotik, zahrnující všechna antibiotika, která obsahují β-laktamový kruh ve své molekulární struktuře. To zahrnuje penicilin a jeho deriváty, cefalosporiny, monobaktamy a karbapenemy. β-laktamová antibiotika jsou baktericidní a inhibicí syntézy peptidoglykanové vrstvy zabraňují tvorbě buněčné stěny *(Giesbrecht a kol., 1998)*. Peptidoglykanová vrstva je u G^+ bakterií důležitá k zajištění strukturální integrity. β-laktamové jádro molekuly antibiotika nezvratně váže zbytek aktivního místa penicilin vázajícího proteinu 2a (penicillin binding protein

PBP2a) (Obr. 1). PBP2a je transpeptidáza, která je nezbytná pro ukončení syntézy peptidoglykanového řetězce *(Zapun a kol., 2008)*. Ireverzibilní inhibice PBP2a zapříčiněná působením β-laktamových antibiotik brání konečnému zesítění peptidoglykanové vrstvy a tak dojde k přerušení syntézy buněčné stěny. β-laktamová antibiotika inhibují mimo bakterie i sinice a funkci fotosyntetických organel eukaryotních buněk *(Katayama a kol., 2003; Kohanski a kol., 2010)*.

Obr. 1: Mechanismus rezistence MRSA na β-laktamová antibiotika. Na stafylokokové chromozomální kazetě mec se nachází *mecA* gen kódující syntézu penicillin-binding proteinu 2a (PBP2a). PBP2a katalyzuje syntézu buněčné stěny a produkcí β-laktamázy dochází k rozkladu β-laktamového kruhu antibiotika. Přítomnost β-laktamových antibiotik inhibuje funkci transpeptidáz, mezi níž se řadí i PBP2a, buňka tak ztrácí

schopnost vytvářet buněčnou stěnu a umírá. PBP2a však vykazuje vůči β-laktamovým antibiotikům nízkou afinitu, proto jejich inhibici nepodléhá.

3.2.3 MRSA

Před více než padesáti lety vedl objev antibiotik k revoluci v léčbě bakteriálních infekcí. Vzápětí se díky nadměrnému používání těchto medikamentů u mnoha bakterií objevily rezistentní kmeny. V poslední době jsou významným problémem např. kmeny *S. aureus* rezistentní k meticilinu, které mají hlavní podíl na šíření nemocničních infekcí. Determinanty rezistence k antibiotikům a jiným baktericidním látkám se u stafylokoků vyskytují na variabilních genetických elementech jako genomové ostrovy patogenity, plazmidy, transpozony aj. Reorganizace bakteriálního genomu způsobená těmito elementy umožňuje vznik a šíření nových rezistentních variant *(Ito, Okuma, Ma, Yuzawaa Hiramatsu, 2003; Fridkin a kol., 2005).*

3.2.3.1 *Stafylokoková chromozomová kazeta mec*

Stafylokoková chromozomová kazeta mec (SCCmec, z angl. staphylococcal chromosome cassette methicillin-resistance island) je fragment DNA dlouhý 21 - 67 kb, který je začleněn do bakteriálního chromozomu poblíž místa počátku replikace *(Ito a kol., 2001).* To je velmi výhodné, protože místo replikace se na chromozomu nachází 2 - 4 krát. Integrací SCCmec do genomu *Staphylococcus aureus* vzniká meticilin-rezistentní kmen (MRSA) odolný vůči téměř všem β-laktamovým antibiotikům *(Ito, Katayama, Asada, Mori, Tsutsumimoto, Tiensasitorna Hiramatsu, 2001).*

3.2.3.2 *Mechanismus rezistence k meticilinu*

Rezistence k meticilinu je dána přítomností penicilin-vázajícího proteinu 2a (PBP2a) a enzymu β-laktamázy, která štěpí β-laktamová antibiotika (antibiotika na bázi penicilinu) a je kódována genem *mecA*. PBP2a je analogem transpeptidáz PBP, jejichž přítomnost je pro normální buňku nepostradatelná, neboť hrají důležitou roli při syntéze buněčné stěny. Přítomnost β-laktamových antibiotik jejich funkci inhibuje, buňka tak

ztrácí schopnost vytvářet buněčnou stěnu a umírá. PBP2a však vykazuje vůči β-laktamovým antibiotikům nízkou afinitu, proto jejich inhibici nepodléhá *(Brakstad a kol., 1997; Hiramatsu a kol., 2001)*.

Exprese genu *mecA* je regulována dvěma základními systémy. Indukčně-represní systém *blaI-blaR1* je lokalizován na plazmidu. Protein BlaI (produkt genu *blaI*) má funkci represoru. Váže se na operátor genu *blaZ* nebo *mecA*, čímž inhibuje jejich transkripci. Gen *blaR1* kóduje transmembránový protein BlaR1, jehož součástí je extracelulární doména vážící penicilin a intracelulární signální sekvence. Navázáním β-laktamového antibiotika na BlaR1 dojde ke spuštění signálu, jehož konečným projevem je uvolnění BlaI represoru z operátoru *blaZ* nebo *mecA*, následná transkripce těchto genů a syntéza β-laktamázy nebo PBP2a. Regulační systém *mecI-mecR1* je lokalizován na bakteriálním chromozomu. Jeho funkce je analogická funkci *blaI-blaR1 (Brakstada Maeland, 1997)*.

3.2.4 Vankomycin-rezistentní *S. aureus*

Vzhledem k výskytu kmenů rezistentních na antibiotika a nedávným vznikem klinických izolátů rezistentních na vankomycin (77), je kontrola *S. aureus* stále obtížnější. *Staphylococcus* hraje hlavní roli v nosokomiálních infekcích a v poslední době byl uznán jako důležitá příčina infekce získané v komunitě (11, 35, 40, 50). Citlivost *S. aureus* vůči vankomycinu je rozdělena do tří tříd: i) vancomycin-intermediate *S. aureus* (VISA), ii) heterogenní VISA (hVISA), iii) vyšší úroveň rezistence vancomycin-resistant *S. aureus* (VRSA) *(Appelbaum, 2007)*.

VISA byl poprvé identifikován v Japonsku v roce 1996 a od té doby byl nalézán v nemocnicích po celém světě. Byl také nazýván GISA (glycopeptide-intermediate *S. aureus*), což poukazuje na odolnost vůči glykopeptidovým antibiotikům *(Hiramatsu a kol., 1997)*. Vankomycin-rezistentní kmeny *S. aureus* se vyskytovaly velmi vzácně a roku 1992 bylo prokázáno, že geny rezistence vůči vankomycinu z bakterie *Enterociccus faecalis* mohly být přeneseny do *S. aureus*. Přítomnost genu rezistence *vanA* u *Enterococcus faecalis* byla potvrzena i u *S. aureus* pomocí polymerázové řetězové reakce, a byla také potvrzena shodnost sekvence tohoto genu *(Courvalin, 2006)*.

3.3 Metody stanovení *S. aureus*

Kvalitativní a kvantitativní stanovení určitého druhu bakterie ve vzorku bylo a stále je prováděno pomocí kultivačních metod v tekutých či agarových živných půdách.

Avšak využití moderních technik vede k velmi rychlé identifikaci bakteriálních druhů v neznámém vzorku. Včasná a přesná identifikace bakterií v klinických materiálech je nutnou a nezbytnou fází při diagnostice, léčbě bakteriálních infekcí, navržení vhodných léčebných postupů a eliminaci šíření těchto infekcí. Pro stanovení *S. aureus* jsou vyvíjeny stále nové postupy, jejichž cílem je, aby byl proces stanovení rychlý, přesný a citlivý.

3.3.1   Kultivační metody

Co se týče kultivace, obecně jsou stafylokoky schopny tolerovat 5 - 15 % NaCl v prostředí, čehož se často v praxi využívá při jejich kultivaci na selektivních médiích obohacených o NaCl. Rostou v širokém rozmezí teplot, udává se rozpětí 18 - 40 °C, přičemž existují rozdíly mezi jednotlivými druhy. Schopnost růstu při dané teplotě je ovlivňována také původem izolovaného kmene. Konvenční identifikace mikroorganismů zahrnuje jejich kultivaci, která trvá 24 – 48 hodin *(Eriksen a kol., 1994)*.

3.3.1.1 *Kvalitativní kultivační metody*

Vzorky potravin, půd, biologické vzorky či jiné obsahují obvykle více druhů bakterií než jednu a to v různých poměrech, které jsou způsobeny parazitismem či symbiózou mezi bakteriálními druhy. Proto je důležité zástupce všech přítomných druhů bakterií neselektivně pomnožit tak, aby mohlo dojít ke kultivaci na selektivním agaru i jedné bakterie přítomné v původním vzorku, konfirmaci a tím k identifikaci. Bakterie vzorku jsou obvykle pomnoženy v neselektivním tekutém živném médiu, které se skládá z trypton-sojového nebo masopeptonového bujónu *(Tanase a kol., 2013)*. Dalším krokem je izolace cílového mikroorganismu z pomnožovacího média na ztužené médium. Po obvykle 18 - 24 hodinové inkubaci vzorku bakterií v tekutém médiu je

pomnožená kultura vyočkovaná na selektivně diagnostickou agarovou živnou půdu frakcionovaně roztěrem pomocí kličky *(Chen a kol.)*.

Stafylokoky jsou selektivně kultivovány nejčastěji na **Baird-Parker agaru**. Baird-Parker agar (BP agar) obsahuje trypton, hovězí a kvasniční extrakt jako zdroj uhlíku a dusíku nezbytný pro růst bakterií, glycin, chlorid litný a telluričitan draselný působící jako selektivní činidla, vaječný žloutek jako substrát pro detekci produkce lecitinázy a lipázy. Morfologické vlastnosti kolonií *S. aureus* na BP agaru jsou tmavě šedé až černé kolonie, což je způsobeno redukcí telluričitanu. Stafylokoky produkující lecitinázu rozkládají vaječný žloutek, což vede k vyčeření zóny kolem kolonií. Typické kolonie *S. aureus* jsou černé nebo šedé, lesklé a vypouklé, 1 - 5 mm velké a jsou obklopeny zónou projasnění, která může být zčásti matná, po nejméně 24 hodinové inkubaci se může v těsné blízkosti kolonií objevit opalescentní prstenec a po 48 hodinách se objevují průsvitné kruhy uvnitř čirých zón. *S. epidermis* tvoří na BP agaru černé, lesklé, nepravidelné kolonie s průsvitnými kruhy již po 24 hodinách inkubace. Mikrokoky rostou na BP agaru jen zřídka a jejich kolonie jsou velmi malé, hnědé až černé bez čirých zón. Kvasinky jsou na BP agaru bílé bez čirých zón *(Baird a kol., 1995; Acco a kol., 2003)*.

Optimální podmínky pro kultivaci *S. aureus* je 37 °C, za přístupu kyslíku.

Dalším selektivně diagnostickým agarem pro kultivaci *S. aureus* je **solný agar s mannitolem**, který vysokým obsahem soli vyselektuje stafylokoky, které jsou halotolerantní. *S. aureus* fermentuje mannitol na rozdíl od ostatních stafylokoků, a proto žluté zbarvení agaru indikuje jeho přítomnost. Ostatní bakterie rostoucí na agaru nezmění jeho zbarvení, tudíž zůstává růžový *(Stoakes a kol., 2006; Han a kol., 2007)*.

Pro selekci stafylokoků ze vzorků se používá **krevní agar s chloridem sodným**. Pro selektivní pomnožení většinou biologických vzorků se používá čtyř různých živných půd. Vzorek je nanesen na krevní agar s 10 % obsahem NaCl sloužící pro selekci stafylokoků (Obr. 2), dále na krevní agar pro růst G^+ i G^- bakterií, pak Endův agar pro selekci G^- bakterií, mezi které patří koliformní bakterie a jako poslední je krevní agar s amikacinem, který slouží pro selekci streptokoků *(Eriksen, Espersen, Rosdahla Jensen, 1994; Brayshaw, 1999)*.

Obr. 2: Izolace *S. aureus* z infekční rány hospitalizovaného pacienta v Úrazové nemocnici v Brně, p.o. na krevním agaru s 10% obsahem NaCl, po 24 hodinové kultivaci při 37 °C.

Mezi kultivační metody patří také inkubace bakterií na **chromogenních médiích**, které obsahují látky podporující růst požadovaných bakterií a látky inhibující růst nestanovovaných bakterií. Média obsahují chromogenní substráty, které štěpí enzymy pouze určitých bakterií a při rozštěpení substrátu bakteriálním enzymem dojde k charakteristickému zabarvení. Chromogenní médium **CHROMagar Staph aureus** či **CHROMagar MRSA** má ve srovnání s tradičními médii velmi vysokou specifitu a senzitivitu pro detekci kmenů *S. aureus* či MRSA. Použitím této diferenciační půdy vypadávají další konfirmační testy jako je katalázový a latexový aglutinační test pro odlišení non-*S. aureus* kmenů. CHROMagar MRSA je jediné komerční médium umožňující spolehlivou detekci MRSA a jehož validně ověřená senzitivita a specifita je na úrovni 100 % *(Merlino a kol., 2000; Stoakes, Reyes, Daniel, Lennox, John, Lannigana Hussain, 2006).*

Stanovení přítomnosti MRSA či jiných rezistentních kmenů kultivačními metodami je možno provést ověřením **testu rezistence** na β-laktamová antibiotika *(Chambersa Deleo, 2009)* metodou inhibičních zón, kdy jsou na Petriho misku pokrytou čerstvou bakteriální kulturou kladeny difúzní disky obsahující β-laktamová antibiotika a po 24 hodinové inkubaci při 37 °C je sledován vznik inhibičních zón, které u rezistentních kmenů nejsou tvořeny *(Chudobova a kol., 2013).* Mezi komerční kultivační soupravy

můžeme zařadit **rehydrovatelné kultivační filmy** (např. Petrifilm), které jsou tvořeny plastickými filmy potaženými vysušeným kultivačním médiem a dehydratovaným gelovým činidlem rozpustným studenou vodou. Inokulum je naneseno do středu spodního filmu a film je následně inkubován za požadovaných podmínek, dle inkubované bakterie. Filmy slouží ke stanovení celkového počtu mikroorganismů a různých indikátorových mikroorganismů i některých patogenů *(Silva a kol., 2005)*.

Otiskové nosiče či kontaktní Petriho misky se používá pro vzorkování otiskem živného média na testovaný povrch, nebo ponořením nosiče do testované tekutiny. Spektrum vyšetření je obvykle omezeno na indikátorové skupiny mikroorganismů *(Moore a kol., 2007)*.

Automatizované metody jako je VITEK 2 nebo systém BD Phoenix jsou založené na fenotypové charakterizaci, které jsou závislé na expresi metabolické aktivity nebo na morfologických znacích *(Ieven a kol., 1995)*. V důsledku toho jsou izoláty nedostatečně identifikovány, a proto jsou nezbytné doplňkové konfirmační metody k přesné identifikaci *(Miller a kol., 1993)*.

3.3.1.2 Kvantitativní kultivační metody

Kvantifikace počtu bakterií ve vzorku je důležitá kvůli přípustným limitům stanovených legislativou například v potravinářství, ale i jako stanovení profilu vzorku půdy, vod, tkání či počtu bakterií na plochách.

Při očkování přelivem se obvykle používá 1 ml inokula, které bývá naředěné tak, aby nedošlo k přerostení Petriho misek koloniemi a následně přelité teplým avšak ne příliš horkým agarem. Počet kolonií pro kvantitativní analýzu bakterií na jednu Petriho misku se pohybuje v rozsahu 30 – 300 KTJ/ml pro celkový počet mikroorganismů a pro selektivně diagnostické živné půdy 15 – 150 KTJ/ml. Půdy pro stanovení počtu *S. aureus* ve vzorku jsou používány stejné jako u kvalitativních kultivačních metod. Výsledná hodnota je udávána v kolonie tvořících jednotkách na mililitr, gram či dm^2 (KTJ/ml, KTJ/g, KTJ/dm^2), dle stanovení v tekutém vzorku, pevném vzorku či plochy *(Schaeg a kol., 1979; Rodriguez a kol., 2005)*.

3.3.2 Konfirmační a identifikační testy *S. aureus*

Konfirmace je založena na pozitivní koagulázové reakci. Konfirmace náhodně vybraných kolonií ze selektivně-diagnostických agarů je prováděna přeočkováním kolonií na krevní agar, který je kultivován při 30 °C po dobu 24 hodin a je jím prokázána **hemolytická aktivita**, kdy může dojít k úplné β-hemolýze nebo neúplné α-hemolýze. Při neúplné hemolýze neboli viridaci dochází k částečnému rozrušení hemoglobinu na zelenohnědý methemoglobin a erytrocyty nejsou lyzovány. Při úplné hemolýze dochází k úplnému rozložení hemoglobinu i k lýze erytrocytů a kolem kolonie je vytvořena průhledná zóna *(Jones a kol., 2006)*.

Dále jako konfirmační test pro průkaz přítomnosti plazmakoagulázy je provedena inkubace s mozkosrdcovou infúzí při 37 °C, 24 hodin *(Knobloch a kol., 2002)*. **Zkumavkový koagulázový test** je standardní test pro rutinní identifikaci *S. aureus*, při kterém se pracuje s králičí plasmou a výsledky jsou odečítány po 4 a 24 hodinách inkubace. Nevýhodou je, že některé stafylokoky, jako jsou *S. schleiferi* a *S. intermedius*, mohou rovněž poskytovat pozitivní výsledky na přítomnost volné koagulázy. Výskyt těchto druhů není ovšem tak častý. Dále některé raritní kmeny *S. aureus* mohou vykazovat neschopnost srážet králičí plazmu. Tento typ testu je pro zmíněná negativa nahrazován latexovými aglutinačními testy *(Hidron a kol., 2008)*.

Pro **latexový aglutinační test** jsou výchozím materiálem kolonie z krevního agaru. Princip testu spočívá v produkci koagulázy, pomocí tzv. clumping factor, bakteriemi *S. aureus*, které obsahují na svém povrchu protein A. Na latexových částicích je navázán králičí imunoglobulin (IgG) a fibrinogen. Při reakci clumping factoru s finbrinogenem nebo proteinu A s IgG dojde k aglutinaci latexové suspenze. Přítomnost proteinu A a clumping factoru jsou indikátory důležité pro detekci *S. aureus* *(Louie a kol., 2000; Felten a kol., 2002)*.

3.3.3 Identifikace stafylokoků pomocí komerčních souprav STAPHYtest

Komerční souprava STAPHYtest je určena pro identifikaci druhů bakterií rodu *Staphylococcus*, která je rychlá, citlivá a jednoduchá pro použití. Historie STAPHYtestu sahá až do roku 1986, kdy byla vyvinuta první souprava pro identifikaci stafylokoků. Rozlišujeme dva typy těchto identifikačních testů a to STAPHYtest 16 a STAPHYtest

24. STAPHYtest 16 umožňuje provést identifikaci 60ti kmenů rodu *Staphylococcus* a dalších G$^+$ kataláza pozitivních koků pomocí šestnácti biochemických testů. Souprava STAPHYtest24 je určena primárně pro definitivní identifikaci druhů rodu *Staphylococcus* izolovaných z klinického materiálu a pro jejich diferenciaci od dalších G$^+$ kataláza pozitivních koků *(Ruzickova, 1994)*. Identifikaci lze dle doporučení vyhodnocovacího software doplnit testy VPtest nebo PYRAtest dodávanými ve formě diagnostických proužků *(Athanasopoulos a kol., 2007)*.

Voges-Proskauer test (VP test) je používán k detekci přítomnosti acetoinu v půdě s bakteriemi a je založen na trávení glukózy na acetylmethylkarbinol. Přidáním α-naftolu a KOH do Voges-Proskauer bujónu naočkovaným bakteriemi dochází při pozitivní reakci k zčervenání bujónu, zatímco žluto-hnědá indikuje negativní výsledek. Přítomnost *S. aureus* vykazuje spolu s dalšími bakteriemi (r. *Enterobacter*, r. *Klebsiella*, *Serratia marcescens*, *Hafnia alvei*) pozitivní reakci VP testu. Naopak negativní reakci projevují *Citrobacter* sp., r. *Shigella*, r. *Yersinia*, r. *Salmonella (Athanasopoulos, Devogel, Beken, Pille, Bemiera Gavage, 2007; Chanchaithong a kol., 2011)*.

Test aktivity enzymu pyrrolidonyl arylamidázy (PYRA test) je založen na hydrolýze β-naftylamidu kyseliny pyroglutamové, který je obsažený v detekčním proužku. Hydrolýza je detekována reakcí s p-dimetylaminocinamaldehydem, který je obsažen v roztoku činidla, za vzniku červeného zbarvení *(Chow a kol., 2014)*.

3.3.4 Imunochemické metody detekce *S. aureus*

Imunochemické metody detekce bakterií jsou založeny na interakci protilátky s antigenem za využití monoklonálních či polyklonálních protilátek. Imunochemické metody jsou rychlé, vysoce specifické a mohou být využity při detekci v komplexní matrici. Nevýhodou je obtížná příprava specifických protilátek. Mezi imunochemické metody patří **ELISA** (Enzyme Linked Immuno Sorbent Assay), při které reaguje antigen s protilátkou na pevné fázi a metoda poskytuje informaci i o koncentraci. Další používanou metodou pro detekci bakterií je **LFIA** (Lateral Flow Immuno Assay), která je kvalitativní a testuje se pomocí testovacích proužků. Přítomnost *S. aureus* bývá imunochemicky testována podle produkovaného enterotoxinu *(Peruski a kol., 2002)*, který je produkován bakterií *S. aureus*. Dále pro stanovení *S. aureus* bývá využíván protein A *(Kessler, 1975)*, což je antigen na povrchu buněčné stěny stafylokoků a

streptokoků *(Frasera Proft, 2008)*. Mezi další specifické antigeny pro *S. aureus* patří fibronectin binding protein *(Foster a kol., 1998)* a pro stanovení MRSA to může být plasmin-sensitive surface protein *(Hilden a kol., 1996)*.

3.3.5 Molekulárně-biologické metody stanovení *S. aureus*

Pro molekulárně-biologickou detekci *S. aureus* je nezbytná znalost genomu této bakterie, a to nalezením specifické části DNA odlišné od ostatních bakterií. Molekulárně-biologickými metodami lze provádět jak kvalitativní tak i kvantitativní stanovení.

Tyto metody jsou obvykle založeny na **polymerázové řetězové reakci (PCR)**. Molekulárně-biologická diagnostika je přímá metoda identifikace bakterií využívající komplementarity vláken nukleových kyselin a je založena na procesu jejich hybridizace. Pro zvýšení citlivosti a specifity stanovení vybraného druhu bakterie je využívána PCR, během které dochází k amplifikaci fragmentu specifického genu *(Grisold a kol., 2002)*. Metoda je nezávislá na bakteriální kultivaci, vysoce citlivá s rychlou detekcí. Před samotným stanovením je potřeba provést lýzu bakteriálních buněk, extrakci a purifikaci nukleové kyseliny a její charakterizaci. Izolace nukleových kyselin může být prováděna fenol-chloroformovou extrakcí, adsorpcí na silikátovou kolonku, anebo automatizovanými metodami využívajícími magnetické částice pokryté specifickými materiály vázajícími nukleové kyseliny jako například MagNA Pure Compact RNA Isolation Kit (Roche, Basel, Switzerland). Takto připravený vzorek DNA je s komplementárními primery pro hledaný gen umístěn do thermocycleru spolu s Taq polymerázou, kde dojde k amplifikaci DNA polymerázovou řetězovou reakcí. Po amplifikaci hledaného genu je PCR produkt vizualizován pomocí gelové elektroforézy a dle přítomnosti správné velikosti tzv. bandu je stanovena přítomnost hledaného kmene ve vzorku *(Cihalova, Chudobova, Michalek, Moulick, Guran, Kopel, Adama Kizek, 2015; Chudobova a kol., 2015)*.

S. aureus je stanovován molekulárně-biologickými metodami pomocí ***nuc* genu**, který kóduje produkci extracelulární termostabilní nukleázu (TNáza) degradující DNA a RNA, jejíž enzymatická aktivita odolává 100 °C po dobu působení nejméně 1 hodinu *(Tang a kol., 2011)*. Pomocí sekvence genu *nuc* je *S. aureus* běžně identifikován, ovšem

TNáza není pro něj specifická. TNáza má pro *S. aureus* specifickou sekvenci aminokyselin, a proto byly vyvinuty protilátky pro imunochemickou detekci *S. aureus* pomocí TNázy *(Brakstad a kol., 1992)*.

Dalším potenciálním markerem pro detekci *S. aureus* je **fnbA gen**. Gen *fnbA* kóduje produkci fibronektin vázajícího proteinu A *(Peacock a kol., 2002)*, který rozpoznává přítomnost fibronektinu a fibrinogenu. Povrchová exprese fibronektin vázajícího proteinu je u *S. aureus* virulentním faktorem *(Wann a kol., 2000)*, který umožňuje kolonizovat hostitelské tkáně a měnit infekční proces *(Ghodousi a kol., 2012)*.

Při stanovení přítomnosti rezistentních kmenů stafylokoků je stanovován gen exprimující protein vyvazující či jinak bránící prostupu antibiotik přes buněčnou stěnu dále do buňky. Stanovení MRSA ve vzorku je prováděno kontrolou přítomnosti **mecA genu** *(van Griethuysen a kol., 1999)*. Gen *mecA* kóduje syntézu transpeptidázy PBP2a, která není inhibována meticilinem, a proto není narušena syntéza buněčné stěny bakterie během působení beta-laktamových antibiotik *(Hao a kol., 2012)*.

Molekulárně-biologicky je možné provést i kvantitativní stanovení bakterií ve vzorku. K tomu slouží **real-time PCR** *(Hein a kol., 2001)*. Princip je stejný jako u klasické PCR, ale metoda navíc umožňuje kvantifikaci sledovaného fragmentu DNA v reálném čase. Při real-time PCR je zaznamenáván každý cyklus PCR ve skutečném čase, zatímco u klasické PCR je analyzován až výsledný produkt. Během amplifikace vzniká fluorescenční signál. Koncentrace izolované DNA je odečtena z hodnoty prahového cyklu, kdy lze detekovat intenzitu fluorescence anebo pomocí kalibrační křivky připravené ze standardních roztoků *(Ludwig a kol., 2000; Elsayed a kol., 2003; Fusco a kol., 2011)*.

Další molekulárně-biologické metody využívají také specifických fragmentů DNA a k nim komplementární oligonukleotidy značené tzv. sondou. Tato metoda se nazývá **fluorescenční *in situ* hybridizace (FISH)** *(Gey a kol., 2013)*. FISH je cytogenetická technika využívající fluorescenčních sond, na které se vážou části DNA s vysokou komplementaritou. Jedná se o RNA sondy, které mohou být navrženy pro jakýkoliv gen nebo jakékoliv sekvence genu. Technika FISH umožňuje analýzu velkých sérií vzorků se snazší identifikací *(Hogardt a kol., 2000; Kempf a kol., 2000)*.

Ve studii Wu et al. (2012) byla právě porovnávána specifita a citlivost metod FISH a PCR. Stanovení přítomnosti bakterie *S. aureus* bylo založeno na detekci 16S rRNA, která je vysoce konzervativní a obsahuje mnoho variabilních oblastí. Byly vytvořeny

primery cílené na různé fylogenetické úrovně bez předešlé kultivace. Obě metody (PCR a FISH) splňují požadavky pro detekci *S. aureus* a nabízí přesnější výsledky za rychlejší dobu než kultivační metody. S ohledem na náklady bylo vykalkulováno, že FISH je výhodnější pro testování menšího počtu vzorků, zatímco PCR je vodná pro testování velkého počtu vzorků *(Wu a kol., 2012).*

Metody využívající PCR patří k základním technikám stanovení bakterií molekulárně-biologickými metodami. Pro podrobnější charakteristiku jednotlivých bakterií jsou využívány **genotypizační metody**. Genotypizační metody jsou založeny na štěpení DNA restrikčními endonukleázami s následnou PCR amplifikací získaných fragmentů, na amplifikaci úseků ohraničených repetitivními sekvencemi nebo na amplifikaci fragmentů náhodnými oligonukleotidy. Tato metoda je hojně využívaná pro detekci rezistentních kmenů *S. aureus*, jako je MRSA *(Predari a kol., 1991; Ghaznavi-Rad a kol., 2010; Chong a kol., 2015).*

Analýza amplifikovaných fragmentů, produktů PCR, je vyhodnocena separační technikou pulzní gelovou elektroforézou či inverzní gelovou elektroforézou, kdy dojde k separaci fragmentů a vizualizace je provedena fluorescenčně.

3.3.6 Genové sekvenování

Pomocí genetických metod lze spolehlivě identifikovat mikroorganismy stanovením nukleotidové sekvence jejich genu kódujícího 16S podjednotku ribozomální RNA (16S rRNA). 16S rRNA obsahuje oblasti velmi konzervované mezi všemi mikroorganismy, stejně tak, jako jsou oblasti variabilní pro každý bakteriální druh. 16S rRNA sekvence určuje příbuznost studovaných bakterií a používá se tak k vytváření fylogenetických stromů.

Na základě genového sekvenování 16S rRNA byly stafylokoky rozděleny do 11 skupin. Díky této metodě lze klasifikovat nové druhy stafylokoků a tím také dochází k novému fylogenetickému členění *(Haas a kol., 2011; Chudobova a kol., 2015).*

3.3.7 Detekce bakterií pomocí hmotnostní spektrometrie MALDI-TOF

Hmotnostní spektrometrie nabízí přesnou a rychlou identifikaci bakterií, plísní a mykobakterií izolovaných z klinických vzorků *(Stevenson a kol., 2010).* Postupy pro

zpracování organismů a jejich analýzu pomocí hmotnostní spektrometrie jsou technicky jednoduché, reprodukovatelné, komerční databáze a interpretační algoritmy jsou k dispozici pro identifikaci širokého spektra klinicky významných organismů využívající ionizaci laserem za přítomnosti matrice (MALDI, matrix assisted laser desorption/ionization) v kombinaci s detektorem doby letu (TOF, time-of-flight). Metoda se využívá pro identifikaci a typizaci nebo pro určení rezistence stanovovaných kmenů *(Wolters a kol., 2011; Wieser a kol., 2012)*.

S. aureus může být detekován hmotnostní spektrometrií na základě identifikace konzervativních proteinů. Specifický protein pro MRSA je PBP2a zajišťující rezistenci vůči beta-laktamovým antibiotikům, nebo toxiny produkující *S. aureus* jako je enterotoxin A, delta-toxin *(Gagnaire a kol., 2012)*, Panton-Valentine leukocidin *(Bittar a kol., 2009)*, TSST-1 (toxic shock syndrome toxin), hemolyziny *(Dinges a kol., 2000)* aj.

3.3.8 Izolace bakterií pomocí paramagnetických částic

Separační technologie jsou jednou z nejsložitějších ale velmi důležitých oblastí biotechnologie. Separační techniky jsou nákladově efektivní a jsou klíčovým faktorem při průmyslové biotechnologické výrobě či rutinních molekulárně-biologických diagnostických postupech. Magnetické mikro či nanočástice jsou využívány v široké škále vědních disciplín, protože jsou snadno manipulovatelné pomocí externího magnetického pole a manipulace s nimi je rychlá a jednoduchá *(Nejdl a kol., 2014)*. Často jsou používány s bioafinitními ligandy jako jsou protilátky či proteiny s vysokou afinitou k cílové molekule *(Chudobova, Cihalova, Skalickova, Zitka, Rodrigo, Milosavljevic, Hynek, Kopel, Vesely, Adama Kizek, 2015)*.

Stejně tak, jako funguje izolace DNA pomocí paramagnetických částic, lze izolovat i bakterie magnetickou separací. Kombinace běžně využívaných imunochemických či molekulárně-biologických technik a magnetické separace je výhodná pro vznik rychlé selektivní metody ke stanovení hledané bakterie. Jednou z takových kombinací je imunomagnetická separace, která zajišťuje selektivní vychytání cílových bakterií pomocí specifické protilátky navázané na magnetickou částici. Protilátka zachytí skupinu bakterií disponující specifickým antigenem na svém povrchu, dochází tak
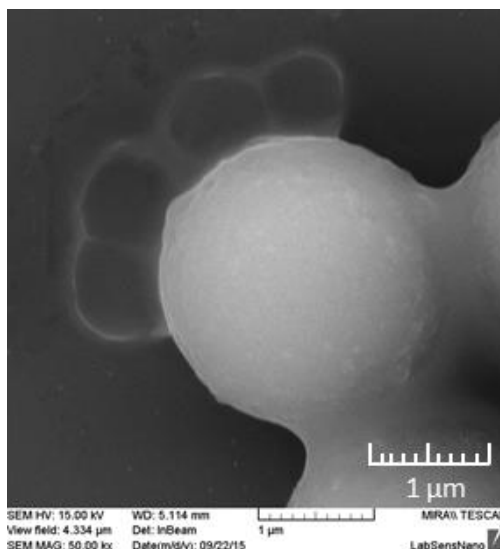
k selekci skupiny bakterií. Stanovení druhu, serotypu či určení druhu rezistence může následně proběhnout pomocí PCR či hmotnostní spektrometrie. Pro stanovení mohou být cílové bakterie, viry, eukaryotické buňky, proteiny a DNA či RNA *(Kolbert a kol., 1995; Krizkova a kol., 2015).*

3.3.8.1 *Magnetické částice používané pro imunomagnetickou separaci*

Magnetické částice pro bioseparaci obsahují jedno nebo více magnetických jader potahovaných matricí z polymerů, oxidu křemičitého nebo hydroxylapatitu s koncovými funkčními skupinami *(Tartaj a kol., 2003).* Velmi často jsou používané magnetické částice Dynabeads produkce Sigma-Aldrich (Sigma-Aldrich, St. Louis, MO, USA) (Obr. 3).

Magnetické jádro se obvykle skládá buď z magnetitu (Fe_3O_4), nebo maghemitu (γ-Fe_2O_3) se superparamagnetickými nebo feromagnetickými vlastnostmi *(Brem a kol., 2006).* Pro separaci DNA/RNA se doporučují feromagnetické částice vzhledem k silnějším magnetickým vlastnostem *(Choi a kol., 2007).*

Molekuly pro funkcionalizaci povrchu částic jsou vybírány podle požadovaných funkčních skupin. Funkcionalizace částic je často prováděna streptavidinem nesoucím silnou afinitu k biotinu, který je vázaný na protilátce, kterou bude magnetická částice modifikována pro použití k imunomagnetické separaci *(McCloskey a kol., 2003).*

Obr. 3: Komerční magnetické částice Dynabeads® M-280 Streptavidin (Sigma-Aldrich, St. Louis, MO, USA) se zachycenou bakterií MRSA na svém povrchu.

3.4 Moderní vývoj komponent s antibakteriálním účinkem

V prostředí vyžadujícím sterilitu, jako jsou operační sály či zařízení, kde dochází k ošetření otevřených ran, je nezbytné používat k ošetření prostředí, ale i pacienta baktericidní anorganické i organické látky, jako jsou chemoterapeutika, antibiotika či různé dezinfekce. Hojné používání dekontaminačních prostředků má za následek vznik bakteriální multirezistence *(Tran a kol., 2002)*. Ve výzkumu je věnována pozornost bakteriální rezistence a řešení nabízí ionty kovů nebo jejich komplexy, jejichž antibakteriální vlastnosti jsou známy již po staletí. V posledních letech však nalezly uplatnění nanotechnologie, co se týče antibakteriálního účinku zejména nanočástice stříbra, oxidu zinečnatého, ale i nanočástice selenu *(Dutta a kol., 2014)*. Nanočástice stříbra jsou v praxi prozatím nejvíce uplatňovány, jelikož vykazují antibakteriální, antivirové a antimykotické účinky *(Rai a kol., 2014)*, to platí i pro Au nanočástice *(Ahmed a kol., 2014)*, TiO$_2$ nanočástice *(Kummer a kol., 2013)*, nebo směs Ag/ZnO nanočástic *(Mirershadi a kol., 2013)*. Srovnáním účinku nanočástic stříbra a selenu došlo k překvapivému závěru, že nanočástice selenu inhibují bakterie *S. aureus* výraznějším způsobem, než nanočástice stříbra *(Chudobova, Cihalova, Dostalova,*

38

Ruttkay-Nedecky, Rodrigo, Tmejova, Kopel, Nejdl, Kudr, Gumulec, Krizkova, Kynicky, Kizeka Adam, 2014). Vliv selenových nanočástic byl také potvrzen v další studii *(Tran a kol., 2013).* Testováním β-laktamových antibiotik, které nemají účinek na MRSA bylo potvrzeno, že v případě vzniku komplexu těchto antibiotik se selenovými nanočásticemi dochází k výrazné inhibici MRSA a ještě výraznější inhibici u *S. aureus (Cihalova, Chudobova, Michalek, Moulick, Guran, Kopel, Adama Kizek, 2015).*

Jak je vidět, nanotechnologie mají velký význam nejen v elektronice, genovém inženýrství, ale i jako léčiva s efektem inhibice nežádoucích bakterií. S neustálým vývojem bakteriální rezistence je vznik antibakteriálních komponent každodenní výzvou pro vědce zabývajících se mikrobiologickou rezistencí.

4 MATERIÁL A METODIKA

4.1 Chemikálie

Všechny chemikálie (v ACS čistotě) byly pořízeny od firmy Sigma-Aldrich (USA), pokud není uvedeno jinak.

4.2 Metody

4.2.1 Kultivace *S. aureus* a MRSA

S. aureus (NCTC 8511) a meticilin-rezistentní *S. aureus* (O. Melter 2/A8) byly získány z České sbírky mikroorganismů, Přírodovědecké fakulty Masarykovy univerzity, Brno, Česká republika. Kmeny byly uchovávány jako suspenze spor v 20% (*v/v*) glycerolu při teplotě -20 °C. Před jejich použitím byly kmeny rozmrazeny a glycerol byl odstraněn promytím destilovanou vodou. Složení Luria Bertani média pro kultivaci bakteriální kultury bylo následující: trypton 10 g/l, kvasničný extrakt 5 g/l, NaCl 5 g/l, sterilní MiliQ voda. pH kultivačního média bylo před sterilizací upraveno na 7,4. Sterilizace média byla prováděna při teplotě 121 °C po dobu 30 minut ve sterilizátoru (Tuttnauer 2450EL, Izrael). Připravená kultivační média byla naočkována bakteriální kulturou v Erlenmeyerově baňce do celkového objemu 25 ml. Po inokulaci byly bakteriální kultury kultivovány po dobu 24 hodin na třepačce (Biosan OS-10, Litva) při 600 rpm a teplotě 37 °C. Bakteriální kultura kultivovaná za těchto podmínek byla následně ředěna kultivačním médiem na OD600 = 0,1 pro použití v dalších experimentech *(Cihalova, Chudobova, Michalek, Moulick, Guran, Kopel, Adama Kizek, 2015).*

4.2.2 Identifikace bakterií pomocí MALDI-TOF hmotnostní spektrometrie

Každá specifická kolonie kultivovaná na krevních agarech byla resuspendovaná v 300 µl deionizované vody. Poté bylo ke vzorku přidáno 900 µl etanolu. Po centrifugaci při 14000 × g po dobu 2 minut byl opět supernatant odstraněn a pelet byl sušen na vzduchu. Vysušený pelet byl rozpuštěn v 70% kyselině mravenčí (*v/v*) a 25 µl acetonitrilu a promísen. Vzorky byly centrifugovány opět při 14000 × g po dobu 2 minut a 1 µl čirého supernatantu byl nanesen na MALDI destičku (MTP 384 destička z leštěné oceli) a vysušen na vzduchu při laboratorní teplotě. Každý spot byl následně

překryt 1 µl matrice α-kyano-4-hydroxyskořicové kyseliny nasycené organickým rozpouštědlem (50% acetonitril a 2,5% kyselina trifluoroctová, obě *v/v*) a zcela vysušen na vzduchu k provedení MALDI-TOF MS analýzy (MALDI-TOF MS, Bruker Daltonics, Brémy, Německo). Spektra byla měřena v rozsahu m/z 2000 Da až 20000 Da a každé spektrum byl výsledek akumulace 1000 laserových pulsů získaných z deseti různých oblastí téhož vzorku. Spektra byla analyzována pomocí softwaru Flex (verze 3.4). Spektra byla vložena do MALDI BioTyper^{TM} 3.1 (Bruker Daltonik GmbH, Brémy, Německo), kde byla následně porovnána s existující databází *(Chudobova, Cihalova, Guran, Dostalova, Smerkova, Vesely, Gumulec, Masarik, Heger, Adama Kizek , 2015).*

4.2.3   Příprava magnetických částic

Magnetické částice byly připraveny rozpuštěním 1,5 g Fe(NO$_3$)$_3$ .9H$_2$O v 80 ml vody a 0,2 g NaBH$_4$ v 3,5 % NH$_3$ (10 ml) byl přidán a následně zahříván při 100 °C po dobu 2 hodin. Po zchlazení byl produkt ponechán v klidu přes noc a pomocí magnetu byly částice promyty. Vzniklý maghemit byl dále modifikován polyetylenglykolem (4 kDa) pro snadnou modifikaci streptavidinem a protilátkami imunoglobulinu G stálým mícháním přes noc. Po promytí byly modifikované částice zahřívány na 40 °C *(Nejdl, Kudr, Cihalova, Chudobova, Zurek, Zalud, Kopecny, Burian, Ruttkay-Nedecky, Krizkova, Konecna, Hynek, Kopel, Prasek, Adama Kizek , 2014).*

4.2.4   Genová exprese

4.2.4.1 Izolace RNA

Bakteriální kultury *S. aureus* a MRSA byly centrifugovány při 6000 × g při 20 °C po dobu 10 minut. K peletům bylo přidáno 100 µl fosfátového pufru (10 mM, pH 7), 100 µl lyzačního roztoku (6 M guanidin hydrochlorid a 0,1 M octan sodný) a 0,1 µl inhibitoru RNáz. Izolace RNA byla provedena pomocí MagNA Pure Compact (Roche, Německo), Nucleic Acid Isolation Kit I dle protokolu pro RNA bakterie v souladu s pokyny výrobce (Roche, Německo).

4.2.4.2 Reverzní transkripce a amplifikace cDNA mecA genu

mRNA byla převedena na cDNA za použití Transcriptor First Strand cDNA Synthesis Kit (Roche, Basel, Switzerland) s náhodnými hexamery. Reakční profil probíhal následovně: 25 °C po dobu 10 minut, 55 °C po dobu 30 minut a 85 °C po dobu 5 minut. Gen *mecA* byl amplifikován pomocí PCR. Sekvence primerů byly 5′-CCCAATTTGTCTGCCAGTTT-3′, and 5′-TGGCAATATTA ACGCACCTC-3′. PCR reakční směs obsahovala Taq reakční pufr (New England Biolabs, Ipswich, Velká Británie), dNTP, reverse a forward primery (Sigma Aldrich, St. Louis, MO, USA), Taq DNA polymerázu. Podmínky pro PCR byly počáteční denaturace 30 cyklů při 94 °C po dobu 3 minut, 53 °C po dobu 30 sekund a 72 °C po dobu 30 sekund a konečné prodloužení při 72 °C po dobu 4 minut. Reakcí vznikl fragment o velikosti 223 párů bází.

4.2.4.3 Vizualizace a kvantifikace genové exprese

cDNA byla smíchána s nanášecím pufrem a poté napipetována do jamek 1,5% agarózového gelu s ethidium bromidem. Elektroforéza probíhala v 1 × TAE pufru (40 mM Tris, 20 mM acetátový pufr, 1 mM ethylendiamintetraoctová kyselina) o pH 8 po dobu 90 minut při napětí 90 V. Vzniklé bandy byly vizualizovány UV světlem v transluminátoru při 312 nm (VilberLourmat, Marne-la-Valle'e Cedex, Francie) a intenzity záření byly kvantifikovány pomocí Carestream molekulární software pro zpracování obrazu pomocí *in vivo* Xtreme Imaging System (Rochester, NY, USA) a normalizovány na 16S gen *(Cihalova, Chudobova, Michalek, Moulick, Guran, Kopel, Adama Kizek, 2015).*

4.2.5 Stanovení růstových křivek

K vyhodnocení antimikrobiálního účinku testovaných antibiotik a komplexů selenových nanočástic s antibiotiky bylo využito měření absorbance pomocí přístroje Multiskan EX (Thermo Fisher Scientific, Německo) a následné analýzy růstových křivek. Bakteriální kultury *S. aureus* a MRSA byly naředěna Luria Bertani médiem na spektrofotometru SPECORD 210 (Analytik Jena, Německo) při vlnové délce 600 nm na absorbanci 0,1 AU. V mikrotitrační destičce byla bakteriální kultura smísena se 100μM roztokem testovaných látek. Celkový objem mikrotitrační destičky byl vždy 300 μl. Měření bylo prováděno vždy v čase 0, poté v půlhodinových intervalech po dobu 24 hodin při teplotě

37 °C a vlnové délce 600 nm. Dosažené hodnoty byly zpracovány do grafické podoby růstových *(Cihalova, Chudobova, Michalek, Moulick, Guran, Kopel, Adama Kizek, 2015).*

5 VÝSLEDKY A DISKUSE

Výsledková část předkládané disertační práce je přiložena ve formě publikací v odborných časopisech a dále doplněna o komentáře autorky.

5.1 Vliv složení bakteriálního mikrobiomu v těžko hojících se ranách na závažnosti onemocnění a délce trvání léčby

5.1.1 Vědecký článek I

CHUDOBOVA, D.; **CIHALOVA, K.**; GURAN, R.; DOSTALOVA, S.; SMERKOVA, K.; VESELY, R.; GUMULEC, J.; MASARIK, M.; HEGER, Z.; ADAM, V.; KIZEK, R. Influence of microbiome species in hard-to-heal wounds on disease severity and treatment duration. *Brazilian Journal of Infectious Diseases*, 2015, roč. 19, č. 6, s. 604-613. ISSN 1413-8670.

Bakteriální infekce vyskytující se ve zdravotnických zařízeních stále častěji a vážně komplikují léčbu hospitalizovaných pacientů *(Dai a kol., 2011)*. Ve zdravotnických zařízeních dochází ke vzniku rezistence bakterií přítomných v infikované ráně vůči používaným antibiotickým léčivům. Včasná identifikace mikrobiomu infekce tak umožní nasadit vhodnou léčbu a předcházení vzniku možných komplikací *(Polaczek-Kornecka a kol., 1991; Mihai a kol., 2014)*.

Cílem práce byla izolace, charakterizace a identifikace mikroorganismů převládajících v povrchových ranách s bakteriální infekcí u pacientů. Bakterie byly kultivovány na selektivních živných půdách: krevní agar obsahující 10% NaCl pro pomnožení stafylokoků, krevní agar pro pomnožení G$^+$ a G$^-$ bakterií, Endův agar pro pomnožení koliformních bakterií a krevní agar s amikacinem pro pomnožení streptokoků. Nejdříve byla provedena identifikace kmenů pomocí MALDI-TOF hmotnostní spektrometrie. Proteinové profily (2-30 kDa) byly srovnávány s databází. Následně byla tato metoda porovnána s genovým sekvenováním genu kódujícího 16S podjednotku ribosolnální RNA.

Touto studií bylo zjištěno, že u vybraných pacientů převládal druh *S. aureus* (70 %) a z toho bylo 11 % meticilin rezistentní formy. Zjištěné kmeny byly porovnány

s diagnózou pomocí neuronové sítě a byl posouzen vztah mezi závažností infekce a hojením s druhovým složením mikrobiomu infikované rány. Neuronové sítě byly následně použity pro prognózu pacientů s 95% úspěšností.

U 50 hospitalizovaných pacientů, kteří byli vybráni pro naši studii, byla identifikována bakteriální infekce a dle navrhované umělé neuronové sítě jsme byli schopni předvídat závažnost infekce a délku léčby.

ELSEVIER

CrossMark

Original Article

Influence of microbiome species in hard-to-heal wounds on disease severity and treatment duration

Dagmar Chudobova [a,b], *Kristyna Cihalova* [a,b], *Roman Guran* [a,b], *Simona Dostalova* [a,b], *Kristyna Smerkova* [a,b], *Radek Vesely* [c], *Jaromir Gumulec* [a,d], *Michal Masarik* [a,d], *Zbynek Heger* [a,b], *Vojtech Adam* [a,b], *Rene Kizek* [a,b,*]

[a] *Department of Chemistry and Biochemistry, Mendel University in Brno, Zemedelska, Czech Republic*
[b] *Central European Institute of Technology, Brno University of Technology, Technicka, Czech Republic*
[c] *Department of Traumatology at the Medical Faculty, Masaryk University and Trauma Hospital of Brno, Ponavka, Czech Republic*
[d] *Department of Pathological Physiology, Faculty of Medicine, Masaryk University, Kamenice, Czech Republic*

ARTICLE INFO

ABSTRACT

Background: Infections, mostly those associated with colonization of wound by different pathogenic microorganisms, are one of the most serious health complications during a medical treatment. Therefore, this study is focused on the isolation, characterization, and identification of microorganisms prevalent in superficial wounds of patients ($n = 50$) presenting with bacterial infection.

Methods: After successful cultivation, bacteria were processed and analyzed. Initially the identification of the strains was performed through matrix-assisted laser desorption/ionization time-of-flight mass spectrometry based on comparison of protein profiles (2–30 kDa) with database. Subsequently, bacterial strains from infected wounds were identified by both matrix-assisted laser desorption/ionization time-of-flight mass spectrometry and sequencing of 16S rRNA gene 108.

Results: The most prevalent species was *Staphylococcus aureus* (70%), and out of those 11% turned out to be methicillin-resistant (*mecA* positive). Identified strains were compared with patients' diagnoses using the method of artificial neuronal network to assess the association between severity of infection and wound microbiome species composition. Artificial neuronal network was subsequently used to predict patients' prognosis ($n = 9$) with 85% success.

* *Corresponding author.*
  E-mail address: kizek@sci.muni.cz (R. Kizek).

Conclusions: In all of 50 patients tested bacterial infections were identified. Based on the proposed artificial neuronal network we were able to predict the severity of the infection and length of the treatment.

Introduction

Skin has an important role in preventing the entry of undesirable substances, organisms, and bacteria into the bloodstream.[1,2] Loss of skin integrity leads to different types of wounds which have the humidity, warmth, and a nurturing environment ideal for colonization and proliferation of undesirable bacterial strains, changing the naturally occurring microbiome. Colonized sites are usually polymicrobial, *i.e.* contain more than one bacterium with pathogenic potential.[3] Wound infections are marked by disturbed host–bacteria equilibrium in a traumatized tissue environment favoring the pathogenic bacteria. A wound infection not only has the possibility to elicit a systemic response (sepsis), but is also able to inhibit the multiple processes involved in the orchestrated progression of normal wound healing.[4]

The concept of microbiome was first suggested in 2001 by Lederberg and McCray and was described as an ecological cohort of commensal, symbiotic, and pathogenic microorganisms sharing a body space.[5] Previously, it was estimated that as much as 20 to 60% of human-associated microbiome is hard-to-identify, which has likely resulted in an underestimation of microbiome diversity.[6] One of the most frequent microorganisms in infected wound is *Staphylococcus aureus*.[7–10] According to numerous studies,[11–13] another common organism in infected wounds is *Pseudomonas aeruginosa* with up to 10% occurrence, causing nosocomial infections together with *S. aureus* and other bacteria. In addition, the *Enterobacteriaceae* family is most often identified in connection with immunocompromised patients or those who have undergone abdominal surgery.[1]

Bacterial infections, increasingly occurring in medical facilities, can seriously complicate the outcome of treated patients.[14,15] This is particularly connected with rising resistance of bacterial strains toward antibiotics or metals,[16,17] thus significantly hindering treatment success. Although being highly debated the mechanism of resistance development has not been satisfactorily elucidated.[18–21]

The elevated occurrence of resistant bacterial strains is strictly linked with increased utilization of invasive surgical techniques, which are often performed in elderly, immunocompromised patients. Simultaneously, with the use of antibiotics, bacterial resistance can evolve in surgical sites, leading to bacteremia and sepsis, and thus significantly prolonging the healing phase of a patient. Although bacterial resistance presents a problem in healthcare facilities, there still exist few possibilities to eliminate the most frequent resistant strains that cause hospital-acquired infection – methicillin-resistant *S. aureus* (MRSA),[22,23] *e.g.* highly potent glycopeptide vancomycin.[24] However, for a correct choice of antibiotics one needs to accurately identify the microbiome composition of infected wounds. Knowledge of the bacterial ecology of wounds may thus lead to increase treatment success, coupled with curbing bacterial resistance as a result of inadequate utilization of antibiotics.[25–28]

Accordingly, this work is focused on identification of the microbiome associated with serious infections in hard-to-heal wounds with the aim to propose a prediction model, comprising both the microbiome composition and patientsˊhealth conditions.

Materials and methods

Chemicals, preparation of deionized water and pH measurement

Chemicals used in this study were acquired from Sigma-Aldrich (St. Louis, MO, USA) in ACS purity unless noted otherwise. Deionized water was prepared using reverse osmosis equipment Aqual 25 (Aqual s.r.o., Brno, Czech Republic) and further purified using Milli-Q Direct QUV equipped with the UV lamp, with 18 MΩ resistance. pH was measured using the pH meter WTW inoLab (Weilheim, Germany).

Preparation of hospital samples and their cultivation

Cohort of patients with bacterial infections
For evaluation, patients with superficial or deep wounds were selected according to infection severity. Detailed information concerning the patients is documented in S1. A total of 50 patients aged 19 through 93 years were enrolled into the clinical study, and 13 patients were 70–79 years old; 23 patients superficial wounds and 27 deep wounds. For all patients, the treatment duration was determined by the traumatologist based severity and extent of infection, associated diseases potentially interfering with treatment outcome and healing of wounds, and other factors such as patient age, concomitant medications, and previous medical history. For confirmation of the functionality of the neural network 9 blank samples from 9 patients identified by MALDI-TOF MS were used. Enrollment of patients into the clinical study was approved by the Ethics Committee of Trauma hospital in Brno.

Collection of wound swabs from patients with bacterial infections
The smears, collected from infected wounds with the agreement of patients, were sampled by rolling motion at the wound using a sterile swab sampler. All patients were divided into two subgroups, on the grounds of infection severity: deep and superficial wound. A detailed description of comorbidities and duration of treatment was obtained. Patients were classified

according to the Classification of surgical wounds – SSI (surgical site infections).[29–31] Infected wounds were sampled by using disposable tampon swabs maximizing collection of representative microflora. Tampons were subsequently stored in transport medium (inorganic salts, sodium thioglycolate, 1% agar, activated charcoal). The important part of our workflow process comprised sampling in duplicates with further transport in both aerobic and anaerobic conditions to preserve bacterial viability.

Cultivation of clinical specimens

Four types of selective nutrient media (blood agar enriched by 10% NaCl, Endo agar, blood agar without any other component, and blood agar with amikacin) we employed for further microbiological selection. Petri dishes, containing the above mentioned media were subsequently incubated according to conventional protocols, as described elsewhere,[32–35] to maintain suitable conditions for growth of all types of bacteria. These Petri dishes were incubated for 24–48 h at 37 °C supplemented by TGY medium (1 g L^{-1} glucose, 5 g L^{-1} tryptone, 2.5 g L^{-1} yeast extract). Subsequently, individual colonies were collected from each Petri dish and stored in 1 μL of enriched media. These samples were processed as described in the *DNA sequencing* section and utilized for both – MALDI-TOF MS identification and PCR with subsequent sequencing.

MALDI-TOF MS identification of bacteria

The following extraction protocol was based on MALDI Biotyper^{TM} 3.0 User Manual Revision 2, also used in a previous report.[36] 500 μL of bacterial culture, cultivated overnight, was centrifuged at 14,000 × *g* for 2 min. The supernatant was discarded and the pellet was re-suspended in 300 μL of deionized water besides adding 900 μL of ethanol. After centrifugation at 14,000 × *g* for 2 min, the supernatant was discarded and the obtained pellet was air-dried. The pellet was then dissolved in 25 μL of 70% formic acid (*v/v*) and 25 μL of acetonitrile and mixed. The samples were centrifuged at 14,000 × *g* for 2 min and 1 μL of the clear supernatant was spotted in duplicate onto the MALDI target and air-dried at room temperature. Then, each spot was overlaid with 1 μL of α-cyano-4-hydroxycinnamic acid (HCCA) matrix solution (20 mg mL^{-1}) in organic solvent (50% acetonitrile and 2.5% trifluoroacetic acid, both *v/v*) and air-dried completely prior to MALDI-TOF MS measurement on UltrafleXtreme MS (Bruker Daltonik GmbH, Bremen, Germany). As matrix solution 2,5-dihydroxybenzoic acid (DHB) was also used in the same concentration and solvent as HCCA. Spectral data were taken in the *m/z* range of 2000–30,000 Da, resulted from the accumulation of 240 laser shots targeted to different regions of the same sample spot. These data were analyzed with the Flex Analysis software (Version 3.4). Final preparation of dendrograms was carried out in the MALDI BioTyper^{TM} 3.1 (Bruker Daltonik GmbH, Bremen, Germany).

DNA sequencing

Bacterial cells were centrifuged at 4450 × *g* and 20 °C for 10 min. The pellet was resuspended in 400 μL of lysis buffer (6 M guanidium hydrochloride, 0.1 M sodium acetate) and cells were lysed for 1 hour at 20 °C and 600 rpm on Multi RS-60 (Biosan, Riga, Latvia). Genomic DNA was isolated from lysed bacterial cultures *via* MagNA Pure Compact (Roche, Mannheim, Germany), using Nucleic Acid Isolation Kit I, protocol DNA_Bacteria.

16S rRNA gene was amplified using *Taq* PCR Mix (New England Biolabs, Ipswich, MA, USA) and MasterCycler realplex[4] epgradient S (Eppendorf, Hamburg, Germany). 100 μL of reaction mixture consisted of: 1× Standard *Taq* Reaction Buffer, 1.6 U of *Taq* DNA polymerase, 200 μM Deoxynucleotide Solution Mix, 0.5 μM primers and 5 μL of isolated genomic DNA. The forward primer E9F 5′-GAGTTTGATCCTGGCTCAG-3′ and reverse primer U1510R 5′-GGTTACCTTGTTACGACTT-3′ were synthesized by Sigma–Aldrich (St. Louis, MO, USA). The reaction profile was as follows: initial denaturation at 94 °C for 4 min; 30 cycles of denaturation at 94 °C for 30 s, annealing at 52 °C for 30 s and elongation at 72 °C for 105 s; with terminal elongation at 72 °C for 10 min. Amplified fragments were purified using MinElute PCR Purification Kit (Qiagen, Hilden, Germany).

For sequencing reaction the DTCS Quick Start Kit (Beckman Coulter, Pasadena, CA, USA) was used. To 20 μL sequencing reaction mixture, 98 ng of purified fragment, 0.75 μL of 10 μM forward primer, 4 μL of DTCS Quick Start Master Mix and 1 μL of Sequencing Buffer were added. The conditions of 30 cycle-reactions were as follows: 96 °C for 20 s; 50 °C for 20 s and 60 °C for 4 min. The purification of sequencing product was carried out using CleanSEQ kit (Beckman Coulter). Purified samples in Sample Loading Solution were transferred to the plate and DNA sequencing was performed using Genetic Analysis System CEQ 8000 (Beckman Coulter). After denaturation at 90 °C for 2 min, a fluorescence-marked DNA fragments were separated in 33 cm long capillary with 75 μm i.d. (Beckman Coulter) filled with linear polyacrylamide denaturing gel. The separation was run at capillary temperature of 50 °C and voltage of 4.0 kV for 85 min. Sequences were identified by comparison with NCBI database.

Amplification of S. aureus genes mecA and fnbA

Isolation of genomic DNA was performed using the same method as described in section *DNA sequencing*. The *mecA* and *fnbA* genes were amplified using polymerase chain reaction (PCR) as previously reported.[37] The primers were synthesized by Sigma-Aldrich and the sequences of forward and reverse primers for *mecA* gene were 5′-CCCAATTTGTCTGCCAGTTT-3′, and 5′-TGGCAATATTAACGCACCTC-3′ and for *fnbA* gene were 5′-GATACAAACCCAGGTGGTGG-3′, and 5′-TGTGCTTGACCAT-GCTCTTC-3′. The volume of PCR reaction mixture was 100 μL containing 1× *Taq* reaction buffer, 0.2 mM dNTP, 1.6 U of *Taq* DNA polymerase (New England Biolabs) and 0.5 mM of each primer. The reaction profile was as follows: initial denaturation at 94 °C for 4 min, 30 cycles of denaturation at 94 °C for 30 s, annealing at 53 °C for 30 s and extension at 72 °C for 1 min with a final extension of 7 min. The amplification generated a 223 bp for *mecA* and 191 bp for *fnbA*.

Agarose gel (2% (*v/v*), high melt, Mercury, San Diego, CA, USA) was prepared with 1× TAE buffer (40 mM Tris, 20 mM acetic acid and 1 mM ethylenediaminetetraacetic acid) and ethidium bromide (5 μL per 100 mL of the gel) as described

elsewhere.[38] 100 bp DNA ladder (New England Biolabs) within the size range from 100 to 1517 bp was used to monitor the size of the analyzed fragment. The electrophoresis (Bio-Rad, Hercules, CA, USA) was run at 60 V and 6 °C for 160 min. The bands were visualized by UV transilluminator at 312 nm (Vilber-Lourmant, Marne-la-Vallée, France).

Statistical processing of obtained results

Automated neuronal network was used as a predictive model. Classification analysis automated neuronal network was used for the estimation of categorical data. The dataset was randomly divided as follows: 80% for learning, 10% for testing, and 10% for validation. Following network types were tested using automated network search: multilayer perceptron network (MLP), and radial basis function (RBF). Number of hidden units to search was determined as follows: 8–24 and 8–11 for MLP and RBF, respectively. Total 1000 networks were trained, and activation functions were searched for identity, logistic, tanh, exponential. Weight decay of 0.0001–0.001 was used for hidden layer and output layer. Weight of input variables for learning was used based on MALDI-TOF classification score. Unless noted otherwise, p-value less than 0.05 was considered significant. Software Statistica 12 (StatSoft, CA, USA) was used for analysis.

Results and discussion

We decided to employ a variety of cultivation approaches (in presence of O_2, CO_2 or in microaerophilic conditions) to reveal the presence of real microbiota associated with superficial infections.

MALDI-TOF MS was explored as an accurate and rapid identification tool, using the protein mass patterns, which are compared with patterns from a commercial Bruker Daltonics database (BDAL) of MALDI Biotyper™ software.[39] Due to a powerful software support, the method can be used for identification within few minutes, which is one of the advantages.[36] Moreover, sequencing of amplified 16S rRNA gene[40] was employed for identification independent of protein patterns. Finally, an artificial neural network (ANN) was developed as a predictive model for evaluation of infection severity and using developed ANN we attempted to find the relationship between disease severity and the microorganisms identified in clinical specimens.

Identification of bacterial strains by MALDI-TOF MS and Sanger sequencing

For the identification of bacterial entities we employed complementary methods for independent evaluation of different biomolecules – proteins and DNA.[36,41,42] Sanger sequencing was utilized as a confirmation method, based on sequencing of 16S rRNA gene. This gene contains hypervariable regions, providing species-specific sequences, hence it can provide enough information for a confident discrimination, and thus became popular in medical microbiology to classify bacteria.[43,44]

When compared to sequencing, MALDI-TOF MS offers much shorter analysis time. By using this technique, wound microbiome could be discriminated within one hour of incubation, and thus this will likely become the method of choice for future microbiome identification. Nevertheless, the classification is based on a still developing database[34]; hence MALDI-TOF MS identification of non-databased bacteria has still to be connected with other confirmation methods. From this reason we firstly employed MALDI-TOF MS with a condition: If score <2.00 = 16S rRNA sequencing.

As shown in S2, 108 bacterial strains were identified[37] of them had to be confirmed by sequencing and confirmed strains were immediately databased to increase future classification success. Strains of *S. aureus* were the most often identified ($n = 35$). Thus, methicillin-resistant *S. aureus* (MRSA) is highly associated with severe infections in post-surgical wounds[45]; we further analyzed the *mecA* gene, encoding a modified penicillin binding protein (PBP) known as PBP2a, with decreased affinity toward β-lactams.[46] The *mecA* positivity was determined in four isolates. Since 67% of patients had deep wound infections and were treated for more than 8 weeks after admission to infectious Department of Trauma Hospital of Brno, presence of *mecA* was shown to be a crucial microbiological factor, affecting patients prognosis. Further, we determined the presence of *fnbA* gene, responsible for adhesins production. Adhesion to human extracellular matrix components and serum proteins is an important facet in the interaction between bacteria and its host cells.[47] Lim and coworkers identified the presence of *fnbA* in 96% of all isolated MRSA strains.[35] In our case, *fnbA* presence was confirmed in all MRSA isolates and in 89% of methicillin-sensitive *S. aureus* isolates. Similarly to *mecA*, *fnbA* was found to be associated with infection severity. In patients with negative *fnbA* and *mecA* the treatment duration was less than four weeks in 75% of cases, despite the fact that patients had deep wound infections. This finding suggests that the severity of staphylococcal infections does not depend solely on antimicrobial resistance, but also on adhesins expression, which enhance the interaction with the target host cells.

Distribution of identified strains within various cohorts of patients

According to duration of treatment, the patients were divided into specific subgroups, where each sector represents one bacterial strain.

The subdivision of patients was based on surgical wounds classification SSI. As shown, patients were divided into two groups - deep and superficial wounds and the associated bacterial strains are depicted in Fig. 1A and B.

As it is obvious from Fig. 1A, in the more serious infections (deep) *S. aureus* was the main bacterium of microbiome composition (28% of identified strains), followed by *Enterococcus faecalis* (15%), and *Escherichia coli* (11%). On the other hand, *E. coli* was not so often identified in surficial wounds (5% – Fig. 1B). Taken together, the microbiome composition in both groups exhibits substantial differences, and thus it can be hypothesized that presence of minority representatives as *Hafnia alvei*, *Proteus vulgaris*, *Staphylococcus lugdunensis*, or
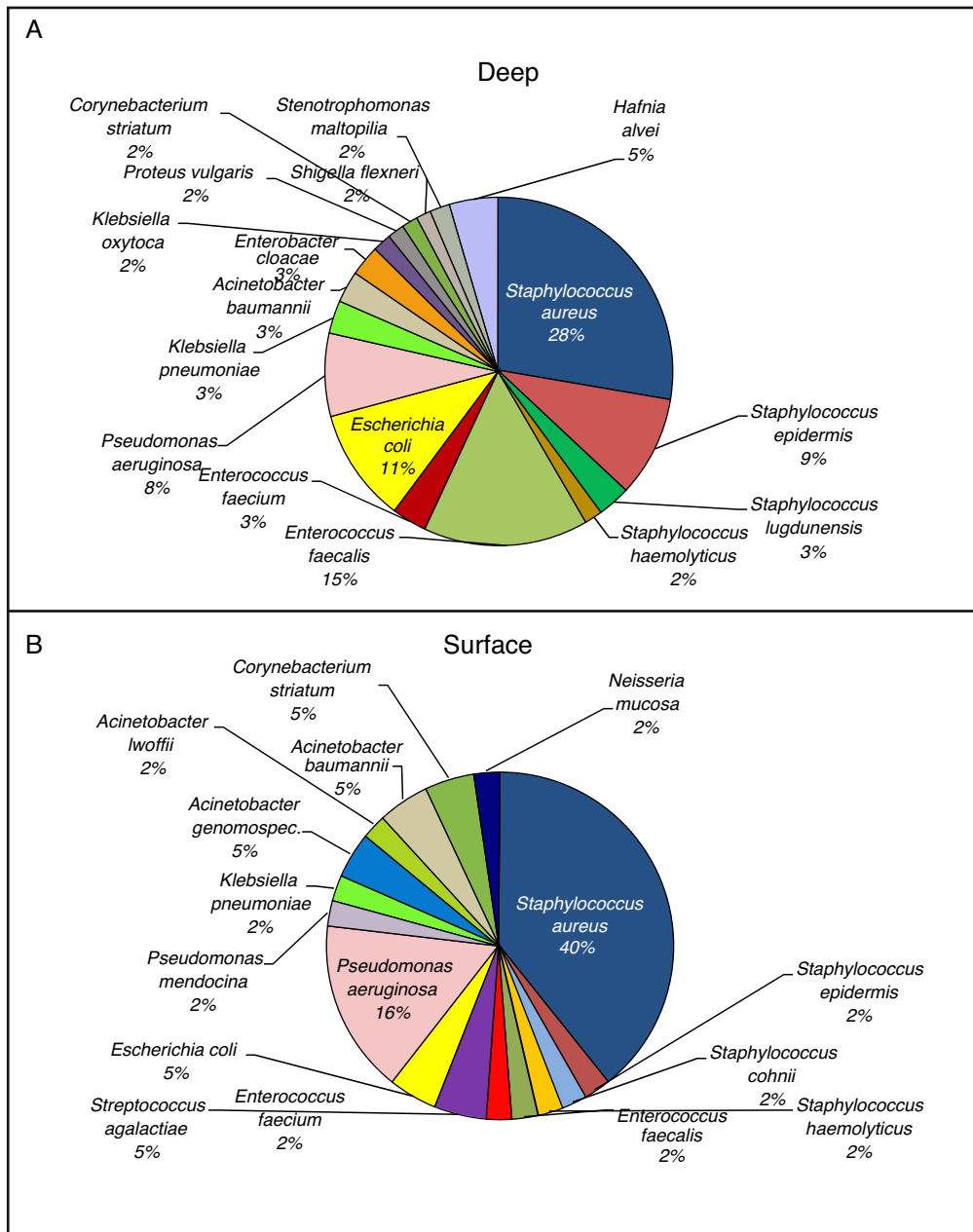
Fig. 1 – Representation of microorganism species present in patients' wounds. Patients were grouped based on infection severity. The graphs show bacterial cultures grown on different selective nutrient media. (A) Infection severity – deep wounds and (B) infection severity – superficial wounds.

Enterobacter cloacae in the wound can significantly influence the infection severity. It can be also stated that increasing duration of treatment leads to increased number of identified *Enterobacteriaceae* and opportunistic pathogens (*Pseudomonas*, *Enterococcus*).

Phylogenetic analysis of protein alterations

As was shown by Rettinger and colleagues,[48] MALDI-TOF mass spectra-based phylogenetic analysis is considered equivalent to 16S rRNA gene sequencing. Therefore, we employed MALDI Biotyper™ for preparation of dendrograms for our groups,

divided by treatment duration (Fig. 2). Dendrograms showed similarity of same bacterial strains (low distance level), but in some cases larger differences were found – usually among bacterial strains from different patients. These differences were caused probably by modifications of bacterial proteins. Karger et al. found methylation as a cause of higher distance level in dendrogram between *Burkholderia pseudomallei* and other types of *B. pseudomallei*.[49] Thus it can be concluded that not only changes in microbiome representatives affect treatment duration and success, but also small changes in protein post-translation modifications can be highly important for patients' recovery.
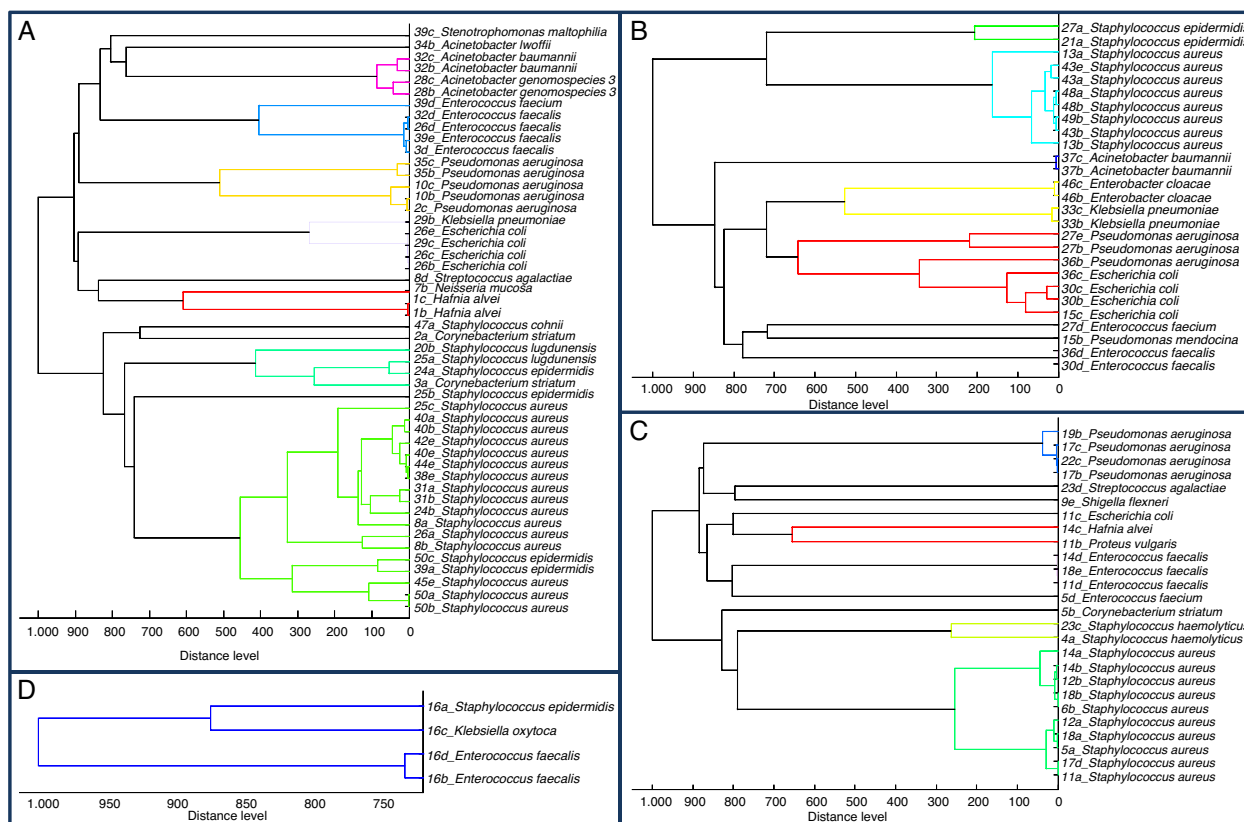
Fig. 2 – Dendrograms from protein mass profiles of microorganisms in different groups based on treatment duration. Created in MALDI Biotyper™. (A) Treatment duration less than four weeks. (B) Treatment duration 4–7 weeks. (C) Treatment duration eight and more weeks. (D) Exitus.

Artificial neural network

Two neuronal networks were created: (1) for the prediction of time-to-heal, and (2) for the prediction of infection severity. The following input parameters were used for the construction of networks: from 2000 networks five were retained and one was used for further final custom neuronal network. The settings of the network created using automated algorithm and used for the custom final learning were Multilayer perceptron 89-13-3 (input-hidden-output neurons), Broyden–Fletcher–Goldfarb–Shanno (BFGS) training algorithm, sum of squares error function, identity function for hidden layer, and then for output layer. The design of the network is displayed in Fig. 3A. With stopping conditions enabled (Fig. 3B), a final network was created in the 17th training cycle with performances of 91.4%, 85.7%, and 71.4% for training, testing, and validation (accuracy in prediction up to 85% – Fig. 3C), respectively.

Consequently, a second neuronal network for the prediction of infection severity was created using an automated algorithm. The best-performing network was trained under following settings: multilayer perceptron 89-19-2 (input-hidden-output neurons) (Fig. 3D) BFGS training algorithm, cross entropy error function, and exponential and softmax activation function for hidden and output layer. The training process is depicted in Fig. 3E (accuracy in prediction up to 85% – Fig. 3F).

The performances of the network were 100.0%, 85.7%, and 85.7% for training, testing, and validation (Table 1), respectively. The accuracy for individual cases is displayed in Table 2.

Sensitivity analysis of input variables for both networks was carried out. For the prediction of infection severity,

Table 1 – Characterization of neuronal network performance for the prediction of patient outcome. Performance displayed in % for training, testing, and validation samples. The number of training cycle for custom network training is displayed in training algorithm column. BFGS, Broyden–Fletcher–Goldfarb–Shanno training algorithm; SOS, sum of squares.

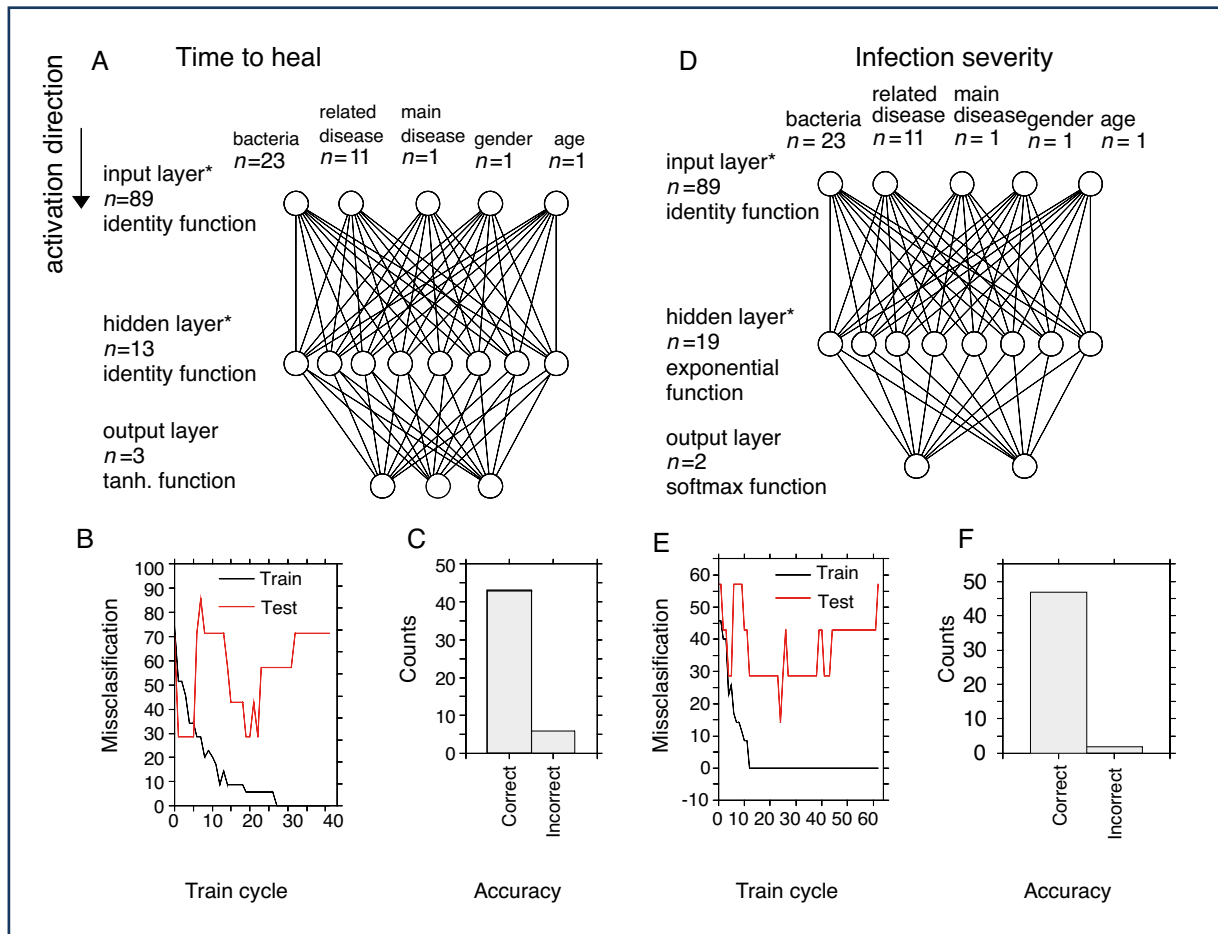| Prediction target	Net. name	Performance			Training algorithm	Error function	Activation	
		Training	Testing	Validation				Train
Infection severity	MLP 89-19-2	100.00	85.71	85.71	BFGS 24	Infection severity	MLP 89-19-2	100.00
Time-to-heal	MLP 89-13-3	91.43	85.71	71.43	BFGS 17	Time-to-heal	MLP 89-13-3	91.43

Fig. 3 – Design and performance of the neuronal networks. (A) Design of classification network for the prediction of time-to-heal. The number of neurons/inputs is indicated by *n*. *Note the number of input and hidden neurons is not displayed exactly. (B) Training process of the classification network with stopping conditions activated. (C) Accuracy of the final network for classification of time-to-heal. (D) Design of classification network for the prediction of infection severity. (E) Training process for creation of this network with stopping criteria activated. (F) Accuracy of the network for the prediction of infection severity.

Table 2 – Performance of the network: verification of the test and validation cohort. Analysis for both networks for prediction of infection severity and time-to-heal. Test cohort was employed for stopping conditions. Validation sample was used to test final network. "target" indicates input data, network output reflects calculated result from the neuronal network. id, identification of patient; w, week.

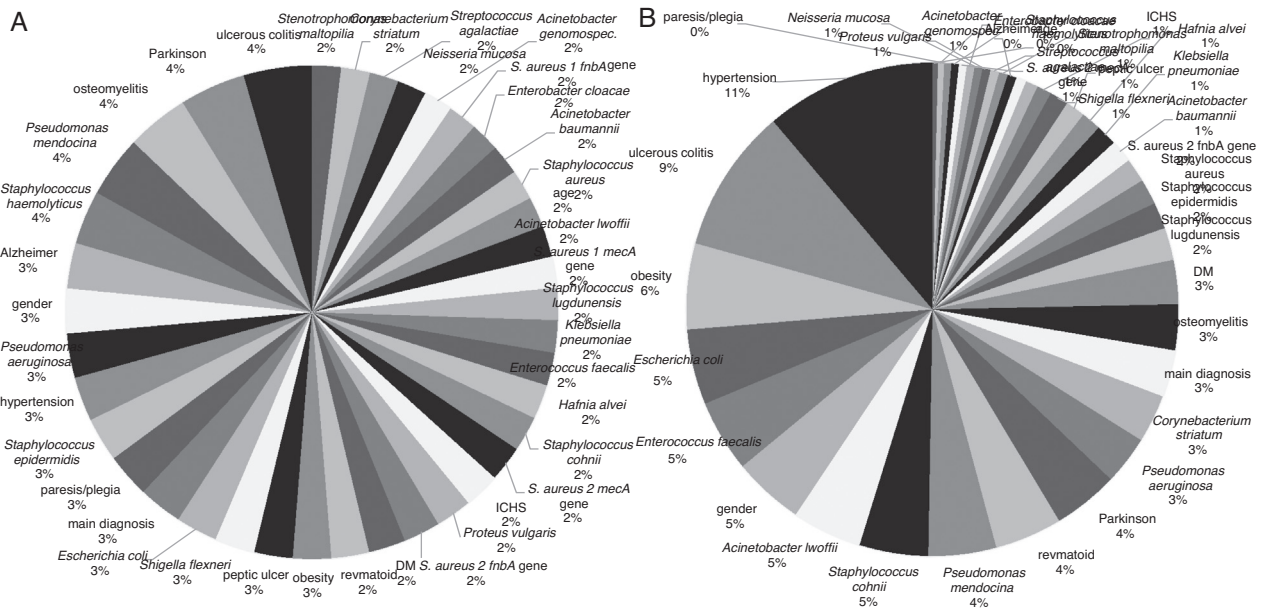| Sample	ID	Case weights	Infection severity				Time-to-heal			
			Target	Network output	Accuracy	Conf. level	Target	Network output	Accuracy	Conf. level
Test	2	1.71	Superficial	Superficial	Correct	1.00	<4 w	<4 w	Correct	0.40
	6	1.81	Deep	Deep	Correct	1.00	>8 w	<4 w	Incorrect	0.47
	8	1.65	Superficial	Superficial	Correct	1.00	<4 w	<4 w	Correct	0.36
	22	2.00	Superficial	Superficial	Correct	1.00	>8 w	>8 w	Correct	0.41
	38	2.06	Deep	Superficial	Incorrect	1.00	<4 w	<4 w	Correct	0.49
	39	2.01	Deep	Deep	Correct	1.00	<4 w	<4 w	Correct	0.56
	40	2.12	Superficial	Superficial	Correct	1.00	<4 w	<4 w	Correct	0.43
Validation	7	1.68	Superficial	Deep	Incorrect	1.00	<4 w	<4 w	Correct	0.40
	23	1.62	Superficial	Superficial	Correct	1.00	>8 w	>8 w	Correct	0.49
	27	2.23	Deep	Deep	Correct	0.87	4–7 w	<4 w	Incorrect	0.58
	28	2.11	Superficial	Superficial	Correct	1.00	<4 w	<4 w	Correct	0.47
	36	2.27	Deep	Deep	Correct	1.00	4–7 w	4–7 w	Correct	0.63
	45	1.88	Deep	Deep	Correct	1.00	<4 w	<4 w	Correct	0.43
	49	2.25	Deep	Deep	Correct	1.00	4–7 w	<4 w	Incorrect	0.56

Fig. 4 – Sensitivity analysis of all factors for prediction of time-to-heal and infection severity. Sensitivity of individual factors depicted as a percentage of total sensitivity. (A) Sensitivity of individual factors for the prediction of time-to-heal. (B) Sensitivity of individual factors for the prediction of infection severity.

the mean sensitivity level was 4.66, ranging from 0.63 to 20.1, and a total sensitivity = 179.9 (Fig. 4) The highest level of sensitivity (thus highest impact on prediction of a network) was observed for hypertension (20.15), ulcerative colitis (17.06), obesity (10.13), *E. coli* (8.87), *E. faecalis* (8.50), and other factors. The factors with sensitivity <1 were *P. vulgaris*, *Neisseria mucosa*, *E. cloacae*, *S. aureus* 2 *mecA* genes, *Staphylococcus haemolyticus*, paresis/plegia, Alzheimer's disease, age.

For the prediction of time-to-heal, the sensitivity was distinctly more homogeneous for the input factors with mean sensitivity = 1.35, (0.99–2.35), total sensitivity = 52.49. The factors with higher sensitivity included ulcerative colitis (2.35), Parkinson's disease (2.27), osteomyelitis (2.15), *Pseudomonas mendocina* (2.11), *S. haemolyticus* (1.84) and others (Fig. 4). The factors with sensitivity <1 include *Streptococcus agalactiae*, *Corynebacterium striatum*, and *Stenotrophomonas maltopilia*.

Conflicts of interest

The authors declare no conflicts of interest.

AcknowledgementS

The study was financially supported by CEITEC CZ.1.05/1.1.00/02.0068. The authors wish also to express their special thanks to Radek Chmela for perfect technical assistance.

Appendix A. Supplementary data

Supplementary data associated with this article can be found, in the online version, at http://dx.doi.org/10.1016/j.bjid.2015.08.013.

REFERENCES

1. Mama M, Abdissa A, Sewunet T. Antimicrobial susceptibility pattern of bacterial isolates from wound infection and their sensitivity to alternative topical agents at Jimma University Specialized Hospital, South-West Ethiopia. Ann Clin Microbiol Antimicrob. 2014;13:1–10.
2. Ndip RN, Malange Takang AE, Echakachi CM, et al. In-vitro antimicrobial activity of selected honeys on clinical isolates of *Helicobacter pylori*. Afr Health Sci. 2007;7:228–32.
3. Dai T, Huang YY, Sharma SK, Hashmi JT, Kurup DB, Hamblin MR. Topical antimicrobials for burn wound infections. Recent Patents Anti-infect Drug Discov. 2010;5:124–51.
4. Dai TH, Tanaka M, Huang YY, Hamblin MR. Chitosan preparations for wounds and burns: antimicrobial and wound-healing effects. Expert Rev Anti-Infect Ther. 2011;9:857–79.
5. Lederberg J, McCray AT. 'Ome sweet' omics – a genealogical treasury of words. Scientist. 2001;15:8–9.
6. Bik EM, Eckburg PB, Gill SR, et al. Molecular analysis of the bacterial microbiota in the human stomach. Proc Natl Acad Sci U S A. 2006;103:732–7.
7. Polaczek-Kornecka B, Dziadur-Goldsztaj Z, Turowski G. Methicillin-oxacillin resistant strains of *Staphylococcus aureus* (MORSA) in infected burn wounds. Mater Med Polona Polish J Med Pharm. 1991;23:304–5.
8. Cooper RA, Molan PC, Harding KG. Antibacterial activity of honey against strains of *Staphylococcus aureus* from infected wounds. J R Soc Med. 1999;92:283–5.
9. Simonetti O, Cirioni O, Ghiselli R, et al. RNAIII-inhibiting peptide enhances healing of wounds infected with methicillin-resistant *Staphylococcus aureus*. Antimicrob Agents Chemother. 2008;52:2205–11.
10. Lima AF, Costa LB, da Silva JL, Maiaiv MBS, Ximenes E. Interventions for wound healing among diabetic patients infected with *Staphylococcus aureus*: a systematic review. Sao Paulo Med J. 2011;129:165–70.

11. Ricotti CA Jr, Cazzaniga A, Feiner A, Davis SC, Mertz PM. Epifluorescent microscopic visualization of an in-vitro biofilm formed by a *Pseudomonas aeruginosa* wound isolate and of an in-vivo polymicrobial biofilm obtained from an infected wound. Abst General Meeting Am Soc Microbiol. 2003;103. J-023.

12. Schmoldt S, Ozkaya I, Gotzfried M, Heesemann J, Hogardt M. Pathotyping of *Pseudomonas aeruginosa* isolated from chronically infected wounds. Int J Med Microbiol. 2007;297:114–5.

13. Wildeboer D, Hill KE, Jeganathan F, et al. Specific protease activity indicates the degree of *Pseudomonas aeruginosa* infection in chronic infected wounds. Eur J Clin Microbiol Infect Dis. 2012;31:2183–9.

14. Chudobova D, Cihalova K, Dostalova S, et al. Comparison of the effects of silver phosphate and selenium nanoparticles on *Staphylococcus aureus* growth reveals potential for selenium particles to prevent infection. FEMS Microbiol Lett. 2014;351:195–201.

15. Hoerr V, Zbytnuik L, Leger C, Tam PPC, Kubes P, Vogel HJ. Gram-negative and Gram-positive bacterial infections give rise to a different metabolic response in a mouse model. J Proteome Res. 2012;11:3231–45.

16. Chudobova D, Dostalova S, Blazkova I, et al. Effect of ampicillin, streptomycin, penicillin and tetracycline on metal resistant and non-resistant *Staphylococcus aureus*. Int J Environ Res Public Health. 2014;11:3233–55.

17. Chudobova D, Dostalova S, Ruttkay-Nedecky B, et al. The effect of metal ions on *Staphylococcus aureus* revealed by biochemical and mass spectrometric analyses. Microbiol Res. 2015;170:147–56.

18. Nasim A, Thompson MM, Naylor AR, Bell PRF, London NJM. The impact of MRSA on vascular surgery. Eur J Vasc Endovasc Surg. 2001;22:211–4.

19. Young MH, Upchurch GR, Malani PN. Vascular graft infections. Infect Dis Clin North Am. 2012;26:41–56.

20. Anderson DJ, Sexton DJ, Kanafani ZA, Auten G, Kaye KS. Severe surgical site infection in community hospitals: epidemiology, key procedures, and the changing prevalence of methicillin-resistant *Staphylococcus aureus*. Infect Control Hosp Epidemiol. 2007;28:1047–53.

21. Earnshaw JJ. Methicillin-resistant *Staphylococcus aureus*: vascular surgeons should fight back. Eur J Vasc Endovasc Surg. 2002;24:283–6.

22. Zhang J, Liu HC, Zhu KK, et al. Antiinfective therapy with a small molecule inhibitor of *Staphylococcus aureus* sortase. Proc Natl Acad Sci U S A. 2014;111:13517–22.

23. Solis N, Parker BL, Kwong SM, Robinson G, Firth N, Cordwell SJ. *Staphylococcus aureus* surface proteins involved in adaptation to oxacillin identified using a novel cell shaving approach. J Proteome Res. 2014;13:2954–72.

24. Rolston KVI, Wang WQ, Nesher L, Coyle E, Shelburne S, Prince RA. In vitro activity of telavancin compared with vancomycin and linezolid against Gram-positive organisms isolated from cancer patients. J Antibiot. 2014;67:505–9.

25. Wang DH, Yuan JF, Tao WY. Identification of a novel antibiotic from myxobacterium stigmatella eracta WXNXJ-B and evaluation of its antitumor effects in-vitro. Iran J Pharm Res. 2014;13:171–80.

26. Verma MS, Chen PZ, Jones L, Gu FX. Chemical nose for the visual identification of emerging ocular pathogens using gold nanostars. Biosens Bioelectr. 2014;61:386–90.

27. Strompfova V, Laukova A. Isolation and characterization of faecal bifidobacteria and lactobacilli isolated from dogs and primates. Anaerobe. 2014;29:108–12.

28. Dulay SB, Gransee R, Julich S, Tomaso H, O' Sullivan CK. Automated microfluidically controlled electrochemical biosensor for the rapid and highly sensitive detection of *Francisella tularensis*. Biosens Bioelectr. 2014;59:342–9.

29. Eisenberg D. Surgical site infections: time to modify the wound classification system? J Surg Res. 2012;175:54–5.

30. Ortega G, Rhee DS, Papandria DJ, et al. An evaluation of surgical site infections by wound classification system using the ACS-NSQIP. J Surg Res. 2012;174:33–8.

31. Klodzinska E, Kupczyk W, Jackowski M, Buszewski B. Capillary electrophoresis in the diagnosis of surgical site infections. Electrophoresis. 2013;34:3206–13.

32. Fon Sing S, Isdepsky A, Borowitzka MA, Lewis DM. Pilot-scale continuous recycling of growth medium for the mass culture of a halotolerant *Tetraselmis* sp. in raceway ponds under increasing salinity: a novel protocol for commercial microalgal biomass production. Bioresour Technol. 2014;161:47–54.

33. Goetz K, Pass T, Wright R, Collins K. Potential new method: a comparability study of M-coliblue24 and M-endo les agar for the verified recoveries of total coliforms and *E. coli*. Abst Gen Meeting Am Soc Microbiol. 1997;97:481.

34. Balazova T, Makovcova J, Sedo O, Slany M, Faldyna M, Zdrahal Z. The influence of culture conditions on the identification of *Mycobacterium* species by MALDI-TOF MS profiling. FEMS Microbiol Lett. 2014;353:77–84.

35. Lim KT, Hanifah YA, Yusof MYM, Thong KL. Investigation of toxin genes among methicillin-resistant *Staphylococcus aureus* strains isolated from a tertiary hospital in Malaysia. Trop Biomed. 2012;29:212–9.

36. Sauer S, Freiwald A, Maier T, et al. Classification and identification of bacteria by mass spectrometry and computational analysis. PLoS ONE. 2008;3:1–10.

37. Stomeo F, Valverde A, Pointing SB, et al. Hypolithic and soil microbial community assembly along an aridity gradient in the Namib Desert. Extremophiles. 2013;17:329–37.

38. Smerkova K, Dostalova S, Skutkova H, et al. Isolation of Xis Gen fragment of lambda phage from agarose gel using magnetic particles for subsequent enzymatic DNA sequencing. Chromatographia. 2013;76:329–34.

39. Nagy E. Matrix-assisted laser desorption/ionization time-of-flight mass spectrometry: a new possibility for the identification and typing of anaerobic bacteria. Future Microbiol. 2014;9:217–33.

40. Kuczynski J, Lauber CL, Walters WA, et al. Experimental and analytical tools for studying the human microbiome. Nat Rev Genet. 2012;13:47–58.

41. Somashekar BS, Amin AG, Tripathi P, et al. Metabolomic signatures in guinea pigs infected with epidemic-associated W-Beijing strains of *Mycobacterium tuberculosis*. J Proteome Res. 2012;11:4873–84.

42. Liu W, Zou DY, Wang XS, et al. Proteomic analysis of clinical isolate of *Stenotrophomonas maltophilia* with bla(NDM-1), bla(L1) and bla(L2) beta-lactamase genes under imipenem treatment. J Proteome Res. 2012;11:4024–33.

43. Pereira F, Carneiro J, Matthiesen R, et al. Identification of species by multiplex analysis of variable-length sequences. Nucleic Acids Res. 2010;38:1–17.

44. Kolbert CP, Persing DH. Ribosomal DNA sequencing as a tool for identification of bacterial pathogens. Curr Opin Microbiol. 1999;2:299–305.

45. Zacharioudakis IM, Zervou FN, Ziakas PD, Mylonakis E. Meta-analysis of methicillin-resistant *Staphylococcus aureus* colonization and risk of infection in dialysis patients. J Am Soc Nephrol. 2014;25:2131–41.

46. Ahmed EF, Gad GFM, Abdalla AM, Hasaneen AM, Abdelwahab SF. Prevalence of methicillin resistant *Staphylococcus aureus* among Egyptian patients after surgical interventions. Surg Infect. 2014;15:404–11.

47. Clarke SR, Foster SJ. Surface adhesins of *Staphylococcus aureus*. In: Poole RK, editor. Advances in microbial physiology, vol 51. London: Academic Press Ltd./Elsevier Science Ltd.; 2006. p. 187–225.

48. Rettinger A, Krupka I, Grunwald K, et al. *Leptospira* spp. strain identification by MALDI TOF MS is an equivalent tool to 16S rRNA gene sequencing and multi locus sequence typing (MLST). BMC Microbiol. 2012;12:1–14.

49. Karger A, Stock R, Ziller M, et al. Rapid identification of *Burkholderia mallei* and *Burkholderia pseudomallei* by intact cell matrix-assisted laser desorption/ionisation mass spectrometric typing. BMC Microbiol. 2012;12:1–15.

5.2 Dálkově ovládaná robotická platforma ORPHEUS jako nový nástroj pro detekci bakterií v prostředí

5.2.1 Vědecký článek II

NEJDL, L.; KUDR, J.; **CIHALOVA, K.**; CHUDOBOVA, D.; ZUREK, M.; ZALUD, L.; KOPECNY, L.; BURIAN, F.; RUTTKAY-NEDECKY, B.; KRIZKOVA, S.; KONECNA, M.; HYNEK, D.; KOPEL, P.; PRASEK, J.; ADAM, V.; KIZEK, R.. Remote-controlled robotic platform ORPHEUS as a new tool for detection of bacteria in the environment. *Electrophoresis*, 2014, roč. 35. č. 16, s. 2333-2345. ISSN 0173-0835.

Jak již bylo zmíněno, rychlá a včasná detekce bakterií hraje důležitou roli pro léčbu pacientů, avšak detekce přítomnosti bakterií ve znečištěném prostředí, ve vodě či místech se špatnou dostupností pro člověka pomocí plně automatizovaného systému je jakýmsi prvním stupněm vývoje detekčních zařízení bakterií tzv. "na dálku" *(Mihai, Holban, Giurcaneanu, Popa, Buzea, Filipov, Lazar, Chifiriuca Popa, 2014)*. Dálkově ovládané robotické systémy jsou používány pro analýzu různých typů analytů v nedostupném prostředí *(Bak a kol., 2004; Bellotto a kol., 2009)*. Cílem této studie bylo vyvinout dálkově ovládanou robotickou platformu (ORPHEUS-HOPE) *(Nejdl a kol., 2015)* pro detekci přítomnosti bakterií v prostředí na bázi vybraných biomarkerů.

Pro platformu ORPHEUS-HOPE byl navržen 3D tištěný čip s kultivační komorou pro objem 600 µl. Průtok byl optimalizován na 500 µl/min. Detekce bakterií byla založena na produkci alkalické fosfatázy bakterií *S. aureus*. Alkalická fosfatáza je metaloenzym, který je zapojen do procesu defosforylace. Pro detekci enzymatické aktivity byla použita elektrochemická detekce. Elektrochemická detekce byla založena na enzymatickém štěpení elektrochemicky inaktivního 1-naftyl fosfátu na elektrochemicky aktivní 1-naftol. Testování čipu bylo prováděno pomocí detekce 1-naftolu diferenční pulzní voltametrií s detekčním limitem 20 nM (S/N = 3). Dále byl optimalizován způsob zachycení bakteriálních buněk *S. aureus*. Pro zachycení byly použity maghemitové nanočástice s různou modifikací; kolagenem, glukózou, grafenem, zlatem, kyselinou hyaluronovou a kombinací grafenu a zlata nebo grafenu a glukózy. Za předpokladu, že jsou v prostředí přítomny nízké koncentrace bakterií, byla důležitá

optimalizace kultivace bakterií s jednotlivými magnetickými nanočásticemi, což bylo prováděno inkubací bakterií s nanočásticemi, promýváním částic a pozorováním růstu bakterií na promytých částicích.

Z výše zmíněných magnetických nanočástic s různou modifikací poskytovaly nejefektivnější výsledky částice modifikované kombinací grafenu a glukózy. Limit detekce celého testu, který zahrnoval zachycení bakterií a jejich detekci za provozu dálkového zařízení, byla stanovena na 30 bakterií na 1 µl.

Lukas Nejdl[1]
Jiri Kudr[1]
Kristyna Cihalova[1]
Dagmar Chudobova[1]
Michal Zurek[1]
Ludek Zalud[2]
Lukas Kopecny[2]
Frantisek Burian[2]
Branislav Ruttkay–
  Nedecky[1,2]
Sona Krizkova[1,2]
Marie Konecna[1,2]
David Hynek[1,2]
Pavel Kopel[1,2]
Jan Prasek[2]
Vojtech Adam[1,2]
Rene Kizek[1,2]

[1]Department of Chemistry and
Biochemistry, Faculty of
Agronomy, Mendel University
in Brno, Czech Republic
[2]Central European Institute of
Technology, Brno University of
Technology, Czech Republic

Research Article

Remote-controlled robotic platform ORPHEUS as a new tool for detection of bacteria in the environment

Remote-controlled robotic systems are being used for analysis of various types of analytes in hostile environment including those called extraterrestrial. The aim of our study was to develop a remote-controlled robotic platform (ORPHEUS-HOPE) for bacterial detection. For the platform ORPHEUS-HOPE a 3D printed flow chip was designed and created with a culture chamber with volume 600 μL. The flow rate was optimized to 500 μL/min. The chip was tested primarily for detection of 1-naphthol by differential pulse voltammetry with detection limit (S/N = 3) as 20 nM. Further, the way how to capture bacteria was optimized. To capture bacterial cells (*Staphylococcus aureus*), maghemite nanoparticles (1 mg/mL) were prepared and modified with collagen, glucose, graphene, gold, hyaluronic acid, and graphene with gold or graphene with glucose (20 mg/mL). The most up to 50% of the bacteria were captured by graphene nanoparticles modified with glucose. The detection limit of the whole assay, which included capturing of bacteria and their detection under remote control operation, was estimated as 30 bacteria per μL.

Additional supporting information may be found in the online version of this article at the publisher's web-site

1 Introduction

Remote sensing is a rapidly developing branch [1]. Progress in the field of electronics and technology constantly restricts the requirement of manpower to carry out dangerous work. The current third generation of "smart" robots richly equipped with sensors can be used in extreme environments (sea depths, space, volcanos). The emphasis is placed mainly on the effective communication and remote control, which gives to the operator a perfect control of the robot and the real-time transmission of an image to the operator's station. Space rovers need a considerable amount of electricity to move and power their equipment, so energy-efficient scientific devices are important for remote sensing [2]. Extraterrestrial environment shows the extremes of temperature, salinity,

dryness, radiation [3, 4] and amorphous land components are similar to the composition of the soil resulting from volcanic igneous rocks [5–7]. The electrochemical applications are suitable for the analysis of such hostile environment and, moreover, for miniaturization to be a part of remote sensing devices [8]. Currently an automated technique is being developed to detect the presence of microorganisms, which should facilitate the collection and detection of samples in the environment for humans hardly accessible. Like terrestrial extremophile organisms, Mars also may have some analogous niches such as sulfur-rich subsurface areas for chemoautotrophic organisms, rocky areas for endolithic communities, cold environment, and the permafrost regions [9]. Therefore, it is necessary to have a robust instrument capable to detect the presence of bacteria based on selected biomarker(s) as some unspecific enzymes.

Alkaline phosphatase (ALP) belonging to above mentioned enzymes is a metalloenzyme involved in the dephosphorylation process. It is a catalyst of the hydrolysis of phosphoric acid monoester to phosphoric acid and alcohol in the alkaline environment [10, 11]. Phosphoric acid

Correspondence: Dr. Rene Kizek, Brno University of Technology, Zemedelska 1, CZ-613 00 Brno, Czech Republic
E-mail: kizek@sci.muni.cz
Fax: +420-5-4521-2044

Abbreviations: ALP, alkaline phosphatase; **CFU**, colony forming unit; **DOF**, degrees of freedom; **LBM**, Luria Bertani medium; **MP**, magnetic particle; **SECM**, scanning electrochemical microscope; **SPE**, screen-printed electrode

Colour Online: See the article online to view Figs. 1–7 in colour.

is represented in most living organisms [10], including extremophilic microorganisms [12, 13], where it affects the metabolism of macroergic phosphate bonds. Thus, it is not surprising that the ALP is produced during the growth and sporulation of various bacterial strains (*Staphylococcus aureus* [14], *Bacillus cereus*, and *Bacillus amyloliquefaciens* [15–17], *Escherichia coli* [18], thermophilic bacteria [19] such as *Thermotoga neapolitana*, *Thermus caldophilus*, *Thermus thermophilus*, *Bacillus stearothermophilus*, *Pyrococcus abyssi*, and *Deinococcus radiodurans*, which is able to live in a radioactive environment [20–22]).

For detection of enzymatic activity, electrochemical detectors (ECD) can provide competitive advantages with respect to other detection systems such as portability, low cost, and low power requirements [23–25]. Additionally, ECD can analyze turbid samples, can be easily miniaturized [26], and requires electrodes that can be fabricated using low cost instrumentation [27]. Recently it can be observed that the interest in 3D printing technology for manufacturing of flow chip and equipment has been growing [28–31]. Described technology (lab-on-a-chip) can be extended to the mobile platform (lab-on-a-robot) [26, 32, 33]. More recently, the first integrated system capable of performing remote analysis of air samples using microchip-CE was presented [33]. The screen-printed electrodes (SPEs) can be used as a suitable detectors in CE microchips [34]. Thus, the technology becomes more accessible in new robotic controls and applications are developed [32, 35–41].

The aim of our study was to create a remote-controlled robotic platform (ORPHEUS-HOPE) capable of carrying different types of detectors for remote-controlled exploration of extreme environments. Combination of the robotic platform ORPHEUS-HOPE and a 3D printed flow chip can perform remote detection of *S. aureus* based on ALP activity, which could be applied also for other bacterial strains. The electrochemical detection was based on enzymatic cleaving of electrochemically inactive 1-naphthyl phosphate to electrochemically active 1-naphthol. Modified magnetic particles (MPs) within the chip were used to attach bacteria from a solution.

2 Materials and methods

2.1 Chemicals and pH measurement

Chemicals used in this study were purchased from Sigma-Aldrich® (St. Louis, Missouri, USA) in ACS purity (chemicals meet the specifications of the American Chemical Society), unless noted otherwise. Washing solutions were prepared in ultrapure water obtained using reverse osmosis equipment Aqual 25 (Aqual, Brno, Czech Republic). The deionized water was further purified by using apparatus Direct-Q 3 UV Water Purification System equipped with the UV lamp from Millipore (Billerica, Massachusetts, USA). The resistance was established to 18 MΩ/cm. The pH was measured using pH meter WTW (inoLab, Weilheim, Germany).

2.2 Fabrication of 3D microfluidic chip

The microfluidic chip was 3D processed in Blender 2.65 (Blender foundation, Amsterdam, the Netherlands) and further edited in NetFabb (Netfabb, Parsberg, Germany). The model was opened in the program G3D maker (DO-IT, Straznice Czech Republic) and printed by Easy 3D maker (DO-IT). Chip was printed with an accuracy of [x, y, z] 0.1/0.1/0.08 mm under the following conditions: the size of the chip was [x, y, z] 40/40/35 mm. Acrylonitrile butadiene styrene was used as a material (DO-IT), and every printed chip was fitted with five input tubes with a diameter of 0.5 mm, one output tube with diameter 0.5 mm, two electromagnets and thermostatic system.

2.3 SPE design and fabrication

Electrode system was designed and fabricated as a disposable planar three-electrode sensor in LabSensNano laboratories (Brno University of Technology, Czech Republic). The properties of design and optimization can be found in the following papers [42, 43]. The working electrode was fabricated using a special carbon paste for electrodes of electrochemical sensors BQ221 (DuPont, Wilmington, USA), reference and auxiliary electrodes were printed using the Ag/AgCl (65:35) paste 5874 (DuPont) and Pt-based paste 5545 (Electroscience, King of Prussia, USA), respectively.

2.4 Microfluidic analysis with differential pulse voltammetric detection

The flow cell for SPE was designed in the shape of a cuboid with sides of 1 cm (width) × 1.5 cm (height) × 3 cm (length). The reaction zone was dimensioned for 20 μL of analyte with 0.7 mm wide inlet and outlet channel. The sample was injected using a peristaltic pump (Amersham Biosciences, Uppsala, Sweden). After optimization of the automated flow system additionally a peristaltic pump Minipuls®3 (Gilson, Middleton, USA) and a stirred water bath WB-4MS (Biosan, Riga, Latvia) were used. Changes of reduction signals were measured with a potentiostat PGSTAT 101 (Metrohm, Herisau, Switzerland) and the results were evaluated by the Software NOVA 1.8 (Metrohm). Settings of the potentiostat were as follows: initial potential -0.2 V, end potential $+0.5$ V, step potential 0.005 V, modulation amplitude 0.1 V, modulation time 0.004 s, interval time 0.1 s, deposition time 60 s, and equilibration time 5 s. For ALP detection 50 mM carbonate buffer (32 mM Na_2CO_3 and 68 mM $NaHCO_3$) pH 9.9 with 1 mM 1-naphthyl phosphate was used [44].

2.5 Preparation of modified MPs

Maghemite nanoparticles (MPs) were prepared according to the following approach [45, 46]. Shortly, 10 g of $FeCl_3.6H_2O$ was dissolved in 800 mL of MilliQ grade water under vigorous stirring at room temperature. 2 g of

NaBH$_4$ solution in ammonia (3.5% v/v, 100 mL) was then quickly added to the mixture. In a short time after the reduction reaction occurrence, the temperature of the system was increased to 100°C and kept constant for 2 h. After 12 h at room temperature, this magnetic product was separated by application of an external magnet and washed several times with water. The step of solution heating to boiling is very important, because it leads to stabilization of particles and oxidizing of Fe^{2+} to Fe^{3+}. Graphite oxide (GPO) was prepared from graphite flakes (Sigma-Aldrich) by the Hummers method [47]. Graphene (GR) was prepared by reduction of GPO by hydrazine [48]. MPs were modified with the following chemicals: graphene (GR), hyaluronic acid (HA), gold (GO), glucose (GL), collagen (CO), graphene (GR) and glucose (GL), graphene (GR), and gold (GO). The experimental details can be found in Supporting Information 1.

2.6 Cultivation of *S. aureus*

S. aureus (NCTC 8511) was obtained from the Czech Collection of Microorganisms, Faculty of Science, Masaryk University, Brno, Czech Republic. Strains were stored in the form of a spore suspension in 20% v/v glycerol at −20°C. Prior to use, the strains were thawed and the glycerol was removed by washing with distilled water in this study. More details about their cultivation are shown in Supporting Information 4.

2.7 Preparation of *S. aureus* samples with modified MPs and microbiological determination of growth curves

A 2.5 mg of each type of modified MPs was weighted and these particles were diluted in 0.5 mL of water in ACS purity. These solutions were resuspended in ultrasonic bath Sonorex digital 10p (Bandelin, Berlin, Germany) for 5 min at 25°C and then added to 0.5 mL of the *S. aureus* bacterial culture (3.7 × 10^7 CFU/mL) and incubated in the thermomixer Comfort (Eppendorf, Hamburg, Germany) at 37°C, 600 rpm for 1 h. After incubation, MPs were separated and washed three times with 1000 μL of phosphate buffer (pH 7) tempered at 37°C. To the washed particles, 1000 μL of cultivation LBM (Himedia, Mumbai, India) containing tryptone 10 g/L, yeast extract 5 g/L, and NaCl 5 g/L was added at 37°C. Particles with LBM were incubated in the thermomixer Comfort (Eppendorf) for 1 h at 37°C and 600 rpm. After cultivation the solution was pipetted off and the MPs with adhered bacteria were three times washed with phosphate buffer (pH 7). To the washed particles 1 mL of the LBM was added and the solution was incubated at the same conditions as mentioned above. The inoculum with released bacteria was then pipetted to the microplate and the absorbance using Multiskan EX (Thermo Fisher Scientific, Bremen, Germany) was measured, and the analysis of the growth curves was used to assess the amount and growth ability of the isolated bacteria. Then the growth curves were measured. Measurements were carried out at time 0, and then in 30 min intervals for 10 h at 37°C, at the wavelength 600 nm. The obtained data were analyzed in graphical form of growth curves for each modification of the MPs.

2.8 UV/Vis spectrophotometry

Absorption spectra were recorded using a SPECORD 210 spectrophotometer (Analytik Jena, Jena, Germany) in λ = 405 nm and λ = 600 nm. Automated spectrophotometric measurements were carried out using chemical analyzer BS-400 (Mindray, Schenzen, China). Alkaline phosphatase was determined in the suspensions of bacteria with culture medium of appropriate cell density (OD$_{600\,nm}$ = 1.5 AU). In a reaction catalyzed by ALP the substrate *p*-nitrophenyl phosphate is split to *p*-nitrophenol and inorganic phosphate. ALP activity is determined kinetically and is based on the rate of *p*-nitrophenol concentration increase during reaction. Experimental details are in Supporting Information 5.

2.9 Mathematical treatment of data and estimation of detection limits

Mathematical analysis of the data and their graphical interpretation was realized by software Matlab (version 7.11., Math-Works, USA). Results are expressed as mean ± SD unless noted otherwise (EXCEL®, Microsoft, USA). Limits of detection S/N = 3, were calculated, whereas N was expressed as SD of noise determined in the signal domain unless stated otherwise [49].

3 Results

3.1 Bacterial activity of ALP

The whole concept of electrochemical detection is based on the capturing of bacteria producing ALP on modified MPs [50] and the subsequent multiplication of bacteria in a culture chamber (Fig. 1A). ALP produced by bacteria cleaves the 1-naphthyl phosphate (electrochemically inactive) to the electrochemically active product 1-naphthol (Fig. 1B), which can be easily detected by voltammetry (Fig. 1C). ALP activity was measured in two bacterial species; Gram-positive *S. aureus* and Gram-negative *E. coli*, with cell count of (2 × 10^7 cells per mL). *S. aureus* showed 2.3 times higher ALP activity in comparison with *E. coli* (Fig. 1D). Due to this fact, the further experiments were performed with *S. aureus* as a model microorganism. It was found that *S. aureus* ALP activity was linear within the range from 1 × 10^5 to 420 × 10^5 per mL with R^2 = 0.9989 (Fig. 1E). Reaction kinetics of the ALP was also studied (Fig. 1F). Michaelis Menten constant of bacterial ALP was determined as 2.3 mM. Finally, the dependence of the *S. aureus* (2 × 10^7 cells per mL) growth was monitored photometrically (λ = 600 nm) in the time interval 0–140 min simultaneously with the formation of the *p*-nitrophenol
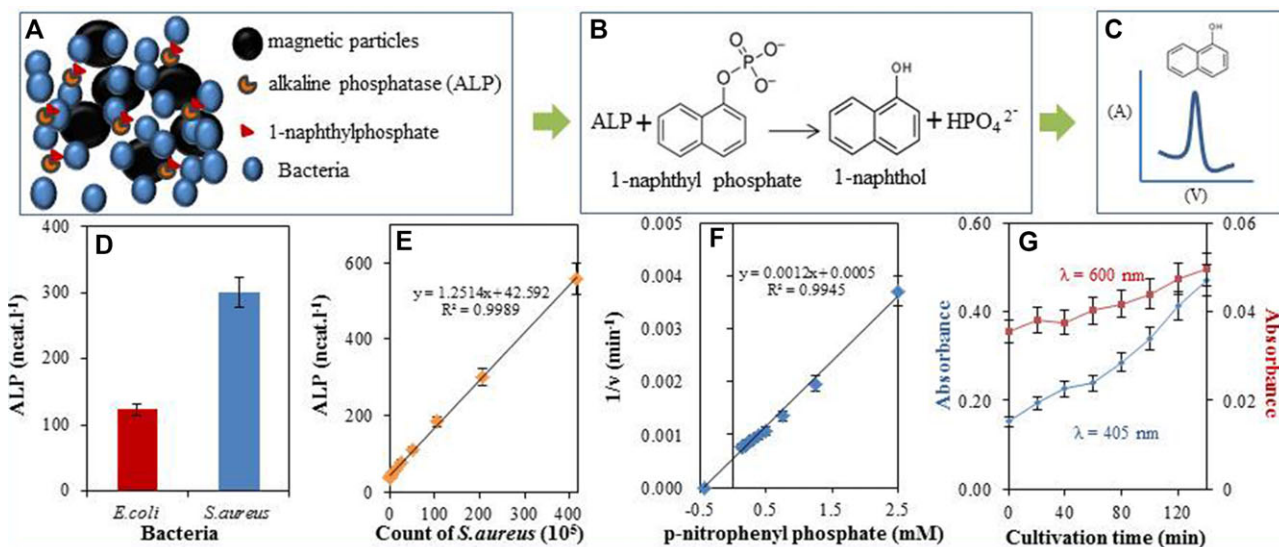
Figure 1. (A) The mechanism, which enables electrochemical detection of *S. aureus*. Alkaline phosphatase (ALP) released by *S. aureus*, which has been captured by magnetic particles (MPs), cleaves 1-naphthyl phosphate in naphthol and phosphate. (B) Chemical reaction, which is the principle of *S. aureus* electrochemical detection. (C) The electrochemical signal of 1-naphthol. (D) Spectrophotometrically measured activity of ALP released by *E. coli* compared with *S. aureus*. (E) The dependence of ALP activity on count of *S. aureus*. (F) Reaction kinetics of ALP. (G) The dependence of *p*-nitrophenol ($\lambda = 405$ nm) and *S. aureus* ($\lambda = 600$ nm) absorbance on mixture of alkaline phosphatase photometric substrate and *S. aureus* (2×10^7 cells) cultivation time.

($\lambda = 405$ nm), a product of the ALP reaction with the photometric ALP substrate (*p*-nitrophenyl phosphate) (Fig. 1G).

3.2 Optimization of 1-naphthol detection

Screen printed electrodes were characterized by cyclic voltammetry (CV) in 50 mM carbonate buffer (pH 9.9). Primarily, the dependence of the CV signals of 10 mM 1-naphthol on the changes of scan rate (5–500 mV/s) was investigated (Fig. 2A-a1). The growing trend of electrochemical signal and peak potentials (Ep) was observed as the scan rate (v) was increased (Fig. 2A-a2). There is no peak in reverse scan, which means that electrode reaction is totally irreversible, which is consistent with Ep shift. A graph of cathodic peak currents (Ip, c) versus square root of scan rate ($v^{1/2}$) was plotted (Fig. 2A-a3). This relationship indicates that diffusion mechanisms are involved in the electrochemical reaction. The same characterization of SPE was done by flow analysis under 500 μL/min (Fig. 2B-b1). When the scan rate (v) was increased, the electrochemical signal of naphthol was increasing in the same way as without flow (Fig. 2B-b3). Peak currents exhibit logarithmic dependence on $v^{1/2}$, which suggests that flow of analyte affects diffusion mechanism of its reduction and partly some adsorption-controlled mechanism can run. This was confirmed by the slope of logIp dependence on log$v$ (not shown). The substrate temperature was optimized by DPV of 2 μM naphthol. From the range of 5–40°C, the optimal temperature of 35 $\pm$ 2°C for 1-naphthol detection was selected (Fig. 2C-c1). Accumulation time was the next parameter, which we were interested in. The difference between the peak height with accumulation time 60 and 120

s was lower than SPE RSD, so accumulation time 60 s was chosen as the best. The calibration curve of 1-naphthol with regression coefficient $R^2 = 0.999$ was measured (Fig. 2C-c3) and the LOD and LOQ were calculated (Table 1).

3.3 Characterization of MPs

Between various magnetic metal oxides, the cubic spinel structured maghemite is technologically important and is widely used for the production of permanent magnetic materials [51, 52]. In this experiment variously modified maghemite MPs were characterized. MPs without surface modification are shown in the first SEM photo (Fig. 3A). The different structures of MPs with modified surface can be recognized in other SEM micrographs (Figs. 3C, E, G, I, K, M, and O). It can be seen that maghemite nanoparticles form clusters unequally deployed on each carrier surface and thus provide perfect paramagnetic properties. The average current of unmodified MPs is 70 nA. The presence of Fe in MPs with typical Skα a Skβ signals corresponding to positions of Fe was proved by X-ray fluorescence (XRF) analysis (Fig. 3B). Taking into account that all MPs have γ-Fe$_2$O$_3$ core, all X-ray spectra are nearly the same. The peak positions are always the same and only their intensity is changing (Figs. 3D, F, H, J, L, N, and P). MPs modified by tetrachlorauric acid are the only exception, because gold nanoparticles are presented after reduction (trisodium citrate dihydrate) on the surface (zoomed part of Fig. 3P).

For scanned current level of collagen modified MPs there are typical transitions between recorded current levels of 40 nA. It means that distribution and the amount of
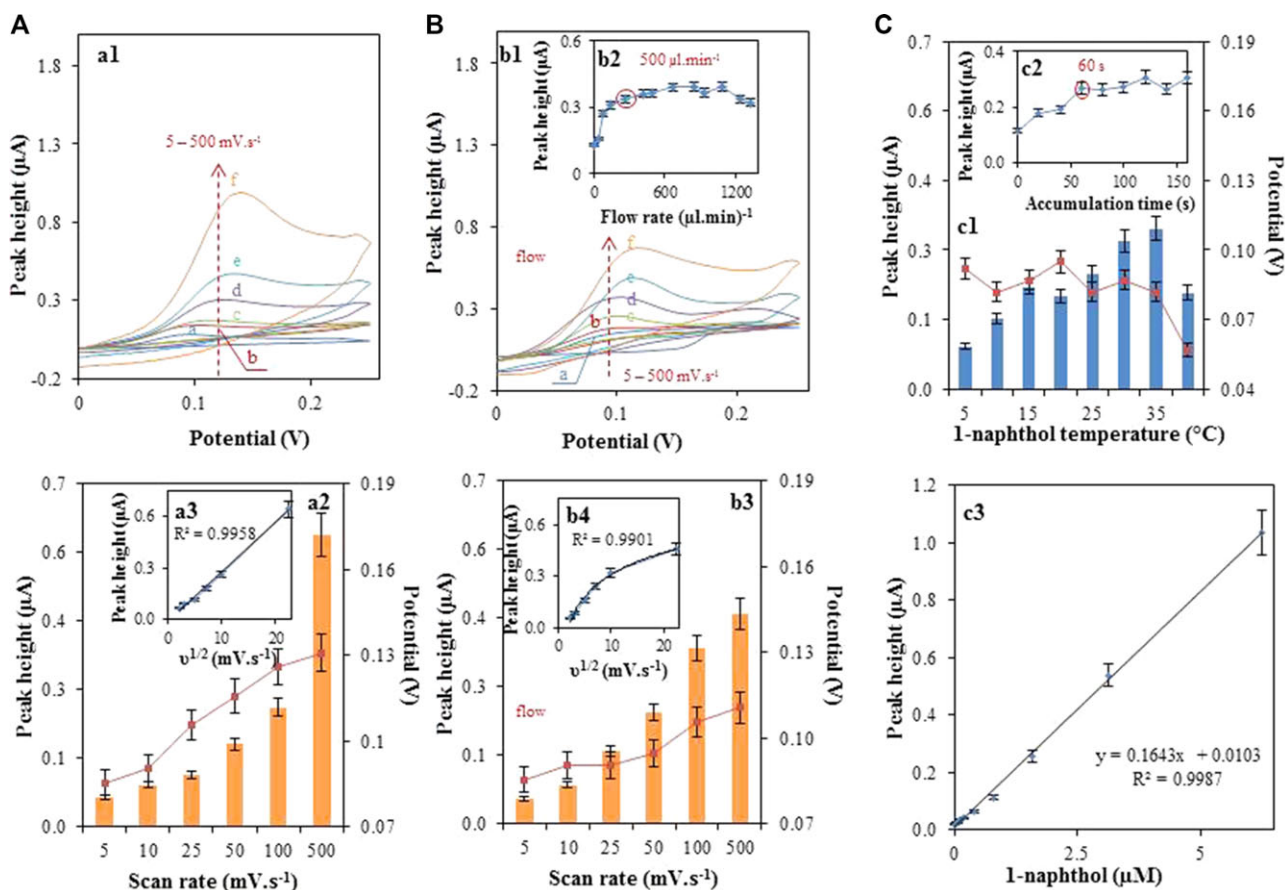
Figure 2. (A) Characterization of 1-naphthol analysis using SPEs. (a1) Cyclic voltammograms measured at different scan rates (mV/s), a = 5, b = 10, c = 25, d = 50, e = 100, and f = 500. (a2) The dependence of the peak height on applied scan rate (5–500 mV/s). (a3) The dependence of the peak height on square root of scan rate. (B) Characterization of 1-naphthol analysis in flow using SPEs. (b1) Cyclic voltammograms measured at different scan rates same as a1. (b2) The dependence of peak height on applied flow rate (0–1300 μL/min). (b3) The dependence peak height on square root of scan rate the flow 500 μL/min. (C) Optimization of measurement by DPV. (c1) The dependence of peak height on temperature (5, 10, 15, 20, 25, 30, 35, and 40°C). (c2) The dependence of peak height on accumulation time (0–120 s). (c3) Calibration curve of 1-naphthol obtained by DPV under the optimized conditions (measurement temperature 35°C, flow rate 500 μL/min, accumulation time 60 s). In all cases the electrochemical response of 10 mM 1-naphthol was studied.

Table 1. Analytical parameters of electrochemical determination of 1-naphthol

Substance	Regression equation	Linear dynamic range (μM)	R^{2} [a]	LOD[b] (nM)	LOQ[c] (nM)	RSD (%)
1-naphthol	$y = 0.1643x + 0.0103$	0.079–6.25	0.999	20	79	6.5

a) Regression coefficients.
b) LOD of detector (S/N = 3).
c) LOQ of detector (S/N = 10).

electrochemical charge are completely different from the values of unmodified MPs (Fig. 3D). The significant changes of electrochemical current levels (30 nA) are shown in Fig. 3E, and the charge is spreading out of larger area. SECM record of hyaluronic acid modified MPs shows little units of MP in current level of 80 nA (Fig. 3H). SECM scan of gold-modified MPs is depicting unequal precipitation of gold on the surface of MPs. The higher current level recorded in this case was 70 nA (Fig. 3J). The graphene-modified MPs create greater units with current level of about 70 nA (Fig. 3L). The MPs modified by graphene and glucose create similar aggregates as in the previous case. In addition, the electrochemical charges are overlaying themselves, thus, particular parts of MPs cannot be recognized (Fig. 3M). The SECM record of MPs modified by graphene and gold nanoparticles differs from other records. These MPs bind specifically to macroelectrode and the difference between gold macroelectrode and immobilized MPs is 10 nA.
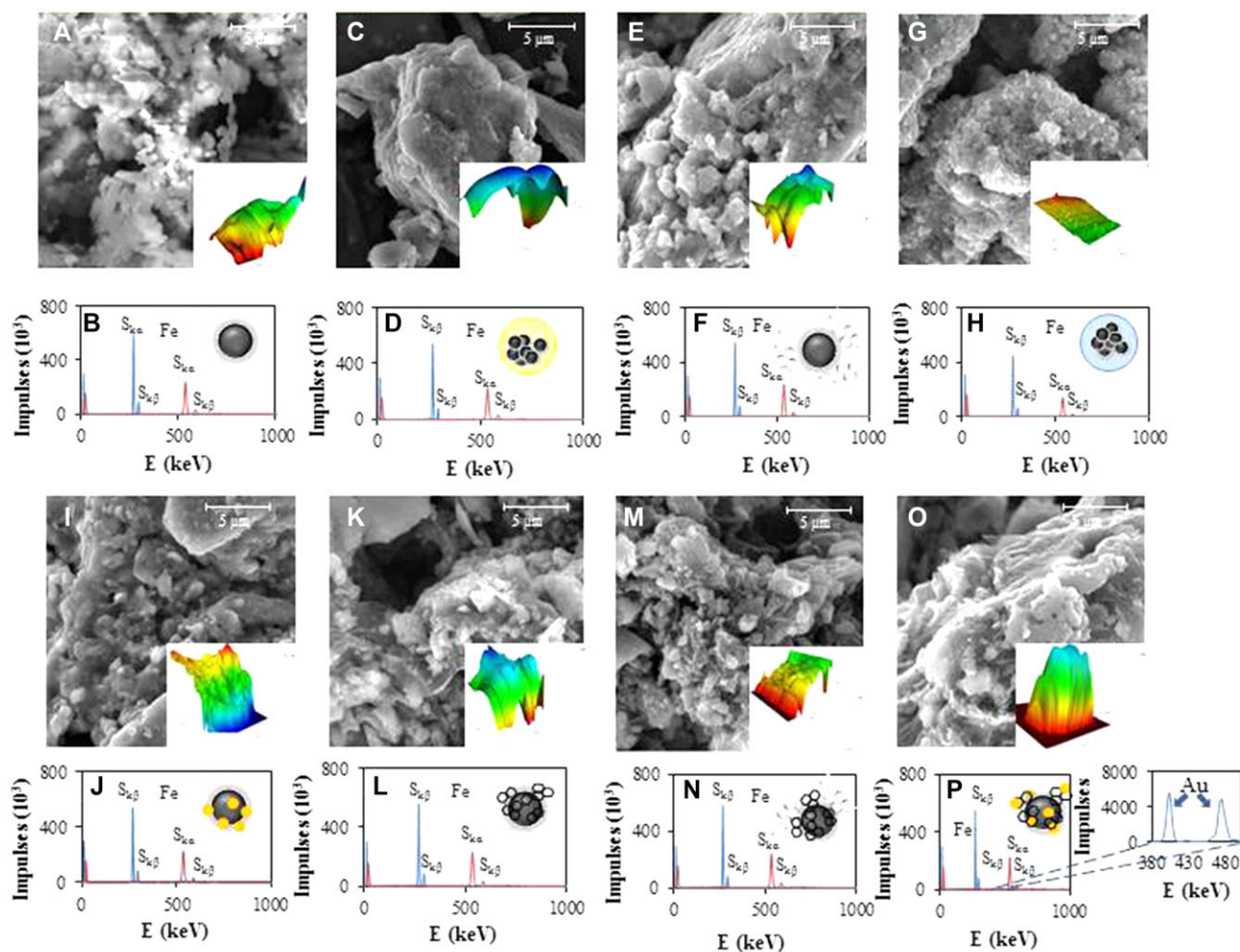
Figure 3. Characterization of different modifications of MPs. (A, B) Maghemite electron microscope image, 3D SECM image (range of current levels 10–80 nA) and XRF spectrum (with typical signals Skα and Skβ) of magnetic particles (MPs) without modification or modified with (C, D) 1% collagen, (E, F) 12.5 mg/mL glucose, (G, H) 12.5 mg/mL glucose and 1.25 mg/mL graphene, (I, J) gold nanoparticles (1 mM HAuCl$_4$), (K, L) 1.25 mg/mL graphene, (M, N) 20 mg/mL hyaluronic acid, and/or (O, P) 1.25 mg/mL graphene with gold nanoparticles (1 mM HAuCl$_4$).

3.4 Optimization of *S. aureus* isolation using modified MPs

The scheme of the sample preparation used for the analysis of growth curves is shown in Fig. 4A. Bacterial culture was isolated using magnetic separation. After separation of MPs from inoculated medium, incurred inoculum was measured under optimal conditions for 10 h (see Section 2.7). The absorbance values for *S. aureus* growth (volume 300 μL, amount of bacteria 3.7×10^7 CFU/mL) after application of 2.5 mg of MPs (1:1) modified in eight different ways were recorded (Fig. 4B-i). Stacked bar chart (Fig. 4J) shows the quantitative growth (CFU/mL) of *S. aureus* bacteria after cultivation on MPs, which differ by its modification. Recording of the CFU was conducted in the tenth hour of bacterial growth after cultivation with MPs according to scheme in Fig. 4A. Cultivation with MPs was run on a thermomixer at 20°C or at 37°C for 1 or 2 h at 600 rpm. The last suitable option for all

modifications of MPs has proved application of the temperature of 20°C with the duration of the 1 h, when the number of bacteria in all MPs except MPs modified by graphene with glucose (1.3×10^8 CFU/mL) ranged from 6.7×10^7 to 8.6×10^7 CFU/mL. Another possibility was to apply temperature of 37°C, again with a shaking period of 1 h with the number of bacteria in the range of 7.5×10^7 to 12.3×10^7 CFU/mL. Increasing CFU at the temperature of 20°C with a shaking period of 2 h confirmed us the fact that for capturing the bacteria on MPs the duration of shaking period plays more important role than temperature. In the case of MPs modified by graphene and gold, number of bacteria is significantly lower (6.3×10^7 CFU/mL^{-1}), but in other modifications of MPs bacterial counts ranged from 8.7×10^7 to 12.6×10^7 CFU/mL. However, the highest number of bacteria was captured by the MPs at application of the temperature of 37°C with a shaking period of 2 h. MPs modified by graphene and gold again showed the lowest value (4.3×10^7 CFU/mL), but for other
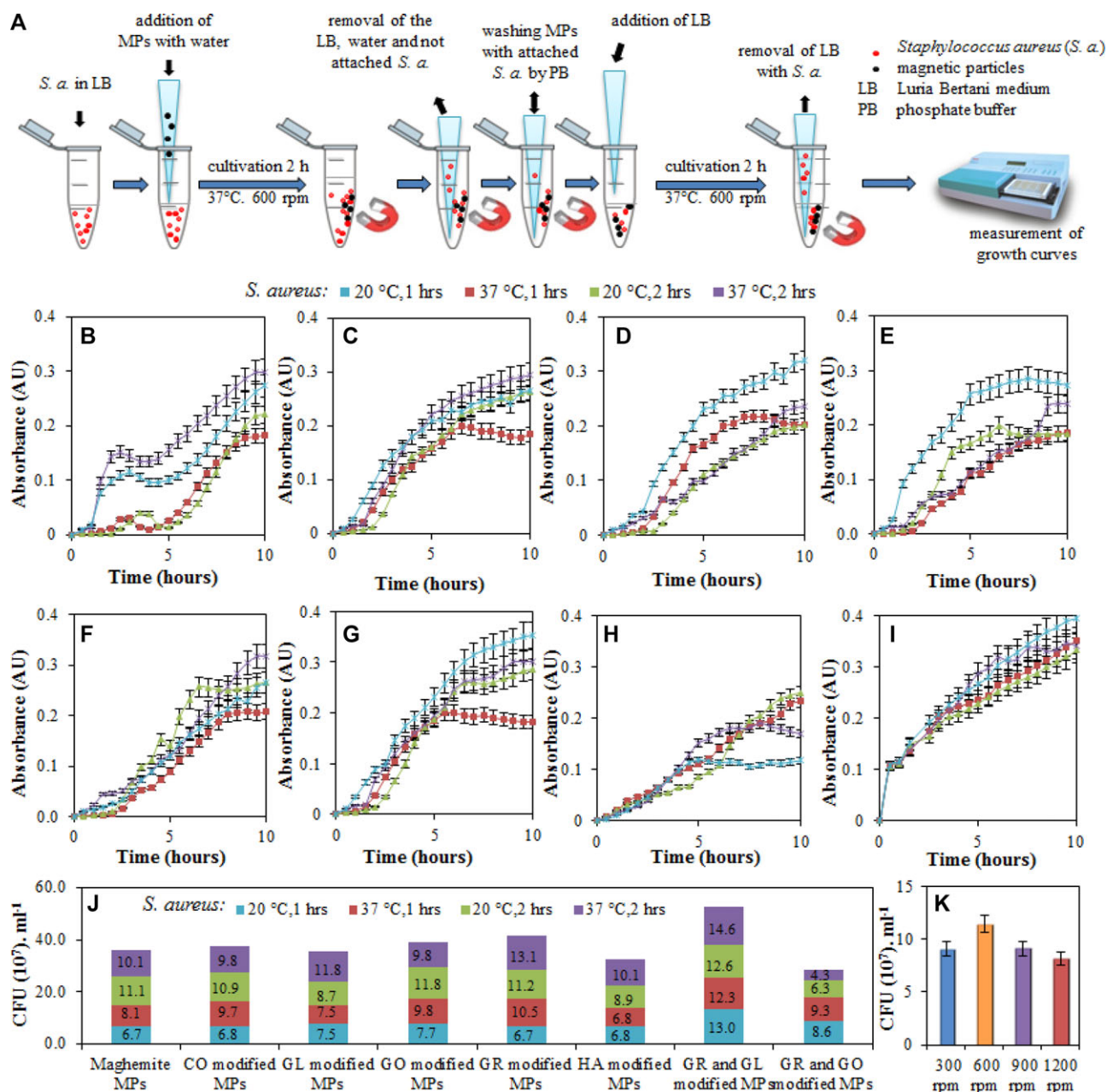
Figure 4. (A) The treatment of *S. aureus* with magnetic particles (MPs) before measurement of growth curves. (B) Dependence of washing buffer temperature and incubation time on *S. aureus* attached to MPs without modification, (C) collagen, (D) glucose, (E) graphene with gold nanoparticles, (F) gold nanoparticles, (G) graphene, (H) hyaluronic acid, (I) graphene with glucose. (J) Spectrophotometric determination of CFU 10^7 per microliter of *S. aureus* obtained by condition changes for different modified MPs (CO – collagen, GL – glucose, GO – gold nanoparticles, GR – graphene, HA – hyaluronic acid). (K) Spectrophotometric determination of CFU 10^7 per microliter of *S. aureus* affected by MPs modified with graphene and glucose after action of different intensity of rotation (300, 600, 900, and 1200 rpm).

modifications, the bacterial count was within the range from 9.8×10^7 to 14.6×10^7 CFU/mL. Best particles were determined as MPs modified by graphene with glucose, when the number of bacteria was determined as 1.46×10^8 CFU/mL after cultivation at 37°C for 2 h. By such modified MPs the

bacterial count values were higher for all applied temperatures and time conditions. This variant was then used for the next steps of the study and was further tested for determination of the optimal number of rotation to achieve the highest yield in terms of the growth of *S. aureus* (Fig. 4K).
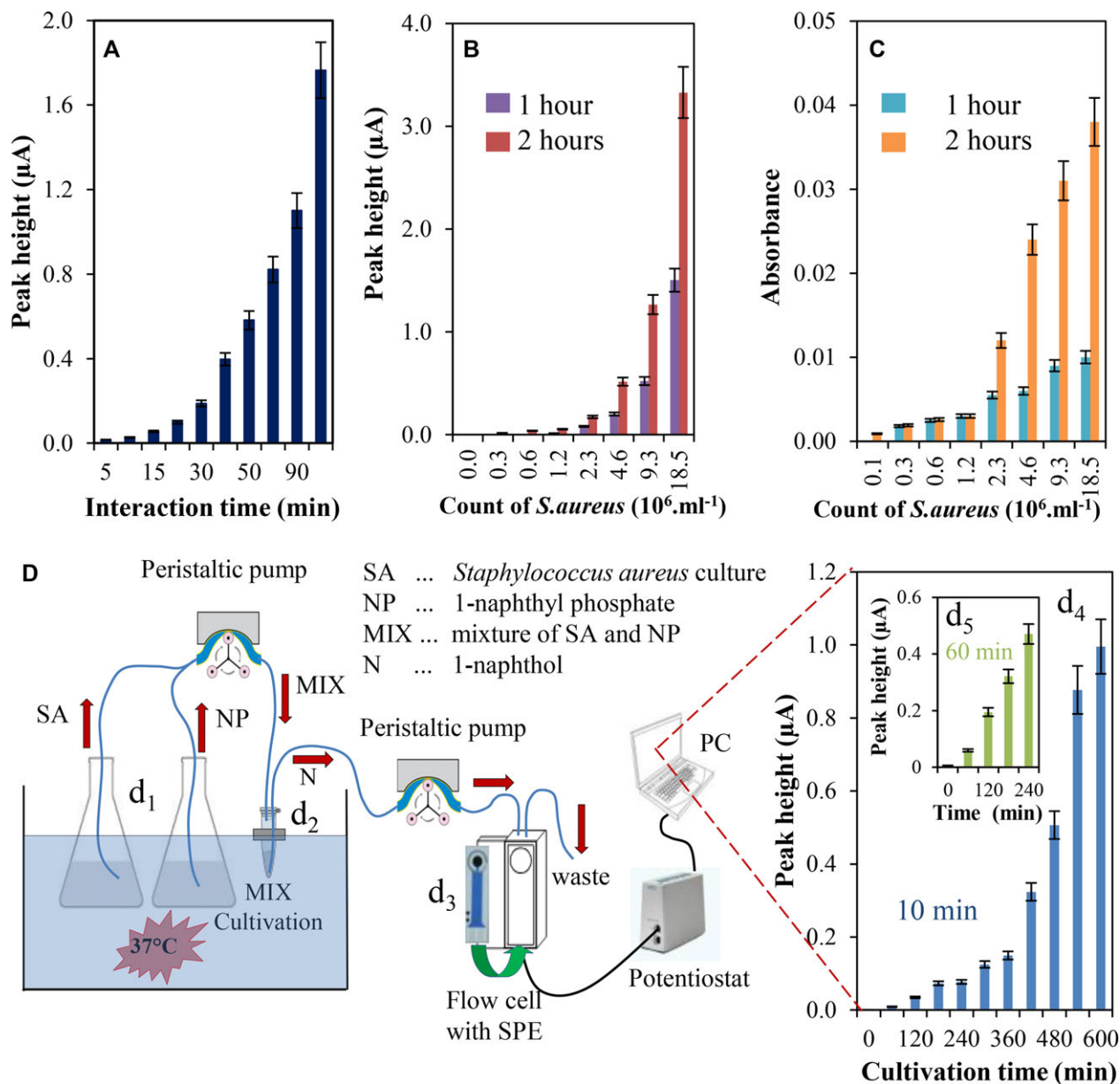
Figure 5. (A) The dependence of 1-naphthol peak height on time (5–120 min) of interaction between 1 mM 1-naphthyl phosphate and culture with same count of *S. aureus*. (B) Mixture of 1 mM 1-naphthyl phosphate and particular *S. aureus* culture was incubated for 1 h (violet line) and 2 h (red line). (C) The counts of *S. aureus* measured spectrometrically ($\lambda = 600$ nm) after 1 (blue line) and 2 h (orange line) of particular bacterial cell culture cultivation. (D) Scheme of the measuring system at laboratory conditions, d1 = stock solutions of *S. aureus* and 1 mM 1-naphthyl phosphate, d2 = mixing chamber, d3 = flow cell with screen printed electrode, d4 = in particular time part of growing *S. aureus* culture was mixed with 1-naphthyl phosphate and incubated for 10 and 60 min (d5).

3.5 Flow analysis of *S. aureus* using an automatic system

At first, the interaction time (5–120 min, 37°C) of 1 mM 1-naphthyl phosphate in 50 mM carbonate buffer (the substrate) and constant *S. aureus* concentration (18.5×10^6 per mL) was studied by electrochemistry. The electrochemical signal of 1-naphthol was increasing with the interaction time (Fig. 5A). One and/or 2 h long interaction (37°C) of different bacterial concentration ($0–18.5 \times 10^6$ mL) with the substrate was investigated. More than 100% increase in electrochemical signal after 2 h of interaction was revealed (Fig. 5B), which corresponds to the reproducing *S. aureus* cells (Fig. 5C).

The optimization of the automatic flow system for *S. aureus* detection was performed. The scheme of this system is shown in Fig. 5D. *S. aureus* bacteria were attached to MPs modified with graphene and glucose according to previous optimization and were mixed with 19 mL of LBM (Fig. 5D-d1). LBM heated at 37°C in water bath and stirred by magnetic stirrer to aerate the medium. MPs were also attached by the

Table 2. Analytical parameters of electrochemical determination of bacteria

Substance	Regression equation	Linear dynamic range (bacteria)	R^{2} [a]	LOD[b] (bacteria/µL)	LOQ[c] (bacteria/µL)	RSD (%)
Bacteria – ALP	$y = 0.1788x - 0.1481$	120–18.5×106	0.9828	30	120	8.5

a) Regression coefficients.
b) LOD of detector (S/N = 3).
c) LOQ of detector (S/N = 10).

stirrer so that MPs could not affect the electroanalysis. The substrate (37°C) together with bacterial culture was pumped to the reaction chamber (Fig. 5D-d2) by peristaltic pump. The multichannel peristaltic pump was used and tubes of the same length and diameter were dosing the substrate and analyte precisely (1:1). The mixture of uncleaved substrate, *S. aureus*, LBM, and finally 1-naphthol was pumped to flow detection cell by another peristaltic pump at flow rate of 500 µL/min (Fig. 5D-d3). After 10 (Fig. 5D-d4) and 60 min long interaction (Fig. 5D-d5) the signal of 1-naphthol was analyzed. The LOD and LOQ was estimated as 3 S/N (Table 2).

3.6. ORPHEUS-HOPE

ORPHEUS-HOPE is a rugged robotic system designed to measure bacterial contamination in field conditions and can be easily equipped with additional devices, such as radiation and biological sensors. The robot is able to go across obstacles up to 20 cm high and work well during night or in bad visibility conditions, because it has sensitive full user control. The maximum ascension angle is 31° and is limited only by adhesion. Robot performs well in mud and snow, but it is also fully capable of indoor operation. Even the control of the robot is ready for narrow space operations, the operator can reverse the control of the robot, thus it can switch the meaning of forward and backward. The robot itself is made to be easy-to-decontaminate. The whole robot is waterproof, with three-layers resistive paintings and the whole mechanical construction is made to repel or at least not keep liquids. Only few parts of the robot are marked as nondecontaminable and have to be replaced (tires, antennas, and two cables). The robot may be operated wirelessly or by wire. Designed for compliance with various MIL-STD-810F environmental and MIL-STD-461E EMI/EMC standards, the ORPHEUS-HOPE robotic system offers exceptional low-temperature operation and resistance to shock and vibration profiles experienced by jet and terrestrial transport. The robot is equipped with two cameras: the first pan/tilt color camera with both manual and automatic parameter settings, and the second rigid high resolution color camera for precise analyte placement and measurement. The robot has one degree of freedom (DOF) manipulator with suction device, while other sensors can be either rigidly connected to the robot body or also placed on the manipulator. The maximum payload on the end of the manipulator is 0.85 kg.

The robot may be controlled with the help of so-called visual telepresence. The operator wears head mounted display (HMD) with inertial measurement unit (IMU) as shown in Fig. 6A. The head-movement data from the IMU are mathematically transformed and sent to the robot. The robot has a camera manipulator with two DOFs (left-to-right and up-to-down). The camera manipulator basically copies movements of the operator's head, while the image from the camera is transmitted to the operator's station and displayed to the operator. Therefore, the operator should feel to be in the robot's place and can intuitively control the main camera movements.

One of the key issues of ORPHEUS-HOPE project is precise "manipulation" with the suction device (Fig. 6B). Positioning of the suction device is performed in four DOFs. In general we are able to move on the Earth's surface and control the "deepness" of the suction device penetration to the liquid. All of these movements have to be precise to be able to achieve precise detection in various conditions. The necessary precision is in the order of millimetres. The control of the robot is currently provided by an operator. Thus, the feedback control loop consists of mechanical parts (motors, gearboxes, and wheels), and electronics, but also human-to-robot user interface and the operator itself.

Rugged operator's station (Fig. 6A-d) was made to control the robot in tactical conditions. The operator's station is battery operated, but may work also continuously when connected to DC power. It is made to allow easy and intuitive operation control of the robot. The movements of robot body are controlled by a joystick, and the other functions are controlled by a series of buttons.

The electronics system of ORPEHUS-HOPE is distributed, and all communication is done via Ethernet or RS-485. Freescale Coldfire microcontroller is responsible for motor control and accelerometer data acquisition, Rabbit microcontroller communicates to the chemical analysis sensors. The cameras and microphone are connected to axis framegrabber. All the main processors, as well as the wireless module are connected to the 5-port miniature Ethernet switch.

3.7 Remote controlled detection of *S. aureus*

Automated analysis of sample containing *S. aureus* bacteria is performed by ORPHEUS-HOPE robotic platform, which is equipped with a flow detection device (Fig. 7A) including the MPs within a chip. The detection flow device consists of a movable robotic arm (Fig. 7A-a), which enables to dip a suction tube (Fig. 7A-b) into the liquid. The resistance detector is responsible for a precise suction tube immersion to analyte. The depth of suction tube immersion can also
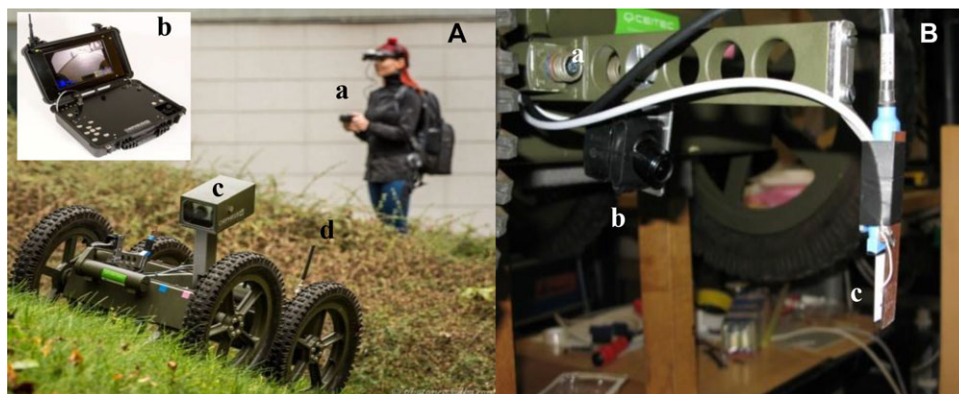
Figure 6. (A) Remote control of ORPHEUS-HOPE (robot dimensions: 881 × 590 × 426 mm, wheel diameter: 426 mm, weight: 42 kg, battery operation: 90 min to 4 h, operating temperatures: −32 to 78°C, charging voltage: 18–32 V, max. charging current: 5 A, max. speed: 3.6 km/h, max. obstacle height: 20 cm, climb ability: 31°, max. reach of cable: 100 m, wireless max. reach: 1 km). Person (a) with joystick and HMD with IMU, which receives signal from camera (b) with two degrees of freedom via wireless transmitter (c). Rugged operator's station (b), which enables to control the robot in tactical conditions. (B) Sensor arm (a) with video camera (b), suction device and submerge detector (c).
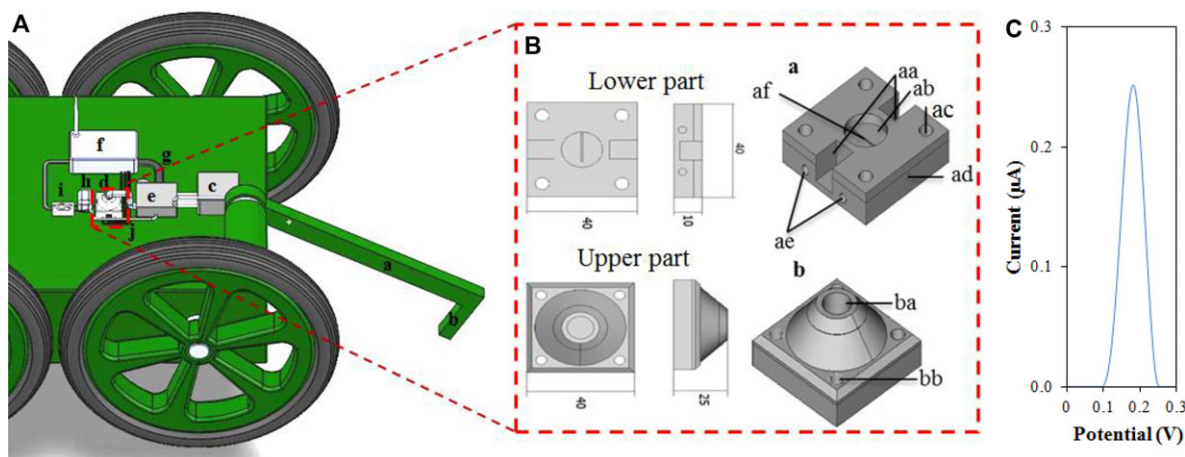

Figure 7. (A) Manipulator (a) with suction device (b) collects the samples of potentially contaminated water with *S. aureus*. It goes through peristaltic pump (c) in tube to cultivation chamber (d) with magnetic particles (MPs) inside, where *S. aureus* is attached to particles. Excess of water is pumped from cultivation chamber to the waste collector (e) by peristaltic pump, which receives instructions from control unit with integrated potentiostat (f) via communication wires (g). Then, LBM is pumped to cultivation chamber (d) from waste collector (e), which serves also as a reagent stock. After several hours of *S. aureus* reproducing, culture is mixed with 1-naphthyl phosphate in a mixing chamber (h). After particular time of alkaline phosphatase (ALP) cleaving of 1-naphthyl phosphate to 1-naphthol, mixture is pumped to flow cell (i), where 1-naphthol can be detected by potentiostat (f). The waste goes through tube (j) to the waste collector (e). The control unit with an integrated potentiostat (Fig. 7AB/a-f) controls actions of peristaltic pump, heating of the chip and magnetic stirring within the chip. The control unit is thus responsible for the alternate turning off and the turning on of the electromagnets. (B) Scheme of the cultivation chip: (a) Lower part of the chip. Places for electromagnets (aa), cultivation chamber (ab), holes for attaching with the cover (ac), the hole for temperature symbol (ad), holes for heating elements (ae) and the outflow canal (af). (b) Upper part of the chip. Hole for injection needles (ba) and holes for attaching to lower part of the chip (bb). (C) DPV signal of 1-naphthol, confirming the presence of bacteria in the sample.

be controlled visually by robotic arm camera. The peristaltic pump (Fig. 7A-c) doses stock solution of the substrate (1-naphthyl phosphate in 50 mM carbonate buffer, pH 9.9) to a cultivation chip (Fig. 7A-d). The control unit with an integrated potentiostat (Fig. 7A-f) controls actions of peristaltic pump, heating of the chip, and magnetic stirring within the chip. All electronic devices are connected via communication cables (Fig. 7A-g). The analyzed sample is mixed with substrate (1:1) in the reaction chamber (Fig. 7A-h) and the mixture is cultivated there for 1 h, then it is pumped with a speed of 500 μL/min to a flow electrode cell (Fig. 7A-i), where electrochemical detection takes place at accumulation time of 60 s.

Cultivation chip consists of two parts (Fig. 7B-a and B-b). Lower part of the chip includes two opposite holes, where two electromagnets are placed (Fig. 7B-aa) next to cultivation chamber of 500 μL volume (Fig. 7B-ab). Every corner has hole to merge upper and lower part of the chip

(Fig. 7B-ac). A thermistor is placed under the cultivation chamber to control the temperature of the chip, which was set to 37°C (Fig. 7B-ad), and the heating elements on the sides of chip (Fig. 7B-ae). The outflow canal is placed in the lower part of the chip (Fig. 7B-af). The upper part of the chip has hole for inflow tube (Fig. 7B-ba) and also holes for the lower part attachment (Fig. 7B-bb).

Robotic remote controlled analysis of *S. aureus* sample (30 cells/µL) was performed automatically. The sample (500 µL) was pumped via suction device to the cultivation chamber, where *S. aureus* was attached to MPs. After attaching period, the excess of solution was pumped to waste collector and LBM (600 µL) was pumped there. During cultivation time (2 h) the sample was stirred. Then, the sample was mixed with substrate for 1 h in mixing chamber. Finally, the sample was pumped (500 µL/min) to flow cell with electrode and electrochemical signal, which detected the presence of bacteria, was recorded at accumulation time of 60 s (Fig. 7C).

4 Discussion

In this study, the remote detection of the bacterial contamination using a microfluidic chip is showed. Automatic detection of microorganisms on the mobile unit allows sampling and determination of the presence of microorganisms in the hardly accessible environment. Mobile unit with a detection device controlled remotely by human is demanding on simple and reliable samples processing and detection itself [53, 54]. Detection of bacterial contamination by classic methods is generally time-consuming and hardly automated, as well as immuno- and PCR-based techniques. Alkaline phosphatase is a thermostable enzyme, which is active in extreme temperatures, even at 308°C [19]. It is produced by wide range of bacteria and archaebacteria [55] and it has been shown that the phosphatases can be used as a marker of life in extreme conditions [55]. Electrochemical detection of ALP using a 1-naphthyl-phosphate is a commonly used and elaborated detection step in electrochemical sensors and immunoassays [44, 56].

The detection limit of 30 bacterial cells per microliter was obtained, which is approximately 50 times higher than beads-based immunoextraction technique for *S. aureus* detection, but the detection limit in this work was obtained after 2 h of cultivation, while in work from Krizkova et al. the enrichment cultivation was performed for 5 h [14]. Whole protocol was possible to realize by remote-controlled robot, which makes it usable for monitoring of distant areas without contamination. Moreover, the process can be easily modified by addition of a specific substrate or an inhibition agent. There are two possibilities how to improve our system for handling several samples. The first possibility is to use a rinsing mechanism with ethanol. The second possibility is to involve several chambers (ca. 10) and each chamber would be used only once.

Wagstaffe et al. developed determination of *S. aureus* in a liquid medium by method based on fluorescence immunoassay, which allows the detection of thermonuclease enzyme produced by *S. aureus* and thus provides confirmation of the presence of *S. aureus* in vitro [57]. The work of Valeriani et al. dealt with methods for the rapid control of the aquatic environment intended for recreational purposes. Their goal was to find a rapid and reliable method for identification of low concentrations of the bacteria *S. aureus*. Using traditional culture microbiological methods is time consuming and therefore molecular techniques are a better choice. Approach of these authors is based on the specific amplification of genomic DNA using the universal primers (23S rDNA), and specific real-time PCR amplification. This procedure refers to the high sensitivity and specificity, which is typical for nucleic acids. The method is suitable for monitoring hygiene and detection of indicators of bacterial pollution [58].

Sensitive method based on fluorescence of carboxymethyl chitosan with cadmium nanoparticles (CMC-CD QDS) was developed by Wang et al. for the specific detection of *S. aureus* in foods and the environment. After a certain period of cultivation of CMC-Cd QDs with *S. aureus* and after removal of the free fluorescent QDs, the bacteria were observed by fluorescence microscopy. The cells of *S. aureus* were recognized as being applicable bioprobes. Using this method, the authors also managed to identify *E. coli* and *Bacillus subtilis* [59].

LaGier et al. aimed at studying the purity and water quality. They decided to develop a biosensor to achieve rapid identification of on-site sampling. The sensor device can simultaneously detect harmful algae, indicators of faecal pollution, and human pathogens in water. The sensor is capable of electrochemical detection of the presence of nucleic acids for matching parameters such as the size, low cost, and low power requirements [60].

In the above mentioned methods, tedious sample preparation procedures are used and a lot of expensive chemicals are required, whereas the capture of bacteria on the MPs and their subsequent proliferation in culture medium and electrochemical detection represents another way, which is unique in its simplicity, versatility, and feasibility.

In summary, due to the availability of technologies, and even more sophisticated detection techniques (lab-on-a-chip) that are compatible with different types of robotic platforms (lab-on-a-robot), it can be expected that the development of remote-controlled robotic systems will be of interest for more and more research teams. In this study, we develop a robotic platform ORPHEUS-HOPE, which can carry different types of detectors. The robot is manufactured as a highly reliable device and meets the requirements of military standards. For this reason robotic platform was designed and printed by a 3D printer. A flow chip was used for electrochemical detection of bacteria. The low chip was completed with the modified MPs that allow capturing and cultivating bacteria inside the chip. In addition, we automated detection system for remote detection of bacteria.

5 References

[1] Noyhouzer, T., Mandler, D., *Electroanalysis* 2013, *25*, 109–115.

[2] Kimura, R., Yoshida, T., *J. Nucl. Sci. Technol.* 2013, *50*, 998–1010.

[3] Crisler, J. D., Newville, T. M., Chen, F., Clark, B. C., Schneegurt, M. A., *Astrobiology* 2012, *12*, 98–106.

[4] Kounaves, S. P., Hecht, M. H., West, S. J., Morookian, J. M., Young, S. M. M., Quinn, R., Grunthaner, P., Wen, X. W., Weilert, M., Cable, C. A., Fisher, A., Gospodinova, K., Kapit, J., Stroble, S., Hsu, P. C., Clark, B. C., Ming, D. W., Smith, P. H., *J. Geophys. Res.-Planets* 2009, *114*, 1–12.

[5] Bish, D. L., Blake, D. F., Vaniman, D. T., Chipera, S. J., Morris, R. V., Ming, D. W., Treiman, A. H., Sarrazin, P., Morrison, S. M., Downs, R. T., Achilles, C. N., Yen, A. S., Bristow, T. F., Crisp, J. A., Morookian, J. M., Farmer, J. D., Rampe, E. B., Stolper, E. M., Spanovich, N., *Science* 2013, *341*, 1–5.

[6] Meslin, P. Y., Gasnault, O., Forni, O., Schroder, S., Cousin, A., Berger, G., Clegg, S. M., Lasue, J., Maurice, S., Sautter, V., Le Mouelic, S., Wiens, R. C., Fabre, C., Goetz, W., Bish, D., Mangold, N., Ehlmann, B., Lanza, N., Harri, A. M., Anderson, R., Rampe, E., McConnochie, T. H., Pinet, P., Blaney, D., Leveille, R., Archer, D., Barraclough, B., Bender, S., Blake, D., Blank, J. G., Bridges, N., Clark, B. C., DeFlores, L., Delapp, D., Dromart, G., Dyar, M. D., Fisk, M., Gondet, B., Grotzinger, J., Herkenhoff, K., Johnson, J., Lacour, J. L., Langevin, Y., Leshin, L., Lewin, E., Madsen, M. B., Melikechi, N., Mezzacappa, A., Mischna, M. A., Moores, J. E., Newsom, H., Ollila, A., Perez, R., Renno, N., Sirven, J. B., Tokar, R., de la Torre, M., d'Uston, L., Vaniman, D., Yingst, A., *Science* 2013, *341*, 1–6.

[7] Stolper, E. M., Baker, M. B., Newcombe, M. E., Schmidt, M. E., Treiman, A. H., Cousin, A., Dyar, M. D., Fisk, M. R., Gellert, R., King, P. L., Leshin, L., Maurice, S., McLennan, S. M., Minitti, M. E., Perrett, G., Rowland, S., Sautter, V., Wiens, R. C., *Science* 2013, *341*, 1–4.

[8] Lukow, S. R., Kounaves, S. R., *Electroanalysis* 2005, *17*, 1441–1449.

[9] Onstott, T. C., McGown, D. J., Bakermans, C., Ruskeeniemi, T., Ahonen, L., Telling, J., Soffientino, B., Pfiffner, S. M., Sherwood-Lollar, B., Frape, S., Stotler, R., Johnson, E. J., Vishnivetskaya, T. A., Rothmel, R., Pratt, L. M., *Microb. Ecol.* 2009, *58*, 786–807.

[10] Chander, R., Thomas, P., *J. Food Biochem.* 2001, *25*, 91–103.

[11] Santos, I. C., Mesquita, R. B. R., Bordalo, A. A., Rangel, A., *Talanta* 2012, *98*, 203–210.

[12] Nicolaus, B., Moriello, V. S., Lama, L., Poli, A., Gambacorta, A., *Orig. Life Evol. Biosph.* 2004, *34*, 159–169.

[13] Seckbach, J., Oren, A., in: Hoover, R. B. (Ed.), *Instruments, Methods, and Missions for Astrobiology III*, Spie-Int Soc Optical Engineering, Bellingham 2000, pp. 89–95.

[14] Krizkova, S., Jilkova, E., Krejcova, L., Cernei, N., Hynek, D., Ruttkay-Nedecky, B., Sochor, J., Kynicky, J., Adam, V., Kizek, R., *Electrophoresis* 2013, *34*, 224–234.

[15] Panosian, T. D., Nannemann, D. P., Watkins, G. R., Phelan, V. V., McDonald, W. H., Wadzinski, B. E., Bachmann, B. O., Iverson, T. M., *J. Biol. Chem.* 2011, *286*, 8043–8054.

[16] Iverson, T. M., Panosian, T. D., Birmingham, W. R., Nannemann, D. P., Bachmann, B. O., *Biochemistry* 2012, *51*, 1964–1975.

[17] Ramesh, A., Sharma, S. K., Joshi, O. P., Khan, I. R., *Indian J. Microbiol.* 2011, *51*, 94–99.

[18] Koksharov, M., Lv, C. Q., Zhai, X. H., Ugarova, N., Huang, E., *Protein Expr. Purif.* 2013, *90*, 186–194.

[19] Takano, Y., Edazawa, Y., Kobayashi, K., Urabe, T., Marumo, K., *Earth Planet. Sci. Lett.* 2005, *229*, 193–203.

[20] Nitzan, Y., Ashkenazi, H., *Photochem. Photobiol.* 1999, *69*, 505–510.

[21] Brim, H., McFarlan, S. C., Fredrickson, J. K., Minton, K. W., Zhai, M., Wackett, L. P., Daly, M. J., *Nat. Biotechnol.* 2000, *18*, 85–90.

[22] Sghaier, H., Bouchami, O., Desler, C., Lazim, H., Saidi, M., Rasmussen, L. J., Ben Hassen, A., *Ann. Microbiol.* 2012, *62*, 493–500.

[23] Wang, J., *Electroanalysis* 2005, *17*, 1133–1140.

[24] Vandaveer, W. R., Pasas-Farmer, S. A., Fischer, D. J., Frankenfeld, C. N., Lunte, S. M., *Electrophoresis* 2004, *25*, 3528–3549.

[25] Nugen, S. R., Asiello, P. J., Connelly, J. T., Baeumner, A. J., *Biosens. Bioelectron.* 2009, *24*, 2428–2433.

[26] Garcia, C. D., Henry, C. S., *Electroanalysis* 2005, *17*, 1125–1131.

[27] Garcia, C. D., Henry, C. S., *Electroanalysis* 2005, *17*, 223–230.

[28] Zhao, L. L., Lee, V. K., Yoo, S. S., Dai, G. H., Intes, X., *Biomaterials* 2012, *33*, 5325–5332.

[29] Dragone, V., Sans, V., Rosnes, M. H., Kitson, P. J., Cronin, L., *Beilstein J. Org. Chem.* 2013, *9*, 951–959.

[30] Mathieson, J. S., Rosnes, M. H., Sans, V., Kitson, P. J., Cronin, L., *Beilstein J. Nanotechnol.* 2013, *4*, 285–291.

[31] Kitson, P. J., Rosnes, M. H., Sans, V., Dragone, V., Cronin, L., *Lab. Chip.* 2012, *12*, 3267–3271.

[32] Lamberti, F., Sanna, A., Paravati, G., Montuschi, P., Gatteschi, V., Demartini, C., *Int. J. Adv. Robot. Syst.* 2013, *10*, 1–11.

[33] Berg, C., Valdez, D. C., Bergeron, P., Mora, M. F., Garcia, C. D., Ayon, A., *Electrophoresis* 2008, *29*, 4914–4921.

[34] Wang, J., Pumera, M., Chatrathia, M. P., Rodriguez, A., Spillman, S., Martin, R. S., Lunte, S. M., *Electroanalysis* 2002, *14*, 1251–1255.

[35] Tao, W. J., Ou, Y., Feng, H. T., *Int. J. Adv. Robot. Syst.* 2012, *9*, 1–9.

[36] Dobie, G., Pierce, S. G., Hayward, G., *NDT E Int.* 2013, *58*, 10–17.

[37] Kulich, M., Chudoba, J., Kosnar, K., Krajnik, T., Faigl, J., Preucil, L., *IEEE Trans. Educ.* 2013, *56*, 18–23.

[38] Li, D. R., Liu, Y., Yuan, X. X., *Sci. China-Inf. Sci.* 2013, *56*, 1–14.

[39] Susperregi, L., Martinez-Otzeta, J. M., Ansuategui, A., Ibarguren, A., Sierra, B., *Int. J. Adv. Robot. Syst.* 2013, *10*, 1–9.

[40] da Costa, E. T., Neves, C. A., Hotta, G. M., Vidal, D. T. R., Barros, M. F., Ayon, A. A., Garcia, C. D., do Lago, C. L., *Electrophoresis* 2012, *33*, 2650–2659.

[41] Valdez, D. C., Garcia, C. D., Ayon, A. A., *Analog Integr. Circuits Process* 2012, *71*, 29–38.

[42] Prasek, J., Trnkova, L., Gablech, I., Businova, P., Drbohlavova, J., Chomoucka, J., Adam, V., Kizek, R., Hubalek, J., *Int. J. Electrochem. Sci.* 2012, *7*, 1785–1801.

[43] Nejdl, L., Merlos, M. A. R., Kudr, J., Ruttkay-Nedecky, B., Konecna, M., Kopel, P., Zitka, O., Hubalek, J., Kizek, R., Adam, V., *Electrophoresis* 2014, *35*, 393–404.

[44] Zitka, O., Krizkova, S., Krejcova, L., Hynek, D., Gumulec, J., Masarik, M., Sochor, J., Adam, V., Hubalek, J., Trnkova, L., Kizek, R., *Electrophoresis* 2011, *32*, 3207–3220.

[45] Magro, M., Sinigaglia, G., Nodari, L., Tucek, J., Polakova, K., Marusak, Z., Cardillo, S., Salviulo, G., Russo, U., Stevanato, R., Zboril, R., Vianello, F., *Acta Biomater.* 2012, *8*, 2068–2076.

[46] Prucek, R., Tucek, J., Kilianova, M., Panacek, A., Kvitek, L., Filip, J., Kolar, M., Tomankova, K., Zboril, R., *Biomaterials* 2011, *32*, 4704–4713.

[47] Hummers, W. S., Offeman, R. E., *J. Am. Chem. Soc.* 1958, *80*, 1339–1339.

[48] Stankovich, S., Dikin, D. A., Piner, R. D., Kohlhaas, K. A., Kleinhammes, A., Jia, Y., Wu, Y., Nguyen, S. T., Ruoff, R. S., *Carbon* 2007, *45*, 1558–1565.

[49] Long, G. L., Winefordner, J. D., *Anal. Chem.* 1983, *55*, A712–A724.

[50] Paleček, E., Kizek, R., Havran, L., Billova, S., Fojta, M., *Anal. Chim. Acta* 2002, *469*, 73–83.

[51] Laurent, S., Forge, D., Port, M., Roch, A., Robic, C., Elst, L. V., Muller, R. N., *Chem. Rev.* 2008, *108*, 2064–2110.

[52] Gupta, A. K., Naregalkar, R. R., Vaidya, V. D., Gupta, M., *Nanomedicine* 2007, *2*, 23–39.

[53] Karl, D. M., *Nat. Rev. Microbiol.* 2007, *5*, 759–769.

[54] Foing, B. H., Stoker, C., Zavaleta, J., Ehrenfreund, P., Thiel, C., Sarrazin, P., Blake, D., Page, J., Pletser, V., Hendrikse, J., Direito, S., Kotler, J. M., Martins, Z., Orzechowska, G., Gross, C., Wendt, L., Clarke, J., Borst, A. M., Peters, S. T. M., Wilhelm, M. B., Davies, G. R., Team, I. E., *Int. J. Astrobiol.* 2011, *10*, 141–160.

[55] Baltar, F., Aristegui, J., Gasol, J. M., Yokokawa, T., Herndl, G. J., *Microb. Ecol.* 2013, *65*, 277–288.

[56] Hayat, A., Andreescu, S., *Anal. Chem.* 2013, *85*, 10028–10032.

[57] Wagstaffe, S. J., Hill, K. E., Williams, D. W., Randle, B. J., Thomas, D. W., Stephens, P., Riley, D. J., *Anal. Chem.* 2012, *84*, 5876–5884.

[58] Valeriani, F., Giampaoli, S., Buggiotti, L., Gianfranceschi, G., Spica, V. R., *Water Sci. Technol.* 2012, *66*, 2305–2310.

[59] Wang, X. H., Du, Y. M., Li, Y., Li, D., Sun, R. C., *J. Biomater. Sci.Polym. Ed.* 2011, *22*, 1881–1893.

[60] LaGier, M. J., Jack, W. F. B., Goodwin, K. D., *Mar. Pollut. Bull.* 2007, *54*, 757–770.

5.3 3D tištěný čip pro detekci meticilin-rezistentní bakterie *S. aureus* značené zlatými nanočásticemi

5.3.1 Vědecký článek III

CHUDOBOVA, D.; **CIHALOVA, K.**; SKALICKOVA, S.; ZITKA, J.; MERLOS RODRIGO, M. A.; MILOSAVLJEVIC, V.; HYNEK, D.; KOPEL, P.; VESELY, R.; ADAM, V.; KIZEK, R. 3D-printed chip for detection of methicillin-resistant *Staphylococcus aureus* labeled with gold nanoparticles. *Electrophoresis*, 2015, roč. 36. č. 3, s. 457-466. ISSN 0173-0835.

Další práce se zabývala detekcí již cílenou na bakterii *S. aureus* s rezistencí vůči β-laktamovým antibiotikům, meticilin-rezistentní *S. aureus*. MRSA je nebezpečný patogen především v nemocničním prostředí, kde způsobuje závažné zdravotní problémy, a to po celém světě *(Fridkin, Hageman, Morrison, Sanza, Como-Sabetti, Jernigan, Harriman, Harrison, Lynfield, Farleya Active Bacterial Core, 2005; Klevens a kol., 2007).* V současné době je diskuze o problematice zvyšující se rezistence a rychlé diagnostice rezistentních bakteriálních kmenů stále častější a vyhledávaná *(Weigel a kol., 2007).* Proto bylo cílem této studie vytvořit konstrukci účinné platformy pro detekci patogenní bakterie MRSA. Princip detekce spočívá v molekulárně-biologickém stanovení přítomnosti genu rezistence vůči β-laktamovým antibiotikům *mecA*, který je přítomný ve stafylokokové chromozomální kazetě mec právě u MRSA *(Shore a kol., 2005).*

V této studii byl pomocí 3D tisku zkonstruován čip, který splňuje podmínky pro kultivaci bakterií, izolaci DNA, polymerázovou řetězovou reakci a detekci amplifikovaného genu za použití zlatých nanočástic jako indikátorových sond přítomnosti genu *mecA*, tedy přítomnosti MRSA. Konfirmace přítomnosti MRSA ve vzorcích byla založena na specifické interakci mezi *mecA* genem a zlatou nanočásticí modifikovanou komplementárním oligonukleotidem (AuNPs sonda) a kolorimetrické detekci této reakce. Při kolorimetrické detekci dochází k agregaci zlatých nanočástic v případě nepřítomnosti komplementárního fragmentu DNA k AuNPs sondě.

Byly analyzovány reálné vzorky, z nichž dva byly pozitivní na přítomnost *mecA* genu. Vzorky obsahující bakterii MRSA poukázaly na přítomnost *mecA* genu barevnou

změnou, která byla zřejmá na první pohled v porovnání s kontrolními vzorky neobsahujícími geny *mecA*. Agregace AuNPs sond se projevuje 75% poklesem absorbance (λ = 530 nm) a změnou velikosti nanočástic zlata z 3 ± 0,05 na 4 ± 0,05 nm (n = 5).

Naše studie poskytuje jednokrokovou identifikaci *mecA* genu pomocí platformy využívající rychlou, finančně nenákladnou a snadno použitelnou kolorimetrickou detekci MRSA z různých vzorků.

Dagmar Chudobova[1,2]
Kristyna Cihalova[1,2]
Sylvie Skalickova[1,2]
Jan Zitka[1,2]
Miguel Angel Merlos Rodrigo[1,2]
Vedran Milosavljevic[1,2]
David Hynek[1,2]
Pavel Kopel[1,2]
Radek Vesely[3]
Vojtech Adam[1,2]
Rene Kizek[1,2]

[1]Department of Chemistry and Biochemistry, Mendel University in Brno, Brno, Czech Republic
[2]Central European Institute of Technology, Brno University of Technology, Technicka, Brno, Czech Republic
[3]Department of Traumatology, Faculty of Medicine, Masaryk University, Trauma Hospital of Brno, Ponavka, Brno, Czech Republic

Research Article

3D-printed chip for detection of methicillin-resistant *Staphylococcus aureus* labeled with gold nanoparticles

Methicillin-resistant *Staphylococcus aureus* (MRSA) is a dangerous pathogen occurring not only in hospitals but also in foodstuff. Currently, discussions on the issue of the increasing resistance, and timely and rapid diagnostic of resistance strains have become more frequent and sought. Therefore, the aim of this study was to design an effective platform for DNA isolation from different species of microorganisms as well as the amplification of *mecA* gene that encodes the resistance to β-lactam antibiotic formation and is contained in MRSA. For this purpose, we fabricated 3D-printed chip that was suitable for bacterial cultivation, DNA isolation, PCR, and detection of amplified gene using gold nanoparticle (AuNP) probes as an indicator of MRSA. Confirmation of the MRSA presence in the samples was based on a specific interaction between *mecA* gene with the AuNP probes and a colorimetric detection, which utilized the noncross-linking aggregation phenomenon of DNA-functionalized AuNPs. To test the whole system, we analyzed several real refractive indexes, in which two of them were positively scanned to find the presence of *mecA* gene. The aggregation of AuNP probes were reflected by 75% decrease of absorbance ($\lambda = 530$ nm) and change in AuNPs size from 3 ± 0.05 to 4 ± 0.05 nm ($n = 5$). We provide the one-step identification of *mecA* gene using the unique platform that employs the rapid, low-cost, and easy-to-use colorimetric method for MRSA detection in various samples.

Keywords:

3D-printed chip / Gold nanoparticles / Methicillin resistant / Pathogen detection / *Staphylococcus aureus*   DOI 10.1002/elps.201400321

1 Introduction

Staphylococcus aureus is a Gram-positive abundantly occurring bacterium, while methicillin-resistant *S. aureus* (MRSA) is a live-threatening pathogen occurring mainly in hospitals [1, 2]. In the period between 2011 and 2012, MRSA was reported in 41.2% of *S. aureus* isolated and typed in healthcare-associated infections in European hospitals [3]. From this it is clear that MRSA was and still is primarily considered as a healthcare-associated pathogen, however, later on, these bacteria were also detected in food products, especially in meats [4]. Therefore, these bacteria can be isolated both from inpatients as well as people not related to medi-

cal environment, and this epidemiological change is important in distribution of infections caused by this pathogen [5].

The design and fabrication of new diagnostic systems necessitates working in collaboration between different disciplines. Recent PCR-based assays for MRSA identification have significantly reduced the time needed to find a diagnosis for a patient [6, 7]. Most importantly, small, field-capable analysis portable systems are critical for timely detection and prevention efforts even in the case of MRSA. Thus, rapid and inexpensive diagnostic systems with high sensitivity and specificity are essential to prevent MRSA to be an emerging public health threat. There are different techniques such as optical, mechanical, magnetic, and electrochemical, and their combinations in detection of biologically related analytes. In labeling strategies, fluorescent dye molecules, quantum dot labels, and metal colloid labels are generally used [8–10]. Recent results show that combining the advantages of microelectromechanical system technology and molecular methods is promising for detection of MRSA [11]. The integration of magnetic bead based detection with loop-mediated

Correspondence: Dr. Rene Kizek, Department of Chemistry and Biochemistry, Mendel University in Brno, Zemedelska 1, CZ-613 00 Brno, Czech Republic
E-mail: kizek@sci.miuni.cz
Fax: +420-5-4521-2044

Abbreviations: AuMNP, gold magnetic nanoparticle; **AuNP**, gold nanoparticle; **CV**, cyclic voltammetry; **MRSA**, methicillin-resistant *Staphylococcus aureus*; **SECM**, scanning electrochemical microscopy

---

Colour Online: See the article online to view Figs. 1–4 in colour.

isothermal amplification process was recently studied by Wang et al. The hybridization was conducted using magnetic bead conjugated complementary probes. Cell lysis, DNA isolation, and amplification using loop-mediated isothermal amplification technique were performed in the microfluidic device only [12]. From these mentioned facts, it follows that there is a great development in the field of manufacturing well portable devices for medical purposes.

Thus, the main objective of this study was to suggest and construct a novel integrated microfluidic platform for rapid and accurate detection of MRSA strain. This platform is capable of colorimetric determination of the target analyte in a microfluidic reactor, rendering its usefulness for in vitro diagnostics. Confirmation of the MRSA presence in the samples is based on isolation of DNA, amplification of *mecA* gene encoding the resistance to β-lactam antibiotics, and specific interaction between *mecA* gene with the gold nanoparticle (AuNP) probes and a colorimetric detection, which utilized the noncross-linking aggregation phenomenon of DNA-functionalized AuNPs.

2 Materials and methods

2.1 Chemicals, preparation of DI water, and pH measurement

Chemicals used in this study were purchased from Sigma-Aldrich (St. Louis, USA) in ACS purity unless noted otherwise. The DI water was prepared using reverse osmosis equipment Aqual 25 (Czech Republic). The DI water was further purified using apparatus MiliQ Direct QUV equipped with the UV lamp. The resistance was 18 MΩ. The pH was measured using pH meter WTW inoLab (Weilheim, Germany).

2.2 Cultivation of bacteria strains

Nonresistant strains (*S. aureus, Escherichia coli, Salmonella typhimurium, and Lactobacillus rhamnosus* and resistant strains of *S. aureus* (MRSA) were obtained from the Czech Collection of Microorganisms, Faculty of Science, Masaryk University, Brno, Czech Republic. The strains were stored as a spore suspension in 20% v/v glycerol at −20°C. Prior to use in this study, the strains were thawed and the glycerol was removed by washing with distilled water. The composition of cultivation medium was as follows: tryptone 10 g/L, yeast extract 5 g/L, NaCl 5 g/L, pH of the cultivation medium was adjusted at 7.4 before sterilization. The sterilization of the media was carried out at 121°C for 30 min in sterilizer (Tuttnauer 2450EL, Beit Shemesh, Israel). The prepared cultivation media were inoculated with bacterial culture into 25 mL Erlenmeyer flasks. After inoculation, the bacterial cultures were cultivated for 24 h in a shaker at 600 rpm and 37°C.

2.3 Preparation of hospital samples and their cultivation

2.3.1 Wound swabs of patients with bacterial infections

Clinical specimens including wound swabs were obtained from Trauma Hospital of Brno, Czech Republic. There were selected patients aged less than 60 years without diagnosis of diabetes mellitus, peripheral arterial disease, nonsmoker, not under corticosteroid treatment or immunosuppressant in regular medication. The smears were taken from infected wounds with the consent of patients. Particularly, smear was made from a patient with perianal abscess before the medical treatment, during treatment using Biseptol (Pabianickie Zaklady Farmaceutyzcne Polfa S.A., Pabianice, Poland), and at regular intervals after completion of the treatment. Smear was done by rolling motion at the site of skin puncture using a sterile swab sampling. The swab was then placed into a tube with a semisolid transport medium and carefully sealed and labeled. Marked tubes were immediately microbiologically examined. The swab sample was left in the transport medium intended for the storage of the sample before culturing in the appropriate medium.

2.3.2 Cultivation of clinical specimens

The isolation of bacterial strains from hospital samples was performed using selective blood agar. The swab sample was cultivated on blood agar with 10% of NaCl, blood agar without other compounds [13], Endo agar [14], and blood agar with amikacin [15]. These Petri dishes were cultivated for 24–48 h in 37°C. The identification of bacterial strains isolated from hospital samples was done using MALDI-TOF MS [16]. The MS experiments were performed on a MALDI-TOF/TOF mass spectrometer Bruker Ultraflextreme (Bruker, Bremen, Germany) equipped with a laser (Bruker) operating at wavelength of 355 nm with an accelerating voltage of 25 kV, cooled with nitrogen, and a maximum energy of 43.2 μJ with repetition rate 2000 Hz in linear and positive mode, and with software for data acquisition and processing of mass spectra flexControl version 3.4 and flexAnalysis version 2.2. A sample of 500 μL *S. aureus* (0.1 OD) culture cultivated overnight was centrifuged at $14\,000 \times g$ for 2 min. After that, supernatant was discarded and the pellet was suspended in 300 μL of DI water. Then, 900 μL of ethanol was added. After centrifugation at $14\,000 \times g$ for 2 min, supernatant was discarded and obtained pellet was air-dried. The pellet was then dissolved in 25 μL of 70% formic acid v/v and 25 μL of ACN, and was mixed. The samples were centrifuged at $14\,000 \times g$ for 2 min and 1 μL of the clear supernatant was spotted in duplicate onto the MALDI target (MTP 384 target polished steel plate; Bruker Daltonics, Bremen, Germany) and air-dried at a room temperature. Then, each spot was overlaid with 1 μL of α-cyano-4-hydroxycinnamic acid matrix solution saturated with organic solvent (50% ACN and 2.5%

TFA, both v/v and air-dried completely prior to MALDI-TOF MS measurement. Spectra were taken in the *m/z* range of 2000–20 000 Da, and each was a result of the accumulation of at least 1000 laser shots obtained from ten different regions of the same sample spot. Prior to analysis, the mass spectrometer was externally calibrated with a peptide mix of bombesin, angiotensin I, glu-fibrinopeptide B, adrenocorticotropic hormone, ubiquitine, and cytochrome c. Spectra with peaks outside the allowed average were not considered. Modified spectra were loaded into the MALDI BioTyper™ 3.1 Version (Bruker Daltonik, Bremen, Germany).

2.4 Synthesis of AuNPs and gold magnetic nanoparticles (AuMNPs)

Water-soluble AuNPs were synthesized as follows. Ten milliliters of 1 mM $HAuCl_4 \cdot 3H_2O$ was added to a 50 mL beaker under magnetic stirring. Aqueous solution of sodium citrate tribasic dihydrate (0.5 mL, 40 mM) was added to $HAuCl_4 \cdot 3H_2O$ solution. The color of the solution slowly changed from yellow to violet. Mixture was left for stirring overnight.

The AuMNPs were prepared according to the following procedure. Two different solutions were prepared separately: (i) 1.5 g of $Fe(NO_3)_3 \cdot 9H_2O$ was dissolved in 80 mL of water in a 250 mL beaker and (ii) 1.4 mL of 25% NH_3 v/v solution was mixed with 8.6 mL of water in a screw-capped tube and poured in a separate beaker. A total of 0.2 g of $NaBH_4$ was mixed with the second solution. A magnetic rotor was used to mix them properly. After 10 min of mixing, the solution was added to the first solution. The color of the solution became black with an initial frothing. Then, it was heated at 100°C for 2 h. The mixture was stirred overnight. Next day, the magnetic particles were separated from the solution by an external magnet and washed several times with DI water. Maghemite nanoparticles were prepared from 1.5 g $Fe(NO_3)_3 \cdot 9H_2O$, as a source of iron was suspended in 80 mL of water and PVP (10 k, 1.5 g in 20 mL of water) was added with stirring. After 3 h of stirring, a solution of $HAuCl_4$ (25 mL, 1 mM) was added. The solution was stirred for 1 h and a solution of trisodium citrate dihydrate (0.75 mL, 0.265 g/10 mL) was added. The solution was stirred overnight, separated by magnet, washed with DI water, and dried at 40°C. Finally, the magnetic AuNPs were air-dried and stored in a glass container.

2.5 Characterization of AuMNPs and AuNPs by SEM

Structure of 3 mM AuMNPs and 1 mM AuNPs was characterized by SEM. For documentation of the nanoparticle structures, a MIRA3 LMU (Tescan, Brno, Czech Republic) was used. This model is equipped with a high brightness Schottky field emitter for low noise imaging at fast scanning rates. The SEM was fitted with in-beam SE detector. Samples were coated by 5 nm of platinum to prevent sample charging. For automated acquisition of selected areas, a TESCAN pro-

prietary software tool called Image Snapper was used. The software enabled automatic acquisition of selected areas with defined resolution. An accelerating voltage of 15 kV and beam currents about 1 nA gave satisfactory results regarding maximum throughput. Magnification for AuMNPs 40 kX, AuNPs 40.9 kX, and aggregated AuNPs 64.6 kX were used.

2.6 Nanoparticles' surface characterization by scanning electrochemical microscope

Surface of AuMNPs and AuNPs was measured by scanning electrochemical microscope (SECM) Model 920C (CH Instruments, Austin, TX, USA). The electrochemical microscope consisted of a 10 μm platinum disc probe electrode, which was controlled by piezoelectric motors driven by all three axes. Electrochemical measurements were performed in a three-electrode configuration using platinum wire as a counterelectrode and Ag/AgCl/ 3 M KCl as a reference electrode. During scanning, the particles were attached on the substrate platinum electrode by magnetic force from neodymium magnet, situated below the electrode. The surfaces were characterized by cyclic voltammetry (CV) in 3 M KCl and 1 mM $FcCH_2OH$ using following parameters—initial potential: 0.2 V, high potential: 0.5 V, and low potential: −0.2 V. Initial scan polarity was positive with scan rate 0.02 V/s. Quiet time was 10 s. Electrochemical scanning method was carried out with potential of working microelectrode of 0.2 V. Gold disc electrodes with an O-ring as the conducting substrate used potential of 0.3 V. Speed of scanning was 250 μm/s. The platinum-measuring electrode moved at least 50 μm above the surface.

2.7 X-ray fluorescence analysis

Qualitative analysis of AuNPs and AuMNPs was measured on Spectro Xepos (Spectro Analytical Instruments, Kleve, Germany). The sample was measured on a Pd anode X-ray tube working at a voltage of 47.63 kV and a current of 0.5 mA, and detected with Barkla scatter aluminum oxide. Measurement time was 300 s. For excitation, an Mo secondary target was used. The excitation geometry was 90°. The AuNPs were measured through the PE bottle side wall 20 mm above the bottom. The Spectro Xepos software and TurboQuant method were applied for data treatment.

2.8 Characterization of nanoparticles' size

The average nanoparticles' size and size distribution were determined by quasielastic laser light scattering with a Malvern Zetasizer (NANO-ZS, Malvern Instruments, Worcestershire, UK). Nanoparticle distilled water solution of 1.5 mL (1 mg/mL) was put into a polystyrene latex cell and measured at detector angle of 173°, wavelength of 633 nm, refractive

index of 0.30, real refractive index of 1.59, and temperature of 25°C.

2.9 Labeling of nanoparticles

The AuNPs and AuMNPs were labeled with thiolated mecA primers 5′-[ThiC6]CCCAATTTGTCTGCCAGTTT-3′ in the case of AuNPS and 5′-[ThiC6]TGGCAATATTAACG CACCTC-3′ in the case of AuMNPs. The protocol was as follows. Ninety microliters of AuNPs was mixed with 10 μL of 100 μM thiolated mecA primers and incubated for 24 h in 4°C.

2.10 Reverse transcription and amplification of *mecA* gene

2.10.1 Thermolysis of bacteria and reverse transcription of mRNA

The lysis of the bacteria was done by heat treatment (99°C) during 30 min. The mRNA was converted to cDNA using PrimeScript One Step RT-PCR Kit (TaKaRa, Mountain View, CA, USA). The reaction profile was as follows: initial denaturation at 94°C for 2 min, 30 cycles of 94°C for 30 s, 50°C for 30 s, and 72°C for 1.5 min.

2.10.2 Binding of DNA with magnetic AuNPs

Ten microliters of paramagnetic particles were washed three times with phosphate buffer (0.1 M NaCl, 0.05 M Na_2HPO_4, and 0.05 M NaH_2PO_4). After that, 10 μL of cDNA and 10 μL of immobilization buffer were added (0.1 M Na_2HPO_4, 0.1 M NaH_2PO_4, 0.6 M guanidinium thiocyanate, 0.15 M Tris-HCl (pH 7.5), and 2.5 M CsCl). This solution was kept for next 1.5 h at 20°C with shaking to bind DNA with magnetic AuNPs. Further, the solution was removed and magnetic AuNPs were washed two times with 20 μL of 5 M NaCl. The obtained magnetic AuNPs with DNA were resuspended in DI water.

2.10.3 PCR and electrophoresis in agarose gel

Taq PCR kit and cDNA (New England Bio-Labs, USA) were used for amplification of MRSA *mecA* gene DNA fragment. The sequences of forward and reverse primers selected from the nucleotide database of NCBI website were 5′-CCC AATTTGTCTGCCAGTTT-3′ and 5′-TGGCAATATTAACGC ACCTC-3′ (Sigma-Aldrich), respectively. Briefly to the experimental protocol, 25 μL of reaction mixture was composed of 1× standard *Taq* reaction buffer, 0.2 mM dNTPs, 0.2 μM primers, 1.25 U *Taq* DNA polymerase, and 10 μL of DNA. PCR was carried out in a thermocycler Mastercycler ep realplex 4S (Eppendorf, Hamburg, Germany) with the following temperature program: initial denaturation at 95°C for 120 s,

25 cycles of denaturation at 95°C for 15 s, annealing at 55°C for 30 s, extension at 72°C for 45 s, and a final extension at 72°C for 5 min. The resulting DNA fragment (113 bp) was electrophoresed in 1.8% m/v agarose gel (Mercury, USA) in 1× TAE buffer (40 mM Trizma-base, 20 mM acetic acid, and 1 mM EDTA, pH 8.0). A DNA ladder (New England BioLabs, USA), within the range from 0.1 to 1.5 kbp, was used as a standard to monitor the size of the analyzed fragments of DNA. The electrophoresis (Bio-Rad, USA) was run at 70 V and 6°C for 135 min. After electrophoresis, the gel was stained with ethidium bromide (31.3 ng/L) in 1× TAE buffer. Bands were visualized using a transilluminator at a wavelength of 312 nm (Vilber-Lourmat, Marne-la-Valle´e, France). Visualized image was recorded by a digital camera Canon G10 (Canon, Japan).

2.11 Confirmation of *mecA* gene in nonresistant and resistant bacterial strains

2.11.1 Isolation of DNA

For analysis of *mecA* gene, 2 mL each of the tested strains (*S. aureus*, MRSA, *E. coli*, *S. typhimurium*, and *L. rhamnosus*) were centrifuged (5000 × *g*, 20°C, 10 min). Lysis was done for 1 h in 400 μL of lysis solution (6 M guanidine hydrochloride and 0.1 M sodium acetate) at 20°C. The isolation of genomic DNA was performed using MagNA Pure Compact (Roche, Germany).

2.11.2 Amplification of DNA for *mecA* gene

The 16S rRNA and *mecA* genes were amplified using multiplex PCR. The sequences of forward and reverse primers of 16S rRNA gene were 5′-GAGTTTGATCCTGGCTCAG-3′ and 5′-GGTTACCTTGTTACGACTT-3′; respectively, and *mecA* primers were 5′-CCCAATTTGTCTGCCAGTTT-3′ and 5′-TGGCAATATTAACGCACCTC-3′, respectively. The final volume of the PCR reaction mixture was 25 μL. The reaction profile was as follows: 94°C for 4 min, 30 cycles of 94°C for 30 s, 52°C for 30 s, and 68°C for 90 s, and a final extension at 68°C for 7 min. The amplification was carried out using Mastercycler ep realplex 4S (Eppendorf) and 1498 bp fragment for 16S rRNA gene and 223 bp fragment for *mecA* gene.

2.11.3 Visualization of the amplified genes

DNA was mixed with loading buffer and then pipetted into the wells, and run in 1.5% agarose gel electrophoresis in 1× TAE buffer with ethidium bromide for 90 min at 90 V. The bands were visualized by UV transilluminator at 312 nm (Vilber-Lourmat) and band intensities were quantified and analyzed by Carestream Molecular Imaging Software (Carestream, Carestream In vivo Xtreme Imaging System, Rochester, USA) and normalized to *mecA* gene control.

2.12 Detection of *mecA* gene fragment or bacterial DNA using AuNPs probe

Absorbance spectra were acquired by multifunctional microplate reader Tecan Infinite 200 PRO (TECAN, Switzerland). The absorbance scan was measured within the range from 230 to 1000 nm per 5 nm steps. Each absorbance value was an average of three measurements. The detector gain was set to 100. The sample (2 μL) was placed in 16-well nanoplate by Tecan NanoQuant plate (TECAN). All measurements were performed at 25°C controlled by Tecan Infinite 200 PRO (TECAN). Ten microliters of AuNPs probe and 10 μL of AuMNPs probe were mixed with 5 μL of PCR product (26 μM). Afterwards the mixture was heated for 5 min at 95°C and slowly cooled to 25°C. For the *mecA* gene detection, 10 μL of 5 M NaCl was added into the cooled mixture (to final concentration of 2 M).

2.13 3D-printed chip design and fabrication

For bacterial cultivation, lysis, DNA isolation, PCR, and detection the 3D-printed chip was fabricated using 3D printer (Profi3Dmaker, Aroja, Czech Republic) controlled by G3Dmaker v1.0 software (Aroja). The reaction chamber was made from acrylonitrile butadiene styrene (Print-plus, Aroja), which is sufficiently rigid and wiry for the final application of the product. The material had also the following properties such as small water absorption and resistance to oils, acids, alkalis, and hydrocarbons. The sample was injected into the chip using programmed syringe pump (Model eVol, SGE Analytical Science, Australia), three-way two-position selector valve (made from six-way valve, Valco, Instruments, USA), and dosing capillary, which was moved into the reaction chamber. To prepare a fully automated system, switching valve enabling switching between the off-waste and sample flow was placed into the system. The sample (10–500 μL) was injected by automated syringe (SGE Analytical Science, Australia) using maximal applied speed of 1.66 μL/s. Mobility and stirring of sample inside chip was arranged using multiturn magnet regulated on working current 200 mA, voltage 12 V, and 1 Hz pulse/frequency. The entire chip is enclosed in a thermostatic box equipped with fan, heater element, and temperature sensor. The heating element was driven by temperature sensors feedback (Instrumentation Temperature Controller, Valco, Instruments). The temperature was automatically operated by control unit Arduino Due (Atmel, USA). Flow measurement chamber in volume of 750 μL fitted with a spectrophotometric detector was used for the final sample absorbance measurement. The detector consists of LED bulb (Roithner Laser, Austria), band-pass filter (Semrock, USA) for 530 nm, and photodiode (Hamamatsu, Japan). All measurements were controlled by Arduino board Due (Atmel) and Arduino IDE (Atmel).

2.14 Descriptive statistics

Mathematical analysis of the data and their graphical interpretation were realized by Microsoft Excel®, Microsoft Word®, Microsoft PowerPoint® (USA), and STATISTICA.CZ (Czech Republic). Results are expressed as mean ± SD unless noted otherwise (EXCEL®).

3 Results and discussion

3.1 Characterization of AuMNPs and nonaggregated or aggregated AuNPs

The used nanoparticles play the crucial role for analysis inside the chip. Using the AuMNPs, the mobility and stirring of solution are ensured. Afterwards the AuNPs provide the spectrophotometric detection of *mecA* gene employing their aggregation in the presence of NaCl [17]. For our experiments, we characterized our fabricated AuMNPs, AuNPs, as well as AuNPs in NaCl presence from the point of view of surface analysis [18], electrochemical properties of particles [19, 20], qualitative analysis [21, 22], and measurement of size and zeta potential [23, 24].

At first, we characterized the AuMNPs by SEM. Iron oxide nanoparticles formed clusters of irregular shape in neutral pH (Fig. 1A, i). In order to image the reduction and oxidation properties of AuMNPs, CV of AuMNPs and surface scans were measured by SECM and the resulting maps are shown in Fig. 1A, ii. The CV scan of AuMNPs provided the lowest reduction signal in comparison to other studied particles. The oxidation potential was determined as 0.3 V, whereas the reduction potential as 0.15 V. From SECM map, it is obvious that the surface current is within the range from 0.6 to 0.9 nA. The qualitative analysis and impurities determination confirm the purity of AuMNPs, which contained bulk of Au^+ and Fe^{3+} ions (data not shown). Finally, we characterized size and zeta potential of magnetic particles. It is shown in Fig. 1A, iii that the size of these particles was found to be 15 ± 3 nm. To confirm that these magnetic nanoparticles carry negative charges, measurement of the zeta potential (or charge density) of samples was done providing important information for predicting their binding capacity. The zeta potential of magnetic nanoparticles covered with gold (19 mV) was found to be higher than that of AuNPs (−25 mV). This indicates that part of citrate on gold surface, which was used for reduction and protection of AuNPs from aggregation, was bounded with iron oxide by covalent bond resulting in increasing of zeta potential and decreasing of free citrate on gold surface.

The SEM characterization of AuNPs is demonstrated in Fig. 1B, i. It follows from the results obtained that AuNPs were spherical and cuboid in shape. CV scan of AuNPs surface shows the oxidation potential at 0.4 V and reduction potential at 0.25 V. In addition, SECM map revealed us AuNPs current within the range from −0.2 to −0.4 nA (Fig. 1B, ii). The qualitative analysis of AuNPs confirmed the presence of trace amount of chloride ions present due to its preparation
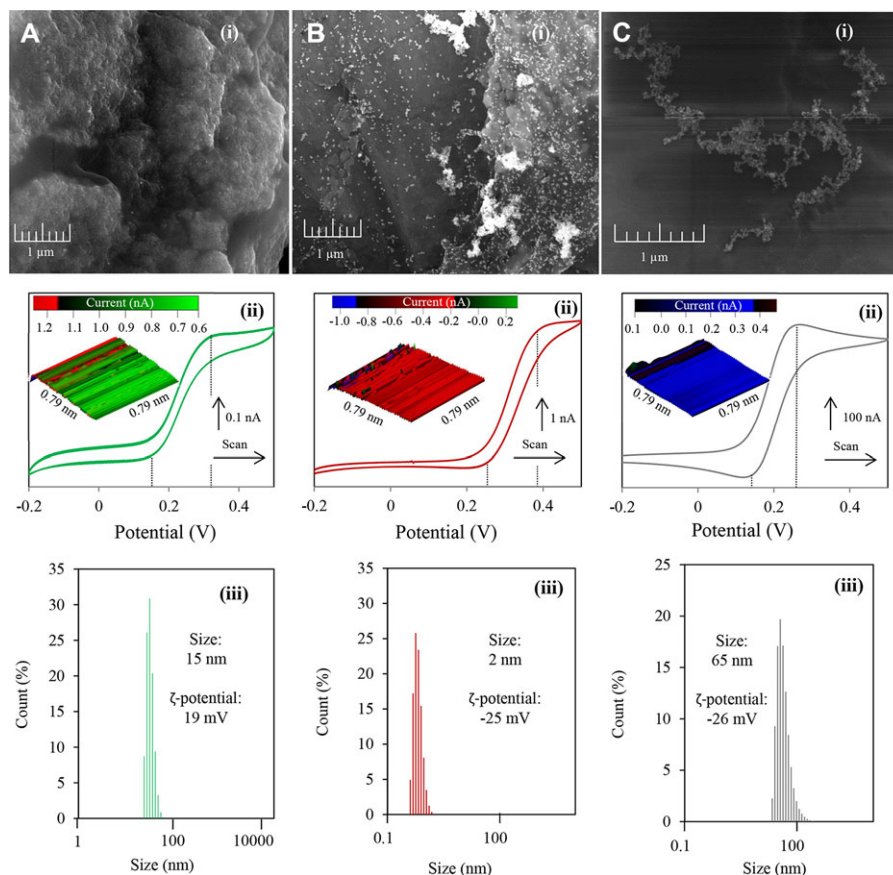
Figure 1. Microscopic and electrochemical characterization of (A) 1 mg/mL AuMNPs, (B) 1 mg/mL AuNPs, and (C) aggregated 1 mg/mL AuNPs dissolved in water by (i) SEM (magnification of 40 kX for AuMNPs, 40.9 kX for AuNPs, and 64.6 kX for aggregated AuNPs), (ii) scanning electrochemical microscope (0.3 V potential of measurement, 250 μm/s speed of scanning, and 50 μm height above the surface), and (iii) the measurements of AuNPs size distribution by Zetasizer. Measuring conditions were: detector angle 173°, wavelength 633 nm, refractive index 0.30, a real refractive index 1.59, and a temperature 25°C.

(data not shown). Moreover, the size of AuNPs was found to be 2 ± 0.5 nm and zeta potential -25 mV (Fig. 1B, iii).

Using the SEM it was found that the AuNPs in the presence of NaCl formed irregular clusters in comparison with AuNPs (Fig. 1C, i). The observation of oxidation or reduction properties of AuNPs in the presence of NaCl demonstrated the oxidation potential as 0.25 V and reduction potential as 1.4 V. Particularly, CV analysis showed higher reduction/oxidation properties in comparison with AuNPs, which could be caused by the increase of particle surface due to particles aggregation. SECM scanning map of AuNPs illustrated the change of surface current within the range from 0.1 to 0.3 nA probably associated with AuNPs aggregation, which is in agreement with CV results (Fig. 1C, ii). Characterization proved that the AuNPs agglomeration and size of these particles were found to be 65 ± 35 nm. Summarization of zeta potential values showed that AuNPs had the lowest zeta potential at -26 mV due to its permanent negative charges (Fig. 1C, iii). Based on all characterizing results obtained, it can be concluded that the particles have the ability to be used for DNA binding and colorimetric detection as other commercial nanoparticles.

3.2 Confirmation of resistance gene presence in different bacterial strains

Scheme in Fig. 2A shows the isolation and confirmation of *mecA* resistance gene expression present in MRSA. mRNA

from bacterial culture proliferating for 24 h under constant conditions was transcribed using reverse transcription into cDNA and isolated using magnetic particles. The *mecA* gene encoding the resistance to the β-lactam antibiotics was amplified and amplicon in response to the absorbance of bacterial culture before isolation (expressed in absorbance values ($\lambda = 600$ nm) 0.0005, 0.005, 0.01, 0.05, 0.1, 0.5, 1 AU) is shown in gels (Fig. 2B). The decreasing intensity of bands (*mecA* fragment, 223 bp) in the gel with the decreasing concentration of MRSA was demonstrated (Fig. 2C).

To confirm the 16S rRNA gene expression, which is naturally present in all bacterial strains, and *mecA* resistance gene, there were selected different bacterial strains of nonresistant *S. aureus*, MRSA, *E. coli*, *S. typhimurium*, *L. rhamnosus* (sample numbers 1–5), and three bacterial strains isolated from the clinical specimens from patients with bacterial infections identified as *S. aureus* (sample numbers 6–8, Fig. 2D). 16S gene expression was expectedly confirmed in all the tested bacterial strains. In the studies [25, 26], the 16S rRNA gene for classification and identification of bacteria was used, while the suitability of this approach was discussed. The expression of the 16S rRNA gene demonstrated ribosome formation in cells, thus the presence of live bacterial cultures was found in our samples. The expression of mecA gene, which is responsible for the emerging of resistance to β-lactam antibiotics, was demonstrated in two samples from eight. The expected result was to confirm the expression of this gene in commercially supplied MRSA, and further to confirm the presence
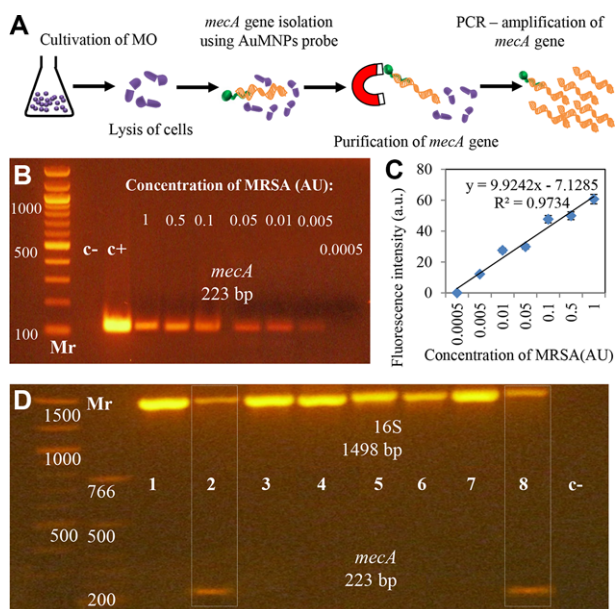
Figure 2. (A) General scheme of steps for cultivation of microorganisms, cell lysis, isolation of DNA by paramagnetic particles, and amplification of *mecA* gene for identification of MRSA inside of the 3D-printed chip using primers modified by gold nanoparticles (AuNPs). (B) Amplification of MRSA *mecA* gene by PCR with specific primers and its detection (λ_{600}). The numbers 1, 2, 3, 4, 5, 6, and 7 correspond to absorbance (λ_{600}) 0.0005, 0.005, 0.01, 0.05, 0.1, 0.5, 1 AU, respectively. C−, negative control (*S. aureus* without *mecA* gene); C+, positive control (MRSA with *mecA* gene). The reverse transcription in *mecA* gene for the confirmation of *mecA* gene expression in MRSA bacterial culture was made. (C) Dependence of MRSA concentration (0.0005, 0.005, 0.01, 0.05, 0.1, 0.5, 1 AU) on fluorescence intensity determined from gel electrophoresis. (D) The amplification of 16S and *mecA* genes by multiplex PCR with 16S and mecA primers in various PCR products of bacterial strains: (1) *S. aureus*, (2) MRSA, (3) *E. coli*, (4) *S. typhimurium*, (5) *L. rhamnosus* and three clinical specimens, where the presence of *S. aureus* was confirmed (sample numbers 6–8) and C− as a negative control. In all samples, the expression of 16S control gene was confirmed. In samples 2 and 8 the expression of *mecA* gene was also confirmed. The confirmation of the expression of 16S control gene and *mecA* gene was performed using multiplex PCR.

of such gene in the sample isolated from the hospital sample, which was identified as an *S. aureus*. Both assumptions were confirmed and the resistance to β-lactam antibiotics was found in MRSA obtained from the collection and also in clinical samples (Fig. 2D). In the other tested bacterial strains the *mecA* gene was not confirmed, therefore constituted nonmethicillin-resistant strains (Fig. 2D). Moussa and Shibl also used 16S rRNA and *mecA* genes for identification of MRSA [27]. Their study was expanded to include the presence of Panton-Valentine Leucocidin, which is a cytotoxin produced by community-associated MRSA bacterial strain [27], and are in good agreement with those found in our study.

3.3 Identification of *mecA* gene fragment to the AuNPs probe

The identification of *mecA* gene fragment is based on noncross-linking DNA hybridization method using the AuNPs probe and its ability to aggregate induced by an increasing salt concentration in the presence of complementary oligonucleotides of the same size [28]. The experimental scheme (Fig. 3A) shows that the *mecA* gene is bound to the AuNPs probe based on the bases complementarity. After the NaCl addition, the unbounded AuNPs probes aggregate. The colloidal solution of AuNPs exhibits a red color and their aggregation is driven by the London–van der Waals attractive force between the nanoparticles, and the color turns to purple red [28]. Based on these facts, we focused on the color change of AuNPs in the presence of MRSA *mecA* gene using the absorbance spectra measurement. Using the agarose gel electrophoresis, it was found that AuNPs probe contained *mecA* primers. Functionality of AuNPs probe bound to the *mecA* gene was proved by multiplex PCR visualized by electrophoresis on agarose gel (Fig. 3B). It is evident from the results shown in Fig. 3B that two bands of approximately same molecular weight of *mecA* gene were found in samples 2 and 8. These results confirmed the suitability of AuNPs probe for *mecA* gene detection because they are in perfect agreement with those shown in Fig. 2D.

Subsequently, we characterized the absorbance properties of AuNPs under various concentrations of NaCl (0–2 M). The AuNPs showed the immediate color change in low concentrations of NaCl. It follows from titration curve (Fig. 3C) that the rapid decrease of AuNPs absorbance in 530 nm in the presence of 0.125 M NaCl occurred and this decreasing trend progressed also with higher NaCl concentration.

Further, we used the described methods to analyze various PCR products of bacterial strains: (1) *S. aureus*, (2) MRSA, (3) *E. coli*, (4) *S. typhimurium*, (5) *L. rhamnosus* and three clinical specimens, where *S. aureus* presence (sample numbers 6–8) was confirmed. First, the isolation of DNA from the bacterial culture and subsequent PCR was carried out. Obtained PCR products were mixed with AuNPs probe functionalized with complementary sequence to *mecA* gene and after hybridization the 10 μL of 5 M NaCl was added into the mixture. We estimated that the color change in the case of AuNPs (0) turned transparent while the samples with noncomplementary DNA to AuNPs probe turned to purple red (samples 1 and 3–7). In the case of MRSA PCR products (2, 8), the mixture showed the stable pink color (Fig. 3D). The typical absorbance spectrum of AuNPs with absorbance maximum at 530 nm is shown in Fig. 3E. In the case of *S. aureus* PCR product, the addition of NaCl into the reaction mixture caused the rapid decrease of absorbance measured at 530 nm. On the other hand, the absorbance spectra of MRSA reaction mixture after NaCl addition shows almost 75% decrease of AuNPs absorbance maximum at 530 nm compared to AuNPs (100%). We analyzed the other bacterial strains in the same way. The absorbance decrease at 530 nm was observed in (3)
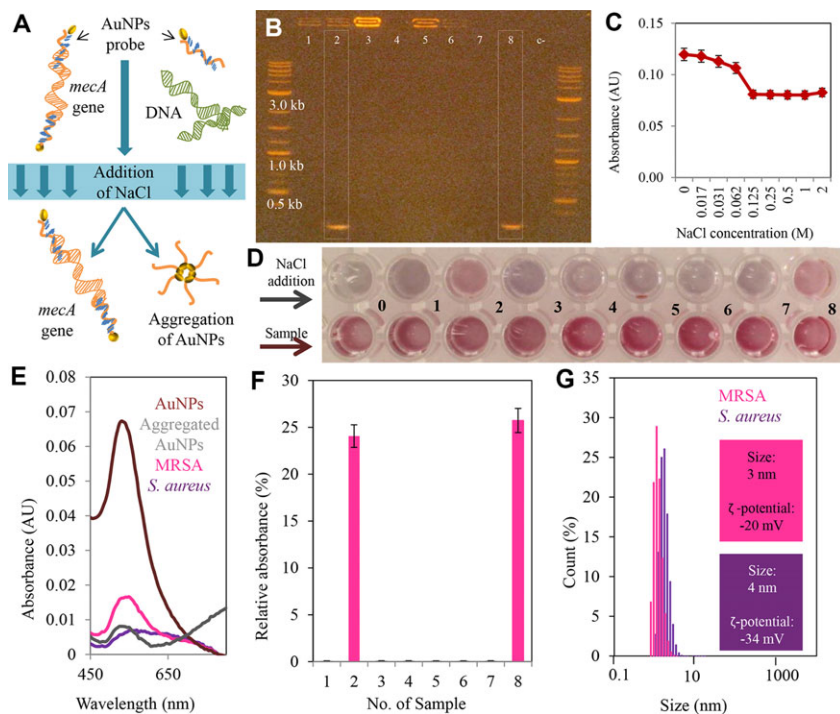
Figure 3. (A) Experimental scheme of *mecA* gene detection. (B) Amplification of *mecA* genes by PCR with AuNPs probe containing *mecA* primers in various PCR products of bacterial strains: (1) *S. aureus*, (2) MRSA, (3) *E. coli*, (4) *S. typhimurium*, (5) *L. rhamnosus* and three clinical specimens, where the presence of *S. aureus* was confirmed (sample numbers 6–8). In samples 2 and 8, the expression of *mecA* gene was confirmed. (C) Titration curve of AuNPs with addition of 0–2 M NaCl. The results are expressed as mean ± SD. (D) The color change of reaction mixtures before 2 M NaCl addition and after NaCl addition into sample: (0) AuNPs, (1) *S. aureus*, (2) MRSA, (3) *E. coli*, (4) *S. typhimurium*, (5) *L. rhamnosus* and three clinical specimens, where the presence of *S. aureus* was confirmed (sample numbers 6–8). (E) The absorbance spectra of reaction mixtures: AuNPs, AuNPs in 2M NaCl, MRSA, and *E. coli*. (F) Comparison of reaction mixtures relative absorbance: various PCR products of bacterial strains 1–8. The results are expressed as percentage of the AuNPs signal (100%). (G) Size distribution of AuNPs in mixture with MRSA (pink line) and *S. aureus* PCR products.

E. coli, (4) *S. typhimurium,* and (5) *L. rhamnosus.* For *S. aureus* (1; 6–7), nearly 90% decrease was observed (Fig. 3F). It follows from the results shown in Fig. 3G that there is a moderate increase in size of aggregated AuNPs in the presence of *mecA* gene to 3 and 4 nm in the case of negative control (*S. aureus* PCR product). Considerable change was visible in zeta potential results. Although the zeta potential of AuNPs in the presence of *mecA* gene was −20 mV, the zeta potential obtained from negative control increased to −34 mV. These results suggest that the AuNPs with sample mixture were weakly aggregated, and simultaneously stabilized the solution electrochemically.

3.4 Characterization of 3D-printed chip device and confirmation of detection inside the chip

Three-dimensional (3D) printed chips are among the new molecular techniques that rapidly monitor the presence of pathogen microorganisms [29, 30], which was demonstrated on detection of the bacterial strains in environment [31]. Their specificity, speed, and the ability to recognize a very low concentration of target molecules belong to the most important features of these chips [32].

In our study, individual steps preceding the detection were included to reaction chamber that was heated allowing the cultivation of microorganisms in Luria Bertani medium under constant conditions of 37°C and stirring. From these cultures, the DNA can be isolated using AuMNPs, and after this procedure the specific gene can be amplified using target primers whose presence can be spectrophotometrically detected by mixing with AuNPs probe and NaCl as an indicator
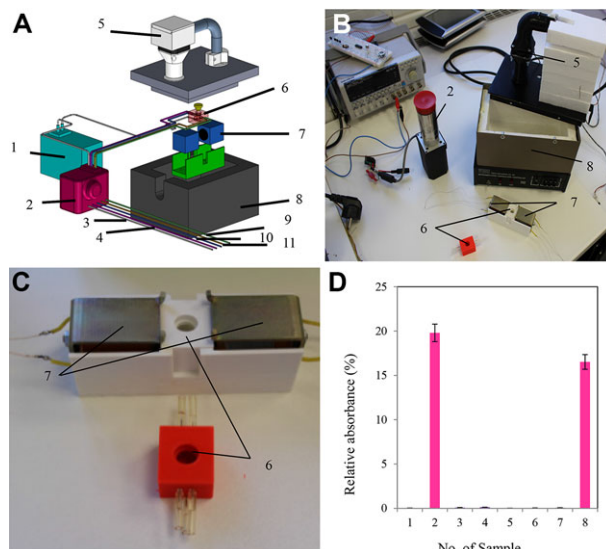

Figure 4. (A) Scheme of 3D-printed chip for detection and confirmation of MRSA presence using binding of MRSA to the gold nanoparticles with specific primers in the chip, (B) system for the identification of MRSA in the sample, and (C) reaction chamber of 3D-printed chip: 1—spectrophotometric detector, 2—pump with the valves, 3—outlet, 4—the first inlet hose, 5—thermoregulatory system, 6—cultivation chip, 7—electromagnet, 8—thermoisolating box, 9—the second inlet hose, 10—the third inlet hose, and 11—the fourth inlet hose. (D) Comparison of reaction mixtures relative absorbance obtained from 3D-printed chip: various PCR products of bacterial strains: (1) *S. aureus*, (2) MRSA, (3) *E. coli*, (4) *S. typhimurium*, (5) *L. rhamnosus* and three clinical specimens, where the presence of *S. aureus* was confirmed (sample numbers 6–8). The results are expressed as percentage of the AuNPs signal (100%).

of MRSA presence (Fig. 4A and B). The mixing and stirring during the bacterial cultivation was enabled using DNA-functionalized AuMNPs, which stirred up the liquids inside the chip. Electromagnets, visible from the picture (Fig. 4C), alternately changed its magnetic field, which resulted in movement of magnetic AuNPs. The magnetic field of electromagnets must be homogenous throughout the chip area, because magnetic particles are not concentrated only in the axis cores of electromagnets. The strength of the magnetic field must be sufficiently large and the time of the pulse, which controls the magnets, must be kept to a minimum. Magnetic particles must pulsate for the longest path. Using the control unit and electromagnets, it is possible to control magnetic particles movement in terms of speed and setting of different intervals of regular and irregular movements. For bacterial cultivation, the period of voltage on magnet connectors was set to 1 Hz. The whole cultivation process in the chip is maintained at a constant temperature of 37°C using a thermostatic box. At the end of the process, the control unit terminates the pulse of the electromagnets and maintains a constant direct current voltage on the terminals. Thus, the magnetic particles are at the right place and the lysis buffer is injected to the reaction chamber. The lysis inside the chip was carried out according to the protocol mentioned in Section 2.10.1. After the bacterial lysis, the purification of isolated DNA was done by rinsing the reaction chamber with water, while the AuMNPs probes functionalized by DNA were attached in magnetic field.

PCR as a second step was performed according to Section 2.10.3. The detection of PCR product inside the chip consisted, as in the case of absorbance detection using multifunctional reader, in the binding of the amplified PCR product (*mecA* gene) to AuNPs labeled by thiol oligonucleotide with specific affinity to gold and complementary sequence to *mecA* gene. The tested samples (1) *S. aureus*, (2) MRSA, (3) *E. coli*, (4) *S. typhimurium*, (5) *L. rhamnosus,* and three clinical specimens, which confirmed *S. aureus* presence (sample numbers 6–8), were subjected to analysis using our fabricated 3D-printed chip. The bacterial cultivation, PCR, and spectrophotometric detection were done by optimized protocols mentioned above. Spectrophotometric signal of tested samples at $\lambda = 530$ nm was expressed as percentage of the AuNPs signal (100%). It clearly follows from the results shown in Fig. 4D that the presence of MRSA was confirmed in samples 2 and 8, where 80% decrease of AuNPs absorbance compared to AuNPs was observed. In other samples, the absorbance decrease was almost 100% indicating the *mecA* gene absence. These results are in good agreement with our previous examination and proved our fabricated chip as a powerful tool for confirming the presence of MRSA.

4 Concluding remarks

Function of 3D-printed chip was tested on detection of *mecA* gene, which occurs in MRSA only. This colorimetric detection was based on specific binding of *mecA* gene to the AuNPs

labeled with thiol oligonucleotides with complementary sequence. Due to this fact, we were able to prove the presence of two positive samples from eight. These samples probably contained the sequence of *mecA* gene, a gene encoding in MRSA strain, the resistance to β-lactam antibiotics. Therefore, we can assume that this platform may be used for rapid detection of a range of other microorganisms, in case, via labeling of AuNPs by thiol oligonucleotides with sequence complementary to specific genes in tested bacterial strains.

The authors have declared no conflict of interest.

5 References

[1] Gould, I. M., *J. Hosp. Infect.* 2005, *61*, 277–282.

[2] Gould, I. M., *Int. J. Antimicrob. Agents* 2009, *34*, S8–S11.

[3] Agnoletti, F., Mazzolini, E., Bacchin, C., Bano, L., Berto, G., Rigoli, R., Muffato, G., Coato, P., Tonon, E., Drigo, I., *Vet. Microbiol.* 2014, *170*, 172–177.

[4] Higginbotham, K. L., Burris, K. P., Zivanovic, S., Davidson, P. M., Stewart, C. N., *Food Control* 2014, *40*, 274–277.

[5] Sadeghi, J., Mansouri, S., *Apmis* 2014, *122*, 405–411.

[6] Costa, A. M., Kay, I., Palladino, S., *Diagn. Microbiol. Infect. Dis.* 2005, *51*, 13–17.

[7] Francois, P., Pittet, D., Bento, M., Pepey, B., Vaudaux, P., Lew, D., Schrenzel, J., *J. Clin. Microbiol.* 2003, *41*, 254–260.

[8] House, D. L., Chon, C. H., Creech, C. B., Skaar, E. P., Li, D. Q., *J. Biotechnol.* 2010, *146*, 93–99.

[9] Focke, M., Stumpf, F., Faltin, B., Reith, P., Bamarni, D., Wadle, S., Muller, C., Reinecke, H., Schrenzel, J., Francois, P., Mark, D., Roth, G., Zengerle, R., von Stetten, F., *Lab Chip* 2010, *10*, 2519–2526.

[10] Shen, F., Du, W. B., Davydova, E. K., Karymov, M. A., Pandey, J., Ismagilov, R. F., *Anal. Chem.* 2010, *82*, 4606–4612.

[11] Koydemir, H. C., Kulah, H., Alp, A., Uner, A. H., Hascelik, G., Ozgen, C., *IEEE Sens. J.* 2014, *14*, 1844–1851.

[12] Wang, C. H., Lien, K. Y., Wu, J. J., Lee, G. B., *Lab Chip* 2011, *11*, 1521–1531.

[13] Bautista-Trujillo, G. U., Solorio-Rivera, J. L., Renteria-Solorzano, I., Carranza-German, S. I., Bustos-Martinez, J. A., Arteaga-Garibay, R. I., Baizabal-Aguirre, V. M., Cajero-Juarez, M., Bravo-Patino, A., Valdez-Alarcon, J. J., *J. Med. Microbiol.* 2013, *62*, 369–376.

[14] Predrag, S., Branislava, K., Miodrag, S., Biljana, M. S., Suzana, T., Natasa, M. T., Tatjana, B., *Braz. J. Microbiol.* 2012, *43*, 215–223.

[15] Bosch-Mestres, J., Martin-Fernandez, R. M., de Anta-Losada, M. T. J., *Enferm. Infecc. Microbiol. Clin.* 2003, *21*, 346–349.

[16] Lasch, P., Fleige, C., Stammler, M., Layer, F., Nubel, U., Witte, W., Werner, G., *J. Microbiol. Methods* 2014, *100*, 58–69.

[17] Chan, W. S., Tang, B. S. F., Boost, M. V., Chow, C., Leung, P. H. M., *Biosens. Bioelectron.* 2014, *53*, 105–111.

[18] Gultekin, A., Karanfil, G., Ozel, F., Kus, M., Say, R., Sonmezoglu, S., *J. Phys. Chem. Solids* 2014, *75*, 775–781.

[19] Kwon, S. J., Bard, A. J., *J. Am. Chem. Soc.* 2012, *134*, 7102–7108.

[20] Latus, A., Noel, J. M., Volanschi, E., Lagrost, C., Hapiot, P., *Langmuir* 2011, *27*, 11206–11211.

[21] Filez, M., Poelman, H., Ramachandran, R. K., Dendooven, J., Devloo-Casier, K., Fonda, E., Detavernier, C., Marin, G. B., *Catal. Today* 2014, *229*, 2–13.

[22] Hertz, H. M., Larsson, J. C., Lundstrom, U., Larsson, D. H., Vogt, C., *Opt. Lett.* 2014, *39*, 2790–2793.

[23] Tabrizi, A., Ayhan, F., Ayhan, H., *Hacettepe J. Biol. Chem.* 2009, *37*, 217–226.

[24] Mitra, M., Kandalam, M., Rangasamy, J., Shankar, B., Maheswari, U. K., Swaminathan, S., Krishnakumar, S., *Mol. Vis.* 2013, *19*, 1029–1038.

[25] Gardete, S., de Lencastre, H., Tomasz, A., *Microbiology (UK)* 2006, *152*, 2549–2558.

[26] Navarro-Noya, Y., Hernandez-Rodriguez, C., Zenteno, J. C., Buentello-Volante, B., Cancino-Diaz, M. E., Jan-Roblero, J., Cancino-Diaz, J. C., *Braz. J. Microbiol.* 2012, *43*, 283–287.

[27] Moussa, I. M., Shibl, A. M., *Saudi Med. J.* 2009, *30*, 611–617.

[28] Sato, K., Hosokawa, K., Maeda, M., *J. Am. Chem. Soc.* 2003, *125*, 8102–8103.

[29] Borchers, K., Weber, A., Hiller, E., Rupp, S., Brunner, H., Tovar, G. E. M., *Abstr. Pap. Am. Chem. Soc.* 2006, *232*, 460–460.

[30] Bernacka-Wojcik, I., Lopes, P., Vaz, A. C., Veigas, B., Wojcik, P. J., Simoes, P., Barata, D., Fortunato, E., Baptista, P. V., Aguas, H., Martins, R., *Biosens. Bioelectron.* 2013, *48*, 87–93.

[31] Jiang, X. R., Shao, N., Jing, W. W., Tao, S. C., Liu, S. X., Sui, G. D., *Talanta* 2014, *122*, 246–250.

[32] Krejcova, L., Nejdl, L., Rodrigo, M. A. M., Zurek, M., Matousek, M., Hynek, D., Zitka, O., Kopel, P., Adam, V., Kizek, R., *Biosens. Bioelectron.* 2014, *54*, 421–427.

5.4 Imunochemická separace meticilin-rezistentního *S. aureus* založená na částicích s nepřímou elektrochemickou detekcí značenými oligonukleotidy

5.4.1   Vědecký článek IV

CIHALOVA, K.; HEGEROVA, D.; DOSTALOVA, S.; JELINKOVA, P.; KREJCOVA, L.; MILOSAVLJEVIC, V.; KRIZKOVA, S.; KOPEL, P.; ADAM, V. Particle-based immunochemical separation of methicillin resistant *Staphylococcus aureus* with indirect electrochemical detection of labeling oligonucleotides. *Analytical Methods*, 2016, roč. 8. č. 25, s. 5123-5128. ISSN 5123-5128.

Další vědecký článek se zabýval stanovením MRSA pomocí principů testu biobarcode *(Muller, 2006)* s nepřímou elektrochemickou detekcí detekčního oligonuklotidu *(Wang a kol., 2003)*. Vzhledem k tomu, že klasické mikrobiologické kultivační metody jsou časově náročné *(Juvonen a kol., 1999)*, rozhodli jsme se vytvořit rychlou, citlivou a přesnou metodu pro stanovení této nebezpečné bakterie.

V této studii byla navržena metoda pro detekci, která je založená na selektivní sendvičové imunomagnetické separaci MRSA. Byly nasyntetizovány superparamagnetické částice a nemagnetické zlaté nanočástice s následnou modifikací povrchu streptavidinem, které sloužily jako nosiče protilátek a oligonukleotidů pro magnetickou separaci. Tyto částice byly charakterizovány pomocí skenovacího elektronového mikroskopu SEM MIRA2 LMU (Tescan, Brno, Česká republika) a velikost byla stanovena pomocí Malvern Zetasizer (NANO-ZS, Malvern Instruments Ltd., Worcestershire, Velká Británie). V metodě bylo využíváno protilátek imunoglobulinu G (IgG) imobilizovaných na superparamagnetických částicích přes afinitní interakci streptavidinu a biotinu a zlatých nemagnetických nanočástic značených specifickými protilátkami anti-Pls specifických k plasmin-sensitive surface proteinu, který je přítomný na povrchu buněčné stěny MRSA. Tyto zlaté nemagnetické nanočástice jsou navíc modifikovány i oligonukleotidem, který slouží k detekci po zachycení MRSA. Vzniklý sendvič je promyt a uvolněný oligonukleotid je po denaturaci detekován elektrochemickou metodou square wave voltametrie.

Velikost superparamagnetických částic byla 2,3 μm a u nemagnetických zlatých nanočástic se velikost pohybovala od 1,3 do 2,3 nm. Při vybraných koncentracích bakterií, které se pohybovaly od 4×10^7 do 2×10^4 KTJ bylo stanoveno, že metoda je dostatečně citlivá pro detekci bakterií v reálném vzorku stěru např. z klinických izolátů od pacientů s infikovanými poraněními, u nichž je infekce zasažena bakteriemi MRSA. V této studii bylo dosaženo závěru, že metoda je vhodná jako rychlé a citlivé imunochemické stanovení s nepřímou elektrochemickou detekcí.

PAPER

Particle-based immunochemical separation of methicillin resistant *Staphylococcus aureus* with indirect electrochemical detection of labeling oligonucleotides

K. Cihalova,[ab] D. Hegerova,[ab] S. Dostalova,[ab] P. Jelinkova,[ab] L. Krejcova,[ab] V. Milosavljevic,[ab] S. Krizkova,[ab] P. Kopel[ab] and V. Adam*[ab]

Early detection of antibiotic-resistant bacteria causing inflammation in patients is a key for an appropriate and timely treatment. Classical microbiological cultivation methods are time-consuming and therefore it is necessary to discover a quick and effective method. The method used in this study is based on a sandwich immunoreaction of bacteria with IgG immobilized on streptavidin-coated polystyrene super-paramagnetic particles and MRSA-specific antibody immobilized on gold non-magnetic nanoparticles labeled with oligonucleotides, which were detected by square wave voltammetry in combination with the adsorptive transfer technique. The assay is suitable for selective detection of methicillin-resistant *Staphylococcus aureus* in samples even at a concentration of 2×10^4 CFU mL^{-1}. The method can be flexibly modified for any other bacteria, depending on the antibodies used.

1 Introduction

Staphylococci are Gram-positive bacteria that cause serious skin and wound infections. Most staphylococcal infections are caused by *Staphylococcus aureus*, which has shown emerging antibiotic resistance.[1] Over 60% of staphylococcal infections in hospitals are currently caused by methicillin-resistant *S. aureus* (MRSA), which is resistant to β-lactam antibiotics.[2,3] Rapid and reliable identification of bacteria is a key for early detection of bacteria in patients suffering from those infections. Moreover, the detection of drug-resistant bacteria, such as MRSA, resistant *Pseudomonas aeruginosa*, extended-spectrum β-lactamase producing Enterobacteriaceae, and vancomycin-resistant *Enterococcus*, is even more urgent. Among others, MRSA is the most widespread resistant human pathogen and colonization with this organism can lead to localized or systemic infections, which may be fatal.[4]

The classical selective incubation with biochemical confirmation,[5] polymerase chain reaction,[6] identification by mass spectrometric methods[7] or immunochemical detection[8] are the most commonly used microbiological methods for the detection of bacteria. However, these methods have considerable disadvantages including expensive instrumentation and/or duration of the analysis. Nowadays, also application of microarrays[9,10] as well as nanoparticle-based detection[11,12] are attracting significant attention. Especially magnetic nano-particles are extremely valuable due to the possibility to be used for magnetic immunoseparation of bacteria from the complex sample mixtures.[13,14] In contrast, non-magnetic nanoparticles are often used as signaling tags[12] with a great advantage of the multiplexing possibility.[15]

For rapid detection of bacteria capture using appropriate surface antigens is beneficial. In the case of *Staphylococcus aureus* (*S. aureus*), several well-characterized surface molecules including protein A, fibrinogen-binding protein and proteins that binding to the extracellular-matrix components fibronectin, laminin and collagen can be employed for such purposes. It has been suggested that these surface proteins mediate the adherence of *S. aureus* to eukaryotic cells and tissues, which is an important initial event in bacterial infection. The surface superantigenic protein A, which is able to bind all mammalian immunoglobulins, was employed for fluorescent labeling of *S. aureus*[16,17] in rapid assays, for indirect chemiluminescence detection of *S. aureus*,[18] and for simultaneous immobilization and labeling of *S. aureus* present in milk.[19] Another application included immunomagnetic separation of staphylococci with consequent detection by surface plasmon resonance,[20] cultivation[21] or amperometry.[22]

The immunoseparation methods employing magnetic particles are beneficial due to the variability of targeted bacteria based on the selection of antibodies used; however, the cross-reactivity of the antibodies as well as their unavailability for certain targets are the main disadvantages of this technique.

[a]Department of Chemistry and Biochemistry, Mendel University in Brno, Zemedelska 1, CZ-613 00 Brno, Czech Republic

[b]Central European Institute of Technology, Brno University of Technology, Purkynova 123, CZ-612 00 Brno, Czech Republic. E-mail: vojtech.adam@mendelu.cz

For detection of MRSA at the whole-bacteria level it is necessary to use specific surface proteins such as antibiotic-binding proteins[16,23] or a specific virulence factor. Certain MRSA strains contain a 230 kDa plasmin-sensitive (Pls) cell-wall protein which is not present on the surface of other staphylococci[24] and therefore can be employed for specific detection of MRSA.[25] To our knowledge, until now this protein has not been used for the construction of a bead-based assay. Pls is a part of the staphylococcal cassette *mec*, which carries the *mecA* gene encoding bacterial resistance to antibiotics. This protein is associated with poor bacterial adherence and attenuates the bacterial binding to immobilized fibronectin and immunoglobulin G.[26]

The aim of this study was to design a rapid and reliable method for resistant bacteria detection. The method can be used to determine all species of bacteria and viruses with known specific antigen and the relevant antibodies.

2 Experimental

2.1 Chemicals

All chemicals of ACS (American Chemical Society) purity were obtained from Sigma-Aldrich (St. Louis, MO, USA) unless stated otherwise.

2.2 Modification of magnetic particles (MPs) with human IgG

Before modification of magnetic particles with IgG, the IgG antibodies were modified with biotin. 500 μL biotinamidohexanoyl-6-aminohexanoic acid *N*-hydroxysuccinimide ester (1 mg mL^{-1}) was added to 100 μL of IgG antibodies (10 mg mL^{-1}) and the solution was stirred in a heating block for 2 hours. The solution was stirred in a heating block for 1.5 hour and then washing with 1 mL of phosphate buffer saline (PBS, 137 mM NaCl, 2.7 mM KCl, 1.4 mM NaH$_2$PO$_4$, 4.3 mM Na$_2$HPO$_4$, pH 7.4) was performed three times. The surface of the magnetic particles was modified with biotinylated human IgG according to the protocol for the modification of Dynabeads M-280 Streptavidin.[27] The particle surface was blocked with 1% bovine serum albumin (BSA).

2.3 Synthesis of gold nanoparticles (AuNPs)

Generally, 10 mL of 1 mM HAuCl$_4$·3H$_2$O was stirred and heated at 120 °C. Then a solution of sodium citrate dihydrate (40 mM, 0.5 mL) was added. The mixture was stirred overnight. Gold nanoparticles (1250 μL) were modified with streptavidin (30 μL, 5 mg mL^{-1}) and stirred in a heating block for 1.5 hour.

2.4 Modification of gold nanoparticles with anti-Pls antibody and oligonucleotide (20 bp)

AuNPs were modified with biotinylated anti-plasminogen antibody (anti-Pls/plasmin/plasminogen (biotin), Baria s.r.o., Czech Republic). 1 mM AuNPs were incubated at 20 °C overnight with the antibody diluted in 0.05 M carbonate buffer (pH 9.6) in ratio of 1 : 3000 (v/v). The unreacted components were washed out by filtration through Amicon Ultra centrifugal filters (Sigma Aldrich, St. Louis, USA) at 14 000 g for 5 min.

The thiolated oligonucleotide (ODN) 5′-[ThiC6]CATA-TCACGCGCGCACTATG-3′ (Sigma-Aldrich, USA) was bound to the gold nanoparticles by sulfur–gold affinity interaction. 2 mM AuNPs were incubated overnight with 10 μM thiolated ODN at 45 °C and 300 rpm. Free ODNs were separated during the washing by magnetic separation.

2.5 Characterization of the particles by scanning electron microscopy (SEM)

The structure of the particles (3 mM solution of Dynabeads M-280 and 1 mM AuNPs in the presence of 2 M NaCl) was characterized by using a SEM MIRA2 LMU (Tescan, Brno, Czech Republic). The SEM was fitted with an In-Beam SE detector. For automated acquisition of the selected area, a TESCAN proprietary software tool Image Snapper was used. An accelerating voltage of 15 kV provided satisfactory results regarding the maximum throughput. Zoom was 40 kX for Dynabeads® M-280 Streptavidin and 40.9 kX for aggregated AuNPs.

2.6 Characterization the of particle size

The average particle size and size distribution were determined by quasielastic dynamic light scattering with a Malvern Zetasizer (NANO-ZS, Malvern Instruments Ltd., Worcestershire, U.K.). A suspension of nanoparticles in distilled water (1.5 mL, 1 mg mL^{-1}) was placed into a polystyrene latex cell and measured at a detector angle of 173°, wavelength of 633 nm, refractive index of 0.30, real refractive index of 1.59, and temperature of 25 °C.

2.7 ELISA

The capacity of the magnetic particles for IgG capture was verified by ELISA. Magnetic particles (50 μg) were washed three times with PBS prior to use and resuspended in 100 μL of PBS. Subsequently, the biotinylated human IgG antibodies (Sigma Aldrich, St. Louis, USA) at different concentrations (0, 1, 2, 4, and 8 μM), dissolved in 0.05 M carbonate buffer (pH 9.6) were added and the mixture was incubated for 1 hour at 37 °C and 300 rpm. The unreacted IgG molecules were removed by washing 5-times with 500 μL of PBS with 0.05% (v/v) Tween-20 (PBST). The surface was subsequently blocked by incubation with 0.1% (m/v) solution of bovine serum albumin in PBS (1 hour at 37 °C) to eliminate the unspecific interactions. After washing with PBST (5×), the particles were incubated with a goat anti-human secondary antibody (goat anti-human antibody labeled with horseradish peroxidase (HRP), Sigma Aldrich, St. Louis, USA) diluted 1 : 30 000 with PBS for 1 hour at 37 °C and 300 rpm. The unbound secondary antibody was removed by washing 5-times with 500 μL of PBST. In order to visualize the interaction of the antibodies, 100 μL of HRP substrate buffer was added (0.001% (w/v) of 3,3′,5,5′-tetramethylbenzidine, 10 μL of hydrogen peroxide (30%, v/v), 0.5 mL of 2 M sodium acetate adjusted to pH 5.8 with 1 M citric acid and 10 mL of Milli-Q water) to magnetic particles in a microplate. After sufficient coloring (30 min at 37 °C), the reaction was stopped with 50 μL of 0.5 M H$_2$SO$_4$. The absorbance of the yellow product was measured at 450 nm using a TECAN Sunrise microplate reader (Switzerland).

2.8 Cultivation of bacteria

Methicillin-resistant *Staphylococcus aureus* (NCTC 8511), *Escherichia coli* (NCTC 13216) and *Proteus mirabilis* (NCTC 11938) were obtained from the Czech Collection of Microorganisms, Faculty of Science, Masaryk University, Brno, Czech Republic. Strains were stored in the form of a spore suspension in 20% (v/v) glycerol at $-20\ ^\circ$C. Prior to use, the strains were thawed and the glycerol was removed by washing with distilled water. The composition of cultivation medium was: tryptone $10\ \text{g L}^{-1}$, yeast extract $5\ \text{g L}^{-1}$, NaCl $5\ \text{g L}^{-1}$, (Himedia, Mumbai, India), and sterilized Milli-Q water. pH of the cultivation medium was adjusted to 7.4 before sterilization. The sterilization of the medium was carried out at $121\ ^\circ$C for 30 min in a sterilizer (Tuttnauer 2450EL, New York, USA). The prepared cultivation medium was inoculated with the bacterial culture in a 25 mL Erlenmeyer flask and cultivated for 24 h on an Environmental Shaker-Incubator ES-20 (Biosan, Riga, Latvia) at 600 rpm and $37\ ^\circ$C. Bacterial cultures were subsequently diluted by using the cultivation medium to $OD_{600} = 0.1$ (determined using a Specord spectrophotometer 210 (Analytik, Jena, Germany)) and used in the following experiments.

2.9 Electrochemical analysis of the specific oligonucleotide (detection of the CA peak)

A reduction signal of cytosine and adenine (CA peak) was measured at a potential of -1.41 ± 0.03 V by square wave voltammetry (SWV) coupled with the adsorptive transfer technique (AdTS). The measurements were carried out using a 663 VA Stand, an 800 Dosino, an 846 Dosing Interface (Metrohm, Herissau, Switzerland) and a standard electrochemical cell with a three-electrode set up. A hanging mercury drop electrode with a drop area of $0.4\ \text{mm}^2$ was used as the working electrode. An Ag/AgCl/3 M KCl electrode was used as the reference and a platinum wire was used as the auxiliary electrode. Parameters of AdTS SWV were the following: initial potential of 0 V, end potential of -1.8 V, potential step of 0.005 V, amplitude of 0.025 V, frequency of 280 Hz, and accumulation time of 120 s. Prior to the measurements, the samples were deoxygenated using argon (99.999%). An acetate buffer pH 5.0 (0.2 M CH_3-COONa, CH_3COOH) was used as a supporting electrolyte. For curve smoothing and baseline correction, the software GPES 4.9 supplied by EcoChemie was employed.

3 Results and discussion

3.1 Characterization of the particles

3.1.1 Magnetic particles. The commercial magnetic nanoparticles Dynabeads M-280 Streptavidin were used as the key component of the procedure. According to the manufacturer's specifications, the nanoparticle size was 2.8 μm in diameter, which was confirmed by the dynamic light scattering measurement that revealed the majority of the nanoparticles to be 2.3 μm in diameter (Fig. 1A). Moreover, the SEM analysis showed the spherical and uniform shape of the particles (Fig. 1B).
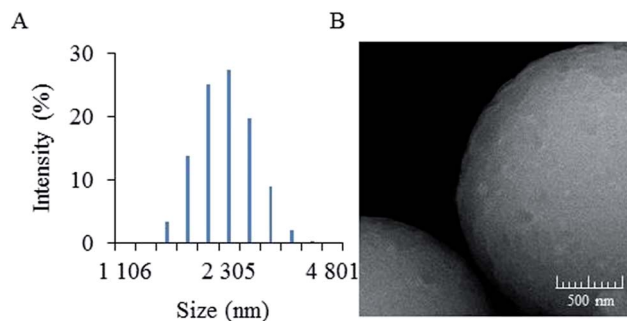

Fig. 1 Characterization of the magnetic particles. (A) Hydrodynamic diameter characterization determined by the dynamic light scattering measurement of Dynabeads M-280 Streptavidin. (B) SEM micrograph of magnetic particles Dynabeads M-280 Streptavidin.

The magnetic particles were modified with IgG antibodies and the binding capacity to IgG was investigated. Different concentrations of antibodies were prepared and conjugated to the magnetic particles. Subsequently, the quantitative determination was performed using ELISA by the measurement of the absorbance intensity at 450 nm. The highest absorbance was determined at 8 μM concentration of IgG per mg of magnetic particles (the value of absorbance intensity was 1.04 AU, Fig. 2A).

To demonstrate the immunoreactivity towards various bacterial strains, the immunoseparation was carried out (1 hour incubation of magnetic particles with bacteria) and the isolated bacteria at the particle surface were cultivated overnight. After 24 hours, the magnetic particles were removed and the absorbance of the newly grown bacteria was measured. As shown in Fig. 2B, in the case of all tested bacterial strains (*MRSA*, *E. coli* and *P. mirabilis*), a significant signal was detected demonstrating the growth of the isolated bacteria. To visualize the interaction between magnetic particles and bacteria, the SEM micrographs were taken. The typical image revealing the MRSA conjugated to the particle is shown in Fig. 2C. From the SEM micrographs, it was found out that up to four bacteria were captured on the surface of one particle.

3.1.2 Nonmagnetic gold nanoparticles (AuNPs). After synthesis and modification with streptavidin, the AuNPs were characterized by dynamic light scattering and SEM. It was found out that the majority of the particles were in the size range of
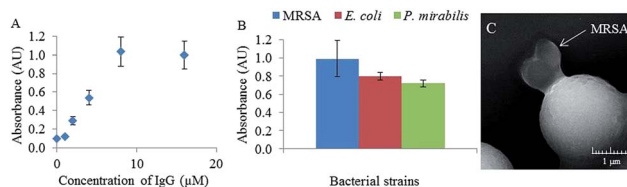

Fig. 2 Interaction of magnetic particles. (A) The binding capacity of magnetic particles was determined by measuring the absorbance intensity of the ELISA reaction (for conditions see Experimental), (B) spectrophotometric signal of the overnight grown bacteria isolated by IgG-modified magnetic particles, and (C) SEM micrograph of the magnetic particle with captured MRSA.
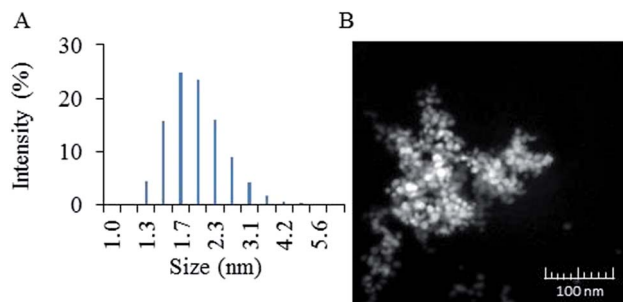
Fig. 3 (A) Hydrodynamic diameter characterization of AuNPs determined by the dynamic light scattering measurement, and (B) micrograph of AuNPs measured using a scanning electron microscope.

1.3–2.3 nm (Fig. 3A). However, as shown in the Fig. 3B, the nanoparticles tended to aggregate and formed clusters.

These AuNPs were surface modified by two components – (1) anti-Pls, which is the specific antibody against the plasmin sensitive surface protein expressed on the surface of MRSA and (2) double-stranded detection ODN. The interaction between the nanoparticles and the anti-Pls was confirmed spectrophotometrically by the presence of the two specific absorption maxima (260 nm for anti-Pls and 510 nm for AuNPs) in the mixture of the AuNPs with anti-Pls. The conjugate was purified by filtration through the centrifugation filters to remove the unreacted components. The absorption spectra of the pure anti-Pls, AuNPs and the conjugate are shown in Fig. 4A.

The interaction between AuNPs and SH-ODN was demonstrated by the SWV measurement. The signal of free denatured ODNs was observed at a potential of -1.42 ± 0.02 V, which is characteristic of adenine and cytosine reduction at the hanging mercury drop electrode.[28] After mixing with AuNPs, the signal was significantly negatively shifted to -1.45 ± 0.02 V, see Fig. 4B.

3.2 Composition of an immunosandwich for MRSA detection

In the present study, the particle-based immunoseparation method with electrochemical detection was proposed. The scheme of the method is shown in Fig. 5.
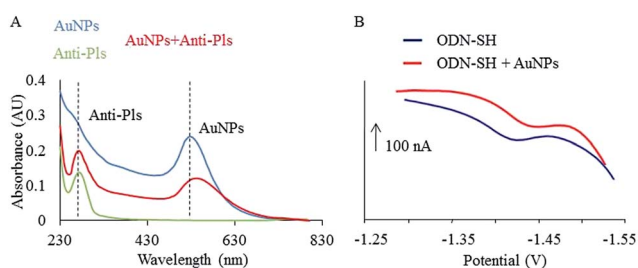

Fig. 4 Confirmation of antibody and oligonucleotide binding to AuNPs. (A) Absorbance spectra of AuNPs (blue) with an absorbance maximum of 510 nm. Absorbance spectra of anti-Pls (66 μM, green) with characteristic absorbance maximum for proteins (260 nm). Absorbance spectra of gold nanoparticles bound to antibodies (red). (B) Electrochemical detection of thiolated oligonucleotide ODN–SH (blue) and ODN–SH on AuNPs (red) by square wave voltammetry (for conditions see Experimental section 2.9).
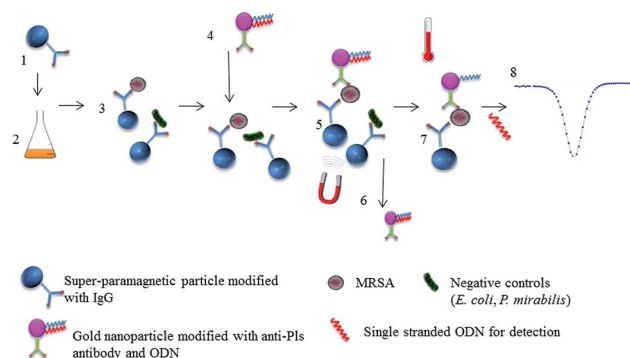

Fig. 5 Scheme of MRSA detection using magnetic separation and electrochemical detection of oligonucleotides. Magnetic particles modified by human IgG (1) incubated with the bacterial culture/sample (2) for nonspecific capture (3). Gold nanoparticles modified by anti-Pls and detection ODNs (4) for specific conjugation to MRSA (5). Removal of the untargeted bacteria and unreacted AuNPs by magnetic separation (6). Thermal denaturation of the double-stranded ODNs from the AuNPs (7) and detection of the released ODNs by SWV (8).

At first, the magnetic nanoparticles were modified with IgG to capture all bacteria expressing immunoglobulin-binding superantigenic proteins. These proteins are expressed on the surface of *Staphylococcus* ssp. (protein A), G-group *Streptococcus* ssp. (protein G), and *Peptostreptococcus* ssp. (protein L).[29] This step simplifies significantly the bacterial mixture, which may be potentially very complex, leading to the immunoseparation of this group of pathogenic bacteria only. After the magnetic separation ensuring the removal of the unreacted components and careful washing with PBS, the non-magnetic AuNPs labeled by specific antibodies against MRSA (anti-Pls) were added to the mixture forming a sandwich with MRSA captured on the magnetic particles. These AuNPs were simultaneously labeled by the short, double-stranded ODNs. All unreacted components were removed by the magnetic separation and washed with PBS. Subsequently, the mixture was heated to thermally release the single-stranded ODNs from the complex. These ODNs were electrochemically detected by AdTS SWV.

The sensor was tested for the detection of 4×10^7 CFU mL^{-1} of MRSA, *E. coli* and *P. mirabilis* using 0.2 μM concentration of the labeling ODN. As shown in Fig. 6, one peak at the position of
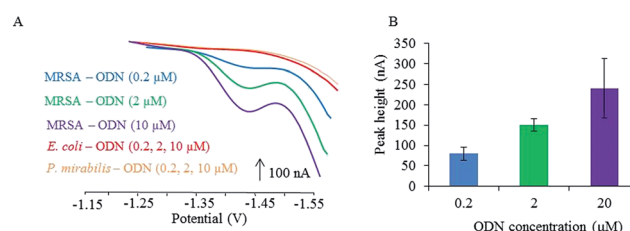

Fig. 6 Detection of MRSA using various concentrations of ODNs bound to AuNPs (0.2, 2 and 10 μM) using SWV. *E. coli* and *P. mirabilis* were used as negative controls (10 μM ODN) (for conditions of the AdTS SWV method see Experimental section 2.9). (A) Voltammograms obtained by the AdTS SWV. (B) Quantification of the voltammetric signals.
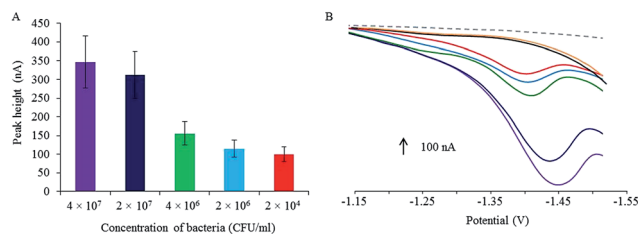
Fig. 7 Detection of MRSA. (A) Dependence of the electrochemical signal (nA) on applied MRSA concentration (CFU), MRSA was isolated and detected by the presented method (key components – 8 μM IgG, 10 μM ODN, 66 μM anti-Pls). (B) Real SWV voltammograms obtained for MRSA detection. *E. coli* and *P. mirabilis* were used as negative controls (dashed line corresponds to the signal of the background electrolyte). The adsorptive transfer stripping technique was used, for conditions see Experimental section 2.9.

-1.45 V was observed for *S. aureus*. In order to increase the signal and investigate the dependence of the signal on the amount of the detection ODN present on the AuNPs, nanoparticles with three different concentrations of the ODN (0.2, 2 and 10 μM) were prepared and compared for the detection of 4×10^7 CFU mL^{-1} of MRSA, *E. coli* and *P. mirabilis* (Fig. 6A). The denatured ODNs were determined by SWV at a potential of -1.45 ± 0.02 V, which is consistent with results obtained in Section 3.1.2. As expected, with decreasing concentration of the ODN on the AuNP surface (0.2–2 μM), the electrochemical signal decreased linearly. As shown in Fig. 6, the negative controls *E. coli* and *P. mirabilis* did not provide any electrochemical signal even at the highest ODN concentration. The quantification of the electrochemical signals is shown in Fig. 6B. This indicated that the ODNs attached on the AuNP surface were not present in the sample due to the fact that they were not captured in the immunosandwich with bacteria and magnetic particles.

3.3 MRSA detection

Finally, the investigation of the response of the method to the MRSA concentration was carried out. It was found out that the electrochemical signal depends on MRSA concentration in the sample (Fig. 7). It was possible to determine MRSA qualitatively and quantitatively in the sample in the range from 4×10^7 to 2×10^4 CFU mL^{-1} (Fig. 7A). The sensitivity of the method is high due to the peak presence in the lowest used concentration (2×10^4 CFU mL^{-1}) (Fig. 7B), which is sufficient for detection in real samples, such as clinical isolates or skin smears.[30–32] In the case of negative controls *E. coli* and *P. mirabilis*, no signal was detected (Fig. 7B), which proves this method to be selective. The principle of the detection mechanism could be used as a platform for the determination of the MRSA presence in clinical infections, in wounds or pus.[32] Our data could be also utilized as a platform for compilation of the detection device for rapid detection of resistant bacteria in a clinical environment.

4   Conclusions

Early detection of bacteria is an important factor in diagnostics of inflammatory diseases in patients. Especially in resistant bacteria, early identification of inflammatory disease plays a significant role in the introduction of an appropriate and timely treatment. In this study, the immunochemical assay for MRSA detection using magnetic particles, gold nanoparticles and oligonucleotide-based labels for electrochemical detection was proposed and tested.

Acknowledgements

Notes and references

1 I. M. Gould, *Int. J. Antimicrob. Agents*, 2008, **32**, S2–S9.
2 R. M. Klevens, M. A. Morrison, J. Nadle, S. Petit, K. Gershman, S. Ray, L. H. Harrison, R. Lynfield, G. Dumyati, J. M. Townes, A. S. Craig, E. R. Zell, G. E. Fosheim, L. K. McDougal, R. B. Carey, S. K. Fridkin and A. B. M. Investigators, *JAMA-J. Am. Med. Assoc.*, 2007, **298**, 1763–1771.
3 H. Wisplinghoff, T. Bischoff, S. M. Tallent, H. Seifert, R. P. Wenzel and M. B. Edmond, *Clin. Infect. Dis.*, 2004, **39**, 309–317.
4 N. Lewis, N. Parmar, Z. Hussain, G. Baker, I. Green, J. Howlett, A. Kearns, B. Cookson, A. McDonald, M. Wilson and D. Ready, *Eur. J. Clin. Microbiol. Infect. Dis.*, 2015, **34**, 1823–1826.
5 J. G. Holt, N. R. Krieg, P. H. Sneath, J. T. Safety and S. T. Williams, *Bergey's Manual of Systematic Bacteriology*, Springer-Verlag, New York, 2009.
6 M. Maurin, *Expert Rev. Mol. Diagn.*, 2012, **12**, 731–754.
7 J. O. Lay, *Mass Spectrom. Rev.*, 2001, **20**, 172–194.
8 N. Pelletier and B. La Scola, *Médecine et Maladies Infectieuses*, 2010, **40**, 506–516.
9 D. R. Call, M. K. Borucki and F. J. Loge, *J. Microbiol. Methods*, 2003, **53**, 235–243.
10 V. Perreten, L. Vorlet-Fawer, P. Slickers, R. Ehricht, P. Kuhnert and J. Frey, *J. Clin. Microbiol.*, 2005, **43**, 2291–2302.
11 Y. W. Chu, D. A. Engebretson and J. R. Carey, *J. Biomed. Nanotechnol.*, 2013, **9**, 1951–1961.
12 N. Sanvicens, C. Pastells, N. Pascual and M. P. Marco, *TrAC, Trends Anal. Chem.*, 2009, **28**, 1243–1252.
13 H. Wang, Y. Li, A. Wang and M. Slavik, *J. Food Prot.*, 2011, **74**, 2039–2047.
14 S. Liebana, A. Lermo, S. Campoy, J. Barbe, S. Alegret and M. Isabel Pividori, *Anal. Chem.*, 2009, **81**, 5812–5820.
15 L. Wang, W. Zhao, M. B. O'Donoghue and W. Tan, *Bioconjugate Chem.*, 2007, **18**, 297–301.
16 W. J. Kong, J. Xiong, H. Yue and Z. F. Fu, *Anal. Chem.*, 2015, **87**, 9864–9868.

17 P. Drake, P. S. Jiang, H. W. Chang, S. C. Su, J. Tanha, L. L. Tay, P. L. Chen and Y. J. Lin, *Anal. Methods*, 2013, **5**, 4152–4158.

18 J. Xiong, W. W. Wang, Y. L. Zhou, W. J. Kong, Z. X. Wang and Z. F. Fu, *Microchim. Acta*, 2016, **183**, 1507–1512.

19 D. Peedel and T. Rinken, *Anal. Methods*, 2014, **6**, 2642–2647.

20 L. L. Chen, L. Deng, L. L. Liu and Z. H. Peng, *Biosens. Bioelectron.*, 2007, **22**, 1487–1492.

21 S. Krizkova, E. Jilkova, L. Krejcova, N. Cernei, D. Hynek, B. Ruttkay-Nedecky, J. Sochor, J. Kynicky, V. Adam and R. Kizek, *Electrophoresis*, 2013, **34**, 224–234.

22 B. E. F. de Avila, M. Pedrero, S. Campuzano, V. Escamilla-Gomez and J. M. Pingarron, *Anal. Bioanal. Chem.*, 2012, **403**, 917–925.

23 A. B. Bandara, Z. W. Zuo, S. Ramachandran, A. Ritter, J. R. Heflin and T. J. Inzana, *Biosens. Bioelectron.*, 2015, **70**, 433–440.

24 P. Hilden, K. Savolainen, J. Tyynela, M. Vuento and P. Kuusela, *Eur. J. Biochem.*, 1996, **236**, 904–910.

25 M. Huesca, R. Peralta, D. N. Sauder, A. E. Simor and M. J. McGavin, *J. Infect. Dis.*, 2002, **185**, 1285–1296.

26 E. Josefsson, K. Juuti, M. Bokarewa and P. Kuusela, *Infect. Immun.*, 2005, **73**, 2812–2817.

27 J. P. Bannantine, J. R. Stabel, D. O. Bayles and B. V. Geisbrecht, *Protein Expression Purif.*, 2010, **72**, 223–233.

28 E. Palecek and M. Bartosik, *Chem. Rev.*, 2012, **112**, 3427–3481.

29 J. D. Fraser and T. Proft, *Immunol. Rev.*, 2008, **225**, 226–243.

30 S. V. Gaidhani, A. V. Raskar, S. Poddar, S. Gosavi, P. K. Sahu, K. R. Pardesi, S. V. Bhide and B. A. Chopade, *Indian J. Med. Res.*, 2014, **140**, 665–671.

31 S. O. Moghadam, M. R. Pourmand and F. Aminharati, *J. Infect. Dev. Countries*, 2014, **8**, 1511–1517.

32 C. Konig, H. P. Simmen and J. Blaser, *J. Antimicrob. Chemother.*, 1998, **42**, 227–232.

5.5 Detekce infekčních bakterií pomocí barcode assay za použití kvantových teček bez účasti protilátek

5.5.1 Vědecký článek V

CIHALOVA, K..; HEGEROVA, D.; JIMENEZ JIMENEZ, A., M.; MILOSAVLJEVIC, V.; KUDR, J.; SKALICKOVA, S.; HYNEK, D.; KOPEL, P.; ADAM, V. Antibody-free detection of infectious bacteria using quantum dots-based barcode assay. *Journal of Pharmaceutical and Biomedical Analysis*. Odesláno.

S. aureus, MRSA a *Klebsiella pneumoniae* (*K. pneumoniae*) jsou nejzastoupenější bakterie způsobující infekční onemocnění. Vzhledem ke zvýšenému užívání antibiotik, bakteriální rezistence u uvedených bakteriálních druhů roste a způsobuje závažné infekce, které komplikují léčbu, prodlužují tak její trvání a hrozí riziko šíření nákazy. Přítomnost zmíněných bakterií způsobujících nosokomiální infekce v nemocnicích roste a představují pro pacienta jisté nebezpečí. Citlivé a rychlé stanovení těchto patogenů je rozhodující pro účinnou léčbu.

Cílem této studie bylo navrhnout účinnou multiplexní metodu pro stanovení *S. aureus*, MRSA a *K. pneumoniae* ve vzorku současně za použití magnetické separace pomocí magnetických částic s nepřímou detekcí kvantových teček. Detekce jednotlivých bakterií byla založena na identifikaci specifického fragmentu genu pomocí oligonukleotidů vázaných k magnetickým částicím a kvantovým tečkám (CdTe). Kvantové tečky byly modifikovány 3´ koncem specifického oligonukleotidu pro hybridizaci a detekci PCR produktu. Pro detekci *S. aureus* byl použit fragment genu *fnbA*, kódující tvorbu proteinu vázající se na fibronektin, pro MRSA to byl *mecA* gen, kódující rezistenci vůči β-laktamovým antibiotikům a pro *K. pneumoniae wcaG* gen, kódující tvorbu enzymu guanosindifosfát-L-fukóza syntázy. Detekce byla založena na různých emisních maximech kvantových teček, což zajistilo provedení multiplexního stanovení. Limit detekce pro tuto metodu byl stanoven na 10^2 KTJ/ml vzorku.

Tato platforma může být použita pro detekci celé řady mikroorganismů. Barcode technika může být provedena jak v laboratorních podmínkách a stejně tak může být zavedena do miniaturizovaných analytických přístrojů. Navrhovaný systém je vhodný

pro implementaci do malovýroby či dokonce do přenosných zařízení. Tyto platformy jsou obvykle navrženy a vytvořeny 3D tiskem *(Park a kol.)* a pracují na principu fluorescence, elektrochemické a spektrofotometrické detekce *(Pinkowitz a kol.; Ming a kol., 2015).*

Antibody-free detection of infectious bacteria using quantum dots-based barcode assay

Kristyna Cihalova[1,2], Dagmar Hegerova[1,2], Ana Maria Jimenez Jimenez[1,2], Vedran Milosavljevic[1,2], Jiri Kudr[1,2], Sylvie Skalickova[1,2], David Hynek[1,2], Pavel Kopel[1,2] and Vojtech Adam[1,2]*

[1] Department of Chemistry and Biochemistry, Mendel University in Brno, Zemedelska 1, CZ-613 00 Brno, Czech Republic, European Union

[2] Central European Institute of Technology, Brno University of Technology, Purkynova 123, CZ-612 00 Brno, Czech Republic, European Union

* Author to whom correspondence should be addressed; E-mail: vojtech.adam@mendelu.cz; Tel.: +420-5-4513-3350; Fax: +420-5-4521-2044.

Abstract

Staphylococcus aureus, methicillin-resistant *Staphylococcus aureus* and *Klebsiella pneumoniae* are the most representative bacteria causing infectious diseases. Due to the increased application of antibiotics, the bacterial resistance is growing causing severe complications. Therefore, a sensitive determination of these pathogens is crucial for effective treatment.

The aim of this study was design an effective method for multiplex detection of *Staphylococcus aureus,* methicillin-resistant *Staphylococcus aureus* and *Klebsiella pneumoniae* taking advantage from properties of magnetic particles as well as fluorescent nanoparticles (quantum dots). The method was able to detect as low concentrations of bacteria as 10^2 CFU/mL using the bacteria-specific genes (*fnbA*, *mecA* and *wcaG*).

Keywords: *Staphylococcus aureus*; Methicillin-resistant *Staphylococcus aureus; Klebsiella pneumoniae*; magnetic particles; barcode; quantum dots

1   Introduction

Microbial antibiotics resistance is one of the biggest threats as well as challenge for numerous scientists [1]. The most attention is paid to such bacteria endangering human health [2-4], i.e. those occurring in hospitals such as *Staphylococcus aureus* (*S. aureus*) [5-8], from which methicillin-resistant *S. aureus* (MRSA) bacteria evolved. MRSA is carrying a penicillin binding protein 2a (PBP2a) encoded by *mecA* gene giving it the ability to be resistant against β-lactam antibiotics [9,10]. Another such resistant specie is gram-negative *Klebsiella pneumoniae (K. pneumoniae)* [11-17] causing nosocomial infections occurring in oropharynx [18,19], gastrointestinal tract [20] and eventually on the skin [21], where strains resistant to antibiotics occur very frequently [22]. The presence of all these strains has been increasing in hospitals representing a threat to a patient. Therefore, fast, robust, simultaneous and easy identification of these bacteria is crucial [23].

Traditional methods of diagnostics of bacterial infections are complex and time-consuming and delay the implementation of the required treatment. Equally important for the speed of analysis is the ability to detect all of these pathogens simultaneously in the pooled sample. For such detection, multiplex polymerase chain reaction (mPCR) is necessary. The mPCR assays have already been featured in a number of reports, but most of these assays have targeted specific bacterial species only [24-26]. Taking into account the abovementioned requirements, barcode assay can be considered effective alternative for these purposes [27,28]. Nowadays, magnetic and non-magnetic micro- and nanoparticles present a suitable platform for barcode assay [29,30]. The particles are used as carriers for molecules detecting a target component. A specific affinity between the capturing molecules immobilized on particles and the target component of the bacteria must be assured for the formation of specific binding [31,32]. The capturing molecules belong mainly to the family of antibodies or nucleic acids in the form of oligonucleotides. In case of bacteria, barcode assay based on oligonucleotides is preferable

due to high costs of antibodies as well as their unavailability [33,34]. To visualize the specific interaction of the capturing oligonucleotide, various forms of labelling can be used [35-38]. For the fluorescence detection, quantum dots have been recently successfully reported [39,40]. In the case of the identification of individual species, quantum dots can be used for confirmation of their presence [41]. With regard to detection of microorganisms in a sample mixture, so-called multiplex analysis containing quantum dots of different color and size giving different fluorescent signals is highly preferable [42,43].

Based on the previously mentioned facts, the aim of this study was to select magnetic particles suitable for isolation of *S. aureus*, MRSA and *K. pneumoniae*. Further, we selected specific genes (*fnbA* for *S. aureus* [44], *mecA* for MRSA [45] and *wcaG* for *K. pneumoniae* [46]), prepared complementary oligonucleotides and optimized their labelling for the simultaneous detection. The resulted biobarcode protocol was tested on bacterial mixture sample.

2   Materials and methods

2.1   Chemicals and pH measurement

Chemicals used in this study were purchased from Sigma-Aldrich (St. Louis, USA) in ACS purity unless noted otherwise. The deionized water was prepared using reverse osmosis equipment Aqual 25 (Czech Republic). The deionized water was further purified by using apparatus MilliQ Direct QUV equipped with the UV lamp. The resistance was 18 MΩ. The pH was measured using pH meter WTW inoLab (Weilheim, Germany).

2.2   Cultivation of bacteria strains

Bacteria causing infections (*Staphylococcus aureus,* methicillin-resistant S*taphylococcus aureus, Klebsiella pneumoniae*) were obtained from the Czech Collection of Microorganisms, Faculty of Science, Masaryk University, Brno, Czech Republic. The strains were stored as a frozen stock suspension in 20% (*v/v*) glycerol at -20 °C until their use. Prior to use, the strains were thawed and the glycerol was removed by washing with distilled water. The composition of GTK cultivation medium was as follows: tryptone 5 g/L, yeast extract 2.5 g/L, glucose 1 g/L. pH of the cultivation medium was adjusted at 7.4 before sterilization. The sterilization of the media was carried out at 121 °C for 30 min in an autoclave (Tuttnauer 2450EL, Beit Shemesh, Israel). The prepared cultivation media were inoculated with the bacterial culture in 25 mL Erlenmeyer flasks. After inoculation, the bacterial cultures were grown for 24 h on a shaker at 600 rpm and 37 °C.

2.3   Synthesis and modification of magnetic particles for bacteria isolation

Maghemite particles were prepared according to published method [47,48]. In this study, we prepared three types called MAN-124, MAN-125 and MAN-132a differing in the experimental conditions of preparation and their properties.

Briefly, $Fe(NO_3)_3 \cdot 9H_2O$ (1.5 g) was dissolved by water (80 mL) and solution of $NaBH_4$ (0.2 g) in ammonia (10 mL, 3.5%) was added followed by heating at 100 °C for 2 h. After cooling, the product was left overnight, separated by magnet, washed several times with water. In case of MAN-124, a water solution of polyethylene glycol (PEG) 8 kDa (3 mL, 40 %) was added during stirring and in case of MAN-125, water solution of polyvinylpyrrolidone (0.2 g, PVP 10 kDa) was added under stirring.

MAN-132a were surface modified by water solution of PEG 4 kDa (0.5 g) and glucose (0.5 g) added under stirring. Subsequently, the mixture was suspended in water and a solution of 1

mM HAuCl$_4$ (25 mL) was added and stirred for 1 h. Solution of trisodium citrate (0.75 mL, 0.0265 g/mL) was poured and stirred overnight.

To finalize the preparation, all suspensions were stirred overnight, separated by external magnetic field, washed several times with water and dried at 40 °C.

2.4 Preparation of CdTe QDs covered with mercaptosuccinic acid (MSA)

CdTe QDs were prepared according to previously published protocol [49,50]. Briefly, solution of CdTe QDs was prepared by reaction of cadmium acetate dihydrate (0.053 g in 76 mL of water) with MSA (60 mg/mL) followed by addition of 1 M NH$_3$ (1.8 mL). Finally, a solution of Na$_2$TeO$_3$ (0.0066 g/mL) was added and after few minutes 40 mg of NaBH$_4$ was poured to the stirred solution. Solution was stirred for 1 h, volume was adjusted to 100 mL with addition of water and after that, it was heated in vials filled with 2 mL of the solution in microwave oven Multiwave 300 (Anton Paar, Graz, Austria) under 300 W for 10 min. For the preparation of green QDs temperature was set to 70 °C, for orange ones to 100 °C and for red ones to 120 °C.

2.4.1 CdTe-orange-PEG

SH-mecA Rv (50 µL, 10 µM) was added to CdTe QDs (orange, 500 µL) and shaken for 1h at 22 ºC). 2 µL of 1,1′-Carbonyldiimidazole (CDI, 1 mg/mL in DMSO) and 2 µL of *N,N′*-Dicyclohexylcarbodiimide (DCC, 1 mg/mL in DMSO) were added followed by addition of 5 µL of Poly(ethylene glycol) 2-aminoethyl ether acetic acid (PEG-NH$_2$, 0.5 mg/mL). The sample was shaken overnight, reduced on Amicon 3k, washed with phosphate buffer saline (PBS) and finally diluted to 1 mL with PBS. By the same procedure, the QDs were labeled with SH-fnbA Rv (green QDs) and with SH-wcaG Rv (red QDs).

2.5   Synthesis and modification of magnetic particles for gene isolation

The preparation of gold magnetic particles MAN-53 (AuMNPs) was described in Chudobova *et al.* [51]. Further, the particles MAN-53 were labelled with CdTe QDs according to the following protocols differing in target gene. For detection of *S. aureus*, the particles were labeled with thiolated fnbA primers 5'-[ThiC6]GCGGAGATCAAAGACAAGTA-3' in the case of MAN-53 and with 5'-[ThiC6]CACCATCTATAGCTGTGTGG-3' in the case of QDs. For MRSA detection, the particles were labeled with thiolated mecA primers 5'-[ThiC6]CCCAATTTGTCTGCCAGTTT-3' in the case of MAN-53 and with 5'-[ThiC6]ACCGTTATAATTGCGTGGAG-3' in the case of QDs. For detection of *K. pneumoniae*, the MAN-53 were labeled with thiolated wcaG primers 5'-[ThiC6]ATTTGAAGAGGTTGCAAACGAT-3' and QDs were labeled by 5'-[ThiC6]AAGTGAGACTTCAAAAGAACACAAG-3'. The labeling was performed in 1 M KH_2PO_4 as follows: 10 µL of MAN-53 (10 mg/mL) was diluted in 1 M KH_2PO_4 and incubated at 45 °C for 1 h under 300 rpm. Further, 90 µl of QDs were mixed with 10 µl of 50 µM thiolated fnbA, mecA and wcaG primers, respectively and incubated for 24 h at 4 °C.

2.6   Characterization of particles by scanning electron microscopy (SEM)

Structure of MAN-124, MAN-125 and MAN-132a was visualized by SEM. For documentation of the particles structure, a MIRA2 LMU (Tescan, Brno, Czech Republic) was used. The SEM was fitted with In-Beam SE detector. An accelerating voltage of 15 kV and beam currents about 1 nA provided satisfactory results regarding maximum throughput. For MAN-124, MAN-127 and MAN-132a, the magnification of 100 kX, 100 kX and 5 kX was used, respectively.

2.7 Characterization of particle size

The average particle size and the size distribution were determined by a dynamic light scattering (DLS) measurement using a Malvern Zetasizer (NANO-ZS, Malvern Instruments Ltd., Worcestershire, U.K.). Nanoparticle solution (1 mg/L) in 1.5 mL of distilled water was placed into a polystyrene latex cell and measured at a detector angle of 173°, a wavelength of 633 nm, a refractive index of 0.30, a real refractive index of 1.59, and temperature 25 °C.

2.8 Analysis of growth curves

The ability of magnetic particles to capture bacteria was determined using a growth-curve method [52]. Bacterial cultures were isolated using the magnetic separation by MAN-124, MAN-125 and MAN-132a. Incubation of bacteria with various types of magnetic particles was carried out at 37 °C for 1 hour at 120 rpm in GTK medium. After the incubation, the magnetic particles were washed by PBS and separated. The magnetic particles with the captured bacteria were incubated at 37 °C for 1 hour at 120 rpm in GTK medium. After the removal of the magnetic particles, the supernatants were used for growth-curves measurement. Growth curves were determined by measuring the absorbance using an apparatus Multiskan EX (Thermo Fisher Scientific, Germany) at 600 nm.

2.9 Optimization of multiplex polymerase chain reaction (mPCR)

2.9.1 DNA isolation

For optimization of mPCR, the genes *fnbA, mecA* and *wcaG* were used. 2 mL of each of tested strain (*S. aureus*, MRSA, *Klebsiella pneumoniae*) were centrifuged (5000 g, 20 °C, 10 min) and the lysis was done at 20 °C for 1 h in 400 μL of lysis solution (6 M guanidine hydrochloride and 0.1 M sodium acetate). Isolation of genomic DNA was performed using MagNA Pure Compact (Roche, Germany).

2.9.2 Amplification of *fnbA, mecA* and *wcaG* genes

The *fnbA, mecA* and *wcaG* genes were amplified using the mPCR. The sequences of primers for amplification of the *fnbA* gene (191bp) were 5'-GATACAAACCCAGGTGGTGG-3'(fnbA-fw) and 5'-TGTGCTTGACCATGCTCTTC-3'(fnbA-rv). For amplification of the *mecA* gene (223bp), the primers 5'-CCCAATTTGTCTGCCAGTTT-3' (mecA-fw) and 5'-TGGCAATATTAACGCACCTC-3' (mecA-rv) were used. For amplification of the *wcaG* gene (133bp), the primers 5'-ATTTGAAGAGGTTGCAAACGAT-3' (wcaG-fw) and 5'-AAGTGAGACTTCAAAAGAACACAAG-3' (wcaG-rv) were used.

The PCR mixture from New England Biolabs (Hitchin, United Kingdom) contained the PCR buffer (10 mM Tris–HCl, pH 8.3, and 50 mM KCl with 2.5 mM $MgCl_2$), 0.2 mM of dNTPs, 0.2 μM of each pair of primers (fnbA-fw, fnbA-rv, mecA-fw, mecA-rv, wcaG-fw, wcaG-rv), 1.5 units/μL of Taq DNA polymerase, and 100 ng of each DNA (*S. aureus*, MRSA, *Klebsiella pneumoniae*). The PCR reaction profile was as follows: 94 °C for 4 min, 35 cycles of 94 °C for 30 s, 45 °C for 30 s and 68 °C for 30 s and a final extension at 68 °C for 7 min. The amplification was carried out using Mastercycler ep realplex4S (Eppendorf AG, Hamburg, Germany).

2.9.3 Visualization of amplified genes

The amplified products were analyzed by agarose gel electrophoresis and the conditions were as follows: 2 % agarose gel (High melt/Medium fragment, Mercury, San Diego, CA, USA) with 1×TAE buffer, 60 V and 160 min (Bio-Rad, Hercules, CA, USA). The 100 bp DNA ladder (New England Biolabs, Ispwich, MA, USA) was used as a molecular weight marker. Bands were visualized via UV transilluminator at 312 nm (Vilber-Lourmat, Marne-la- Valle´e Cedex, France) and band intensities were quantified and analyzed by Carestream Molecular

Imaging Software (Carestream, Carestream In vivo Xtreme Imaging System, Rochester, NY, USA) and normalized to *fnbA, mecA* and *wcaG* genes control.

2.10   Biobarcoding

Three bacterial strains were prepared together at different concentrations. The concentrations of bacteria were: 10^2, 10^4, or 10^7 CFU/mL. After the PCR amplification, the PCR products were denatured and incubated with MAN-53 modified with *fnbA, mecA* and *wcaG* forward primers and CdTe (green, orange, red) modified with *fnbA, mecA* and *wcaG* reverse primers (complementary to 3' end of PCR amplicons). The hybridization of the PCR products was performed in 20 mM Tris-HCl, pH 7.4. The fluorescence intensity of CdTe QDs captured by the formed constructs was determined by Tecan NanoQuant plate (TECAN, Mannedorf, Switzerland). For determination of areas and signal intensity, the measured signals were subjected to deconvolution. Absorbance scan of oligonucleotides for calculation of the calibration was performed on Tecan NanoQuant plate (TECAN, Mannedorf, Switzerland).

3   Results and Discussion

3.1   Characterization of particles

The superparamagnetic iron oxide particles are very often used for separation of different kinds of analytes [53,54]. Maghemite (γ-Fe$_2$O$_3$) can be prepared in a relatively easy way, it has perfect magnetic properties and its surface, containing also hydroxide groups, and can be modified by numerous reagents [55]. In this study, the surface was modified with PEG (MAN-124), PVP (MAN-125), and PEG followed by addition of tetrachloroauric acid and reducing agent (MAN-132a). The presence of iron and gold, respectively, were confirmed by X-ray fluorescence analyses (data not shown). Primarily, the magnetic particles were characterized by SEM (Fig. 1A-a, B-a, C-a) to obtain the information about morphology of

the surface. From the SEM images, it is obvious that modification by PVP led to a better stabilization of nanoparticles in comparison with nanoparticles covered by PEG. From the size distribution diagram obtained by the DLS (Fig. 1A-b, 2B-b and 2C-b), it was also visible that the most abundant particle diameters were within the range from 340 to 825 nm and from 90 to 164 nm for MAN-124 and MAN-125, respectively. In the case of MAN-132a, the situation was different. The last step of synthesis, reduction of chloroauric acid with citrate, led to great changes on the surface and probably to a higher agglomeration of already formed PEG modified maghemite nanoparticles. The surface was not as porous as in previous cases and the particles were in micrometer dimensions, which was also confirmed by DLS, where the most abundant particle diameters were within the range from 2.5 to 3.6 μm.

Subsequently, three sizes of CdTe QDs were prepared by microwave heating at 70, 100 and 120 °C. The color was controlled under UV light using illumination by the light with a wavelength of 312 nm and green, orange and red color, respectively, were observed. These CdTe QDs were further modified either by PEG-NH$_2$ or by thiolated oligonucleotides followed by addition of PEG-NH$_2$. DLS was used to assess diameters of CdTe QDs (Fig. 1D). The diameters of green, orange and red CdTe QDs modified by PEG-NH$_2$ only were 1.7 ± 0.4, 3.5 ± 0.7 and 4.8 ± 0.8 nm, respectively. The modification of CdTe QDs by oligonucleotides led to formation of bigger nanoparticles i.e. 8.7 ± 1.2, 13.5 ± 1.8 and 15.7 ± 2.5 nm, respectively. The QDs labelled by specific primers for bacteria detection were characterized by fluorescence spectroscopy. Figure 1E-a shows the excitation spectra of studied QDs (2 μM) within the range from 200 to 500 nm. The common excitation wavelength of 250 nm was found to be optimal for all QDs. After the excitation wavelength optimization, the emission spectra of QDs were measured within the range from 400 to 800 nm (Fig. 1E-b). For the primers-modified QDs (green CdTe-fnbA, orange CdTe-mecA

and red CdTe-wcaG), the emission maxima were determined at 526, 590 and 686 nm, respectively.
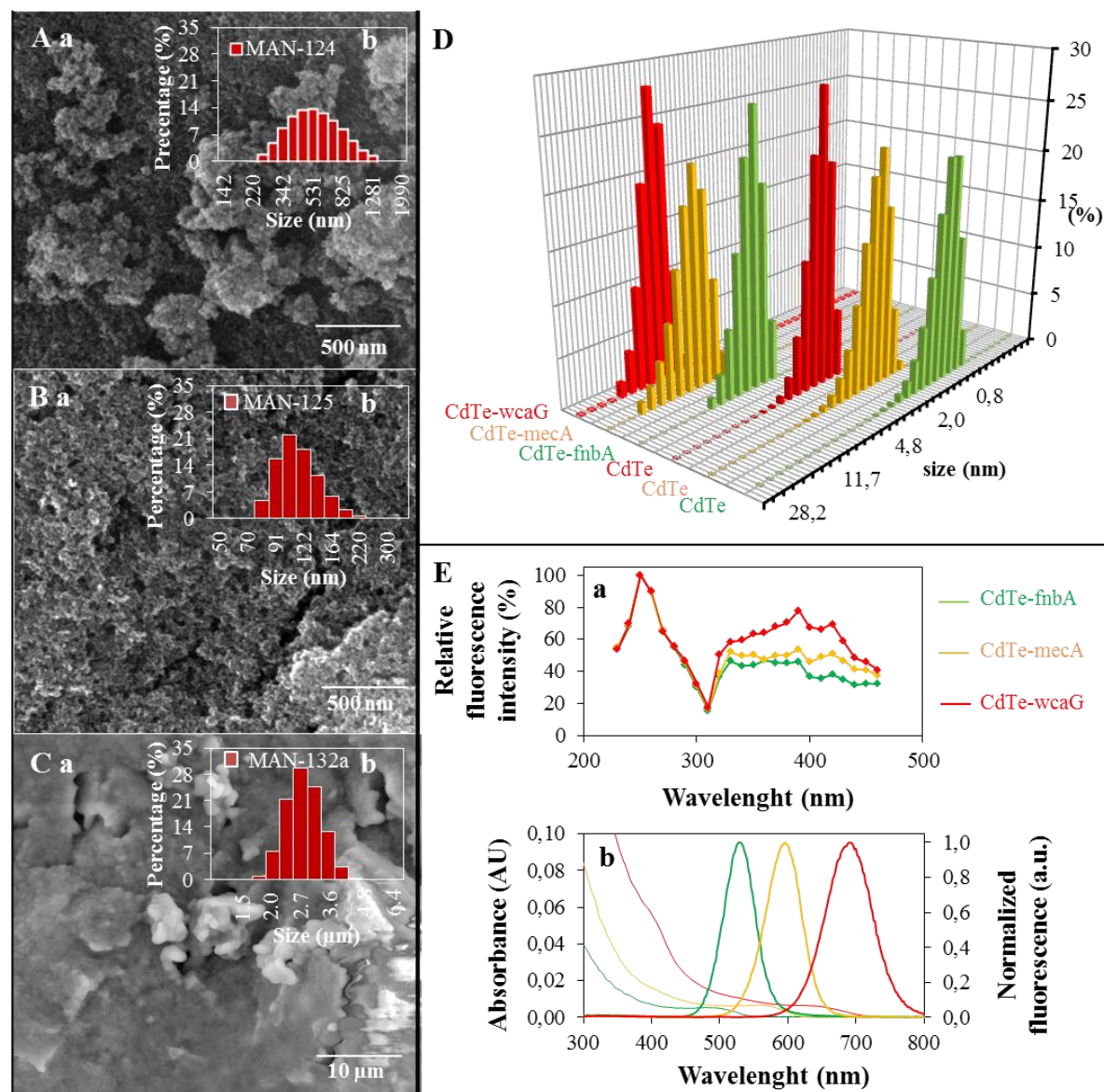

Figure 1: Characterization of each component. A - C) characterization of different magnetic particles – MAN-124 A, MAN-125 B, MAN-132 C (SEM (a), the size distribution of particles (b) and SECM images (c)). Characterization of quantum dots: D) size distribution of CdTe QDs modified by oligonucleotides. Ea) Excitation maxima of QDs, and E-b) absorption and emission maxima of QDs.

3.2   Optimization of bacteria isolation using modified MPs

The scheme of sample preparation used for the analysis of the growth curves is shown in Fig. 2A. Mixture of three tested bacterial strains was used for incubation and measurement of growth curves. The growth curves were measured after incubation of magnetic particles (MAN-124, MAN-125 and MAN-132a) with bacteria. The absorbance values for *S. aureus*, MRSA and *K. pneumoniae* growth ware dependent on binding ability of the individual magnetic particles. The growth curves (Fig. 2B-D) shows the quantitative growth of bacteria after cultivation on MPs, which differed by its modification. All chosen particles exhibited the ability to capture bacteria but in the case of MAN-132a, the growth curves showed the highest absorbance for all chosen bacteria. Therefore, the MAN-132a were chosen for the further experiments. A similar methodology for binding of bacteria to magnetic particles was previously suggested for *S. aureus* binding [47]. The magnetic particles were modified by graphene and glucose that was determined using biochemical reaction with electrochemical detection of 1-naphtol. Other studies used for bacterial capture magnetic particles modified by antibody or enzyme [38,56]. In case of method presented in this study, it is advantageous that no antibodies are required since these are expensive and may not be available for all targeted bacteria.
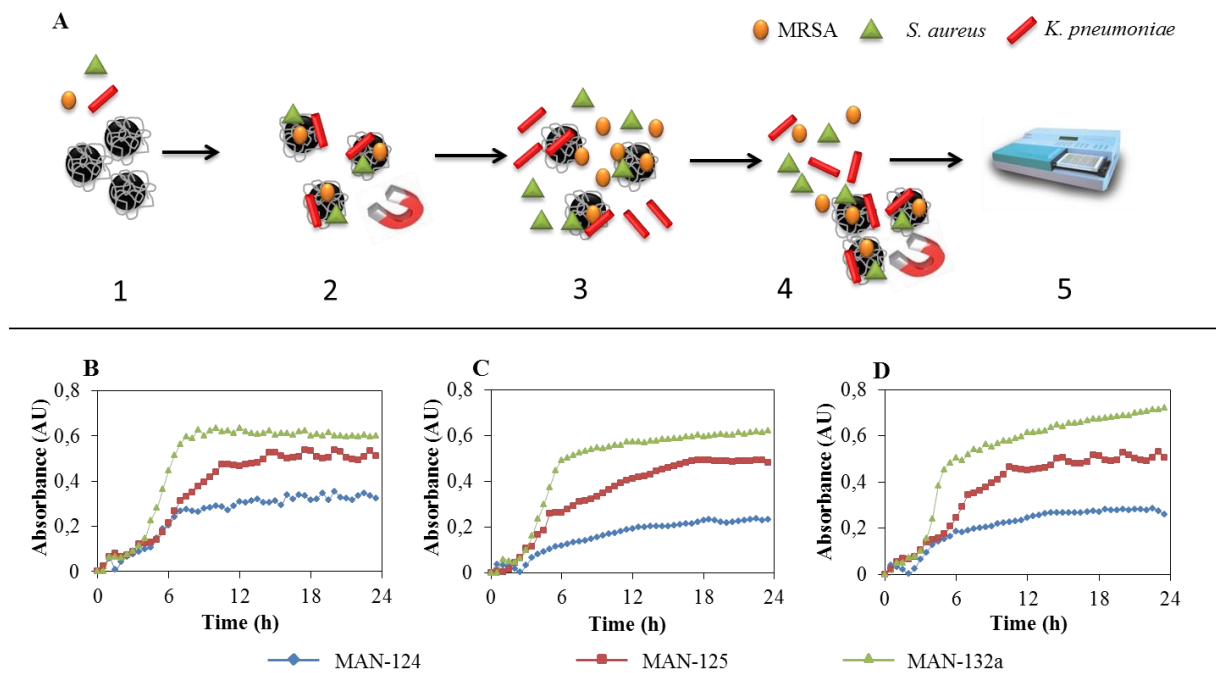
Figure 2: The selection of MPs for bacterial capture. A) Scheme of the process (1- incubation of bacteria with MPs for 1 hour, at 37 °C, 600 rpm in GTK medium, 2 – magnetic purification of the captured bacteria, 3 – cultivation of captured bacteria for 1 hour, at 37 °C, 600 rpm in GTK medium, 4 – removal of MPs, 5 - measurement of growth curves of bacteria, B) growth curves of MRSA, C) growth curves of *S. aureus*, D) growth curves of *K. pneumoniae*.

3.3   mPCR

For determination of *S. aureus*, MRSA and *K. pneumoniae,* the detection of specific genes was chosen. For *S. aureus, fnbA* gene with the size of 191 bp was chosen, MRSA was monitored by resistance gene *mecA* in size of 223 bp and *K. pneumoniae* was determined by the presence of *wcaG* gene of size of 133 bp. Primarily, the conditions of mPCR for all three genes were optimized individually. Optimal conditions for mPCR were determined to be 45 °C for *S. aureus*, 53 °C for MRSA and 50 °C for *K. pneumonia*, amplification time was determined for all genes as 30 s (Fig. 3A). In all cases, 1.2 unit/µl of Taq polymerase was employed.

Fig. 3A shows the scheme of the process of individual testing of mPCR as well as the positive amplification of genes by multiplex PCR. The bacteria capture on the surface of MAN-132a were lysed and the targeted genes were amplified. The visualization by gel electrophoresis proved the successful and specific amplification of the genes with no contaminations. The position of the bands was in a good agreement with the gene sizes.

Subsequently, the procedure was repeated using a mixture of all three bacterial strains. The conditions of the mPCR were - 45 °C for 30 s and 1.5 unit/µl of Taq polymerase. It was confirmed (Fig. 3B) that the genes were amplified even from the mixtures as visualized on the agarose gel.
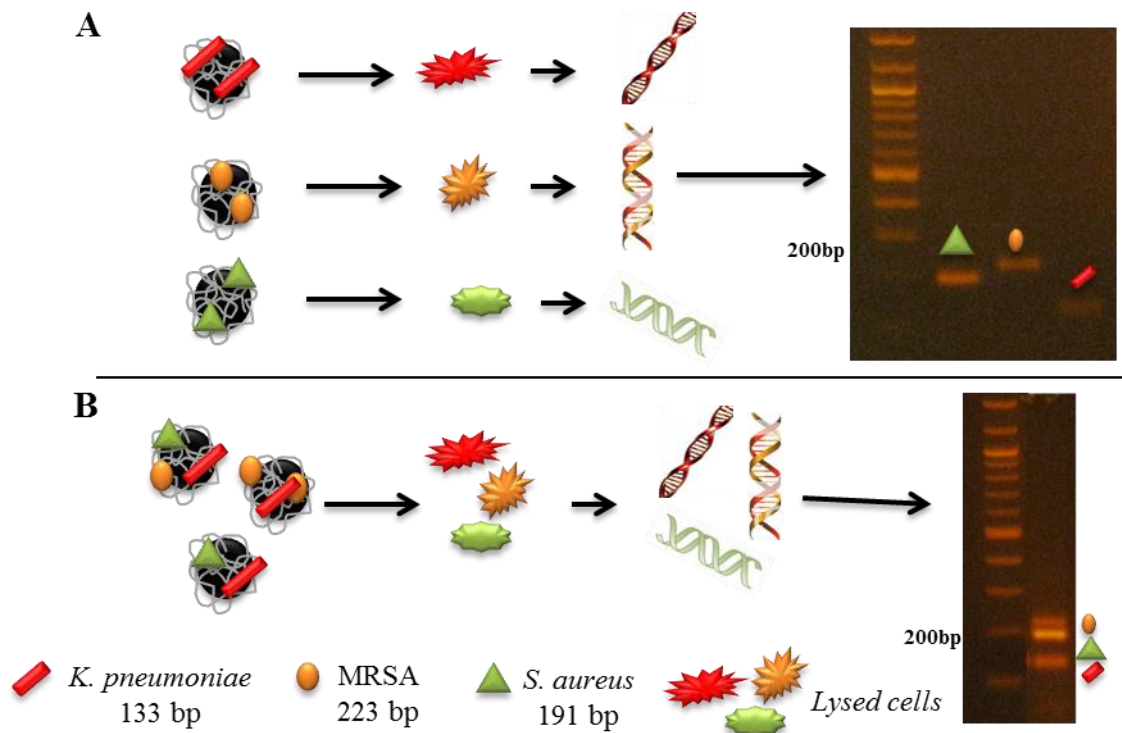

Figure 3: Multiplex PCR for detection of bacteria (*S. aureus*, MRSA, *K. pneumoniae)*: A) Optimal conditions for individual bacterial genes, 1.2 unit/µL Taq 100 ng each bacteria, annealing conditions: *fnbA – S. aureus* 53 °C, 30 sec*, mecA –* MRSA 45 °C, 30 sec, *wcaG – K. pneumoniae* 50 °C, 30 sec); B) Multiplex PCR (45 °C, 30 sec, 100 ng of each bacteria DNA.

3.4   Biobarcoding using MP-based isolation and QD-based detection

Finally, the whole biobarcoding method was tested. The workflow of the entire process is shown in the Fig. 4. First, selected bacteria ware captured on the surface of magnetic particles enabling their isolation from the biological matrix. Subsequently, the captured bacterial cells ware lysed and the mPCR was carried out to amplify the specific genes as described in the previous chapter. Subsequently, the PCR amplicons were denatured by heating at 95 °C for 3 min. Then, the magnetic gold nanoparticles (MAN-53) modified with fnbA, mecA and wcaG forward primers for detection of *S. aureus*, MRSA and *K. pneumoniae* respectively, were hybridized with denatured PCR products at 45 °C for 10 min. After this first hybridization, unbound impurities and unreacted components of the PCR reaction were washed by PBS using magnetic separation. Finally, CdTe QDs modified by oligonucleotides complementary to the 3' end of the denatured PCR products (fragment of *fnbA, mecA, wcaG* gene) were added as shown in Fig 4. These sandwich constructs were washed using magnetic separation and the signal of CdTe-fnbA, CdTe-mecA and CdTe-wcaG was detected by measurement of the fluorescence intensity at 530, 598 and 695 nm for *S. aureus*, MRSA and *K. pneumoniae*, respectively.

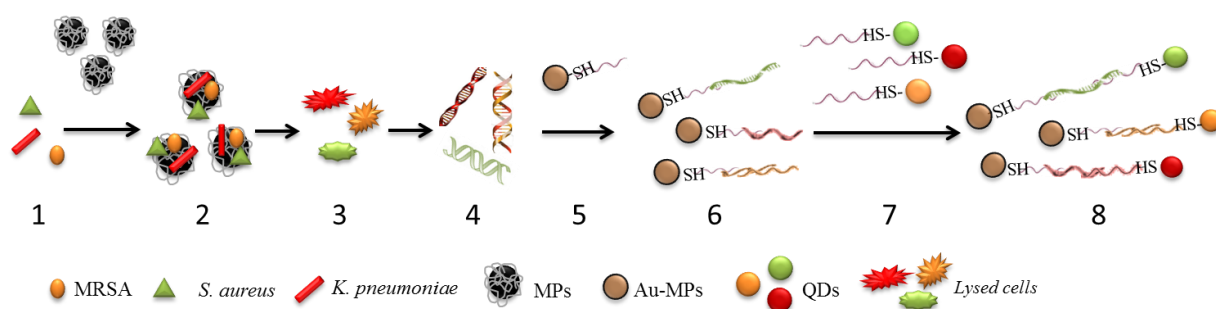**Figure 4:** Scheme of bacteria determination by multiplex barcoding. 1) mixture of bacteria (MRSA, S. aureus, K pneumoniae), 2) addition of MPs and nonspecific capture of bacteria, 3) lysis of bacterial cells dirrectly on the MPs surface, 4) multiplex PCR from the bacterial lysate, 5) addition of Au-MPs labeled by specific oligonucleotides for amplified fragments, 6)

magnetic purification from the PCR mixture, 7) addition of QDs labelled with specific oligonucleotides for amplified fragments captured on Au-MPs, 8) magnetic purification of the final product from unreacted QDs.

The typical signal of the biobarcode analysis obtained for the bacterial mixture is shown in Fig. 5A. The determination is taking advantage from the fact that emission wavelength of QDs is size dependent and therefore the nanoparticle of the same composition may provide emission with several emission maxima and moreover, all these QDs can be excited by a single wavelength (e.g. 250 nm). In this way, a flexible platform can be easily prepared to set up the method upon request by selecting the appropriate oligonucleotide sequences.

To demonstrate the applicability of the method in practice, detection of bacteria at various concentrations was carried out. As shown in Fig. 5B, the proposed method was capable to detect selected bacteria already at 10^2 CFU/ml, which is sufficient even for clinical applications [57-59]. Moreover, the method exhibited the highest sensitivity for MRSA, which presents currently one of the biggest problems due to the fact that the increasing occurrence of these bacteria, resistant to the antibiotics, leads to spread of the nosocomial infections, which are extremely hard to treat. Therefore, the early stage sensitive detection of these resistant bacterial strains is crucial for implementation of the proper treatment.
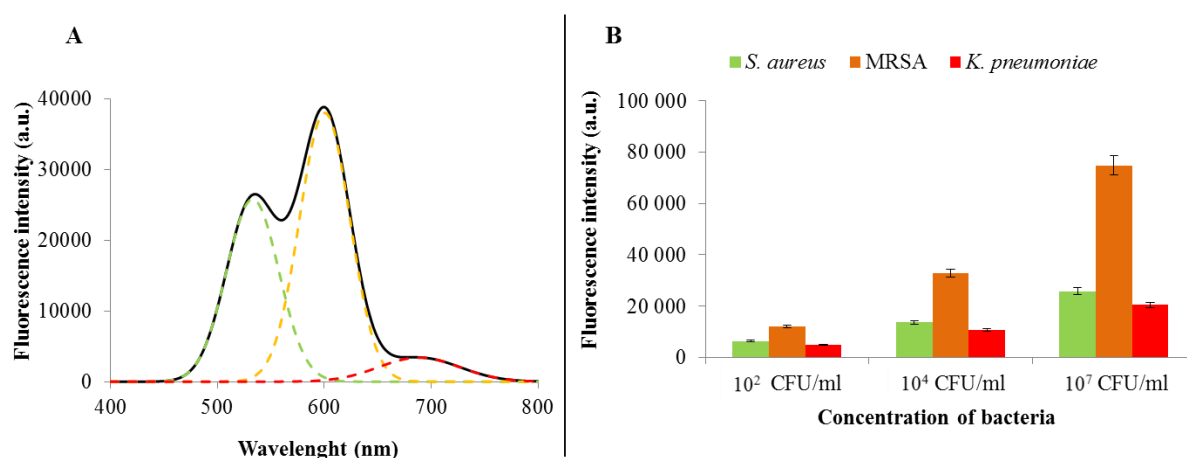
Figure 5: Quantification of bacteria. A) Typical emission spectrum of QDs mixture of isolated bacterial specific genes, B) Dependence of fluorescence intensity of QDs on increasing amount of bacteria.

Conclusions

In the presented work, a biobarcode assay using CdTe QDs was suggested and tested for the detection of presence of *S. aureus*, MRSA and *K. pneumoniae*. This detection was based on various emission maxima of CdTe QDs modified by specific oligonucleotides complementary to 3' end of detection PCR product. This platform can be used also for rapid detection of a range of other microorganisms. Barcode technique can be carried out either under laboratory conditions and using the classic laboratory equipment and also in a wide range of automated instruments, however due to the rapid development of miniaturized analytical devices, the proposed method is well suitable to be implemented into small-scale or even portable devices. These platforms are usually designed and formed by 3D printing [60] and operate mostly on the principle of fluorescence, electrochemical and spectrophotometric detection [61,62] or acquiring of a barcode using a camera [63].

Conflict of Interest

The authors declare no conflict of interests.

References

[1] S. Ruer, N. Pinotsis, D. Steadman, G. Waksman, H. Remaut, Virulence-targeted Antibacterials: Concept, Promise, and Susceptibility to Resistance Mechanisms, Chem. Biol. Drug Des. 86 (2015) 379-399.

[2] I. Livshiz-Riven, A. Borer, R. Nativ, S. Eskira, E. Larson, Relationship between shared patient care items and healthcare-associated infections: A systematic review, Int. J. Nurs. Stud. 52 (2015) 380-392.

[3] H.A. Khan, A. Ahmad, R. Mehboob, Nosocomial infections and their control strategies, Asian Pac J Trop Biomed 5 (2015) 509-514.

[4] S. Lal, S.K. Singhrao, U.E.M. Achilles-Day, L.H.G. Morton, M. Pearce, S. Crean, Risk Assessment for the Spread of Serratia marcescens Within Dental-Unit Waterline Systems Using Vermamoeba vermiformis, Curr. Microbiol. 71 (2015) 434-442.

[5] H.R. Rose, R.S. Holzman, D.R. Altman, D.S. Smyth, G.A. Wasserman, J.M. Kafer, M. Wible, R.E. Mendes, V.J. Torres, B. Shopsin, Cytotoxic Virulence Predicts Mortality in Nosocomial Pneumonia Due to Methicillin-Resistant Staphylococcus aureus, J. Infect. Dis. 211 (2015) 1862-1874.

[6] A.F. Shorr, L.A. Puzniak, P. Biswas, M.S. Niederman, Predictors of Clinical Success in the Treatment of Patients with Methicillin-Resistant Staphylococcus aureus (MRSA) Nosocomial Pneumonia (NP), PLoS One 10 (2015).

[7] C.J. Kim, H.B. Kim, M.D. Oh, Y. Kim, A. Kim, S.H. Oh, K.H. Song, E.S. Kim, Y.K. Cho, Y.H. Choi, J. Park, B.N. Kim, N.J. Kim, K.H. Kim, E.J. Lee, J.B. Jun, Y.K. Kim, S.M. Kiem, H.J. Choi, E.J. Choo, K.M. Sohn, S. Lee, H.H. Chang, J.H. Bang, S.J. Lee, J.H. Lee, S.Y. Park, M.H. Jeon, N.R. Yun, K.S. Grp, G. Korea Infect Dis Study, The burden of nosocomial staphylococcus aureus bloodstream infection in South Korea: a prospective hospital-based nationwide study, BMC Infect. Dis. 14 (2014).

[8] I.F. Chaberny, E. Ott, Multiresistant pathogens in surgery, Unfallchirurg 114 (2011) 193-196.

[9] R.R. Watkins, M.Z. David, R.A. Salata, Current concepts on the virulence mechanisms of meticillin-resistant Staphylococcus aureus, J. Med. Microbiol. 61 (2012) 1179-1193.

[10] S.J. Peacock, G.K. Paterson, in R.D. Kornberg (Editor), Annual Review of Biochemistry, Vol 84, Annual Reviews, Palo Alto, 2015, p. 577-601.

[11] P. Lagace-Wiens, A. Walkty, J.A. Karlowsky, Ceftazidime-avibactam: an evidence-based review of its pharmacology and potential use in the treatment of Gram-negative bacterial infections, 9 (2014) 13-25.

[12] M. Bassetti, M. Merelli, C. Temperoni, A. Astilean, New antibiotics for bad bugs: where are we?, Ann. Clin. Microbiol. Antimicrob. 12 (2013).

[13] A.H. Kashani, D. Eliott, The emergence of Klebsiella pneumoniae endogenous endophthalmitis in the USA: basic and clinical advances, 3 (2013) 28.

[14] L.W.K. Chang, K.L. Buising, C.J. Jeremiah, K. Cronin, Y.S.P. Lorenzo, B.P. Howden, J. Kwong, J. Cocks, A. Blood, J. Greenough, M.J. Waters, Managing a nosocomial outbreak of carbapenem-resistant Klebsiella pneumoniae: an early Australian hospital experience, Intern. Med. J. 45 (2015) 1037-1043.

[15] J.D.D. Pitout, P. Nordmann, L. Poirel, Carbapenemase-Producing Klebsiella pneumoniae, a Key Pathogen Set for Global Nosocomial Dominance, Antimicrob. Agents Chemother. 59 (2015) 5873-5884.

[16] G.G. Gaspar, F. Bellissimo-Rodrigues, L.N. de Andrade, A.L. Darini, R. Martinez, Induction and nosocomial dissemination of carbapenem and polymyxin-resistant Klebsiella pneumoniae, Rev. Soc. Bras. Med. Trop. 48 (2015) 483-487.

[17]   S. Hoppe, F.F. Bier, M. von Nickisch-Rosenegk, Identification of Antigenic Proteins of the Nosocomial Pathogen Klebsiella pneumoniae, PLoS One 9 (2014).

[18]   C.M. Luna, I. Bledel, A. Raimondi, The role of surveillance cultures in guiding ventilator-associated pneumonia therapy, Curr. Opin. Infect. Dis. 27 (2014) 184-193.

[19]   D.M. Kusahara, L.T. Friedlander, M.A.S. Peterlini, M.L.G. Pedreira, Oral care and oropharyngeal and tracheal colonization by Gram-negative pathogens in children, Nurs. Crit. Care 17 (2012) 115-122.

[20]   P. Torres-Gonzalez, M.E. Cervera-Hernandez, M.D. Niembro-Ortega, F. Leal-Vega, L.P. Cruz-Hervert, L. Garcia-Garcia, A. Galindo-Fraga, A. Martinez-Gamboa, M. Bobadilla-del Valle, J. Sifuentes-Osornio, A. Ponce-de-Leon, Factors Associated to Prevalence and Incidence of Carbapenem-Resistant Enterobacteriaceae Fecal Carriage: A Cohort Study in a Mexican Tertiary Care Hospital, PLoS One 10 (2015).

[21]   M. Shokouhfard, R.K. Kermanshahi, R.V. Shahandashti, M.M. Feizabadi, S. Teimourian, The inhibitory effect of a Lactobacillus acidophilus derived biosurfactant on biofilm producer Serratia marcescens, Iran. J. Basic Med. Sci. 18 (2015) 1001-1007.

[22]   O. Blennow, P. Ljungman, The challenge of antibiotic resistance in haematology patients, Br. J. Haematol. 172 (2016) 497-511.

[23]   M. Cainzos, Review of the guidelines for complicated skin and soft tissue infections and intra-abdominal infections-are they applicable today?, Clin. Microbiol. Infect. 14 (2008) 9-18.

[24]   I. Altinok, Multiplex PCR assay for detection of four major bacterial pathogens causing rainbow trout disease, Dis. Aquat. Org. 93 (2011) 199-206.

[25]   M.A. Tsai, P.Y. Ho, P.C. Wang, Y.J. E, L.L. Liaw, S.C. Chen, Development of a multiplex polymerase chain reaction to detect five common Gram-negative bacteria of aquatic animals, J. Fish Dis. 35 (2012) 489-495.

[26]   D.F. Zhang, Q.Q. Zhang, A.H. Li, Development of a multiplex PCR assay for rapid and simultaneous detection of four genera of fish pathogenic bacteria, Lett. Appl. Microbiol. 59 (2014) 471-478.

[27]   S.E. Brunker, K.B. Cederquist, C.D. Keating, Metallic barcodes for multiplexed bioassays, Nanomedicine 2 (2007) 695-710.

[28]   D. Begerow, H. Nilsson, M. Unterseher, W. Maier, Current state and perspectives of fungal DNA barcoding and rapid identification procedures, Appl. Microbiol. Biotechnol. 87 (2010) 99-108.

[29]   Y.J. Zhao, Y. Cheng, L.R. Shang, J. Wang, Z.Y. Xie, Z.Z. Gu, Microfluidic Synthesis of Barcode Particles for Multiplex Assays, Small 11 (2015) 151-174.

[30]   Y.G. Li, D. Luo, Multiplexed molecular detection using encoded microparticles and nanoparticles, Expert Rev. Mol. Diagn. 6 (2006) 567-574.

[31]   Y. Ma, L. Lu, DNA barcode technology, 23 (2012) 185-190, 205.

[32]   G. Wang, Y.-D. Dong, T.-Y. Zhao, ADVANCES OF DNA BARCODING, 21 (2014) 65-72.

[33]   H.D. Hill, C.A. Mirkin, The bio-barcode assay for the detection of protein and nucleic acid targets using DTT-induced ligand exchange, Nat. Protoc. 1 (2006) 324-336.

[34]   A.S. Tanabe, H. Toju, Two New Computational Methods for Universal DNA Barcoding: A Benchmark Using Barcode Sequences of Bacteria, Archaea, Animals, Fungi, and Land Plants, PLoS One 8 (2013).

[35]   M. Tintore, S. Grijalvo, R. Eritja, C. Fabrega, Synthesis of oligonucleotides carrying fluorescently labelled O-6-alkylguanine for measuring hAGT activity, Bioorg. Med. Chem. Lett. 25 (2015) 5208-5211.

[36] C.L. Ren, R. Schlapak, R. Hager, I. Szleifer, S. Howorka, Molecular and Thermodynamic Factors Explain the Passivation Properties of Poly(ethylene glycol)-Coated Substrate Surfaces against Fluorophore-Labeled DNA Oligonucleotides, Langmuir 31 (2015) 11491-11501.

[37] A.Y. Skoblov, M.V. Vichuzhanin, V.M. Farzan, O.A. Veselova, T.A. Konovalova, A.T. Podkolzin, G.A. Shipulin, T.S. Zatsepin, Solid- and solution-phase synthesis and application of R6G dual-labeled oligonucleotide probes, Bioorg. Med. Chem. 23 (2015) 6749-6756.

[38] Q.R. Xiong, X. Cui, J.K. Saini, D.F. Liu, S. Shan, Y. Jin, W.H. Lai, Development of an immunomagnetic separation method for efficient enrichment of Escherichia coli O157:H7, Food Control 37 (2014) 41-45.

[39] A.H. Huang, Z.G. Qiu, M. Jin, Z.Q. Shen, Z.L. Chen, X.W. Wang, J.W. Li, High-throughput detection of food-borne pathogenic bacteria using oligonucleotide microarray with quantum dots as fluorescent labels, Int. J. Food Microbiol. 185 (2014) 27-32.

[40] R.Q. Liang, W. Li, Y. Li, C.Y. Tan, J.X. Li, Y.X. Jin, K.C. Ruan, An oligonucleotide microarray for microRNA expression analysis based on labeling RNA with quantum dot and nanogold probe, Nucleic Acids Res. 33 (2005).

[41] H. Yao, Z.-h. Huang, Z. Li, R. He, F. Gao, D.-x. Cui, Biological activity of survivin antisense oligonucleotide labeled with quantum dots or green fluorescein: a comparative study, J South Med Uni 27 (2007) 663-666.

[42] M. Liong, C. Tassa, S.Y. Shaw, H. Lee, R. Weissleder, Multiplexed Magnetic Labeling Amplification Using Oligonucleotide Hybridization, Adv. Mater. 23 (2011) H254-H258.

[43] K. Faulds, R. Jarvis, W.E. Smith, D. Graham, R. Goodacre, Multiplexed detection of six labelled oligonucleotides using surface enhanced resonance Raman scattering (SERRS), Analyst 133 (2008) 1505-1512.

[44] M. Mirzaee, S. Najar-Peerayeh, M. Behmanesh, M.F. Moghadam, Relationship Between Adhesin Genes and Biofilm Formation in Vancomycin-Intermediate Staphylococcus aureus Clinical Isolates, Curr. Microbiol. 70 (2015) 665-670.

[45] T. Wang, Z. Zhang, Y.Y. Li, G.M. Xie, Amplified electrochemical detection of mecA gene in methicillin-resistant Staphylococcus aureus based on target recycling amplification and isothermal strand-displacement polymerization reaction, Sens. Actuator B-Chem. 221 (2015) 148-154.

[46] J.Y. Ho, T.L. Lin, C.Y. Li, A. Lee, A.N. Cheng, M.C. Chen, S.H. Wu, J.T. Wang, T.L. Li, M.D. Tsai, Functions of Some Capsular Polysaccharide Biosynthetic Genes in Klebsiella pneumoniae NTUH K-2044, PLoS One 6 (2011).

[47] L. Nejdl, J. Kudr, K. Cihalova, D. Chudobova, M. Zurek, L. Zalud, L. Kopecny, F. Burian, B. Ruttkay-Nedecky, S. Krizkova, M. Konecna, D. Hynek, P. Kopel, J. Prasek, V. Adam, R. Kizek, Remote-controlled robotic platform ORPHEUS as a new tool for detection of bacteria in the environment, Electrophoresis 35 (2014) 2333-2345.

[48] Z. Heger, N. Cernei, S. Krizkova, M. Masarik, P. Kopel, P. Hodek, O. Zitka, V. Adam, R. Kizek, Paramagnetic Nanoparticles as a Platform for FRET-Based Sarcosine Picomolar Detection, Sci Rep 5 (2015).

[49] S. Krizkova, S. Dostalova, P. Michalek, L. Nejdl, M. Kominkova, V. Milosavljevic, A. Moulick, M. Vaculovicova, P. Kopel, V. Adam, R. Kizek, SDS-PAGE as a Tool for Hydrodynamic Diameter-Dependent Separation of Quantum Dots, Chromatographia 78 (2015) 785-793.

[50] E. Guszpit, S. Krizkova, M. Kepinska, M.A.M. Rodrigo, H. Milnerowicz, P. Kopel, R. Kizek, Fluorescence-tagged metallothionein with CdTe quantum dots analyzed by the chip-CE technique, J. Nanopart. Res. 17 (2015).

[51] D. Chudobova, K. Cihalova, S. Skalickova, J. Zitka, M.A.M. Rodrigo, V. Milosavljevic, D. Hynek, P. Kopel, R. Vesely, V. Adam, R. Kizek, 3D-printed chip for detection of methicillin-resistant Staphylococcus aureus labeled with gold nanoparticles, Electrophoresis 36 (2015) 457-466.

[52] K. Cihalova, D. Chudobova, P. Michalek, A. Moulick, R. Guran, P. Kopel, V. Adam, R. Kizek, Staphylococcus aureus and MRSA Growth and Biofilm Formation after Treatment with Antibiotics and SeNPs, Int. J. Mol. Sci. 16 (2015) 24656-24672.

[53] A.J. Kell, K. Somaskandan, G. Stewart, M.G. Bergeron, B. Simard, Superparamagnetic nanoparticle-polystyrene bead conjugates as pathogen capture mimics: A parametric study of factors affecting capture efficiency and specificity, Langmuir 24 (2008) 3493-3502.

[54] A.K. Gupta, R.R. Naregalkar, V.D. Vaidya, M. Gupta, Recent advances on surface engineering of magnetic iron oxide nanoparticles and their biomedical applications, Nanomedicine 2 (2007) 23-39.

[55] A. Drenkova-Tuhtan, K. Mandel, A. Paulus, C. Meyer, F. Hutter, C. Gellermann, G. Sextl, M. Franzreb, H. Steinmetz, Phosphate recovery from wastewater using engineered superparamagnetic particles modified with layered double hydroxide ion exchangers, Water Res. 47 (2013) 5670-5677.

[56] S. Mun, S.J. Choi, Detection of Salmonella typhimurium by antibody/enzyme-conjugated magnetic nanoparticles, BioChip J. 9 (2015) 10-15.

[57] S.V. Gaidhani, A.V. Raskar, S. Poddar, S. Gosavi, P.K. Sahu, K.R. Pardesi, S.V. Bhide, B.A. Chopade, Time dependent enhanced resistance against antibiotics & metal salts by planktonic & biofilm form of Acinetobacter haemolyticus MMC 8 clinical isolate, Indian J. Med. Res. 140 (2014) 665-671.

[58] C. Konig, H.P. Simmen, J. Blaser, Bacterial concentrations in pus and infected peritoneal fluid - implications for bactericidal activity of antibiotics, J. Antimicrob. Chemother. 42 (1998) 227-232.

[59] S.O. Moghadam, M.R. Pourmand, F. Aminharati, Biofilm formation and antimicrobial resistance in methicillin-resistant Staphylococcus aureus isolated from burn patients, Iran, J. Infect. Dev. Ctries. 8 (2014) 1511-1517.

[60] G.D. Park, K.D. Park, in, p. 19.

[61] K. Ming, J. Kim, M.J. Biondi, A. Syed, K. Chen, A. Lam, M. Ostrowski, A. Rebbapragada, J.J. Feld, W.C.W. Chan, Integrated Quantum Dot Barcode Smartphone Optical Device for Wireless Multiplexed Diagnosis of Infected Patients, ACS Nano 9 (2015) 3060-3074.

[62] R.A. Pinkowitz, M.J. Ockham, G.V. Williams, N.X. Krueger, A. Han, L.S. Mungo, J.L. Dowling, J.S. Minahan, J. Kessler, G. Chevalier, R.T. Lacroix, in, p. 134.

[63] K. Yang, S. Lee, S. Je, K.S. Yang, S.E. Lee, S.M. Je, in, p. 19.

5.6 Růst a tvorba biofilmu *S. aureus* a MRSA po léčbě antibiotik a SeNPs

5.6.1 Vědecký článek VI

CIHALOVA, K.; CHUDOBOVA, D.; MICHALEK, P.; MOULICK, A.; GURAN, R.; KOPEL, P.; ADAM, V.; KIZEK, R. *Staphylococcus aureus* and MRSA Growth and Biofilm Formation after Treatment with Antibiotics and SeNPs. *International Journal of Molecular Sciences*, 2015, roč. 16. č. 10, s. 24656-24672. ISSN 1422-0067.

Po rychlé, přesné a citlivé diagnostice bakteriálních druhů v infekčním onemocnění následuje nasazení vhodného léčiva v podobě antibiotika, které je vybráno tak, aby bylo na přítomnou skupinu bakterií v infekci co nejúčinnější *(Paterson a kol., 2005)*. Vzhledem k výskytu a neustálému vývoji bakteriální rezistence, je důležité zvolit skupinu antibiotik tak, aby obsažené druhy bakterií byly cílem účinku těchto antibiotik *(Doern a kol., 1997)*. Ovšem dlouhodobým podáváním jednoho druhu antibiotik je vznik rezistence u bakterií v infekci pravděpodobnější, a proto je možností tato antibiotika nahradit alternativou, která může být v podobě nanočástic kovů *(Doern, Brueggemann, Pierce, Holleya Rauch, 1997)*, anebo jen účinek antibiotik nanočásticemi podpořit. Jak již bylo zmíněno, MRSA disponuje rezistencí vůči β-laktamovým antibiotikům, mezi které patří penicilin, oxacilin či ampicilin, a tak je jeho léčba komplikovaná *(Baba a kol., 2002; Rand a kol., 2004)*. V této studii jsme se rozhodli testovat, jaký účinek mají tato antibiotika na *S. aureus* a MRSA v kombinaci s nanočásticemi selenu (SeNPs), které samy o sobě způsobují inhibici růstu bakterií *(Chudobova, Cihalova, Dostalova, Ruttkay-Nedecky, Rodrigo, Tmejova, Kopel, Nejdl, Kudr, Gumulec, Krizkova, Kynicky, Kizeka Adam, 2014)*.

Cílem této práce bylo sledování růstových vlastností a schopnosti tvorby biofilmu u *S. aureus* a MRSA po aplikaci antibiotik a SeNPs v komplexu s antibiotiky. Výsledky poukazují na silný inhibiční účinek komplexů SeNPs a antibiotik. Měřením impedance bylo pozorováno i vyšší narušení biofilmu účinkem komplexů než samotných antibiotik. Tvorba biofilmu byla pro *S. aureus* inhibována o 99 % ± 7 % a pro MRSA o 94 % ± 4 % účinkem komplexů SeNPs s antibiotiky, zatímco pro antibiotika samotná byl inhibiční účinek pro *S. aureus* 79 % ± 5 % a pro MRSA jen 16 % ± 2 %. Po vystavení

působení nízké koncentrace β-laktamových antibiotik (50 μM) a jejich komplexů se selenovými nanočásticemi byla stanovena intenzita exprese *mecA* genu pro *S. aureus* a MRSA. Výsledkem byla vysoká exprese tohoto genu u MRSA v případě působení samotných antibiotik. U komplexů antibiotik a selenových nanočástic byla exprese tohoto genu nižší. V případě *S. aureus* byla exprese jen v některých případech, a to nepatrná. Změny byly pozorovány i v proteinovém složení bakterií po aplikaci antibiotik a testovaných komplexů. Výsledky získané touto studií poskytují základ pro použití SeNPs jako nástroje pro léčbu bakteriálních infekcí, které mohou být vzhledem ke zvyšující se bakteriální rezistenci vůči konvenčním léčivům vysoce komplikované.

Article

Staphylococcus aureus and MRSA Growth and Biofilm Formation after Treatment with Antibiotics and SeNPs

Kristyna Cihalova [1,2], Dagmar Chudobova [1,2], Petr Michalek [1,2], Amitava Moulick [1,2], Roman Guran [1,2], Pavel Kopel [1,2], Vojtech Adam [1,2,3] and Rene Kizek [1,2,*]

[1] Department of Chemistry and Biochemistry, Mendel University in Brno, Zemedelska 1, CZ-613 00 Brno, Czech Republic; E-Mails: kriki.cihalova@seznam.cz (K.C.); dagmar.chudobova@centrum.cz (D.C.); petrmichalek85@gmail.com (P.M.); amitavamoulick@gmail.com (A.M.); r.guran@email.cz (R.G.); paulko@centrum.cz (P.K.); vojtech.adam@mendelu.cz (V.A.)

[2] Central European Institute of Technology, Brno University of Technology, Technicka 3058/10, CZ-616 00 Brno, Czech Republic

[3] Department of Microelectronics, Faculty of Electrical Engineering and Communication, Brno University of Technology, Technicka 3058/10, CZ-616 00 Brno, Czech Republic

* Author to whom correspondence should be addressed; E-Mail: kizek@sci.muni.cz; Tel.: +420-5-4513-3350; Fax: +420-5-4521-2044.

Academic Editor: Bing Yan

Abstract: Methicillin-resistant *Staphylococcus aureus* (MRSA) is a dangerous pathogen resistant to β-lactam antibiotics. Due to its resistance, it is difficult to manage the infections caused by this strain. We examined this issue in terms of observation of the growth properties and ability to form biofilms in sensitive *S. aureus* and MRSA after the application of antibiotics (ATBs)—ampicillin, oxacillin and penicillin—and complexes of selenium nanoparticles (SeNPs) with these ATBs. The results suggest the strong inhibition effect of SeNPs in complexes with conventional ATBs. Using the impedance method, a higher disruption of biofilms was observed after the application of ATB complexes with SeNPs compared to the group exposed to ATBs without SeNPs. The biofilm formation was intensely inhibited (up to 99% ± 7% for *S. aureus* and up to 94% ± 4% for MRSA) after application of SeNPs in comparison with bacteria without antibacterial compounds whereas ATBs without SeNPs inhibited *S. aureus* up to 79% ± 5% and MRSA up to 16% ± 2% only. The obtained results provide a basis for the use of SeNPs as a tool for the treatment

of bacterial infections, which can be complicated because of increasing resistance of bacteria to conventional ATB drugs.

1. Introduction

The formation of biofilms is a natural property of a wide range of bacterial species [1,2]. These species can cause many serious bacterial infections initiating serious complications [3–5]. Staphylococci are recognized as the most frequent causes of biofilm-associated infections [6], dental plaque [7] and this exceptional status among biofilm-associated pathogens is due to the fact that they are frequent commensal bacteria on the human skin and mucous surfaces (and those of many other mammals).

Excessive use of methicillin antibiotics (ATBs) led to the formation of methicillin-resistant *S. aureus* (MRSA) with adhesion properties. The occurrence of resistant strains of bacteria is a complication of all medical practices that are commonly encountered in recent time with CA-MRSA (community-associated methicillin-resistant *S. aureus*) [8] and HA-MRSA (hospital-acquired methicillin-resistant *S. aureus*) [9]. These strains are unlike non-resistant *S. aureus* resistant to β-lactam ATBs [10]. All MRSA strains carry an acquired genetic determinant-*mecA* or *mecC*- which encodes low affinity penicillin binding proteins-PBP2a [11]. The *mecA* gene is present on a Staphylococcal cassette chromosome *mec* (SCC*mec*), which is a genomic island that concentrates β-lactam ATBs resistance genes and other resistance genes [12]. The majority of MRSA found in clinical testing are multidrug resistant (MDR) [13]. MRSA may be resistant to other groups of antibiotics such as aminoglycosids, cefalosporins, penicillins or glycopeptides. Included in the glycopeptides group is vancomycin, which has long been considered the antibiotic of last resort against serious and multi-drug-resistant infections caused by Gram-positive bacteria. However, vancomycin resistance has emerged, first in enterococci [14,15] and, more recently, in *Staphylococcus aureus* [16].

Because of an increasing resistance of bacterial species to ATBs, it is necessary to develop new methods for bacterial inhibition. Recently, scientists were increasingly focused on the activity of silver nanoparticles that exhibit antibacterial, antiviral and antifungal effects [17], as in the case of gold nanoparticles [18], TiO_2 nanoparticles [19], or a mixture of Ag/ZnO nanoparticles [20]. A study [21] compared the antibacterial effect between silver and selenium nanoparticles; antibacterial effects of selenium nanoparticles inhibited the bacteria *S. aureus* surprisingly better than nanoparticles of silver phosphate. In another study, selenium nanoparticles (SeNPs) showed good properties as antibacterial drugs. The effect of selenium nanoparticles was confirmed in a study by Tran *et al.* [22] that showed that the growth of *S. aureus* is inhibited after three hours of incubation with SeNPs. The combination of ATBs drugs, which are aimed at groups of multi-drug resistant bacteria [23], with the metal nanoparticles can also represent a new alternative as pharmaceutical tools with a high antibacterial effect on a broad spectrum of both resistant and non-resistant bacteria [24]. Metal nanoparticles interacting with cellular components (DNA, RNA and ribosomes) deactivate and effectively alter cellular processes [25]. Metal nanoparticles penetrate the cell membrane to reach the cytosol due to

their ability to dissolve slowly while releasing ions, but the exact mechanism of the metal nanoparticles antimicrobial action remains unclear [21].

For determining antibacterial effect to resistant bacteria we compared non-resistant *S. aureus* and methicillin-resistant *S. aureus*. This study examined the changes on the cellular level in cultures of *S. aureus* and MRSA after incubation with ATBs and complexes of SeNPs with ATBs. At the same time, attention was focused on the changes of biofilm formation after ATBs and complexes of SeNPs with ATBs treatment. Real-time cell analysis (RTCA) on xCELLigence device was used for this determination [26,27]. The method works on the principle of cell adhesion on the surface of electrodes, which modulates the resulting impedance [28]. In the case of bacteria adherence of biofilm on the surface of the electrodes occurs [29] and thereby the change of the relative impedance is observed [30]. The study was supported through monitoring of the activity of the expression process of ATB resistance genes.

2. Results and Discussion

2.1. Influence of Antibacterial Compounds to Growth Properties

Microbiological determination of the inhibition zone sizes showed evident inhibitory effect resulting from the application of SeNPs enhanced by forming a complex with ampicillin, oxacillin and penicillin. The ATBs alone demonstrated antibacterial properties only for sensitive *S. aureus* with sizes of the growth inhibition zones within the range of 4–12 mm (Figure 1A). However, the complexes of SeNPs with ATBs showed the significant antibacterial effect with inhibition zone sizes within the range of 6–13 mm for sensitive *S. aureus* (Figure 1(Aa)) and 3–5 mm for MRSA (Figure 1(Ab)). After the application of ampicillin, the observed sizes of growth inhibition zones were 4 and 6 mm for non-resistant *S. aureus* (Figure 1(Aa)) and 0 and 4 mm for MRSA (Figure 1(Ab)). Application of oxacillin provided the highest growth inhibition zones with sizes of 12 and 13 mm for non-resistant *S. aureus* (Figure 1(Aa)) and 0 and 5 mm for MRSA (Figure 1(Ab)). In the case of penicillin, the sizes of inhibition zones were 7 and 8 mm for non-resistant *S. aureus* (Figure 1(Aa)) and 0 and 3 mm for MRSA (Figure 1(Ab)). Application of other drugs exhibited similar results. Although MRSA did not form inhibition zones after application of the discs containing ATBs without SeNPs, complexes of SeNPs with ATBs manifested inhibition zones between 4–6 mm. Application of complex of SeNPs with AMP, OXA, PNC has about 0%, 25%, 54% higher inhibition effect than SeNPs alone for non-resistant *S. aureus*, respectively, and about 25%, 40%, 0% higher inhibition effect than SeNPs alone for MRSA, respectively. The inhibition effect of SeNPs is about 50% higher for non-resistant *S. aureus* than for MRSA. In the case of non-resistant *S. aureus*, larger inhibition zones were observed after the application of complexes of SeNPs with ATBs than ATBs alone. In the non-resistant *S. aureus* case, ampicillin, oxacillin and penicillin caused higher inhibitory effects (44%, 8% and 13% respectively) when applied in combination with SeNPs than ATBs alone (Figure 1(Aa)). Application of ATBs in combination with SeNPs caused 100% higher inhibition effect because ATBs do not cause formation of the inhibition zones (Figure 1(Ab)). Muhsin *et al.* [31] reported that the application of silver nanoparticles caused a 17 mm wide growth inhibition zone for *S. aureus*. On the other hand, the use of gentamycin alone could cause a growth inhibition zone of larger size (31 mm). However, the

modification of silver nanoparticles with gentamycin showed a small increase of the inhibition zone width up to 33 mm [31].

Figure 1. (**A**) Determination of inhibition zones after application of circular discs on the *S. aureus* (**a**) and MRSA (**b**) strains with 100 µM concentration of ampicillin, oxacillin, penicillin or complexes (100 µM of nanoparticles and 100 µM of ATBs) of SeNPs with ampicillin, SeNPs with oxacillin and SeNPs with penicillin. Cultivation was carried out at 37 °C for 24 h; (**B**) Optimization of SeNPs concentration for non-resistant *S. aureus* (**a**) and MRSA (**b**) for other measurements; (**C**) Growth curves after application of ATBs (ampicillin—red line, oxacillin-green line, penicillin—purple line) on *S. aureus* (**a**) and MRSA (**c**)—blue line and complexes of SeNPs (100 µM) with the same ATBs (100 µM) *S. aureus* (**b**) and MRSA (**d**)—blue line. All data represent mean ± S.D. NS, not significant, * $p < 0.05$.

The antibacterial activity of ATBs or their complexes with SeNPs after 24 h was confirmed by the method of the growth curves [21]. The 50% inhibitory concentration was determined in the previous study [21] and for our study, 100 μM concentrations of SeNPs in combination with 100 μM of ATB (Figure 1(Ba,b)) was used. Concentration of SeNPs that showed inhibitory differences between non-resistant *S. aureus* and MRSA were selected for measurements in this paper. ATBs concentrations were chosen on the basis of previous measurements. For the comparison of ATBs with or without SeNPs, we used only one concentration (100 μM) of ATBs, and it was found that the ATBs applied in combination with SeNPs (100 μM) showed a greater antibacterial effect than ATBs alone. The inhibition effect of ATBs was significant on a non-resistant *S. aureus* (Figure 1(Ca)). But in the case of MRSA, ATBs, as expected, were mostly ineffective (Figure 1(Cc)). Only oxacillin showed low antibacterial activity with MRSA without antibacterial compounds. The application of complexes of SeNPs with ATBs caused almost complete inhibition of both strains (non-resistant *S. aureus* and MRSA) in the case of all 3 types of applied ATBs-ampicillin, oxacillin, penicillin (Figure 1(Cb,d)).

2.2. Influence of Antibacterial Compounds to Biofilm Formation

The assessment of the antimicrobial components was further carried out to test the viability of the cells. The relative impedance depending on the adherence of cell culture to the gold electrodes in real time was used for this purpose. Real time xCELLigence analysis system is an impedance-based cell detection platform that provides a non-invasive, label-free way for continuous cellular monitoring [32–34]. This method has been used in many published research studies [27,35–37]. Junka *et al.* [28] showed that xCELLigence system can also be useful for microbiological tests, including (i) measurements of morphological changes in prokaryotic cells; (ii) measurement of bacterial biofilm formation and (iii) impact of antiseptics on the biofilm structure.

Figure 2A depicts the application of SeNPs on the non-resistant *S. aureus* and MRSA, showing that the biofilm formation was more hampered in presence of SeNPs than in control (*S. aureus* or MRSA without application of antibacterial components). The xCELLigence suitability for the microbiological tests was confirmed in the same way as in the study previously conducted by Junka *et al.* [28]. The tested bacteria must always be able to adhere on the surface of electrode at the bottom in the measuring well [7,38]. The ability to destroy the biofilm formation is one of the virulence factors in bacteria with low sensitivity to ATBs [39].

After application of the antibacterial agents, the biofilm is disrupted and bacterial cells are released from the surface of electrodes. This trend is measured as an impedance values and depicted in the graph (Figure 2A,B). The differences in the relative impedance of *S. aureus* showed decreases in the values of all components applied in comparison with the control, which is caused by balanced violation of the biofilm formed on the electrode surface. In the case of non-resistant *S. aureus*, ATBs and complexes of SeNPs with ATBs disrupted the bacterial biofilm, and after that a higher effect on these bacteria could be seen (Figure 2A). The biofilm formed by MRSA (Figure 2(Bb,c)) was more resistant to ATBs and complexes of SeNPs with ATBs than the biofilm formed by the non-resistant *S. aureus* (Figure 2(Ab,c)). Figure 2B shows the percentage decrease of biofilm formation after application of ATBs and complexes of SeNPs with ATBs in comparison with control. The control sample of non-resistant *S. aureus* reached the relative impedance values of 0.29 and the control sample

of MRSA reached 0.52 after 24-h measurement and from these values the decrease of the relative impedance after application of ATBs and complexes of SeNPs with ATBs was calculated. The measurements were performed in triplicates. Low adhesion showed a decreasing trend caused by the biofilm formation on the electrodes, and from this we can conclude that the application of ATBs and complexes of SeNPs with ATBs caused disruption of the biofilm on the electrodes. The results are summarized in Table 1.
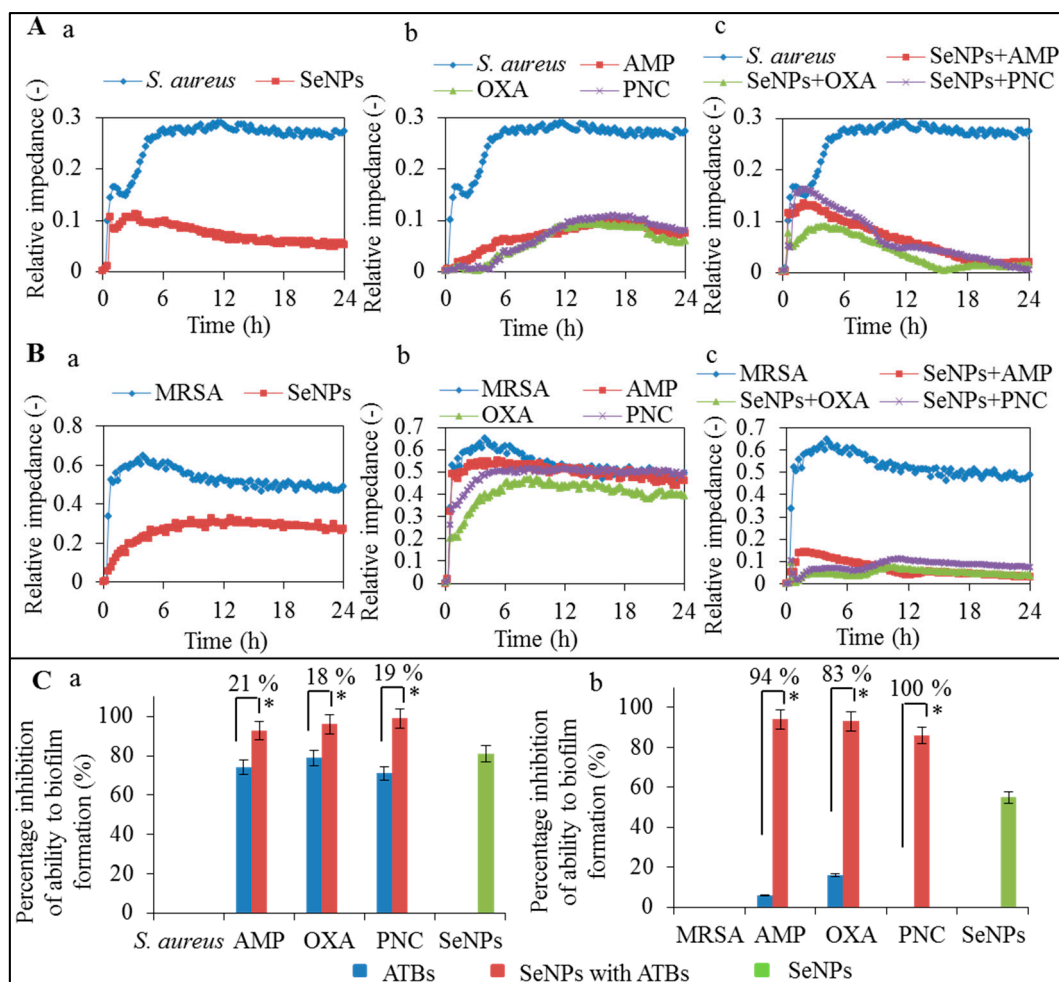

Figure 2. (**A**) Monitoring of biofilm disruption after application of 100 μM SeNPs on *S. aureus*—blue line (**a**) and ATBs (100 μM): ampicillin—red line, oxacillin—green line, penicillin—purple line on *S. aureus*—blue line (**b**) and complexes of SeNPs (100 μM) with the same ATBs (100 μM) on *S. aureus*—blue line (**c**); (**B**) Monitoring of biofilm disruption after application of 100 μM SeNPs on MRSA—blue line (**a**) and ATBs (100 μM) ampicillin—red line, oxacillin—green line, penicillin—purple line on MRSA—blue line (**b**) and complexes of SeNPs (100 μM) with the same ATBs (100 μM) on MRSA—blue line (**c**); (**C**) Comparison of differences in relative impedance after application of 100 μM concentration of ATBs or complexes of ATBs with SeNPs (100 μM) and SeNPs alone (100 μM) on *S. aureus* (**a**) and MRSA (**b**) after 24 h of measurement. All data represent mean ± S.D. from three measurements, NS, not significant, * $p < 0.05$.

Table 1. Percentage disruption of biofilm after treatment of antibacterial component (ATBs, SeNPs + ATBs) after 24 h (Figure 2(Ca,b)).

Compounds	Biofilm Disruption (%)			
	S. aureus		MRSA	
	ATB	SeNPs + ATBs	ATB	SeNPs + ATBs
AMP	74 ± 2	93 ± 3	6 ± 5	94 ± 4
OXA	79 ± 5	96 ± 2	16 ± 2	93 ± 4
PNC	71 ± 2	99 ± 7	0	86 ± 2
SeNPs	81 ± 4		55 ± 3	

The application of complex of SeNPs with ATBs (SeNPs with ampicillin, SeNPs with oxacillin, SeNPs with penicillin) caused a twofold decrease in the relative impedance compared to ATBs only. For non-resistant *S. aureus* the significantly higher effect of SeNPs with ATBs was not observed, however increased inhibition of biofilm formation in case of complexes of SeNPs with ATBs was confirmed.

2.3. Determination of Expression Intensity of mecA Gene

The *mecA* gene is responsible for bacterial resistance to β-lactam ATBs and occurs at staphylococcal chromosome cassette *mec* (SCC*mec*), which besides *mecA* gene contains a number of other genes causing the resistance [10]. Its expression was monitored after application and also after 24-h cultivation in the presence of ATBs alone (50 μM) or at same concentration of ATBs in complexes with SeNPs (100 μM). Bacterial strain MRSA even without drugs application always exhibited the expression of this gene in comparison with the strain of *S. aureus*, where this expressed gene was absent.

Expression of the *mecA* gene in MRSA without antibacterial compounds was higher (by 84%) than the standard expression of the *16S* gene. Fluorescence values of *16S* (the housekeeping gene with a luminescence level 13,098 a.u. (absorbance units) for non-resistant *S. aureus* and 12,544 a.u. for MRSA) ware subtracted from the *mecA* (Figure 3A).

For non-resistant *S. aureus* the expression of *mecA* gene reached the intensity of fluorescence of 13,059 a.u. while for MRSA was the fluorescence intensity much higher (36 times). *S. aureus* grew only in the presence of 50 μM ampicillin and penicillin, but not in the presence of 50 μM concentration of oxacillin. For ampicillin and penicillin, non-resistant *S. aureus* reached a very low expression of *mecA* gene (17,315 and 15,543 a.u., respectively). MRSA showed higher expression by 14% in the case of using 50 μM concentrations of ampicillin or oxacillin, and low expression of *mecA* gene after 24 h cultivation with 50 μM penicillin, when comparing with MRSA without application of antibacterial compounds (Figure 3A).

In MRSA, the expression of the *mecA* gene was decreased after application of ATBs with selenium nanoparticles when compared with expression of the *mecA* gene in MRSA without antibacterial compounds. Higher fluorescence intensity of *mecA* gene expression was observed in MRSA after incubation with 50 μM of ATBs (ampicillin, oxacillin and penicillin) alone (Figure 3), as compared to complexes of SeNPs with ATBs, for which the fluorescence intensities of expression were 48%, 70% and 90% lower, respectively (Figure 3B).

In non-resistant *S. aureus*, *mecA* gene expression was observed to be 37% higher after incubation with 50 μM concentration of ampicillin in comparison with control (*S. aureus* without antibacterial compounds). Non-resistant *S. aureus* did not grow after application of oxacillin (50 μM) thus, gene expression could not be determined (Figure 3B). In the case of ATBs with selenium nanoparticles, the growth of non-resistant *S. aureus* was observed only after application of 50 μM concentration of penicillin (Figure 3B). The expression was measurable only in the case of penicillin. This expression was by 7% higher compared to non-resistant *S. aureus* without antibacterial compounds.

MecA gene expression in resistant strains of bacteria was discussed in the study of Rudkin *et al.* [40], where the use of different concentrations of oxacillin increased the level of expression of *mecA* gene and they detected a higher level of toxicity in CA-MRSA than in HA-MRSA. It was observed, that in the HA-MRSA, high expression of PBP2a reduced the toxicity by disrupting the *agr* quorum sensing system, which controls the expression of virulence.
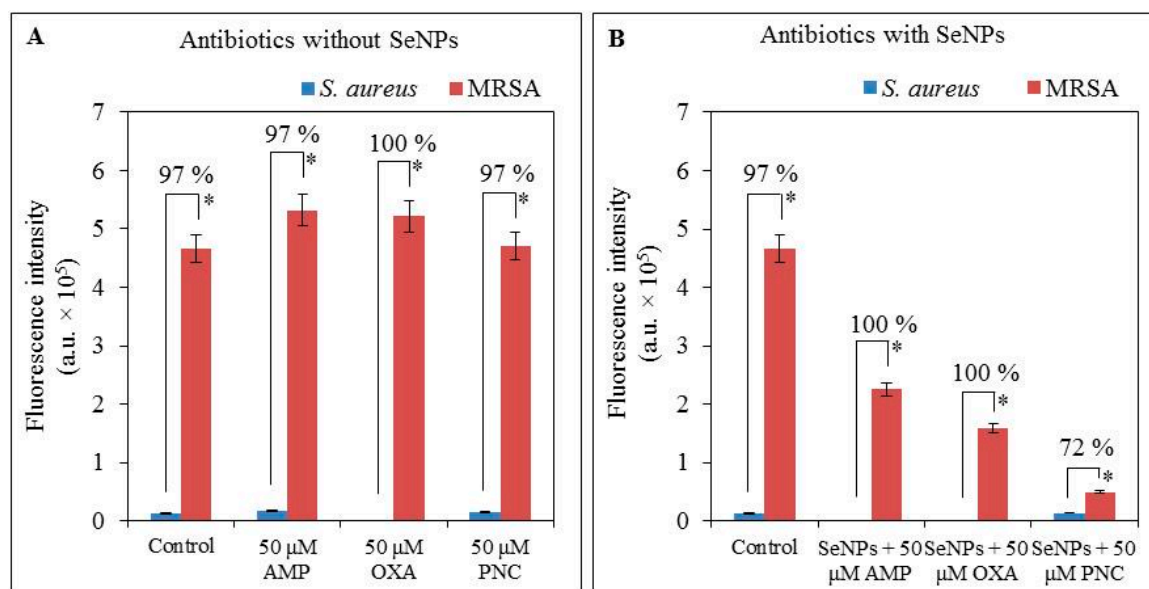

Figure 3. Monitoring of *mecA* gene expression in bacterial strains *S. aureus* and MRSA after 24 h of growth with (**A**) 50 µM ATBs concentration and with (**B**) 100 µM concentration of SeNPs with 50 µM ATBs concentration in complexes using PCR and subsequent gel electrophoresis. Controls are bacterial strains (*S. aureus* and MRSA) without application of antibacterial component. All data represent mean ± S.D. NS, not significant, * *p* < 0.05.

2.4. Determination of Changes in Protein Structure

The significant changes in the protein composition of bacterial strains caused by the effect of selenium nanoparticles were observed using mass spectrometry. In the mass spectra of non-resistant *S. aureus* with different ATBs, three peaks with *m/z* 4306, 6355 and 6845 were selected as significant peaks showing the differences between mass spectra (Figure 4A). Similarly, in the mass spectra of MRSA, peaks with *m/z* 5303, 6356 and 7567 were selected (Figure 4B). Peaks with the same or similar *m/z* value were described in various publications [41,42]. It is obvious that the presence of selenium nanoparticles causes distinct changes in protein profiles—according to the mass spectra, the most

efficient were SeNPs with oxacillin in the case of non-resistant *S. aureus* (Figure 4A) and with ampicillin and penicillin in the case of MRSA (Figure 4B). These compounds caused the suppressed expression of almost all proteins compared to the control strain of non-resistant *S. aureus* and MRSA without the addition of SeNPs (Figure 4A,B). These results can be a suitable basis for comparison of the protein representation and their effect on the pathogenicity of bacteria.

Figure 4. The comparison of MALDI-TOF mass spectra of (**A**) *S. aureus* and (**B**) MRSA with ampicillin, SeNPs with ampicillin, oxacillin, SeNPs with oxacillin, penicillin and SeNPs with penicillin. The analysis was performed in linear positive mode. A solution of 2,5-dihydroxybenzoic acid (concentration 20 mg·mL^{-1}) in 30% acetonitrile and 0%, 1% trifluoroacetic acid was used as a matrix. The laser power was set to 75%. The highlighted peaks show the biggest differences in compared spectra.

These protein changes may affect the pathogenicity of bacteria. Interaction of metal ions with DNA can affect the protein-DNA interactions [43]. In the case of silver nanoparticles, the interaction with

DNA or proteins can occur through Ag-N bonding [44] and selenium can assume a similar mechanism of bonding to DNA. This process in prokaryotes regulates the expression of a number of genes in virulence and pathogenesis [45]. Similarly, the study of Gopal *et al.* [46] refers to the changes in the protein profile of bacteria measured by mass spectrometry in bacterial cultures of *S. aureus* and *Pseudomonas aeruginosa*, which were incubated for 24 h with Ag, ZnO, TiO_2, NiO and Pt nanoparticles. Between 2–6 h of incubation, no change in the signal was observed, while rapid decrease of signal occurred between 12–24 h of incubation with Ag, ZnO and TiO_2 nanoparticles in both tested bacterial strains in comparison with the control. After the application of NiO NPs and Pt NPs, no changes were observed.

This test determined minimum inhibitory concentration of individual substance for non-resistant *S. aureus* and MRSA and from these values were calculated FICI (fractional inhibitory concentration index) indicating the synergy or antagonism of two substances. For *S. aureus*, the values of FICI were for SeNPs with AMP and SeNPs with PNC was partly synergistic and for SeNPs with oxacillin had additive effect. In the case of MRSA, complexes of SeNPs with AMP and SeNPs with PNC were determined the FICI as 0.53 and for SeNPs with OXA 0.57 indicating partial synergy between the SeNPs and ATBs (Table 2). These results are very important for inhibition of resistant bacteria, because a synergism occurs between the SeNPs and ATBs, due to that bacteria in the sample are inhibited by the effect of both substances in the complex. The results thus suggest that the combinations of SeNPs with ATBs exhibited improved inhibition of methicillin-resistant bacteria with partial synergy or additive effect. Drugs were assayed separately, thus confirming the hypothesis that antibiotic-resistant inhibitors combined with antibiotics are a potential method for solving the problem caused by resistant bacteria.

Table 2. Minimum inhibitory concentration and FICI values of SeNPs with antibiotics.

Strain	MIC (µM)				FICI		
	AMP	OXA	PNC	SeNPs	SeNPs + AMP	SeNPs + OXA	SeNPs + PNC
S. aureus	50	25	50	10	0.70	0.90	0.70
MRSA	300	150	300	20	0.53	0.57	0.53

3. Experimental Section

3.1. Cultivation of S. aureus and MRSA

S. aureus (NCTC 8511) and MRSA (ST239) were obtained from the Czech Collection of Microorganisms, Faculty of Science, Masaryk University, Brno, Czech Republic. Cultivation media (LB = Luria Bertani) were inoculated with bacterial culture and were cultivated for 24 h on a shaker at $40 \times g$ and 37 °C. Bacterial culture was diluted by cultivation medium to OD_{600} = 0.1 for the following experiments.

3.2. Testing of Antibacterial Properties

Inhibition zones and growth curves were used to test of the antibacterial properties. Petri dishes were covered by 24-h grown culture of non-resistant *S. aureus* and MRSA with 3 mL of LB medium.

Circular pieces of fabric (VUP Medical Brno, Brno, Czech Republic) with a diameter of 1 cm were soaked with solutions of ampicillin, oxacillin and penicillin (100 μM) or complexes of selenium nanoparticles (SeNPs) with 100 μM concentration of the same ATBs. The Petri dishes were incubated at 37 °C for 24 h.

The antimicrobial effect of tested compounds was determined by measuring the absorbance using an apparatus Multiskan EX (Thermo Fisher Scientific, Schwerte, Germany). In a microtitration plate, *S. aureus* and MRSA cultures were mixed with ATBs and complexes of SeNPs with ATBs. The total volume in the microtitration plate wells was always 300 μL [21].

3.3. Preparation of the SeNPs and Complexes of SeNPs with ATBs

Chitosan at 0.1 g was dissolved in 9 mL of water. Then, 0.1 mL of acetic acid was added with 1 mL of $Na_2SeO_3·5H_2O$ (0.263 g/50 mL) solution. After, the solution was mixed for 1 h. Subsequently, 10 μL of mercaptopropionic acid was added and the solution was stirred for 1 h. Then the pH of the solution was adjusted to 7 by 1 M NaOH (1.4 mL), and the color of the samples became pale orange. The samples were stirred vigorously for 3 h at 25 °C. Then the samples were left at 60 °C for 24 h on magnetic stirrer. After 24 h, the ATBs (ampicillin, oxacillin and penicillin) were added and the final concentrations of ATBs for each complex of SeNPs with ATBs were 1 mM.

3.4. Measuring the Biofilm Formed by S. aureus and MRSA Followed by Application of ATBs

The xCELLigence system consists of four main components: the Real time cell analyzer dual plate (RTCA DP), the RTCA DP station, the RTCA computer with integrated software and disposable E-plate 16. Firstly, the optimal seeding concentration for proliferation and RTCA assay of non-resistant *S. aureus* and MRSA were determined. For further measurements, a concentration of $3.7 × 10^7$ CFU/mL was selected. *S. aureus* and MRSA with ATBs (ampicillin, oxacillin and penicillin) were put in to the appropriate wells of E-Plate 16 in concentration of 100 μM in a total volume of 250 μL. The measuring was conducted at 37 °C for 48 h in 15-min intervals.

3.5. Gene Expression

3.5.1. Isolation of RNA

Bacterial cultures ($1 × 10^8$ of cells) were centrifuged at 6000 rpm and 20 °C for 10 min and the pellets were resuspended in 100 μL of PBS buffer, 100 μL of Tissue Lysis Buffer and 0.1 μL of RNase inhibitors. This volume was pipetted into the sample tube from MagNA Pure Compact RNA Isolation Kit (Roche, Basel, Switzerland), and inserted with other instruments on the appropriate place in the machine. In the second row of the machine, the vials with 20 μL of DNAase were inserted. Next steps were carried out according to the manufacturer's instructions ("RNA Cell" protocol MagNA).

3.5.2. Reverse Transcription and Amplification of cDNA for *mecA* Gene

The mRNA was converted to cDNA using Transcriptor First Strand cDNA Synthesis Kit (Roche, Basel, Switzerland), using random hexamers. The reaction profile was as follows: 25 °C for 10 min, 55 °C for 30 min and 85 °C for 5 min.

The *mecA* gene was amplified using polymerase chain reaction. The sequences of forward and reverse primers for *mecA* gene were 5′-CCCAATTTGTCTGCCAGTTT-3′, and 5′-TGGCAATATTA ACGCACCTC-3′, respectively. The final volume of the PCR reaction mixture was 25 μL containing 17.3 μL of sterile water, 2.5 μL of 1× Taq reaction buffer, 0.5 μL of 100 mM dNTP, 1 μL of forward primer, 1 μL of reverse primer and 0.2 μL of Taq DNA polymerase (Sigma-Aldrich, St. Louis, MO, USA) and 2.5 μL of cDNA. The reaction profile was as follows: 30 cycles of 94 °C for 3 min, 53 °C for 30 s and 72 °C for 30 s and a final extension at 72 °C for 4 min. The amplification was carried out using Mastercycler ep realplex4S (Eppendorf AG, Hamburg, Germany) and a 223 bp fragment for *mecA* gene was obtained.

3.5.3. Visualization and Quantification of Gene Expression

cDNA was mixed with loading buffer and then pipetted into the wells of 1.5% agarose gel with ethidium bromide and the electrophoresis was run in 1× TAE buffer for 90 min at 90 V. The bands were visualized by UV transilluminator at 312 nm (VilberLourmat, Marne-la-Valle´e Cedex, France) and band intensities were quantified and analyzed by Carestream Molecular Imaging Software using *In vivo* Xtreme Imaging System (Rochester, NY, USA) and normalized to *16S* gene.

3.6. Determination of Protein Fingerprints by MALDI-TOF

Overnight culture (500 μL, 0.1 OD) was centrifuged at 14,000× *g* for 2 min. The supernatant was discarded and the pellet was suspended in 300 μL of de-ionized water. Then, 900 μL of ethanol was added. After centrifugation at 14,000× *g* for 2 min, the supernatant was discarded and the obtained pellet was air-dried. Then it was dissolved in 25 μL of 70% formic acid (*v/v*) and 25 μL of acetonitrile. The samples were centrifuged at 14,000× *g* for 2 min and 1 μL of the clear supernatant was spotted in duplicate onto the MALDI target (MTP 384 target polished steel plate; Bruker Daltonics, Bremen, Germany) and air-dried at a room temperature. Each spot was overlaid with 1 μL of 2,5-dihydroxybenzoic acid matrix solution. The spectra were measured on MALDI-TOF/TOF Bruker in the *m/z* range of 2–20 kDa.

3.7. The Checkerboard Dilution Test

The antibacterial effects that resulted from combining the two antimicrobial agents were assessed by the checkerboard test. The antimicrobial combination we assayed included selenium nanoparticles and antibiotics (ampicillin, oxacillin, penicillin). The inocula were prepared from colonies that had been grown in LB overnight. The final bacterial concentration after inoculation was 2×10^5 CFU/mL. The MIC was determined after 24 h of incubation at 37 °C. The fractional inhibitory concentration (FIC) index was determined by the formula: FIC index = FIC A + FIC B = [A]/MIC A + [B]/MIC B, where [A] is the concentration of drug A, MICA is its MIC and FICA is the FIC of drug A for the

organism, while [B], MICB, and FICB are defined in the same fashion for drug B. The FIC index thus obtained was interpreted as follows: <0.5, synergy; 0.5 to 0.75, partial synergy; 0.76 to 1.0, additive effect; >1.0 to 4.0, indifference; and >4.0, antagonism [47]. Finally, the varying rates of synergy between two agents were determined [48].

3.8. Descriptive Statistics

Data were processed using MICROSOFT EXCEL® (Microsoft, Albuquerque, NM, USA) with the pair assay for comparison between sensitive *S. aureus* and methicillin-resistant *S. aureus*. The results are expressed as mean ± standard deviation (S.D.) unless noted otherwise (EXCEL®).

4. Conclusions

The study was performed to investigate the growth properties and ability to form biofilms in non-resistant *S. aureus* and MRSA after the application of ATBs or complexes of SeNPs with ATBs. Particularly, MRSA, as a common agent of nosocomial infections with resistance to antibiotics, has been the major focus in our investigations of alternatives for inhibition of its growth and multiplication. Our results point to significant antimicrobial effects of SeNPs in with ATBs. The components in the complex can act independently or synergistically and can perform better on a wider spectrum of bacterial species, including antibiotic-resistant species. By the impedance monitoring of biofilms formation revealed that SeNPs can cause biofilm disruption compared with controls without the application of nanoparticles. After the application of nanoparticles or complexes with antibiotics, gene expression was monitored, and was found to be decreasing with increasing concentration of ATBs. The reported results can be used for further experiments concerning ATBs resistance, and especially for the use of selenium nanoparticles as a tool for the treatment of bacterial infection, in the cases where antibiotics are not effective.

Acknowledgments

Author Contributions

Kristyna Cihalova cultivated sensitive *S. aureus* and methicillin-resistant *S. aureus* with antibacterial compounds and prepared samples for other analyzes, participated on microbiological analyzes-measuring of inhibition zones and growth curves. Dagmar Chudobova determined the biofilm formation and evaluated the results. Petr Michalek determined the gene expression. Amitava Moulick participated on preparation of the manuscript and optimized the sample preparation. Roman Guran measured the changes in protein structure. Pavel Kopel prepared the complexes of selenium nanoparticles with antibiotics. Rene Kizek participated on design and coordination of the study and drafted manuscript. Vojtech Adam conceived of the study, and participated on its design.

Conflicts of Interest

The authors declare no conflict of interest.

References

1. Ding, Y.L.; Wang, W.; Fan, M.; Tong, Z.C.; Kuang, R.; Jiang, W.K.; Ni, L.X. Antimicrobial and anti-biofilm effect of Bac8c on major bacteria associated with dental caries and Streptococcus mutans biofilms. *Peptides* **2014**, *52*, 61–67.
2. Abucayon, E.; Ke, N.; Cornut, R.; Patelunas, A.; Miller, D.; Nishiguchi, M.K.; Zoski, C.G. Investigating catalase activity through hydrogen peroxide decomposition by bacteria biofilms in real time using scanning electrochemical microscopy. *Anal. Chem.* **2014**, *86*, 498–505.
3. Chudobova, D.; Nejdl, L.; Gumulec, J.; Krystofova, O.; Rodrigo, M.A.M.; Kynicky, J.; Ruttkay-Nedecky, B.; Kopel, P.; Babula, P.; Adam, V.; *et al.* Complexes of silver(I) ions and silver phosphate nanoparticles with hyaluronic acid and/or chitosan as promising antimicrobial agents for vascular grafts. *Int. J. Mol. Sci.* **2013**, *14*, 13592–13614.
4. Zaidi, S.T.R.; Al Omran, S.; Al Aithan, A.S.M.; Al Sultan, M. Efficacy and safety of low-dose colistin in the treatment for infections caused by multidrug-resistant gram-negative bacteria. *J. Clin. Pharm. Ther.* **2014**, *39*, 272–276.
5. Buru, A.S.; Pichika, M.R.; Neela, V.; Mohandas, K. *In vitro* antibacterial effects of Cinnamomum extracts on common bacteria found in wound infections with emphasis on methicillin-resistant Staphylococcus aureus. *J. Ethnopharmacol.* **2014**, *153*, 587–595.
6. Bjarnsholt, T.; Ciofu, O.; Molin, S.; Givskov, M.; Hoiby, N. Applying insights from biofilm biology to drug development—Can a new approach be developed? *Nat. Rev. Drug Discov.* **2013**, *12*, 791–808.
7. Besinis, A.; de Peralta, T.; Handy, R.D. Inhibition of biofilm formation and antibacterial properties of a silver nano-coating on human dentine. *Nanotoxicology* **2014**, *8*, 745–754.
8. Banaszkiewicz, T.; Krukowski, H. Pathogenicity of MRSA for humans and animals. *Med. Weter.* **2014**, *70*, 151–156.
9. Lall, M.; Sahni, A.K. Prevalence of inducible clindamycin resistance in *Staphylococcus aureus* isolated from clinical samples. *Armed. Forces Med. J. India* **2014**, *70*, 43–47.
10. Zhu, C.; He, N.A.; Cheng, T.; Tan, H.L.; Guo, Y.Y.; Chen, D.S.; Cheng, M.Q.; Yang, Z.; Zhang, X.L. Ultrasound-targeted microbubble destruction enhances human beta-defensin 3 activity against antibiotic-resistant Staphylococcus biofilms. *Inflammation* **2013**, *36*, 983–996.
11. Kim, C.; Mwangi, M.; Chung, M.; Milheirco, C.; de Lencastre, H.; Tomasz, A. The mechanism of heterogeneous beta-lactam resistance in MRSA: Key role of the stringent stress response. *PLoS ONE* **2013**, *8*, 1–10.
12. Vanderhaeghen, W.; Vandendriessche, S.; Crombe, F.; Dispas, M.; Denis, O.; Hermans, K.; Haesebrouck, F.; Butaye, P. Species and staphylococcal cassette chromosome mec (SCCmec) diversity among methicillin-resistant non-*Staphylococcus aureus* staphylococci isolated from pigs. *Vet. Microbiol.* **2012**, *158*, 123–128.

13. Chang, L.-J.; Jia, B.; Wei, X.-Y.; Huang, W.-X.; Liu, C.-W. Tracing the outbreak of methicilin resistant *Staphylococcus aureus* in intensive care units. *Zhongguo Kangshengsu Zazhi* **2012**, *37*, 615–618. (In Chinese)

14. Boneca, I.G.; Chiosis, G. Vancomycin resistance: Occurrence, mechanisms and strategies to combat it. *Expert Opin. Ther. Targets* **2003**, *7*, 311–328.

15. Doron, S.; Hibberd, P.L.; Goldin, B.; Thorpe, C.; McDermott, L.; Snydman, D.R. Effect of lactobacillus rhamnosus GG administration on vancomycin-resistant enterococcus colonization in adults with comorbidities. *Antimicrob. Agents Chemther.* **2015**, *59*, 4593–4599.

16. Hiramatsu, K.; Okuma, K.; Ma, X.X.; Yamamoto, M.; Hori, S.; Kapi, M. New trends in *Staphylococcus aureus* infections: Glycopeptide resistance in hospital and methicillin resistance in the community. *Curr. Opin. Infect. Dis.* **2002**, *15*, 407–413.

17. Rai, M.; Kon, K.; Ingle, A.; Duran, N.; Galdiero, S.; Galdiero, M. Broad-spectrum bioactivities of silver nanoparticles: The emerging trends and future prospects. *Appl. Microbiol. Biotechnol.* **2014**, *98*, 1951–1961.

18. Ahmed, R.A.; Fadl-allah, S.A.; El-Bagoury, N.; El-Rab, S. Improvement of corrosion resistance and antibacterial effect of NiTi orthopedic materials by chitosan and gold nanoparticles. *Appl. Surf. Sci.* **2014**, *292*, 390–399.

19. Kummer, K.M.; Taylor, E.N.; Durmas, N.G.; Tarquinio, K.M.; Ercan, B.; Webster, T.J. Effects of different sterilization techniques and varying anodized TiO_2 nanotube dimensions on bacteria growth. *J. Biomed. Mater. Res. Part B* **2013**, *101B*, 677–688.

20. Mirershadi, F.; Jafari, A.; Janati, E.; Roohi, E.; Sarabi, M. Ag/ZnO nano-composites as novel antibacterial agent against strain of MRSA. *J. Pure Appl. Microbiol.* **2013**, *7*, 947–956.

21. Chudobova, D.; Cihalova, K.; Dostalova, S.; Ruttkay-Nedecky, B.; Rodrigo, M.A.M.; Tmejova, K.; Kopel, P.; Nejdl, L.; Kudr, J.; Gumulec, J.; *et al.* Comparison of the effects of silver phosphate and selenium nanoparticles on Staphylococcus aureus growth reveals potential for selenium particles to prevent infection. *FEMS Microbiol. Lett.* **2014**, *351*, 195–201.

22. Tran, P.A.; Webster, T.J. Selenium nanoparticles inhibit Staphylococcus aureus growth. *Int. J. Nanomed.* **2011**, *6*, 1553–1558.

23. Singh, R.; Smitha, M.S.; Singh, S.P. The role of nanotechnology in combating multi-drug resistant bacteria. *J. Nanosci. Nanotechnol.* **2014**, *14*, 4745–4756.

24. Noh, H.J.; Kim, H.S.; Jun, S.H.; Kang, Y.H.; Cho, S.; Park, Y. Biogenic silver nanoparticles with chlorogenic acid as a bioreducing agent. *J. Nanosci. Nanotechnol.* **2013**, *13*, 5787–5793.

25. Grigor'eva, A.; Saranina, I.; Tikunova, N.; Safonov, A.; Timoshenko, N.; Rebrov, A.; Ryabchikova, E. Fine mechanisms of the interaction of silver nanoparticles with the cells of Salmonella typhimurium and *Staphylococcus aureus*. *Biometals* **2013**, *26*, 479–488.

26. Garcia, S.N.; Gutierrez, L.; McNulty, A. Real-time cellular analysis as a novel approach for *in vitro* cytotoxicity testing of medical device extracts. *J. Biomed. Mater. Res. Part A* **2013**, *101A*, 2097–2106.

27. Scrace, S.; O'Neill, E.; Hammond, E.M.; Pires, I.M. Use of the xCELLigence system for real-time analysis of changes in cellular motility and adhesion in physiological conditions. In *Adhesion Protein Protocols*, 3rd ed.; Coutts, A.S., Ed.; Humana Press Inc: Totowa, UK, 2013; Volume 1046, pp. 295–306.

28. Junka, A.F.; Janczura, A.; Smutnicka, D.; Maczynska, B.; Secewicz, A.; Nowicka, J.; Bartoszewicz, M.; Gosciniak, G. Use of the real time xCelligence system for purposes of medical microbiology. *Pol. J. Microbiol.* **2012**, *61*, 191–197.

29. Wagner, C.; Aytac, S.; Hansch, G.M. Biofilm growth on implants: Bacteria prefer plasma coats. *Int. J. Artif. Organs* **2011**, *34*, 811–817.

30. Anastasiadis, P.; Mojica, K.D.A.; Allen, J.S.; Matter, M.L. Detection and quantification of bacterial biofilms combining high-frequency acoustic microscopy and targeted lipid microparticles. *J. Nanobiotechnol.* **2014**, *12*, 1–11.

31. Muhsin, T.M.; Hachim, A.K. Mycosynthesis and characterization of silver nanoparticles and their activity against some human pathogenic bacteria. *World J. Microbiol. Biotechnol.* **2014**, *30*, 2081–2090.

32. Wang, S.-Y.; Wang, X.-J.; Ma, J. Progress in real time xCELLigence analysis system on drug cardiotoxicity screening. *Zhongguo Yaolixue Yu Dulixue Zazhi* **2013**, *27*, 908–912. (In Chinese)

33. Himmel, H.; Herbold, S. Drug-induced functional cardiotoxicity screening with the xcelligence system: Effects of reference compounds in human iPSC-versus mouse eSC-derived cardiomyocytes. *J. Pharmacol. Toxicol. Methods* **2013**, *68*, E9–E10.

34. Xi, B.A.; Wang, T.X.; Li, N.; Ouyang, W.; Zhang, W.; Wu, J.Y.; Xu, X.; Wang, X.B.; Abassi, Y.A. Functional cardiotoxicity profiling and screening using the xCELLigence RTCA cardio system. *J. Assoc. Lab. Autom.* **2011**, *16*, 415–421.

35. Macdonald, C.; Unsworth, C.P.; Graham, E.S. Enrichment of differentiated hNT neurons and subsequent analysis using flow-cytometry and xCELLigence sensing. *J. Neurosci. Methods* **2014**, *227*, 47–56.

36. Bruening-Wright, A.; Obejero-Paz, C.; Kojukhova, M.; Brown, A. Quantification of cardioactive drug effects using xCELLigence RTCA cardio and human stem cell-derived cardiomyocytes. *J. Pharmacol. Toxicol. Methods* **2013**, *68*, E6.

37. Golke, A.; Cymerys, J.; Slonska, A.; Dzieciatkowski, T.; Chmielewska, A.; Tucholska, A.; Banbura, M.W. The xCELLigence system for real-time and label-free analysis of neuronal and dermal cell response to Equine Herpesvirus type 1 infection. *Pol. J. Vet. Sci.* **2012**, *15*, 151–153.

38. Dowling, C.M.; Ors, C.H.; Kiely, P.A. Using real-time impedance-based assays to monitor the effects of fibroblast-derived media on the adhesion, proliferation, migration and invasion of colon cancer cells. *Biosci. Rep.* **2014**, *34*, 415–427.

39. Murugan, K.; Usha, M.; Malathi, P.; Al-Sohaibani, A.S.; Chandrasekaran, M. Biofilm forming multi drug resistant staphylococcus spp. Among Patients with Conjunctivitis. *Pol. J. Microbiol.* **2010**, *59*, 233–239.

40. Rudkin, J.K.; Laabei, M.; Edwards, A.M.; Joo, H.S.; Otto, M.; Lennon, K.L.; O'Gara, J.P.; Waterfield, N.R.; Massey, R.C. Oxacillin alters the toxin expression profile of community-associated methicillin-resistant Staphylococcus aureus. *Antimicrob. Agents Chemother.* **2014**, *58*, 1100–1107.

41. Ueda, O.; Tanaka, S.; Nagasawa, Z.; Hanaki, H.; Shobuike, T.; Miyamoto, H. Development of a novel matrix-assisted laser desorption/ionization time-of-flight mass spectrum (MALDI-TOF-MS)-based typing method to identify meticillin-resistant Staphylococcus aureus clones. *J. Hosp. Infect.* **2015**, *90*, 147–155.

42. Josten, M.; Reif, M.; Szekat, C.; Al-Sabti, N.; Roemer, T.; Sparbier, K.; Kostrzewa, M.; Rohde, H.; Sahl, H.G.; Bierbaum, G. Analysis of the Matrix-Assisted Laser Desorption Ionization-Time of Flight Mass Spectrum of Staphylococcus aureus Identifies Mutations That Allow Differentiation of the Main Clonal Lineages. *J. Clin. Microbiol.* **2013**, *51*, 1809–1817.

43. Zambelli, B.; Musiani, F.; Ciurli, S. Metal Ion-Mediated DNA-Protein Interactions. In *Interplay between Metal Ions and Nucleic Acids*; Sigel, A., Sigel, H., Sigel, R.K.O., Eds.; Springer: Dordrecht, The Netherlands, 2012; Volume 10, pp. 135–170.

44. Bovenkamp, G.L.; Zanzen, U.; Krishna, K.S.; Hormes, J.; Prange, A. X-Ray absorption near-edge structure (XANES) spectroscopy study of the interaction of silver ions with *Staphylococcus aureus*, *Listeria monocytogenes*, and *Escherichia coli*. *Appl. Environ. Microbiol.* **2013**, *79*, 6385–6390.

45. Kumar, R.; Rao, D.N. Role of DNA methyltransferases in epigenetic regulation in bacteria. *Subcell. Biochem.* **2013**, *61*, 81–102.

46. Gopal, J.; Manikandan, M.; Hasan, N.; Lee, C.H.; Wu, H.F. A comparative study on the mode of interaction of different nanoparticles during MALDI-MS of bacterial cells. *J. Mass Spectrom.* **2013**, *48*, 119–127.

47. Choi, J.G.; Kang, O.H.; Lee, Y.S.; Oh, Y.C.; Chae, H.S.; Jang, H.J.; Shin, D.W.; Kwon, D.Y. Antibacterial Activity of Methyl Gallate Isolated from Galla Rhois or Carvacrol Combined with Nalidixic Acid Against Nalidixic Acid Resistant Bacteria. *Molecules* **2009**, *14*, 1773–1780.

48. Patel, J.B.; Eliopoulos, G.M.; Hindler, J.A.; Jenkins, S.G.; Lewis, J.S.; Limbago, B.; Miller, L.A.; Nicolau, D.P.; Powell, M.; *et al. Methods for Dilution Antimicrobial Susceptibility Tests for Bacteria That Grow Aerobically*, 10th ed.; Clinical and Laboratory Standards Institute: Wayne, PA, USA, 2015.

6 ZÁVĚR

O běžných mikrobiologických stanoveních bakterií pojednává mnoho literatury a mnoho metod je běžně využívaných a stále jsou vyvíjeny a objevovány nové, které se snaží tato stanovení zpřesnit, urychlit a hlavně zvýšit jejich senzitivitu. Důležitá jsou především rychlá stanovení v prostředí nemocničních zařízení, kde dochází k velmi rychlému šíření bakteriální infekce mezi pacienty.

Neustálý vývoj rychlých detekčních metod je pro vědce výzvou a otevřenou kapitolou, který vždy nalezne své uplatnění v praxi . Do popředí se dostávají metody detekce bakterií založené na molekulárně-biologických principech, díky kterým se metody stanovení stávají citlivějšími a přesnějšími. Kombinací těchto metod s imunologickými stanoveními vzniká tak nový směr, kterým je možné se dále ubírat. Cílem je ovšem tyto metody co nejvíce urychlit a zajistit, aby byla identifikace nenáročná a opakovatelná. Pro zajištění selektivní separace je výhodné používat magnetickou separaci za použití maghemitových částic, které jsou modifikovány afinitní molekulou ke specifickému antigenu.

Tato práce, pojednávající o nejzastoupenější bakterii *S. aureus* a její formě odolné vůči antibiotikům, meticilin-rezistentní *S. aureus*, se zabývá různými možnostmi návrhů detekčních zařízení, jejichž cílem je efektivněji stanovovat přítomnost těchto bakterií ve vzorku bez předešlé kultivace, která je časově nejnáročnější z celého stanovení a konfirmace bakteriálních druhů.

Součástí práce bylo také hledání alternativ léčby infekčních onemocnění. Časté používání antibiotik vede ke vzniku bakteriální rezistence vůči použité skupině antibiotika. Vzhledem ke stále častější rezistenci bakterií je nutno vzít v potaz i toto riziko. Proto byl poslední experiment celé práce zaměřen na sledování efektu β-laktamových antibiotik a komplexů nanočástic selenu s těmito antibiotiky na *S. aureus* a MRSA, kdy byla u obou bakteriálních kmenů v případě komplexů nanočástic selenu s antibiotiky výrazně vyšší inibice růstu než u antibiotik samotných.

Včasná a rychlá diagnostika bakteriálních druhů v infekci hraje důležitou roli při léčbě, stejně tak jako navržení vhodného antibakteriálního léčiva. Vzhledem ke stále častějšímu výskytu bakteriální rezistence je v nanotechnologiích a aplikacích na bázi kombinace antibiotik s nanočásticemi kovů stále objevovaná velká uplatnitelnost. Vývoj

moderních diagnostik a antibakteriálních léčiv je tak neustále otevřenou kapitolou a je třeba se jí nadále věnovat.

7 LITERATURA

ACCO, M., FERREIRA, F. S., HENRIQUES, J. A. P. a TONDO, E. C. Identification of multiple strains of Staphylococcus aureus colonizing nasal mucosa of food handlers. *Food Microbiology*,2003, roč. 20. č. 5, s. 489-493.

ADAMS, D. W. a ERRINGTON, J. Bacterial cell division: assembly, maintenance and disassembly of the Z ring. *Nature Reviews Microbiology*,2009, roč. 7. č. 9, s. 642-653.

AHMED, R. A., FADL-ALLAH, S. A., EL-BAGOURY, N. a EL-RAB, S. Improvement of corrosion resistance and antibacterial effect of NiTi orthopedic materials by chitosan and gold nanoparticles. *Applied Surface Science*,2014, roč. 292. č., s. 390-399.

AMAGAI, M., MATSUYOSHI, N., WANG, Z. H., ANDL, C. a STANLEY, J. R. Toxin in bullous impetigo and staphylococcal scalded-skin syndrome targets desmoglein 1. *Nature Medicine*,2000, roč. 6. č. 11, s. 1275-1277.

AMOOZEGAR, M. A., BAGHERI, M., MAKHDOUMI-KAKHKI, A., DIDARI, M., SCHUMANN, P., NIKOU, M. M., SANCHEZ-PORRO, C. a VENTOSA, A. Aliicoccus persicus gen. nov., sp nov., a halophilic member of the Firmicutes isolated from a hypersaline lake. *International Journal of Systematic and Evolutionary Microbiology*,2014, roč. 64. č., s. 1964-1969.

ANSARI, M. A., KHAN, H. M., KHAN, A. A., CAMEOTRA, S. S. a ALZOHAIRY, M. A. Anti-biofilm efficacy of silver nanoparticles against MRSA and MRSE isolated from wounds in a tertiary care hospital. *Indian Journal of Medical Microbiology*,2015, roč. 33. č. 1, s. 101-109.

APPELBAUM, P. C. Reduced glycopeptide susceptibility in methicillin-resistant Staphylococcus aureus (MRSA). *International Journal of Antimicrobial Agents*,2007, roč. 30. č. 5, s. 398-408.

ARCHUNAN, G. (2004). Microbiology, Sarup & Sons.

ATHANASOPOULOS, A., DEVOGEL, P., BEKEN, C., PILLE, C., BEMIER, I. a GAVAGE, P. Comparison of three selective chromogenic media for Methicillin-Resistant Staphylococcus aureus detection. *Pathologie Biologie*,2007, roč. 55. č. 8-9, s. 366-369.

BABA, T., TAKEUCHI, F., KURODA, M., YUZAWA, H., AOKI, K., OGUCHI, A., NAGAI, Y., IWAMA, N., ASANO, K., NAIMI, T., KURODA, H., CUI, L., YAMAMOTO, K. a HIRAMATSU, K. Genome and virulence determinants of high virulence community-acquired MRSA. *Lancet*,2002, roč. 359. č. 9320, s. 1819-1827.

BAIRD, R. M. a LEE, W. H. MEDIA USED IN THE DETECTION AND ENUMERATION OF STAPHYLOCOCCUS-AUREUS. *International Journal of Food Microbiology*,1995, roč. 26. č. 1, s. 15-24.

BAK, T. a JAKOBSEN, H. Agricultural robotic platform with four wheel steering for weed detection. *Biosystems Engineering*,2004, roč. 87. č. 2, s. 125-136.

BECKER, K., FRIEDRICH, A. W., LUBRITZ, G., WEILERT, M., PETERS, G. a VON EIFF, C. Prevalence of genes encoding pyrogenic toxin superantigens and exfoliative toxins among strains of Staphylococcus aureus isolated from blood and nasal specimens. *Journal of Clinical Microbiology*,2003, roč. 41. č. 4, s. 1434-1439.

BELLOTTO, N. a HU, H. S. Multisensor-Based Human Detection and Tracking for Mobile Service Robots. *Ieee Transactions on Systems Man and Cybernetics Part B-Cybernetics*,2009, roč. 39. č. 1, s. 167-181.

BENNE, R. a SLOOF, P. EVOLUTION OF THE MITOCHONDRIAL PROTEIN SYNTHETIC MACHINERY. *Biosystems*,1987, roč. 21. č. 1, s. 51-68.

BINGEN, E., MARIANI-KURKDJIAN, P. a NEBBAD, B. Optimal vancomycin serum level in Staphylococcus aureus infections. *Medecine Et Maladies Infectieuses*,2006, roč. 36. č. 9, s. 439-442.

BITTAR, F., OUCHENANE, Z., SMATI, F., RAOULT, D. a ROLAIN, J. M. MALDI-TOF-MS for rapid detection of staphylococcal Panton-Valentine leukocidin. *International Journal of Antimicrobial Agents*,2009, roč. 34. č. 5, s. 467-470.

BOURGEOIS-NICOLAOS, N., PIRIOU, O., BUTEL, M. J. a DOUCET-POPULAIRE, F. Linezolid: antibacterial activity, clinical efficacy and resistance. *Annales De Biologie Clinique*,2006, roč. 64. č. 6, s. 549-564.

BOYD, E. F. a BRUSSOW, H. Common themes among bacteriophage-encoded virulence factors and diversity among the bacteriophages involved. *Trends in Microbiology*,2002, roč. 10. č. 11, s. 521-529.

BRAKSTAD, O. G., AASBAKK, K. a MAELAND, J. A. DETECTION OF STAPHYLOCOCCUS-AUREUS BY POLYMERASE CHAIN-REACTION AMPLIFICATION OF THE NUC GENE. *Journal of Clinical Microbiology*,1992, roč. 30. č. 7, s. 1654-1660.

BRAKSTAD, O. G. a MAELAND, J. A. Mechanisms of methicillin resistance in staphylococci. *Apmis*,1997, roč. 105. č. 4, s. 264-276.

BRAYSHAW, D. P. Methicillin-resistant Staphylococcus aureus: evaluation of detection techniques on laboratory-passaged organisms. *British Journal of Biomedical Science*,1999, roč. 56. č. 3, s. 170-176.

BREM, F., HIRT, A. M., WINKLHOFER, M., FREI, K., YONEKAWA, Y., WIESER, H. G. a DOBSON, J. Magnetic iron compounds in the human brain: a comparison of

tumour and hippocampal tissue. *Journal of the Royal Society Interface*,2006, roč. 3. č. 11, s. 833-841.

BUDIN, I. a DEVARAJ, N. K. Membrane Assembly Driven by a Biomimetic Coupling Reaction. *Journal of the American Chemical Society*,2012, roč. 134. č. 2, s. 751-753.

CIHALOVA, K., CHUDOBOVA, D., MICHALEK, P., MOULICK, A., GURAN, R., KOPEL, P., ADAM, V. a KIZEK, R. Staphylococcus aureus and MRSA Growth and Biofilm Formation after Treatment with Antibiotics and SeNPs. *International Journal of Molecular Sciences*,2015, roč. 16. č. 10, s. 24656-24672.

COURVALIN, P. Vancomycin resistance in gram-positive cocci. *Clinical Infectious Diseases*,2006, roč. 42. č., s. S25-S34.

COX, L., WILLIAMS, B., SICHERER, S., OPPENHEIMER, J., SHER, L., HAMILTON, R. a GOLDEN, D. Pearls and pitfalls of allergy diagnostic testing: report from the American College of Allergy, Asthma and Immunology/American Academy of Allergy, Asthma and Immunology Specific IgE Test Task Force. *Annals of Allergy Asthma & Immunology*,2008, roč. 101. č. 6, s. 580-592.

CZERNILO.AP, COLLATZ, E. E., STOFFLER, G. a KUECHLER, E. PROTEINS AT TRANSFER-RNA BINDING-SITES OF ESCHERICHIA-COLI RIBOSOMES. *Proceedings of the National Academy of Sciences of the United States of America*,1974, roč. 71. č. 1, s. 230-234.

DAI, T. H., TANAKA, M., HUANG, Y. Y. a HAMBLIN, M. R. Chitosan preparations for wounds and burns: antimicrobial and wound-healing effects. *Expert Review of Anti-Infective Therapy*,2011, roč. 9. č. 7, s. 857-879.

DELEO, F. R., OTTO, M., KREISWIRTH, B. N. a CHAMBERS, H. F. Community-associated meticillin-resistant Staphylococcus aureus. *Lancet*,2010, roč. 375. č. 9725, s. 1557-1568.

DEURENBERG, R. H. a STOBBERINGH, E. E. The evolution of Staphylococcus aureus. *Infection Genetics and Evolution*,2008, roč. 8. č. 6, s. 747-763.

DINGES, M. M., ORWIN, P. M. a SCHLIEVERT, P. M. Exotoxins of Staphylococcus aureus. *Clinical Microbiology Reviews*,2000, roč. 13. č. 1, s. 16-+.

DOERN, G. V., BRUEGGEMANN, A. B., PIERCE, G., HOLLEY, H. P. a RAUCH, A. Antibiotic resistance among clinical isolates of Haemophilus influenzae in the United States in 1994 and 1995 and detection of beta-lactamase-positive strains resistant to amoxicillin-clavulanate: Results of a national multicenter surveillance study. *Antimicrobial Agents and Chemotherapy*,1997, roč. 41. č. 2, s. 292-297.

DREISBACH, A., VAN DIJL, J. M. a BUIST, G. The cell surface proteome of Staphylococcus aureus. *Proteomics*,2011, roč. 11. č. 15, s. 3154-3168.

DUNCAN, C. H., WILSON, G. A. a YOUNG, F. E. MECHANISM OF INTEGRATING FOREIGN DNA DURING TRANSFORMATION OF BACILLUS-SUBTILIS. *Proceedings of the National Academy of Sciences of the United States of America*,1978, roč. 75. č. 8, s. 3664-3668.

DUNNE, D. W., RESNICK, D., GREENBERG, J., KRIEGER, M. a JOINER, K. A. THE TYPE-I MACROPHAGE SCAVENGER RECEPTOR BINDS TO GRAM-POSITIVE BACTERIA AND RECOGNIZES LIPOTEICHOIC ACID. *Proceedings of the National Academy of Sciences of the United States of America*,1994, roč. 91. č. 5, s. 1863-1867.

DUTTA, R. K., NENAVATHU, B. P. a TALUKDAR, S. Anomalous antibacterial activity and dye degradation by selenium doped ZnO nanoparticles. *Colloids and Surfaces B-Biointerfaces*,2014, roč. 114. č., s. 218-224.

ELSAYED, S., CHOW, B. L., HAMILTON, N. L., GREGSON, D. B., PITOUT, J. D. D. a CHURCH, D. L. Development and validation of a molecular beacon probe-based real-time polymerase chain reaction assay for rapid detection of methicillin resistance in Staphylococcus aureus. *Archives of Pathology & Laboratory Medicine*,2003, roč. 127. č. 7, s. 845-849.

EMMETT, M. a KLOOS, W. E. AMINO-ACID REQUIREMENTS OF STAPHYLOCOCCI ISOLATED FROM HUMAN SKIN. *Canadian Journal of Microbiology*,1975, roč. 21. č. 5, s. 729-733.

ERIKSEN, N. H. R., ESPERSEN, F., ROSDAHL, V. T. a JENSEN, K. EVALUATION OF METHODS FOR THE DETECTION OF NASAL CARRIAGE OF STAPHYLOCOCCUS-AUREUS. *Apmis*,1994, roč. 102. č. 6, s. 407-412.

EVANS, J. B., BRADFORD, W. L. a NIVEN, C. F. COMMENTS CONCERNING THE TAXONOMY OF THE GENERA MICROCOCCUS AND STAPHYLOCOCCUS. *International Bulletin of Bacteriological Nomenclature and Taxonomy*,1955, roč. 5. č. 2, s. 61-66.

FELTEN, A., GRANDRY, B., LAGRANGE, P. H. a CASIN, I. Evaluation of three techniques for detection of low-level methicillin-resistant Staphylococcus aureus (MRSA): a disk diffusion method with cefoxitin and moxalactam, the Vitek 2 system, and the MRSA-screen latex agglutination test. *Journal of Clinical Microbiology*,2002, roč. 40. č. 8, s. 2766-2771.

FORSYTH, R. A., HASELBECK, R. J., OHLSEN, K. L., YAMAMOTO, R. T., XU, H., TRAWICK, J. D., WALL, D., WANG, L. S., BROWN-DRIVER, V., FROELICH, J. M., KEDAR, G. C., KING, P., MCCARTHY, M., MALONE, C., MISINER, B., ROBBINS, D., TAN, Z. H., ZHU, Z. Y., CARR, G., MOSCA, D. A., ZAMUDIO, C., FOULKES, J. G. a ZYSKIND, J. W. A genome-wide strategy for the identification of essential genes in Staphylococcus aureus. *Molecular Microbiology*,2002, roč. 43. č. 6, s. 1387-1400.

FOSTER, T. J. a HOOK, M. Surface protein adhesins of Staphylococcus aureus. *Trends in Microbiology*,1998, roč. 6. č. 12, s. 484-488.

FRASER, J. D. a PROFT, T. The bacterial superantigen and superantigen-like proteins. *Immunological Reviews*,2008, roč. 225. č., s. 226-243.

FRIDKIN, S. K., HAGEMAN, J. C., MORRISON, M., SANZA, L. T., COMO-SABETTI, K., JERNIGAN, J. A., HARRIMAN, K., HARRISON, L. H., LYNFIELD, R., FARLEY, M. M. a ACTIVE BACTERIAL CORE, S. Methicillin-resistant staphylococcus aureus disease in three communities. *New England Journal of Medicine*,2005, roč. 352. č. 14, s. 1436-1444.

FUSCO, V., QUERO, G. M., MOREA, M., BLAIOTTA, G. a VISCONTI, A. Rapid and reliable identification of Staphylococcus aureus harbouring the enterotoxin gene cluster (egc) and quantitative detection in raw milk by real time PCR. *International Journal of Food Microbiology*,2011, roč. 144. č. 3, s. 528-537.

GAGNAIRE, J., DAUWALDER, O., BOISSET, S., KHAU, D., FREYDIERE, A. M., ADER, F., BES, M., LINA, G., TRISTAN, A., REVERDY, M. E., MARCHAND, A., GEISSMANN, T., BENITO, Y., DURAND, G., CHARRIER, J. P., ETIENNE, J., WELKER, M., VAN BELKUM, A. a VANDENESCH, F. Detection of Staphylococcus aureus Delta-Toxin Production by Whole-Cell MALDI-TOF Mass Spectrometry. *Plos One*,2012, roč. 7. č. 7.

GEY, A., WERCKENTHIN, C., POPPERT, S. a STRAUBINGER, R. K. Identification of pathogens in mastitis milk samples with fluorescent in situ hybridization. *Journal of Veterinary Diagnostic Investigation*,2013, roč. 25. č. 3, s. 386-394.

GHAZNAVI-RAD, E., SHAMSUDIN, M. N., SEKAWI, Z., VAN BELKUM, A. a NEELA, V. A simplified multiplex PCR assay for fast and easy discrimination of globally distributed staphylococcal cassette chromosome mec types in meticillin-resistant Staphylococcus aureus. *Journal of Medical Microbiology*,2010, roč. 59. č. 10, s. 1135-1139.

GHODOUSI, A., NOMANPOUR, B., DAVOUDI, S., MALEKNEJAD, P., OMRANI, M., KASHEF, N., SALEHI, T. Z. a FEIZABADI, M. M. Application of fnbA gene as new target for the species-specific and quantitative detection of Staphylococcus aureus directly from lower respiratory tract specimens by real time PCR. *Indian Journal of Pathology and Microbiology*,2012, roč. 55. č. 4, s. 490-495.

GIESBRECHT, P., KERSTEN, T., MAIDHOF, H. a WECKE, J. Staphylococcal cell wall: Morphogenesis and fatal variations in the presence of penicillin. *Microbiology and Molecular Biology Reviews*,1998, roč. 62. č. 4, s. 1371-+.

GILL, S. R., FOUTS, D. E., ARCHER, G. L., MONGODIN, E. F., DEBOY, R. T., RAVEL, J., PAULSEN, I. T., KOLONAY, J. F., BRINKAC, L., BEANAN, M., DODSON, R. J., DAUGHERTY, S. C., MADUPU, R., ANGIUOLI, S. V., DURKIN, A. S., HAFT, D. H., VAMATHEVAN, J., KHOURI, H., UTTERBACK, T., LEE, C., DIMITROV, G., JIANG, L. X., QIN, H. Y., WEIDMAN, J., TRAN, K., KANG, K.,

HANCE, I. R., NELSON, K. E. a FRASER, C. M. Insights on evolution of virulence and resistance from the complete genome analysis of an early methicillin-resistant Staphylococcus aureus strain and a biofilm-producing methicillin-resistant Staphylococcus epidermidis strain. *Journal of Bacteriology*,2005, roč. 187. č. 7, s. 2426-2438.

GONZALEZ, B. E., RUEDA, A. M., SHELBURNE, S. A., MUSHER, D. M., HAMILL, R. J. a HULTEN, K. G. Community-associated strains of methicillin-resistant Staphylococccus aureus as the cause of healthcare-associated infection. *Infection Control and Hospital Epidemiology*,2006, roč. 27. č. 10, s. 1051-1056.

GRISOLD, A. J., LEITNER, E., MUHLBAUER, G., MARTH, E. a KESSLER, H. H. Detection of methicillin-resistant Staphylococcus aureus and simultaneous confirmation by automated nucleic acid extraction and real-time PCR. *Journal of Clinical Microbiology*,2002, roč. 40. č. 7, s. 2392-2397.

GRUMANN, D., NUBEL, U. a BROKER, B. M. Staphylococcus aureus toxins - Their functions and genetics. *Infection Genetics and Evolution*,2014, roč. 21. č., s. 583-592.

GUERRERO, R. Bergey's manuals and the classification of prokaryotes. *International Microbiology*,2001, roč. 4. č. 2, s. 103-109.

HAAS, B. J., GEVERS, D., EARL, A. M., FELDGARDEN, M., WARD, D. V., GIANNOUKOS, G., CIULLA, D., TABBAA, D., HIGHLANDER, S. K., SODERGREN, E., METHE, B., DESANTIS, T. Z., PETROSINO, J. F., KNIGHT, R., BIRREN, B. W. a HUMAN MICROBIOME, C. Chimeric 16S rRNA sequence formation and detection in Sanger and 454-pyrosequenced PCR amplicons. *Genome Research*,2011, roč. 21. č. 3, s. 494-504.

HAAS, P. J., DE HAAS, C. J. C., KLEIBEUKER, W., POPPELIER, M., VAN KESSEL, K. P. M., KRUIJTZER, J. A. W., LISKAMP, R. M. J. a VAN STRIJP, J. A. G. N-terminal residues of the chemotaxis inhibitory protein of Staphylococcus aureus are essential for blocking formylated peptide receptor but not C5a receptor. *Journal of Immunology*,2004, roč. 173. č. 9, s. 5704-5711.

HACKER, J., BLUMOEHLER, G., MUHLDORFER, I. a TSCHAPE, H. Pathogenicity islands of virulent bacteria: Structure, function and impact on microbial evolution. *Molecular Microbiology*,1997, roč. 23. č. 6, s. 1089-1097.

HAN, Z. L., LAUTENBACH, E., FISHMAN, N. a NACHAMKIN, I. Evaluation of mannitol salt agar, CHROMagar Staph aureus and CHROMagar MRSA for detection of meticillin-resistant Staphylococcus aureus from nasal swab specimens. *Journal of Medical Microbiology*,2007, roč. 56. č. 1, s. 43-46.

HAO, H. H., DAI, M. H., WANG, Y. L., HUANG, L. L. a YUAN, Z. H. Key genetic elements and regulation systems in methicillin-resistant Staphylococcus aureus. *Future Microbiology*,2012, roč. 7. č. 11, s. 1315-1329.

HARRAGHY, N., KERDUDOU, S. a HERRMANN, M. Quorum-sensing systems in staphylococci as therapeutic targets. *Analytical and Bioanalytical Chemistry*,2007, roč. 387. č. 2, s. 437-444.

HARTFORD, O., MCDEVITT, D. a FOSTER, T. J. Matrix-binding proteins of Staphylococcus aureus: functional analysis of mutant and hybrid molecules. *Microbiology-Uk*,1999, roč. 145. č., s. 2497-2505.

HE, Y. S., KEEN, J. E., WESTERMAN, R. B., LITTLEDIKE, E. T. a KWANG, J. Monoclonal antibodies for detection of the H7 antigen of Escherichia coli. *Applied and Environmental Microbiology*,1996, roč. 62. č. 9, s. 3325-3332.

HEDGES, R. W., DATTA, N., KONTOMIC.P a SMITH, J. T. MOLECULAR SPECIFICITIES OF R FACTOR-DETERMINED BETA-LACTAMASES - CORRELATION WITH PLASMID COMPATIBILITY. *Journal of Bacteriology*,1974, roč. 117. č. 1, s. 56-62.

HEILMANN, C., THUMM, G., CHHATWAL, G. S., HARTLEIB, J., UEKOTTER, A. a PETERS, G. Identification and characterization of a novel autolysin (Aae) with adhesive properties from Staphylococcus epidermidis. *Microbiology-Sgm*,2003, roč. 149. č., s. 2769-2778.

HEIN, I., LEHNER, A., RIECK, P., KLEIN, K., BRANDL, E. a WAGNER, M. Comparison of different approaches to quantify Staphylococcus aureus cells by real-time quantitative PCR and application of this technique for examination of cheese. *Applied and Environmental Microbiology*,2001, roč. 67. č. 7, s. 3122-3126.

HIDRON, A. I., EDWARDS, J. R., PATEL, J., HORAN, T. C., SIEVERT, D. M., POLLOCK, D. A., FRIDKIN, S. K., NATL HEALTHCARE SAFETY NETWORK, T. a PARTICIPATING NATL HEALTHCARE, S. Antimicrobial-Resistant Pathogens Associated With Healthcare-Associated Infections: Annual Summary of Data Reported to the National Healthcare Safety Network at the Centers for Disease Control and Prevention, 2006-2007. *Infection Control and Hospital Epidemiology*,2008, roč. 29. č. 11, s. 996-1011.

HILDEN, P., SAVOLAINEN, K., TYYNELA, J., VUENTO, M. a KUUSELA, P. Purification and characterisation of a plasmin-sensitive surface protein of Staphylococcus aureus. *European Journal of Biochemistry*,1996, roč. 236. č. 3, s. 904-910.

HIRAMATSU, K., CUI, L., KURODA, M. a ITO, T. The emergence and evolution of methicillin-resistant Staphylococcus aureus. *Trends in Microbiology*,2001, roč. 9. č. 10, s. 486-493.

HIRAMATSU, K., HANAKI, H., INO, T., YABUTA, K., OGURI, T. a TENOVER, F. C. Methicillin-resistant Staphylococcus aureus clinical strain with reduced vancomycin susceptibility. *Journal of Antimicrobial Chemotherapy*,1997, roč. 40. č. 1, s. 135-136.

HOGARDT, M., TREBESIUS, K., GEIGER, A. M., HORNEF, M., ROSENECKER, J. a HEESEMANN, J. Specific and rapid detection by fluorescent in situ hybridization of bacteria in clinical samples obtained from cystic fibrosis patients. *Journal of Clinical Microbiology*,2000, roč. 38. č. 2, s. 818-825.

CHAMBERS, H. F. a DELEO, F. R. Waves of resistance: Staphylococcus aureus in the antibiotic era. *Nature Reviews Microbiology*,2009, roč. 7. č. 9, s. 629-641.

CHANCHAITHONG, P. a PRAPASARAKUL, N. Biochemical markers and protein pattern analysis for canine coagulase-positive staphylococci and their distribution on dog skin. *Journal of Microbiological Methods*,2011, roč. 86. č. 2, s. 175-181.

AUTHOR, Culture medium silica gel stick for bacterial cultivation, has ring-shaped coating device that comprises fixing rod, and inoculating needle that is movably connected with fixed rod. Lanzhou Veterinary Res Inst China Agric (Cags-C): 5.

CHOI, J. H., NGUYEN, F. T., BARONE, P. W., HELLER, D. A., MOLL, A. E., PATEL, D., BOPPART, S. A. a STRANO, M. S. Multimodal biomedical imaging with asymmetric single-walled carbon nanotube/iron oxide nanoparticle complexes. *Nano Letters*,2007, roč. 7. č. 4, s. 861-867.

CHONG, Y. P., PARK, K. H., KIM, E. S., KIM, M. N., KIM, S. H., LEE, S. O., CHOI, S. H., JEONG, J. Y., WOO, J. H. a KIM, Y. S. Clinical and Microbiologic Analysis of the Risk Factors for Mortality in Patients with Heterogeneous Vancomycin-Intermediate Staphylococcus aureus Bacteremia. *Antimicrobial Agents and Chemotherapy*,2015, roč. 59. č. 6, s. 3541-3547.

CHOW, S. K. a CLARRIDGE, J. E. Identification and Clinical Significance of Helcococcus species, with Description of Helcococcus seattlensis sp nov from a Patient with Urosepsis. *Journal of Clinical Microbiology*,2014, roč. 52. č. 3, s. 854-858.

CHUDOBOVA, D., CIHALOVA, K., DOSTALOVA, S., RUTTKAY-NEDECKY, B., RODRIGO, M. A. M., TMEJOVA, K., KOPEL, P., NEJDL, L., KUDR, J., GUMULEC, J., KRIZKOVA, S., KYNICKY, J., KIZEK, R. a ADAM, V. Comparison of the effects of silver phosphate and selenium nanoparticles on Staphylococcus aureus growth reveals potential for selenium particles to prevent infection. *Fems Microbiology Letters*,2014, roč. 351. č. 2, s. 195-201.

CHUDOBOVA, D., CIHALOVA, K., GURAN, R., DOSTALOVA, S., SMERKOVA, K., VESELY, R., GUMULEC, J., MASARIK, M., HEGER, Z., ADAM, V. a KIZEK, R. Influence of microbiome species in hard-to-heal wounds on disease severity and treatment duration. *Brazilian Journal of Infectious Diseases*,2015, roč. 19. č. 6, s. 604-613.

CHUDOBOVA, D., CIHALOVA, K., SKALICKOVA, S., ZITKA, J., RODRIGO, M. A. M., MILOSAVLJEVIC, V., HYNEK, D., KOPEL, P., VESELY, R., ADAM, V. a KIZEK, R. 3D-printed chip for detection of methicillin-resistant Staphylococcus aureus labeled with gold nanoparticles. *Electrophoresis*,2015, roč. 36. č. 3, s. 457-466.

CHUDOBOVA, D., NEJDL, L., GUMULEC, J., KRYSTOFOVA, O., RODRIGO, M. A. M., KYNICKY, J., RUTTKAY-NEDECKY, B., KOPEL, P., BABULA, P., ADAM, V. a KIZEK, R. Complexes of Silver(I) Ions and Silver Phosphate Nanoparticles with Hyaluronic Acid and/or Chitosan as Promising Antimicrobial Agents for Vascular Grafts. *International Journal of Molecular Sciences*,2013, roč. 14. č. 7, s. 13592-13614.

IEVEN, M., VERHOEVEN, J., PATTYN, S. R. a GOOSSENS, H. RAPID AND ECONOMICAL METHOD FOR SPECIES IDENTIFICATION OF CLINICALLY SIGNIFICANT COAGULASE-NEGATIVE STAPHYLOCOCCI. *Journal of Clinical Microbiology*,1995, roč. 33. č. 5, s. 1060-1063.

ITO, T., KATAYAMA, Y., ASADA, K., MORI, N., TSUTSUMIMOTO, K., TIENSASITORN, C. a HIRAMATSU, K. Structural comparison of three types of staphylococcal cassette chromosome mec integrated in the chromosome in methicillin-resistant Staphylococcus aureus. *Antimicrobial Agents and Chemotherapy*,2001, roč. 45. č. 5, s. 1323-1336.

ITO, T., OKUMA, K., MA, X. X., YUZAWA, H. a HIRAMATSU, K. Insights on antibiotic resistance of Staphylococcus aureus from its whole genome: genomic island SCC. *Drug Resistance Updates*,2003, roč. 6. č. 1, s. 41-52.

JONES, R. N., ROSS, J. E., FRITSCHE, T. R. a SADER, H. S. Oxazolidinone susceptibility patterns in 2004: report from the Zyvox (R) Annual Appraisal of Potency and Spectrum (ZAAPS) Program assessing isolates from 16 nations. *Journal of Antimicrobial Chemotherapy*,2006, roč. 57. č. 2, s. 279-287.

JOSEFSSON, E., JUUTI, K., BOKAREWA, M. a KUUSELA, P. The surface protein Pls of methicillin-resistant Staphylococcus aureus is a virulence factor in septic arthritis. *Infection and Immunity*,2005, roč. 73. č. 5, s. 2812-2817.

JUVONEN, R., SATOKARI, R., MALLISON, K. a HAIKARA, A. Detection of spoilage bacteria in beer by polymerase chain reaction. *Journal of the American Society of Brewing Chemists*,1999, roč. 57. č. 3, s. 99-103.

KATAYAMA, N., TAKANO, H., SUGIYAMA, M., TAKIO, S., SAKAI, A., TANAKA, K., KUROIWA, H. a ONO, K. Effects of antibiotics that inhibit the bacterial peptidoglycan synthesis pathway on moss chloroplast division. *Plant and Cell Physiology*,2003, roč. 44. č. 7, s. 776-781.

KAWAMURA, Y., HOU, X. G., SULTANA, F., HIROSE, K., MIYAKE, M., SHU, S. E. a EZAKI, T. Distribution of Staphylococcus species among human clinical specimens and emended description of Staphylococcus caprae. *Journal of Clinical Microbiology*,1998, roč. 36. č. 7, s. 2038-2042.

KAYSER, F. H. a BIENZ, K. A. (2011). Medical microbiology, Thieme.

KEMPF, V. A. J., TREBESIUS, K. a AUTENRIETH, I. B. Fluorescent in situ hybridization allows rapid identification of microorganisms in blood cultures. *Journal of Clinical Microbiology*,2000, roč. 38. č. 2, s. 830-838.

KESSLER, S. W. RAPID ISOLATION OF ANTIGENS FROM CELLS WITH A STAPHYLOCOCCAL PROTEIN A-ANTIBODY ADSORBENT - PARAMETERS OF INTERACTION OF ANTIBODY-ANTIGEN COMPLEXES WITH PROTEIN-A. *Journal of Immunology*,1975, roč. 115. č. 6, s. 1617-1624.

KLEVENS, R. M., MORRISON, M. A., NADLE, J., PETIT, S., GERSHMAN, K., RAY, S., HARRISON, L. H., LYNFIELD, R., DUMYATI, G., TOWNES, J. M., CRAIG, A. S., ZELL, E. R., FOSHEIM, G. E., MCDOUGAL, L. K., CAREY, R. B., FRIDKIN, S. K. a INVESTIGATORS, A. B. M. Invasive methicillin-resistant Staphylococcus aureus infections in the United States. *Jama-Journal of the American Medical Association*,2007, roč. 298. č. 15, s. 1763-1771.

KLOOS, W. E., GEORGE, C. G., OLGIATE, J. S., VAN PELT, L., MCKINNON, M. L., ZIMMER, B. L., MULLER, E., WEINSTEIN, M. P. a MIRRETT, S. Staphylococcus hominis subsp. novobiosepticus subsp. nov., a novel trehalose- and N-acetyl-D-glucosamine-negative, novobiocin- and multiple-antibiotic-resistant subspecies isolated from human blood cultures. *International Journal of Systematic Bacteriology*,1998, roč. 48. č., s. 799-812.

KNOBLOCH, J. K. M., HORSTKOTTE, M. A., ROHDE, H. a MACK, D. Evaluation of different detection methods of biofilm formation in Staphylococcus aureus. *Medical Microbiology and Immunology*,2002, roč. 191. č. 2, s. 101-106.

KOBAYASHI, S. D., BRAUGHTON, K. R., PALAZZOLO-BALLANCE, A. M., KENNEDY, A. D., SAMPAIO, E., KRISTOSTURYAN, E., WHITNEY, A. R., STURDEVANT, D. E., DORWARD, D. W., HOLLAND, S. M., KREISWIRTH, B. N., MUSSER, J. M. a DELEO, F. R. Rapid Neutrophil Destruction following Phagocytosis of Staphylococcus aureus. *Journal of Innate Immunity*,2010, roč. 2. č. 6, s. 560-575.

KOHANSKI, M. A., DWYER, D. J. a COLLINS, J. J. How antibiotics kill bacteria: from targets to networks. *Nature Reviews Microbiology*,2010, roč. 8. č. 6, s. 423-435.

KOLBERT, C. P., CONNOLLY, J. E., LEE, M. J. a PERSING, D. H. DETECTION OF THE STAPHYLOCOCCAL MECA GENE BY CHEMILUMINESCENT DNA HYBRIDIZATION. *Journal of Clinical Microbiology*,1995, roč. 33. č. 8, s. 2179-2182.

KRIZKOVA, S., NGUYEN, H. V., STANISAVLJEVIC, M., KOPEL, P., VACULOVICOVA, M., ADAM, V. a KIZEK, R. Microchip capillary electrophoresis: quantum dots and paramagnetic particles for bacteria immunoseparation: rapid superparamagnetic-beads-based automated immunoseparation of Zn-Proteins from Staphylococcus aureus with nanogram yield. *Methods in molecular biology (Clifton, N.J.)*,2015, roč. 1274. č., s. 67-79.

KUMMER, K. M., TAYLOR, E. N., DURMAS, N. G., TARQUINIO, K. M., ERCAN, B. a WEBSTER, T. J. Effects of different sterilization techniques and varying anodized TiO2 nanotube dimensions on bacteria growth. *Journal of Biomedical Materials Research Part B-Applied Biomaterials*,2013, roč. 101B. č. 5, s. 677-688.

KURODA, M., OHTA, T., UCHIYAMA, I., BABA, T., YUZAWA, H., KOBAYASHI, I., CUI, L. Z., OGUCHI, A., AOKI, K., NAGAI, Y., LIAN, J. Q., ITO, T., KANAMORI, M., MATSUMARU, H., MARUYAMA, A., MURAKAMI, H., HOSOYAMA, A., MIZUTANI-UI, Y., TAKAHASHI, N. K., SAWANO, T., INOUE, R., KAITO, C., SEKIMIZU, K., HIRAKAWA, H., KUHARA, S., GOTO, S., YABUZAKI, J., KANEHISA, M., YAMASHITA, A., OSHIMA, K., FURUYA, K., YOSHINO, C., SHIBA, T., HATTORI, M., OGASAWARA, N., HAYASHI, H. a HIRAMATSU, K. Whole genome sequencing of meticillin-resistant Staphylococcus aureus. *Lancet*,2001, roč. 357. č. 9264, s. 1225-1240.

KWOK, A. Y. C. a CHOW, A. W. Phylogenetic study of Staphylococcus and Macrococcus species based on partial hsp60 gene sequences. *International Journal of Systematic and Evolutionary Microbiology*,2003, roč. 53. č., s. 87-92.

LAMBERT, L. H., COX, T., MITCHELL, K., ROSSELLO-MORA, R. A., DEL CUETO, C., DODGE, D. E., ORKAND, P. a CANO, R. J. Staphylococcus succinus sp. nov., isolated from Dominican amber. *International Journal of Systematic Bacteriology*,1998, roč. 48. č., s. 511-518.

LINA, G., PIEMONT, Y., GODAIL-GAMOT, F., BES, M., PETER, M. O., GAUDUCHON, V., VANDENESCH, F. a ETIENNE, J. Involvement of Panton-Valentine leukocidin-producing Staphylococcus aureus in primary skin infections and pneumonia. *Clinical Infectious Diseases*,1999, roč. 29. č. 5, s. 1128-1132.

LOUIE, L., MATSUMURA, S. O., CHOI, E., LOUIE, M. a SIMOR, A. E. Evaluation of three rapid methods for detection of methicillin resistance in Staphylococcus aureus. *Journal of Clinical Microbiology*,2000, roč. 38. č. 6, s. 2170-2173.

LOWY, F. D. Staphylococcus aureus infections - Reply. *New England Journal of Medicine*,1998, roč. 339. č. 27, s. 2026-2027.

LUDWIG, W. a SCHLEIFER, K. H. How quantitative is quantitative PCR with respect to cell counts? *Systematic and Applied Microbiology*,2000, roč. 23. č. 4, s. 556-562.

MAHILLON, J. a CHANDLER, M. Insertion sequences. *Microbiology and Molecular Biology Reviews*,1998, roč. 62. č. 3, s. 725-+.

MARRAFFINI, L. A., DEDENT, A. C. a SCHNEEWIND, O. Sortases and the art of anchoring proteins to the envelopes of gram-positive bacteria. *Microbiology and Molecular Biology Reviews*,2006, roč. 70. č. 1, s. 192-+.

MCCLOSKEY, K. E., CHALMERS, J. J. a ZBOROWSKI, M. Magnetic cell separation: Characterization of magnetophoretic mobility. *Analytical Chemistry*,2003, roč. 75. č. 24, s. 6868-6874.

MCCORMICK, J. K., YARWOOD, J. M. a SCHLIEVERT, P. M. Toxic shock syndrome and bacterial superantigens: An update. *Annual Review of Microbiology*,2001, roč. 55. č., s. 77-104.

MERLINO, J., LEROI, M., BRADBURY, R., VEAL, D. a HARBOUR, C. New chromogenic identification and detection of Staphylococcus aureus and methicillin-resistant S. aureus. *Journal of Clinical Microbiology*,2000, roč. 38. č. 6, s. 2378-2380.

MIHAI, M. M., HOLBAN, A. M., GIURCANEANU, C., POPA, L. G., BUZEA, M., FILIPOV, M., LAZAR, V., CHIFIRIUC, M. C. a POPA, M. J. Identification and phenotypic characterization of the most frequent bacterial etiologies in chronic skin ulcers. *Romanian Journal of Morphology and Embryology*,2014, roč. 55. č. 4, s. 1401-1408.

MILLER, J. M., BIDDLE, J. W., QUENZER, V. K. a MCLAUGHLIN, J. C. EVALUATION OF BIOLOG FOR IDENTIFICATION OF MEMBERS OF THE FAMILY MICROCOCCACEAE. *Journal of Clinical Microbiology*,1993, roč. 31. č. 12, s. 3170-3173.

MING, K., KIM, J., BIONDI, M. J., SYED, A., CHEN, K., LAM, A., OSTROWSKI, M., REBBAPRAGADA, A., FELD, J. J. a CHAN, W. C. W. Integrated Quantum Dot Barcode Smartphone Optical Device for Wireless Multiplexed Diagnosis of Infected Patients. *Acs Nano*,2015, roč. 9. č. 3, s. 3060-3074.

MIRERSHADI, F., JAFARI, A., JANATI, E., ROOHI, E. a SARABI, M. Ag/ZnO Nano-composites as Novel Antibacterial Agent against Strain of MRSA. *Journal of Pure and Applied Microbiology*,2013, roč. 7. č. 2, s. 947-956.

MLYNARCZYK, A., MLYNARCZYK, G. a JELJASZEWICZ, J. The genome of Staphylococcus aureus: A review. *Zentralblatt Fur Bakteriologie-International Journal of Medical Microbiology Virology Parasitology and Infectious Diseases*,1998, roč. 287. č. 4, s. 277-314.

MOORE, G. a GRIFFITH, C. Problems associated with traditional hygiene swabbing: the need for in-house standardization. *Journal of Applied Microbiology*,2007, roč. 103. č. 4, s. 1090-1103.

MULLER, U. R. Protein detection using biobarcodes. *Molecular Biosystems*,2006, roč. 2. č. 10, s. 470-476.

NANDAKUMAR, R., NANDAKUMAR, M. P., MARTEN, M. R. a ROSS, J. M. Proteome analysis of membrane and cell wall associated proteins from Staphylococcus aureus. *Journal of Proteome Research*,2005, roč. 4. č. 2, s. 250-257.

NEJDL, L., KUDR, J., CIHALOVA, K., CHUDOBOVA, D., ZUREK, M., ZALUD, L., KOPECNY, L., BURIAN, F., RUTTKAY-NEDECKY, B., KRIZKOVA, S., KONECNA, M., HYNEK, D., KOPEL, P., PRASEK, J., ADAM, V. a KIZEK, R.

Remote-controlled robotic platform ORPHEUS as a new tool for detection of bacteria in the environment. *Electrophoresis*,2014, roč. 35. č. 16, s. 2333-2345.

NEJDL, L., KUDR, J., RUTTKAY-NEDECKY, B., HEGER, Z., ZIMA, L., ZALUD, L., KRIZKOVA, S., ADAM, V., VACULOVICOVA, M. a KIZEK, R. Remote-Controlled Robotic Platform for Electrochemical Determination of Water Contaminated by Heavy Metal Ions. *International Journal of Electrochemical Science*,2015, roč. 10. č. 4, s. 3635-3643.

NISHIFUJI, K., SUGAI, M. a AMAGAI, M. Staphylococcal exfoliative toxins: "Molecular scissors" of bacteria that attack the cutaneous defense barrier in mammals. *Journal of Dermatological Science*,2008, roč. 49. č. 1, s. 21-31.

NOVICK, R. P., ROSS, H. F., PROJAN, S. J., KORNBLUM, J., KREISWIRTH, B. a MOGHAZEH, S. SYNTHESIS OF STAPHYLOCOCCAL VIRULENCE FACTORS IS CONTROLLED BY A REGULATORY RNA MOLECULE. *Embo Journal*,1993, roč. 12. č. 10, s. 3967-3975.

OTERO, M. C. a NADER-MACIAS, M. E. Inhibition of Staphylococcus aureus by H2O2-producing Lactobacillus gasseri isolated from the vaginal tract of cattle. *Animal Reproduction Science*,2006, roč. 96. č. 1-2, s. 35-46.

AUTHOR, Random type identification block for three dimensional (3D) identification device has index pattern that can be print on which barcode or specific image pattern is printed, and for storing index information on one surface of body. 19.

PATEL, R. Biofilms and antimicrobial resistance. *Clinical Orthopaedics and Related Research*,2005, roč. č. 437, s. 41-47.

PATERSON, D. L. a BONOMO, R. A. Extended-spectrum beta-lactamases: a clinical update. *Clinical Microbiology Reviews*,2005, roč. 18. č. 4, s. 657-+.

PAULSSON, J. Multileveled selection on plasmid replication. *Genetics*,2002, roč. 161. č. 4, s. 1373-1384.

PEACOCK, S. J., MOORE, C. E., JUSTICE, A., KANTZANOU, M., STORY, L., MACKIE, K., O'NEIL, G. a DAY, N. P. J. Virulent combinations of adhesin and toxin genes in natural populations of Staphylococcus aureus. *Infection and Immunity*,2002, roč. 70. č. 9, s. 4987-4996.

PERUSKI, A. H., JOHNSON, L. H. a PERUSKI, L. F. Rapid and sensitive detection of biological warfare agents using time-resolved fluorescence assays. *Journal of Immunological Methods*,2002, roč. 263. č. 1-2, s. 35-41.

PIETTE, A. a VERSCHRAEGEN, G. Role of coagulase-negative staphylococci in human disease. *Veterinary Microbiology*,2009, roč. 134. č. 1-2, s. 45-54.

AUTHOR, Assay device for assay detection system for analyzing presence of e.g. bacterial in e.g. blood of e.g. bacterial infections of patient, has optical reader apparatus comprising light source, where device comprises barcode scanner. 134.

PLACE, R. B., HIESTAND, D., BURRI, S. a TEUBER, M. Staphylococcus succinus subsp casei subsp nov., a dominant isolate from a surface ripened cheese. *Systematic and Applied Microbiology*,2002, roč. 25. č. 3, s. 353-359.

POLACZEK-KORNECKA, B., DZIADUR-GOLDSZTAJ, Z. a TUROWSKI, G. Methicillin-oxacillin resistant strains of Staphylococcus aureus (MORSA) in infected burn wounds. *Materia medica Polona. Polish journal of medicine and pharmacy*,1991, roč. 23. č. 4, s. 304-305.

PREDARI, S. C., LIGOZZI, M. a FONTANA, R. GENOTYPIC IDENTIFICATION OF METHICILLIN-RESISTANT COAGULASE-NEGATIVE STAPHYLOCOCCI BY POLYMERASE CHAIN-REACTION. *Antimicrobial Agents and Chemotherapy*,1991, roč. 35. č. 12, s. 2568-2573.

PROCTOR, R. A., KAHL, B., VON EIFF, C., VAUDAUX, P. E., LEW, D. P. a PETERS, G. Staphylococcal small colony variants have novel mechanisms for antibiotic resistance. *Clinical Infectious Diseases*,1998, roč. 27. č., s. S68-S74.

RAI, M., KON, K., INGLE, A., DURAN, N., GALDIERO, S. a GALDIERO, M. Broad-spectrum bioactivities of silver nanoparticles: the emerging trends and future prospects. *Applied Microbiology and Biotechnology*,2014, roč. 98. č. 5, s. 1951-1961.

RAND, K. H. a HOUCK, H. J. Synergy of daptomycin with oxacillin and other beta-lactams against methicillin-resistant Staphylococcus aureus. *Antimicrobial Agents and Chemotherapy*,2004, roč. 48. č. 8, s. 2871-2875.

RAO, A. S. (1997). Introduction to microbiology, PHI Learning Pvt. Ltd.

RODRIGUEZ, E., CALZADA, J., ARQUES, J. L., RODRIGUEZ, J. M., NUNEZ, M. a MEDINA, M. Antimicrobial activity of pediocin-producing Lactococcus lactis on Listeria monocytogenes, Staphylococcus aureus and Escherichia coli O157 : H7 in cheese. *International Dairy Journal*,2005, roč. 15. č. 1, s. 51-57.

RUZICKOVA, V. CHARACTERISTICS OF STRAINS OF STAPHYLOCOCCUS-AUREUS ISOLATED IN DAIRY FARMS. *Veterinarni Medicina*,1994, roč. 39. č. 1, s. 37-44.

SHORE, A., ROSSNEY, A. S., KEANE, C. T., ENRIGHT, M. C. a COLEMAN, D. C. Seven novel variants of the staphylococcal chromosomal cassette mec in methicillin-resistant Staphylococcus aureus isolates from Ireland. *Antimicrobial Agents and Chemotherapy*,2005, roč. 49. č. 5, s. 2070-2083.

SCHAEG, W., BRUCKLER, J. a BLOBEL, H. IMPROVED METHOD FOR THE DEMONSTRATION OF PROTEIN-A OF STAPHYLOCOCCUS-AUREUS. *Zentralblatt Fur Bakteriologie Mikrobiologie Und Hygiene Series a-Medical*

Microbiology Infectious Diseases Virology Parasitology,1979, roč. 245. č. 4, s. 442-449.

SILVA, B. O., CARAVIELLO, D. Z., RODRIGUES, A. C. a RUEGG, P. L. Evaluation of petrifilm for the isolation of Staphylococcus aureus from milk samples. *Journal of Dairy Science*,2005, roč. 88. č. 8, s. 3000-3008.

SINGER, S. J. a NICOLSON, G. L. FLUID MOSAIC MODEL OF STRUCTURE OF CELL-MEMBRANES. *Science*,1972, roč. 175. č. 4023, s. 720-&.

SINHA, B., FRANCOIS, P. P., NUSSE, O., FOTI, M., HARTFORD, O. M., VAUDAUX, P., FOSTER, T. J., LEW, D. P., HERRMANN, M. a KRAUSE, K. H. Fibronectin-binding protein acts as Staphylococcus aureus invasin via fibronectin bridging to integrin alpha(5)beta(1). *Cellular Microbiology*,1999, roč. 1. č. 2, s. 101-117.

STANDISH, A. J., SALIM, A. A., ZHANG, H., CAPON, R. J. a MORONA, R. Chemical Inhibition of Bacterial Protein Tyrosine Phosphatase Suppresses Capsule Production. *Plos One*,2012, roč. 7. č. 5.

STEVENS, D. L., MA, Y. S., SALMI, D. B., MCINDOO, E., WALLACE, R. J. a BRYANT, A. E. Impact of antibiotics on expression of virulence-associated exotoxin genes in methicillin-sensitive and methicillin-resistant Staphylococcus aureus. *Journal of Infectious Diseases*,2007, roč. 195. č. 2, s. 202-211.

STEVENSON, L. G., DRAKE, S. K. a MURRAY, P. R. Rapid Identification of Bacteria in Positive Blood Culture Broths by Matrix-Assisted Laser Desorption Ionization-Time of Flight Mass Spectrometry. *Journal of Clinical Microbiology*,2010, roč. 48. č. 2, s. 444-447.

STEWART, P. S. a COSTERTON, J. W. Antibiotic resistance of bacteria in biofilms. *Lancet*,2001, roč. 358. č. 9276, s. 135-138.

STOAKES, L., REYES, R., DANIEL, J., LENNOX, G., JOHN, M. A., LANNIGAN, R. a HUSSAIN, Z. Prospective comparison of a new chromogenic medium, MRSASelect, to CHROMagar MRSA and mannitol-salt medium supplemented with oxacillin or cefoxitin for detection of methicillin-resistant Staphylococcus aureus. *Journal of Clinical Microbiology*,2006, roč. 44. č. 2, s. 637-639.

TANASE, C., CARAMIHAI, M. a MUNTEAN, O. Study of the Growth Kinetic Models of a Bacterium for a Human Use Therapeutic Product. *Revista De Chimie*,2013, roč. 64. č. 2, s. 182-185.

TANG, J. N., TANG, C., CHEN, J., DU, Y. W., YANG, X. N., WANG, C. T., ZHANG, H. R. a YUE, H. Phenotypic Characterization and Prevalence of Enterotoxin Genes in Staphylococcus aureus Isolates from Outbreaks of Illness in Chengdu City. *Foodborne Pathogens and Disease*,2011, roč. 8. č. 12, s. 1317-1320.

TARTAJ, P., MORALES, M. D., VEINTEMILLAS-VERDAGUER, S., GONZALEZ-CARRENO, T. a SERNA, C. J. The preparation of magnetic nanoparticles for applications in biomedicine. *Journal of Physics D-Applied Physics*,2003, roč. 36. č. 13, s. R182-R197.

TRAN, J. H. a JACOBY, G. A. Mechanism of plasmid-mediated quinolone resistance. *Proceedings of the National Academy of Sciences of the United States of America*,2002, roč. 99. č. 8, s. 5638-5642.

TRAN, P. A. a WEBSTER, T. J. Antimicrobial selenium nanoparticle coatings on polymeric medical devices. *Nanotechnology*,2013, roč. 24. č. 15.

VAN GRIETHUYSEN, A., POUW, M., VAN LEEUWEN, N., HECK, M., WILLEMSE, P., BUITING, A. a KLUYTMANS, J. Rapid slide latex agglutination test for detection of methicillin resistance in Staphylococcus aureus. *Journal of Clinical Microbiology*,1999, roč. 37. č. 9, s. 2789-2792.

VAN HAL, S. J., JENSEN, S. O., VASKA, V. L., ESPEDIDO, B. A., PATERSON, D. L. a GOSBELL, I. B. Predictors of Mortality in Staphylococcus aureus Bacteremia. *Clinical Microbiology Reviews*,2012, roč. 25. č. 2, s. 362-386.

VANDAMME, P., POT, B., GILLIS, M., DEVOS, P., KERSTERS, K. a SWINGS, J. Polyphasic taxonomy, a consensus approach to bacterial systematics. *Microbiological Reviews*,1996, roč. 60. č. 2, s. 407-+.

VERHOEF, J., PETERSON, P. K. a VERBRUGH, H. A. HOST - PARASITE RELATIONSHIP IN STAPHYLOCOCCAL INFECTIONS - ROLE OF THE STAPHYLOCOCCAL CELL-WALL DURING THE PROCESS OF PHAGOCYTOSIS. *Antonie Van Leeuwenhoek Journal of Microbiology*,1979, roč. 45. č. 1, s. 49-53.

WANG, J., LIU, G. D. a MERKOCI, A. Electrochemical coding technology for simultaneous detection of multiple DNA targets. *Journal of the American Chemical Society*,2003, roč. 125. č. 11, s. 3214-3215.

WANG, Q. F., SUZUKI, A., MARICONDA, S., PORWOLLIK, S. a HARSHEY, R. M. Sensing wetness: a new role for the bacterial flagellum. *Embo Journal*,2005, roč. 24. č. 11, s. 2034-2042.

WANG, Z. Q., ORLIKOWSKY, T., DUDHANE, A., TREJO, V., DANNECKER, G. E., PERNIS, B. a HOFFMANN, M. K. Staphylococcal enterotoxin B-induced T-cell anergy is mediated by regulatory T cells. *Immunology*,1998, roč. 94. č. 3, s. 331-339.

WANN, E. R., GURUSIDDAPPA, S. a HOOK, M. The fibronectin-binding MSCRAMM FnbpA of Staphylococcus aureus is a bifunctional protein that also binds to fibrinogen. *Journal of Biological Chemistry*,2000, roč. 275. č. 18, s. 13863-13871.

WEIDENMAIER, C., KOKAI-KUN, J. F., KRISTIAN, S. A., CHANTURIYA, T., KALBACHER, H., GROSS, M., NICHOLSON, G., NEUMEISTER, B., MOND, J. J. a

PESCHEL, A. Role of teichoic acids in Staphylococcus aureus nasal colonization, a major risk factor in nosocomial infections. *Nature Medicine*,2004, roč. 10. č. 3, s. 243-245.

WEIGEL, L. M., DONLAN, R. M., SHIN, D. H., JENSEN, B., CLARK, N. C., MCDOUGAL, L. K., ZHU, W. M., MUSSER, K. A., THOMPSON, J., KOHLERSCHINIDT, D., DUMAS, N., LIMBERGER, R. J. a PATEL, J. B. High-level vancomycin-resistant staphylococcus aureus isolates associated with a polymicrobial biofilm. *Antimicrobial Agents and Chemotherapy*,2007, roč. 51. č. 1, s. 231-238.

WENDT, C., SCHINKE, S., WURTTEMBERGER, M., OBERDORFER, K., BOCK-HENSLEY, O. a VON BAUM, H. Value of whole-body washing with chlorhexidine for the eradication of methicillin-resistant Staphylococcus aureus: A randomized, placebo-controlled, double-blind clinical trial. *Infection Control and Hospital Epidemiology*,2007, roč. 28. č. 9, s. 1036-1043.

WIESER, A., SCHNEIDER, L., JUNG, J. T. a SCHUBERT, S. MALDI-TOF MS in microbiological diagnostics-identification of microorganisms and beyond (mini review). *Applied Microbiology and Biotechnology*,2012, roč. 93. č. 3, s. 965-974.

WOLTERS, M., ROHDE, H., MAIER, T., BELMAR-CAMPOS, C., FRANKE, G., SCHERPE, S., AEPFELBACHER, M. a CHRISTNER, M. MALDI-TOF MS fingerprinting allows for discrimination of major methicillin-resistant Staphylococcus aureus lineages. *International Journal of Medical Microbiology*,2011, roč. 301. č. 1, s. 64-68.

WU, Q., LI, Y., HU, H. X., WANG, M., WU, Z. G. a XU, W. Z. Rapid Identification of Staphylococcus aureus: FISH Versus PCR Methods. *Labmedicine*,2012, roč. 43. č. 6, s. 276-280.

ZAPUN, A., CONTRERAS-MARTEL, C. a VERNET, T. Penicillin-binding proteins and beta-lactam resistance. *Fems Microbiology Reviews*,2008, roč. 32. č. 2, s. 361-385.

8 SEZNAM OBRÁZKŮ

Obr. 1: Mechanismus rezistence MRSA na β-laktamová antibiotika. Na stafylokokové chromozomální kazetě mec se nachází *mecA* gen kódující syntézu penicillin-binding proteinu 2a (PBP2a). PBP2a katalyzuje syntézu buněčné stěny a produkcí β-laktamázy dochází k rozkladu β-laktamového kruhu antibiotika. Přítomnost β-laktamových antibiotik inhibuje funkci transpeptidáz, mezi níž se řadí i PBP2a, buňka tak ztrácí schopnost vytvářet buněčnou stěnu a umírá. PBP2a však vykazuje vůči β-laktamovým antibiotikům nízkou afinitu, proto jejich inhibici nepodléhá.

Obr. 2: Izolace *S. aureus* z infekční rány hospitalizovaného pacienta v Úrazové nemocnici v Brně, p.o. na krevním agaru s 10% obsahem NaCl, po 24 hodinové kultivaci při 37 °C.

Obr. 3: Komerční magnetické částice Dynabeads® M-280 Streptavidin (Sigma-Aldrich, St. Louis, MO, USA) se zachycenou bakterií MRSA na svém povrchu.